

**VERSLAGEN EN VERHANDELINGEN**

**REPORTS AND TRANSACTIONS**

**NATIONAAL LUCHT- EN RUIMTEVAART-  
LABORATORIUM**

**NATIONAL AERO- AND ASTRONAUTICAL RESEARCH INSTITUTE**

**AMSTERDAM**

**XXVI — 1962**

## P R E F A C E.

This volume of "Verslagen en Verhandelingen" (= "Reports and Transactions") of the "Nationaal Lucht- en Ruimtevaartlaboratorium" (N.L.R.) (= "National Aero- and Astronautical Research Institute") contains a selection of reports by the N.L.R. completed in recent years.

The investigations reported in TR S. 527, TR S. 542, TR W. 3 and TR W. 5 have been performed under contract with the "Netherlands Aircraft Development Board" (N. I. V.). The research reported in TR S. 529 has been carried out under contract with the "Netherlands Civil Aviation Department" upon a recommendation made by the "Netherlands Committee for structural strength requirements for civil aircraft". The permission for publication is herewith acknowledged.

The printed reports of the N.L.R. which are collected at more or less regular intervals in the volumes of "Verslagen en Verhandelingen", form only a part of the publications issued by the N.L.R. A series of multigraphed reports and of publications in scientific and technical journals on research subjects studied by the N.L.R. is continuously growing. Both the multigraphed reports and the reprints of the reports meant for bound volumes of "Verslagen en Verhandelingen" are distributed as soon as they become available.

A complete list of publications issued between the years 1921 and 1960 is available upon request.

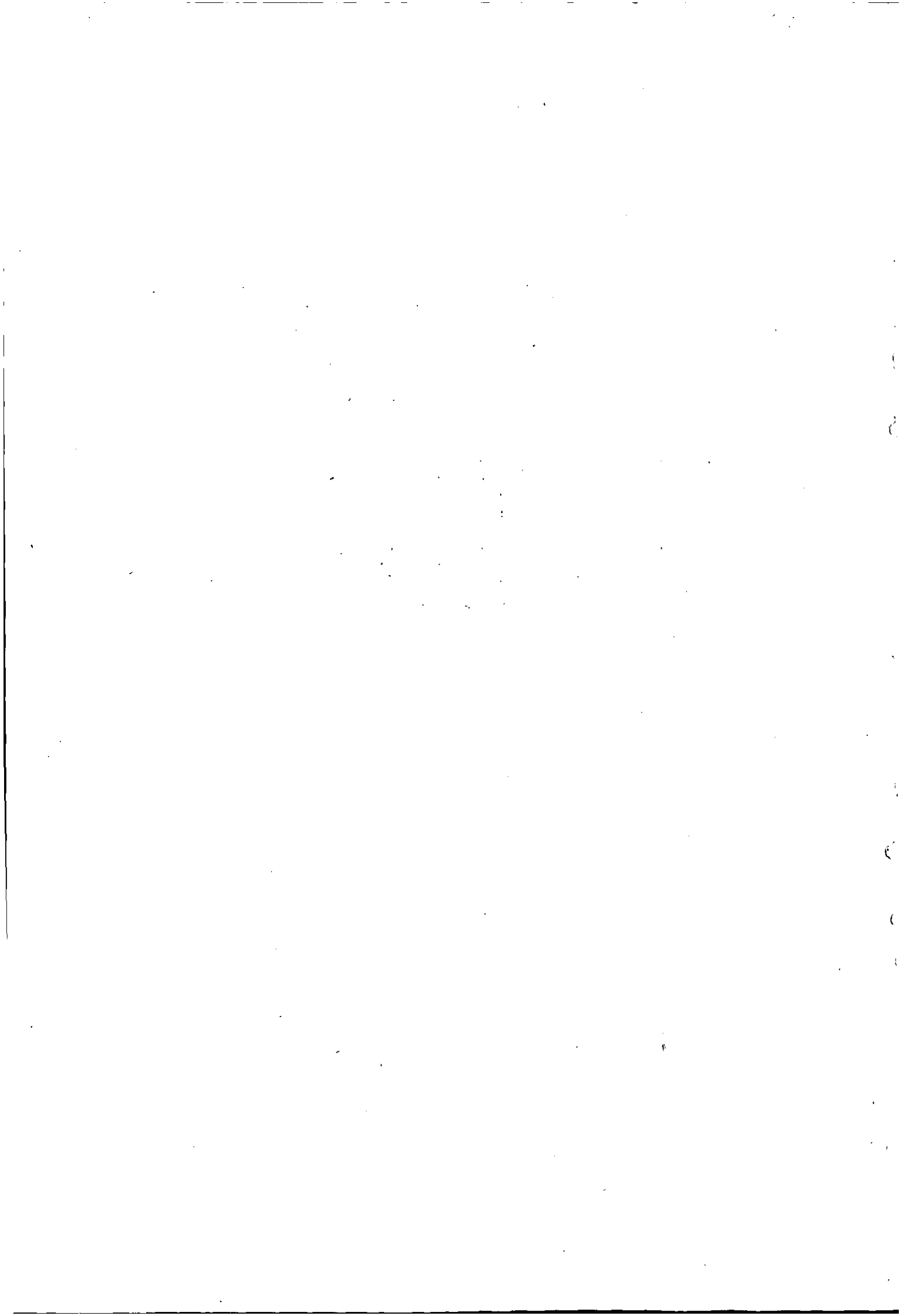
Amsterdam, september 1962.

A. J. Marx

Director of the  
"Nationaal Lucht- en Ruimtevaartlaboratorium"

### CONTENTS.

Report:	Author(s):	Title:	Com- pleted:	Pages:
TR S. 527	Benthem, J. P.	The buckling load of flat panels that change in thickness across the bay.	1958	1
TR S. 529	Hakkeling, B.	Airplane loads in pitching manoeuvres.	1958	9
TR S. 542	Benthem, J. P. and van der Vooren, J.	A stress diffusion problem for a wedge-shaped plate with three stiffeners.	1959	41
TR W. 3	de Jager, E. M.	Oscillating rectangular wings in supersonic flow with arbitrary bending and torsion mode shapes. <i>Part 1: Development of the theory.</i>	1959	71
TR W. 5	de Jager, E. M.	Oscillating rectangular wings in supersonic flow with arbitrary bending and torsion mode shapes. <i>Part 2: Numerical results.</i>	1959	103



NLI-TR S. 527

# The buckling load of flat panels that change in thickness across the bay

by

J. P. BENTHEM.

## Summary.

The compressive buckling load of infinitely long panels with simply-supported longitudinal edges, that have two symmetrical discontinuous changes in thickness across the width, has been calculated by CAPEY. This derivation holds also for an infinite set of such panels simply supported in longitudinal direction at equal distances. The present paper deals with an infinite set of equal unsymmetrical panels, buckling load and mode of which are not equal to those of such a single simply supported panel.

### Contents.

#### Notations.

1 Introduction.

2 Method of solution.

3 Numerical evaluation.

4 Discussion of diagrams.

5 References.

Appendix A: Comparison with semi-empirical values of ref. 5.

2 tables.

7 figures.

This investigation has been performed under contract with the Netherlands Aircraft Development Board (N.I.V.).

#### Notations.

$s$	width of one panel.	} see fig. 5
$b$	width of panel part with thickness $t_1$	
$c$	width of panel part with thickness $t_2$	
$t_1$	thickness of panel part	
$t_2$	thickness of panel part	
$\gamma$	$t_2/t_1$	
$\eta$	$b/s$	
$x_1, y_1, z_1$	coordinates of panel part with thickness $t_1$	
$x_2, y_2, z_2$	coordinates of panel part with thickness $t_2$	
$w_{1,n}$	deflections from the plane (i.e. in the direction of the $z_1$ axis) of the part with thickness $t_1$ of the $n$ -th panel.	

 $w_{2,n}$ 

deflections from the plane (i.e. in the direction of the  $z_2$  axis) of the part with thickness  $t_2$  of the  $n$ -th panel.

 $l$ 

half-wave length of buckling mode.

 $\sigma_x$ 

buckling stress (compressive stress taken positive).

 $E$ 

elasticity modulus.

 $\nu$ 

Poisson's ratio ( $\nu = 0.3$ ).

 $K_1, K_2$ 

differential operators defined in (2.6)

 $H_1, H_2$ 

differential operators defined in (2.11)

 $\lambda$ 

$l/s$

 $k$ 

from  $\sigma_x = k\pi^2 E t_2^2 / 12(1 - \nu^2) s^2$

 $\xi$ 

$\lambda \sqrt{k}$

 $p_1, q_1$  $\alpha_1, \beta_1$ 

} defined in (2.25)

 $p_2, q_2$  $\alpha_2, \beta_2$ 

} defined in (2.28)

 $a_1, a_2, a_3, a_4$ 

} defined in (2.33)

## 1 Introduction.

CAPEY, ref. 1, calculates for longitudinal compression the buckling load of single panels, infinite in length, simply supported at the longitudinal edges, and which show a variation in skin thickness across the bay according to fig. 1, which may be considered as an approximation to the more practical cross-section, fig. 2. Such a configuration may occur in integral construction of stringer sheet, whether by extrusion or by machining from the solid, and the variation in skin thickness may result in a gain in efficiency. The buckling stress and mode of such a panel are identical to those of an infinite set of such panels simply supported in longitudinal direction at equal distances.

A configuration like fig. 2 (or fig. 3) may also occur in structures where stringers are bonded

with their flanges to the skin. The derivation of CAPEY for his case is extended for the unsymmetrical configuration with cross section fig. 3, which is also simplified to that of cross section fig. 4. In that case the buckling load and mode of an infinite set of identical panels (the case actually considered, fig. 5) are no longer those of a single simply supported panel.

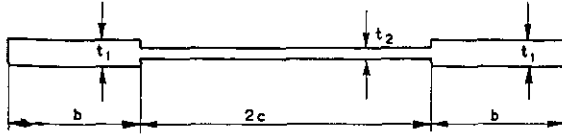


Fig. 1. Cross section of symmetrical panel analysed by CAPEY.

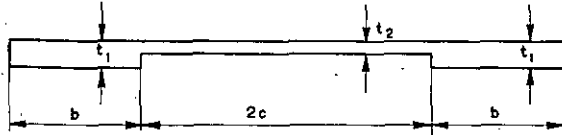


Fig. 2. Cross section of symmetrical panel as it may be applied in practice.

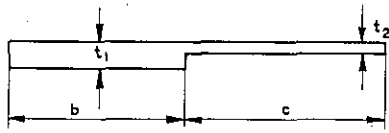


Fig. 3. Cross section of unsymmetrical panel as it may be applied in practice.

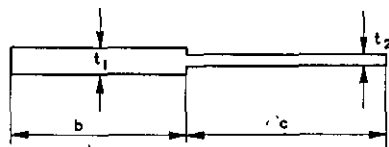


Fig. 4. Simplification of the cross section of fig. 3.

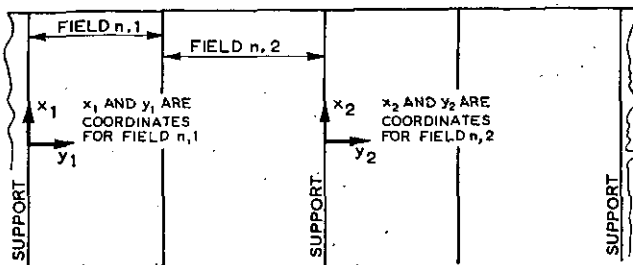
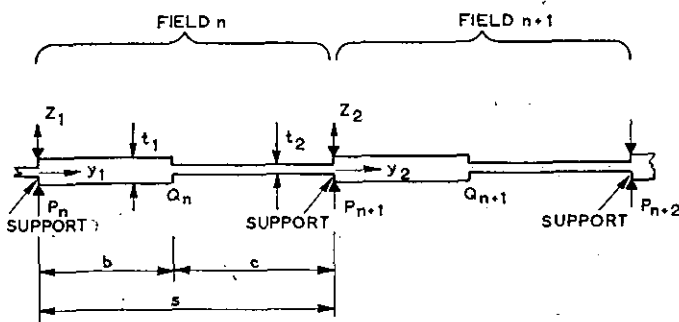


Fig. 5. Part of the infinite set of unsymmetrical panels.

The derivation of the buckling load of panels with cross section like fig. 1 or fig. 4 is closely connected to the well established theories on the buckling of uniform panels. Determination of the buckling load of a uniform panel results in the solution of a homogeneous linear differential equation of the fourth order; for the present case it results in the solution of two simultaneous equations of the fourth order. Besides, other work on the buckling load of compression members built up from flat plates is present (refs. 2, 3 and 4).

In ref. 5 the author describes tests on panels with three unsymmetrical bays. The intention of these tests was in the first place to determine the load-carrying capacity and a load-deflection curve. The buckling load could not be determined with very great accuracy due to initial deflections or other unavoidable irregularities. Therefore in analysing the results of ref. 5 (the present computations not yet being performed) use was made of buckling loads computed in a semi-empirical way<sup>1)</sup>.

## 2 Method of solution.

Fig. 5 shows the n-th panel between two supports, with its two parts of unequal thickness  $t_1$  and  $t_2$  respectively. Both parts have their own coordinate axes  $x, y, z$  (note that the coordinate  $y_2$  in the plate with thickness  $t_2$  is always negative). It is supposed that there is an infinite sequence of equal configurations to both sides (in the direction of the  $y$ -axes). The supports cause no restraint against rotations  $\varphi_x$  of the panels. The supports are supposed not to be able to suppress uniform expansion in  $y$  direction at uniform compression in  $x$ -direction.

In the n-th panel the displacements normal to the plate with thickness  $t_1$  are  $w_{1,n}$ , those of the plate with thickness  $t_2$  are  $w_{2,n}$ .

The buckling stress  $\sigma_x$  is to be determined from the equations (ref. 6)

$$\frac{\partial^4 w_{1,n}}{\partial x_1^4} + 2 \frac{\partial^4 w_{1,n}}{\partial x_1^2 \partial y_1^2} + \frac{\partial^4 w_{1,n}}{\partial y_1^4} = - \frac{t_1}{D_1} \sigma_x \frac{\partial^2 w_{1,n}}{\partial x_1^2} \quad (2.1)$$

$$\frac{\partial^4 w_{2,n}}{\partial x_2^4} + 2 \frac{\partial^4 w_{2,n}}{\partial x_2^2 \partial y_2^2} + \frac{\partial^4 w_{2,n}}{\partial y_2^4} = - \frac{t_2}{D_2} \sigma_x \frac{\partial^2 w_{2,n}}{\partial x_2^2} \quad (2.2)$$

where

$$D_1 = \frac{E t_1^3}{12(1-\nu^2)}, \quad D_2 = \frac{E t_2^3}{12(1-\nu^2)}$$

All equations (2.1), (2.2) have coupled boundary conditions. At point  $P_n$

$$w_{2,n-1} = w_{1,n} = 0 \quad (2.3)$$

$$\frac{\partial w_{2,n-1}}{\partial y_2} = \frac{\partial w_{1,n}}{\partial y_1} \quad (2.4)$$

$$t_2^3 K_2 w_{2,n-1} = t_1^3 K_1 w_{1,n} \quad (2.5)$$

where

<sup>1)</sup> A comparison is made between the latter values and the exact ones (for an infinite sequence of bays) in appendix A.

$$K_1 = \frac{\partial^2}{\partial y_1^2} + \nu \frac{\partial^2}{\partial x_1^2}, \quad K_2 = \frac{\partial^2}{\partial y_2^2} + \nu \frac{\partial^2}{\partial x_2^2}. \quad (2.6)$$

At point  $Q_n$

$$w_{1,n} = w_{2,n} \quad (2.7)$$

$$\frac{\partial w_{1,n}}{\partial y_1} = \frac{\partial w_{2,n}}{\partial y_2} \quad (2.8)$$

$$t_1^3 K_1 w_{1,n} = t_2^3 K_2 w_{2,n} \quad (2.9)$$

where  $K_1, K_2$  according (2.6)

$$t_1^3 H_1 w_{1,n} = t_2^3 H_2 w_{2,n} \quad (2.10)$$

where

$$H_1 = \frac{\partial^3}{\partial y_1^3} + (2 - \nu) \frac{\partial^3}{\partial x_1^2 \partial y_1}, \quad H_2 = \frac{\partial^3}{\partial y_2^3} + (2 - \nu) \frac{\partial^3}{\partial x_2^2 \partial y_2} \quad (2.11)$$

Equations (2.3), (2.4), (2.7) and (2.8) result from the requirement of geometrical continuity, (2.5) and (2.9) from the continuity of bending moments  $M_y$ , and (2.10) from the continuity of  $Q_y - \partial M_{xy} / \partial x$  ( $Q_y$  shear force,  $M_{xy}$  twisting moment).

In fact (2.3) ... (2.11) form an infinite set of conditions ( $n$  ranges from  $-\infty$  to  $+\infty$ ) but they may be made to a finite set by supposing that the buckling mode is repeated after one panel (with the displacements reversed in sign)

$$\left. \begin{aligned} w_{1,n} &= -w_{1,n+1} \\ w_{2,n} &= -w_{2,n+1} \end{aligned} \right\} \quad (2.12)$$

Then the infinite number of equations (2.3) ... (2.11) result into 8 equations (2.13) ... (2.20) with 8 unknowns

$$\text{at } P_n \quad w_{2,n} = 0 \quad (2.13)$$

$$w_{1,n} = 0 \quad (2.14)$$

$$\frac{\partial w_{1,n}}{\partial y_1} + \frac{\partial w_{2,n}}{\partial y_2} = 0 \quad (2.15)$$

$$t_1^3 K_1 w_{1,n} + t_2^3 K_2 w_{2,n} = 0 \quad (2.16)$$

$$\text{at } Q_n \quad w_{1,n} - w_{2,n} = 0 \quad (2.17)$$

$$\frac{\partial w_{1,n}}{\partial y_1} - \frac{\partial w_{2,n}}{\partial y_2} = 0 \quad (2.18)$$

$$t_1^3 K_1 w_{1,n} - t_2^3 K_2 w_{2,n} = 0 \quad (2.19)$$

$$t_1^3 H_1 w_{1,n} - t_2^3 H_2 w_{2,n} = 0 \quad (2.20)$$

A buckling mode is sought of the shape<sup>1)</sup>

$$w_{1,n} = f_{1,n}(y_1) \sin \pi x_1 / l \quad (2.21)$$

$$w_{2,n} = f_{2,n}(y_2) \sin \pi x_2 / l \quad (2.22)$$

Equation (2.21) substituted into (2.1) gives

<sup>1)</sup> There are no geometrical restrictions on the wave length, since the panels are infinitely long in the direction of the x-axis.

$$\frac{\pi^4}{l^4} f_{1,n} - 2 \frac{\pi^2}{l^2} \frac{d^2 f_{1,n}}{dy_1^2} + \frac{d^4 f_{1,n}}{dy_1^4} = \frac{t_1}{D_1} \sigma_x \frac{\pi^2}{l^2} f_{1,n} \quad (2.23)$$

or

$$\frac{d^4 f_{1,n}}{dy_1^4} + \frac{\beta_1^2 - \alpha_1^2}{s^2} \frac{d^2 f_{1,n}}{dy_1^2} - \frac{\alpha_1^2 \beta_1^2}{s^4} f_{1,n} = 0 \quad (2.24)$$

where

$$\alpha_1 = \frac{\pi p_1}{\lambda}, \quad p_1 = \sqrt{\gamma \xi + 1}, \quad \lambda = l/s$$

$$\beta_1 = \frac{\pi q_1}{\lambda}, \quad q_1 = \sqrt{\gamma \xi - 1}$$

$$\gamma = t_2/t_1, \quad \xi = \lambda \sqrt{k} \text{ and } k \text{ from } \sigma_x =$$

$$= k \frac{\pi_2 E t_2^2}{12(1 - \nu^2) s^2}$$

$s$  = distance between two supports.

The general solution of (2.23) is ( $\beta_1 \neq 0$ )

$$f_{1,n} = A_{1,n} \sinh \alpha_1 y_1 / s + A_{2,n} \sin \beta_1 y_1 / s + A_{3,n} \cosh \alpha_1 y_1 / s + A_{4,n} \cos \beta_1 y_1 / s \quad (2.25)$$

Substitution of (2.22) into (2.2) gives

$$\frac{d^4 f_{2,n}}{dy_2^4} + \frac{\beta_2^2 - \alpha_2^2}{s^2} \frac{d^2 f_{2,n}}{dy_2^2} - \frac{\alpha_2^2 \beta_2^2}{s^4} f_{2,n} = 0 \quad (2.27)$$

where

$$\alpha_2 = \frac{\pi p_2}{\lambda}, \quad p_2 = \sqrt{\xi + 1}$$

$$\beta_2 = \frac{\pi q_2}{\lambda}, \quad q_2 = \sqrt{\xi - 1}$$

and the general solution is ( $\beta_2 \neq 0$ )

$$f_{2,n} = B_{1,n} \sinh \alpha_2 y_2 / s + B_{2,n} \sin \beta_2 y_2 / s + B_{3,n} \cosh \alpha_2 y_2 / s + B_{4,n} \cos \beta_2 y_2 / s \quad (2.29)$$

The solutions (2.26) and (2.29) inserted into the boundary conditions (2.13) ... (2.20) deliver 8 homogeneous equations for the unknown integration constants

$$A_{1,n} \dots A_{4,n}, \quad B_{1,n} \dots B_{4,n}.$$

These equations in matrix form have the shape

$$U Z = 0 \quad (2.30)$$

where  $U$  is a square matrix given in table 1,  $Z$  a column matrix with elements  $A_{1,n} \dots B_{4,n}$ , and  $0$  a zero column matrix.

Because the equations (2.30) are homogeneous a non zero solution for the unknowns is only possible if the determinant of the matrix  $U$  vanishes

$$\det U = 0. \quad (2.31)$$

In table 1 the further substitutions have taken place

$$\frac{b}{s} = \eta, \quad \frac{c}{s} = 1 - \eta \quad (2.32)$$

$$\left. \begin{aligned} \gamma \xi + 1 - \nu &= a_1 \\ -\gamma \xi + 1 - \nu &= a_2 \\ \gamma^3 (\xi + 1 - \nu) &= a_3 \\ \gamma^3 (-\xi + 1 - \nu) &= a_4 \end{aligned} \right\} (2.33)$$

### 3 Numerical evaluation.

The method of solution of (2.31) for given values of  $\gamma = t_2/t_1$  and of  $\eta = b/s$  is to choose a value for  $\lambda = l/s$  and to determine by trial and error the value of  $\xi$  for which the determinant (2.31) vanishes. This process is repeated with a number of different values of  $\lambda$ . The value of  $\lambda$  at which

$$\xi/\lambda = \sqrt{k}, \quad k \text{ from } \sigma_x = \frac{k \pi^2 E t_2^2}{12(1-\nu^2)s^2}$$

(see (2.25)) reaches a minimum delivers the actual wave length and the buckling stress  $\sigma_x$ <sup>1)</sup>.

It was desirable that the calculations had only to be performed with real numbers. It may however occur that  $q_1 = \sqrt{\gamma \xi - 1}$  and  $q_2 = \sqrt{\xi - 1}$  (from (2.25) and (2.28) respectively) become imaginary (in practice only  $q_1$  did so). In that case substitutions like

$$q_1 = i q_1' \quad (3.1)$$

$$\beta_1 = i \beta_1' \quad (3.2)$$

where  $q_1'$  and  $\beta_1'$  are real quantities are desirable. Further in the matrix table 1

$$\sin \beta_1 \eta = \sin i \beta_1' \eta = i \sinh \beta_1' \eta$$

etc. and  $i$  can be divided from the determinant (2.31), table 1.

The general solution (2.26) may for this case be written as

$$f_{1,n} = A_{1,n} \sinh \alpha_1 y_1/s + A_{2,n}' \sinh \beta_1' y_1/s + A_{3,n} \cosh \alpha_1 y_1/s + A_{4,n} \cosh \beta_1' y_1/s \quad (3.3)$$

where  $\beta_1'$  from (3.2) and  $A_{2,n}'$  are real quantities.

It is easily observed that the determinant (2.31), table 1 for all values of  $\gamma$  and  $\eta$  is zero if  $\beta_1 = 0$ , i.e.  $\xi = 1/\gamma$  and if  $\beta_2 = 0$ , i.e.  $\xi = 1$ . These solutions, however, are without meaning since at, for example,  $\beta_1 = 0$ , the general solution of (2.26) is not:

$$f_{1,n} = A_{1,n} \sinh \alpha_1 y_1/s + A_{3,n} \cosh \alpha_1 y_1/s + A_{4,n}, \quad (3.4)$$

but

$$f_{1,n} = A_{1,n} \sinh \alpha_1 y_1/s + A_{2,n} \frac{y_1}{s} + A_{3,n} \cosh \alpha_1 y_1/s + A_{4,n}. \quad (3.5)$$

In practice, should this occur at a certain combination of  $\gamma$ ,  $\eta$ , the special case can be avoided by slight alterations of the value for  $\gamma$  or  $\eta$ .

The computations were performed on the electronic computer Z.E.B.R.A. of the Nat. Aeronau-

tical Research Institute. The combinations of  $\gamma$ ,  $\eta$ ,  $\lambda$  investigated which delivered indeed a minimum for  $\sqrt{k}$  are given in table 2. For a certain combination  $\gamma$ ,  $\eta$  the minimum value of  $\sqrt{k}$  (as a function of  $\lambda$ ) could be determined with great accuracy but, as is to be expected, not the value of  $\lambda$  at which this minimum, which was sometimes very flat, occurs.

It even turned out that in the region  $\eta = 0.4$ ,  $\gamma = 0.3$  a minimum altered into a maximum (see table 2). In such a region only with very much trouble the wave length could be determined.

Similar difficulties were met in the region  $\eta = 0.2$ ,  $\gamma = 0.5$ . Here it was almost impossible to obtain proper solutions following the procedure just mentioned. These difficulties are, however, of no practical importance.

### 4 Discussion of diagrams.

Fig. 6 and fig. 7 give diagrams as they are drawn from the computed values of table 2. Values of  $\gamma$  only between 0 and 1 are dealt with, but by changing  $t_1$  into  $t_2$  ( $\gamma$  into  $1/\gamma$ ) and  $\eta$  into  $1-\eta$ , values of  $\gamma$  larger than 1 can be met.

For every  $\eta$  there are two branches which (for

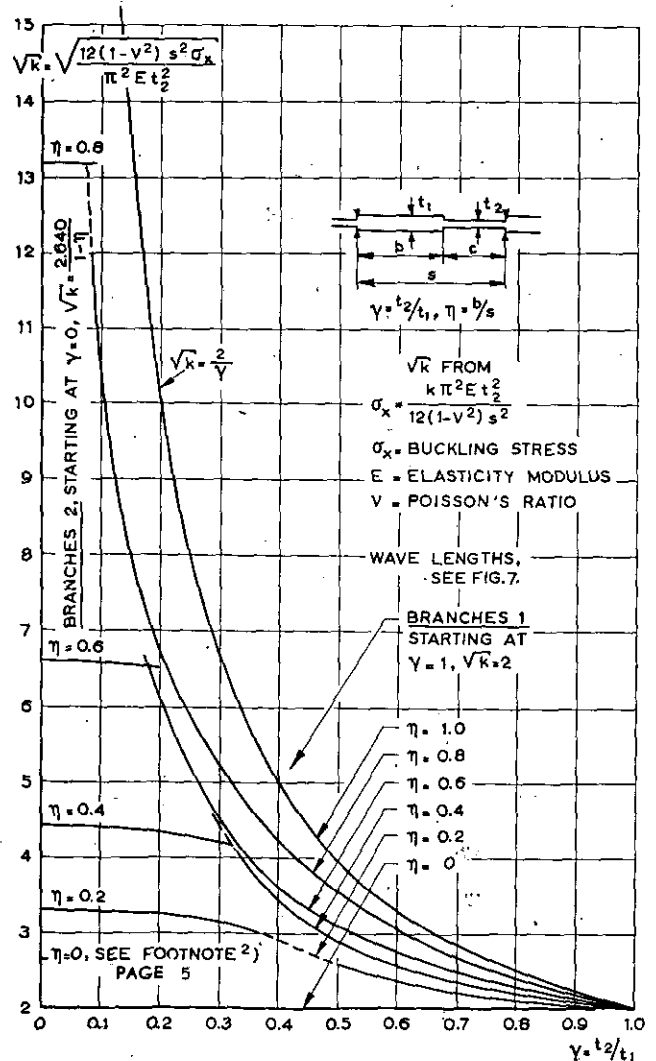


Fig. 6. Results for the buckling stress.

<sup>1)</sup> In the work of CAPEY, ref. 1, the determinant which had to vanish was, due to the symmetry properties of the configuration, only of the 4th order.

$\eta = 0.8, 0.6$  and  $0.4$ ) in fig. 6 intersect. At this intersection belong, however, quite different values for the wavelength (fig. 7).

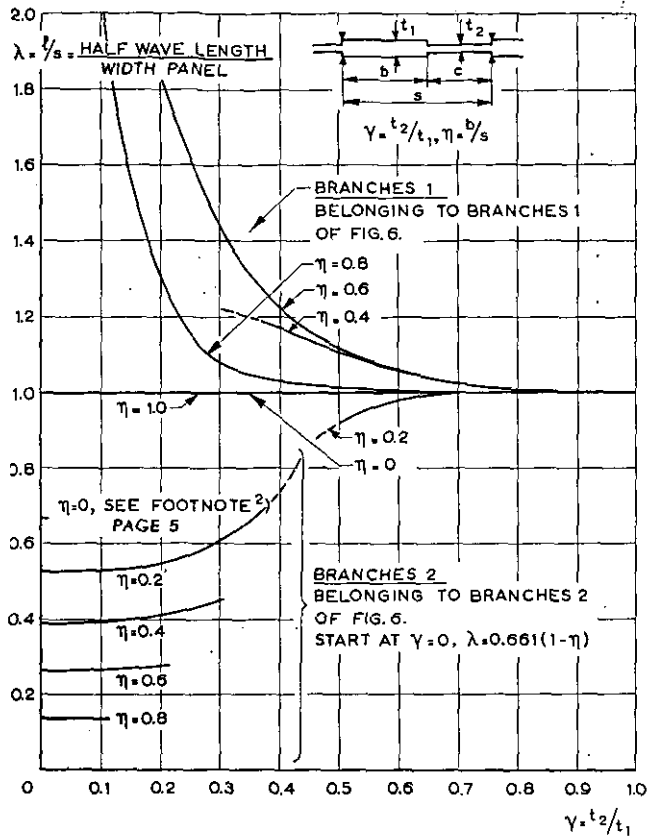


Fig. 7. Wave-lengths.

In fig. 6, the branches 1 all start at  $\gamma = 1$ ,  $\sqrt{k} = 2$ . The branches in this point represent the buckling of simply supported constant thickness panels (or an infinite sequence of such panels).

The branches 2 of fig. 6 start at  $\gamma = 0$  ( $t_1 = \infty$ ),  $\sqrt{k} = 2.640/(1 - \eta)$ , they represent the buckling

of a clamped panel of width  $(1 - \eta)s$  and thickness  $t_2$ . The wavelength is  $0.661(1 - \eta)^{-1}$ .

The branches 2 deliver for  $\gamma = 0$ ,  $\eta = 0$   $\sqrt{k} = 2.640$ . However  $\gamma = \text{finite}$ ,  $\eta = 0$  delivers  $\sqrt{k} = 2^2$ ). Obviously the curves (be it of branches 2, or 1 or both) in the region for very small values of  $\gamma$  and  $\eta$  have strong gradients, but this region, representing dimensions which do not occur in practice, is not further investigated.

#### Acknowledgement.

The author wishes to express his gratitude to Mr. Burgerhout, under whose direction the calculations for the Z.E.B.R.A. electronic computer were programmed and were carried out.

#### 5 References.

1. CAPEY, E. C. The buckling under longitudinal compression of a simply supported panel that changes in thickness across the width. Ministry of Supply, Aeronautical Research Council, C. P. No. 235, London, 1956.
2. V. D. NEUT, A. The local instability of compression members built up from flat plates. Techn. Univ. Delft. Aero. Dept. V. T. H. - 47, Aug. 1952. Also: University Volume on Applied Mechanics dedicated to C. B. Biezeno, Haarlem, 1953.
3. KLIMM, G. Beitrag zur Stabilität dünnwandiger U-Profile mit konstanter Wandstärke im elastischen Bereich. Luftfahrtforschung Bnd 18, S. 155, 1941.
4. HEMP, W. S. and GRIFFEN, K. H. The buckling in compression of panels with square top hat section stringers. Min. of Supply, London, R and M. Rep. no. 2635, 1949. Also: The College of Aeronautics Rep. no. 29, 1949.
5. BENTHEM, J. P. Experiments on the post buckling behaviour of simply supported panels that change in thickness across the bay. N.L.L.-Techn. Memo S. 522, 1958.
6. TIMOSHENKO, S. Theory of elastic stability. McGraw-Hill Book Company, Inc. New York and London, 1936.

<sup>1)</sup> Values for this case of ref. 3 are based on  $\nu = 1/4$ , the present numbers on  $\nu = 0.3$ , which makes only little difference for the wave length.

<sup>2)</sup> Actually the limit of  $\sqrt{k}$  if both  $\eta$  and  $\gamma$  limit to zero remains indeterminate and can only be solved if the quotient  $\eta^c/\gamma$  is constant during the limiting process, where  $\eta^c$  will be a certain (not necessary integral) positive power of  $\eta$ .

## APPENDIX A.

Comparison with semi-empirical values of ref. 5.

$\eta$	$\gamma$	$\sqrt{k}$ from fig. 6	$t_2$ , mm	buckling stress	
				$\sigma_x$	$\sigma_x$ ref. 5
0.2	0.543	2.46	0.978	1.63	1.56
0.2	0.555	2.44	0.973	1.58	1.52
0.4	0.547	2.76	0.982	2.07	2.07
0.4	0.551	2.73	0.977	2.00	2.03
0.2	0.377	2.96	1.003	2.48	2.65
0.2	0.376	2.96	0.995	2.44	2.62
0.4	0.368	3.73	1.005	3.95	3.87
0.4	0.353	3.85	0.975	3.96	3.88

Values of  $\sigma_x$  in kg/mm<sup>2</sup> ( $E = 7000$  kg/mm<sup>2</sup>).

TABLE 1.

Matrix  $U$  occurring in (2.30) and (2.31).

0	0	0	0	0	0	0	0	1	1
0	0	1	1	1	0	0	0	0	0
$-\alpha_1$	$-\beta_1$	0	0	0	$-\alpha_2$	0	$-\beta_2$	0	0
0	0	$-a_1$	$-a_2$	$-a_2$	0	0	0	$-a_3$	$-a_4$
$\sinh \alpha_1 \eta$	$\sin \beta_1 \eta$	$\cosh \alpha_1 \eta$	$\cos \beta_1 \eta$	$\cosh \alpha_1 \eta$	$\sinh \alpha_2 (1 - \eta)$	$\sin \beta_2 (1 - \eta)$	$\sin \beta_2 (1 - \eta)$	$-\cosh \alpha_2 (1 - \eta)$	$-\cos \beta_2 (1 - \eta)$
$p_1 \cosh \alpha_1 \eta$	$q_1 \cos \beta_1 \eta$	$p_1 \sinh \alpha_1 \eta$	$-q_1 \sin \beta_1 \eta$	$p_1 \sinh \alpha_1 \eta$	$-p_2 \cosh \alpha_2 (1 - \eta)$	$-q_2 \cos \beta_2 (1 - \eta)$	$-q_2 \cos \beta_2 (1 - \eta)$	$p_2 \sinh \alpha_2 (1 - \eta)$	$-q_2 \sin \beta_2 (1 - \eta)$
$a_1 \sinh \alpha_1 \eta$	$a_2 \sin \beta_1 \eta$	$a_1 \cosh \alpha_1 \eta$	$a_2 \cos \beta_1 \eta$	$a_1 \cosh \alpha_1 \eta$	$a_3 \sinh \alpha_2 (1 - \eta)$	$a_4 \sin \beta_2 (1 - \eta)$	$a_4 \sin \beta_2 (1 - \eta)$	$-a_3 \cosh \alpha_2 (1 - \eta)$	$-a_4 \cos \beta_2 (1 - \eta)$
$-p_1 a_2 \cosh \alpha_1 \eta$	$-q_1 a_1 \cos \beta_1 \eta$	$-p_1 a_2 \sinh \alpha_1 \eta$	$q_1 a_1 \sin \beta_1 \eta$	$-p_1 a_2 \sinh \alpha_1 \eta$	$p_2 a_4 \cosh \alpha_2 (1 - \eta)$	$q_2 a_3 \cos \beta_2 (1 - \eta)$	$q_2 a_3 \cos \beta_2 (1 - \eta)$	$-p_2 a_4 \sinh \alpha_2 (1 - \eta)$	$q_2 a_3 \sin \beta_2 (1 - \eta)$

$$\alpha_1 = \pi p_1 / \lambda$$

$$\beta_1 = \pi q_1 / \lambda$$

$$\alpha_2 = \pi p_2 / \lambda$$

$$\beta_2 = \pi q_2 / \lambda$$

$$p_1 = \sqrt{\gamma \xi + 1}$$

$$p_2 = \sqrt{\xi + 1}$$

$$q_1 = \sqrt{\gamma \xi - 1}$$

$$q_2 = \sqrt{\xi - 1}$$

$$a_1 = \gamma \xi + 1 - \nu$$

$$a_2 = -\gamma \xi + 1 - \nu$$

$$a_3 = \gamma^3 (\xi + 1 - \nu)$$

$$a_4 = \gamma^3 (-\xi + 1 - \nu)$$

$$\nu = 0.3$$

TABLE 2.

Computed minima for  $\sqrt{k}$  (diagrams fig. 6 and fig. 7).

$\eta$	$\gamma$	$\lambda$	$\sqrt{k}$
0.2	1.0	1	2
0.2	0.8	1.00	2.11585
0.2	0.6	0.985	2.3647
0.2	0.5	0.922	2.5958
0.2	0.4	0.7485	2.904
0.2	0.3	0.605	3.138
0.2	0.2	0.546	3.255
0.2	0.01 <sup>1)</sup>	0.5288	3.30
0.4	1.0	1	2
0.4	0.8	1.009	2.20596
0.4	0.6	1.05	2.5792
0.4	0.5	1.099	2.9110
0.4	0.42	1.153	3.3233
0.4	0.4	1.169	3.458
0.4	0.38	1.183	3.6098
0.4	0.34	1.20	3.9753
0.4	0.3	1.22	4.4851
0.4	0.3	1.079	4.44578
0.4	0.3	0.450	4.215
0.4	0.2	0.407	4.3530
0.4	0.01	0.3966	4.40
0.6	1.0	1	2
0.6	0.8	1.01	2.29699
0.6	0.6	1.05	2.7684
0.6	0.4	1.22	3.626
0.6	0.2	1.842	6.095
0.6	0.2	0.2705	6.534
0.6	0.01	0.2644	6.61
0.8	1.0	1	2
0.8	0.8	1.00	2.4028
0.8	0.6	1.005	3.07102
0.8	0.4	1.030	4.25962
0.8	0.2	1.295	6.699
0.8	0.1	2.06	10.49
0.8	0.01	0.1322	13.20

maximum

<sup>1)</sup> Values  $\gamma = 0.01$  give practically the same result as  $\gamma = 0$  and are used because the programme of the calculations did not allow  $\gamma$  being zero.

## REPORT S. 529.

## Airplane Loads in Pitching Manoeuvres

by

B. HAKKELING.

## Summary.

In the present structural airworthiness requirements the pitching manoeuvres are formulated in a rather vague and unsatisfactory way.

In order to obtain an impression of the value of these requirements and to introduce possible improvements, calculations were performed on the tail loads, load factors, and stick forces of two transport airplanes of different sizes in longitudinal manoeuvres.

The starting-point was a prescribed elevator motion; a deflection-time history as an unequal-sided triangle has been chosen as an approximation of actual elevator motions. Two parameters were varied: the time in which the elevator reaches its maximum deflection and the time in which the elevator returns to its initial position.

In addition, the effects of location of centre of gravity, airplane weight and moment of inertia on the tail loads, were determined.

The results of the computations for the two airplanes of quite different sizes are analogous in most respects.

## Contents.

List of symbols.
1 Introduction.
2 Assumptions.
3 Derivation of equations.
3.1 Airplane response.
3.1.1 Increment of aerodynamic tail load.
3.1.2 Load factor.
3.1.3 Pitching acceleration.
3.1.4 Increment of total tail load.
3.2 Stick force.
4 Numerical data.
5 Results.
5.1 Introduction.
5.2 Variation of the centre of gravity (other parameters constant).
5.3 Variation of airplane weight (other parameters constant).
5.4 Variation of moment of inertia (other parameters constant).
5.5 Combined variation of centre of gravity, weight and moment of inertia.
5.6 Variation of elevator deflection-time history.
5.6.1 Variation of $k = \frac{\tau_2}{\tau_1}$ .
5.6.2 Variation of the control time $\tau_1$ .
5.7 Discussion.
6 Conclusions.
7 References.
Appendix A. The coefficients $K_i'$ of equation (8).
Appendix B. The coefficients of equation (14).
Appendix C. Stick force required to balance bob-weight.
2 Tables.
44 Figures.

## List of symbols.

$a$	$= b_1 \alpha_t + b_2 \delta$ .
$b$	wing span.
$b_t$	span of horizontal tail.
$b_1$	$= \frac{dC_H}{d\alpha_t}$ .
$b_2$	$= \frac{dC_H}{d\delta}$ .
$b_3$	$= \frac{dC_H}{d\delta_t}$ .
$c$	chord.
$g$	acceleration of gravity.
$h$	distance between aerodynamic centre without tail and centre of gravity.
$k$	$= \frac{\tau_2}{\tau_1} = \frac{t_2}{t_1}$ (fig. 1).
$k_y$	radius of gyration with respect to $y$ -axis.
$m$	airplane mass.
$m_c$	$= \frac{F}{H}$ .
$n$	airplane load factor.
$q$	dynamic pressure.
$t$	time.
$t_1$	time in which the elevator reaches its maximum deflection.
$t_2$	time in which the elevator returns to neutral.
$x_t$	distance between centre of gravity of airplane and aerodynamic centre of tail (negative for conventional airplanes).
$C$	spring constant of spring tab (eq. (20)).
$C_L$	lift coefficient.
$C_M$	pitching moment coefficient of airplane without tail with respect to aerodynamic centre.
$C_{MCG}$	pitching moment coefficient of airplane

without tail with respect to centre of gravity.

$F$  stick force.

$F_{bw}$  stick force required to balance bobweight alone.

$F_1$  largest stick force at which spring tab will not deflect.

$H$  hinge moment of elevator.

$I$  moment of inertia with respect to  $y$ -axis.

$I'$   $= Ig$ .

$K$  empirical constant denoting ratio of damping moment of complete airplane to damping moment of tail alone.

$K_i$  coefficients of eq. (6).

$K_i'$  coefficients of eq. (8).

$L$  lift on tail.

$L_1$  first maximum of tail load including balancing load.

$L_2$  second maximum of tail load including balancing load.

$L_{2\max}$  maximum of  $(L_2)$  as a function of  $k$ .

$L_{bal.}$  balancing tail load in level flight condition

$\Delta L_1$  first maximum of incremental tail load due to a manoeuvre (fig. 5).

$\Delta L_2$  second maximum of incremental tail load due to a manoeuvre (fig. 5).

$\Delta L_{2\max}$  maximum of  $\Delta L_2$  as a function of  $k$ .

$M$  pitching moment of airplane without tail with respect to aerodynamic centre.

$M_{CG}$  pitching moment of airplane without tail with respect to centre of gravity.

$S$  wing area.

$S_t$  area of horizontal tail.

$S_e$  area of elevator behind hinge line.

$\Delta S_1$  first maximum of tail load (including inertia loadings) due to a manoeuvre.

$\Delta S_2$  second maximum of tail load (including inertia loadings) due to a manoeuvre.

$V$  airspeed.

$V_A$  design manoeuvring speed.

$V_C$  design cruising speed.

$V_D$  design dive speed.

$W$  airplane weight.

$W_t$  weight of horizontal tail.

$\alpha$  wing angle of attack.

$\gamma$  flight-path angle.

$\delta$  elevator deflection from trimmed configuration.

$\hat{\delta}$  maximum elevator deflection during a manoeuvre.

$\delta_{\max}$  maximum possible elevator deflection (elevator against its stop).

$\delta_t$  spring tab deflection.

$\epsilon$  downwash angle.

$\eta$  ratio of dynamic head at tail to dynamic head at wing.

$\theta$  angle of pitch.

$\lambda$  coefficient used in fig. 3.

$\rho$  mass density of air.

$\tau$  aerodynamic time (dimensionless, eq. (7)).

$\tau_1$  dimensionless time in which the elevator reaches its maximum deflection.

$\tau_2$  dimensionless time in which the elevator returns to neutral.

$\omega$  frequency of airplane pitching oscillation (eq. (11)).

$\Delta$  means an increment of a quantity from the unaccelerated flight condition due to a manoeuvre.

$\phi_i$  coefficients of eq. (14); see appendix B.

$\psi$  coefficients of eq. (14); see appendix B.

### Subscripts:

max maximum value.

$t$  tail, except  $\delta_t$ .

$w$  wing.

$e$  elevator.

1, 2 denote first and second maximum respectively.

The notations  $\alpha, \ddot{\alpha}$  etc. denote single and double differentiations with respect to  $\tau$ .

The notations  $\bar{\alpha}, \bar{\alpha}$  denote the results of superposition referred to in par. 3.1.

### 1 Introduction.

In order to judge the present structural airworthiness requirements concerning pitching manoeuvres on their merits and to have a starting-point for possible improvements, the knowledge of airplane accelerations and tail-loads due to different types of elevator movements is needed.

The problem of determining dynamic tail loads in a rational way has been treated by many authors (e.g. bibliography of ref. 1), but most approaches have other aims.

In the present work particular attention has been devoted to the variation of airplane normal acceleration and tail load as a function of:

- location of the centre of gravity.
- airplane weight.
- airplane moment of inertia.
- the shape of the elevator deflection-time history.

In all cases the elevator deflection as a function of time is assumed to be triangular and in case  $d$  two parameters are varied: the "control time"  $t_1$  (the time in which the elevator has reached its maximum deflection) and the ratio  $k = t_2/t_1$  (see fig. 1).

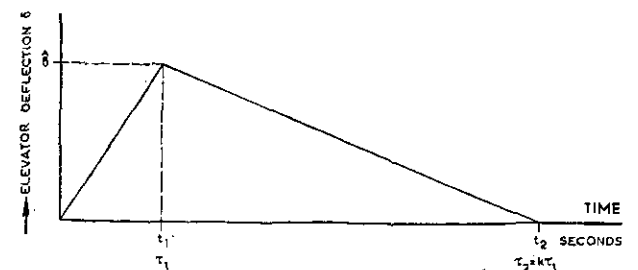


Fig. 1. Assumed shape of elevator deflection-time history.

Account was taken of the control force, required to apply the assumed elevator-deflection history of fig. 1.

In order to gain an insight into the behaviour

of airplanes of different sizes the computations were performed for two types:

Airplane A, a twin-engined light transport, design take-off weight 15,500 kg (34,170 lb); control column directly connected with elevator, no mechanical or aerodynamic servo-system.

Airplane B, a four engine medium transport, design take-off weight 48,081 kg (106,000 lb); elevator control system provided with a spring tab.

The numerical data used in the computations were derived from reports on two airplanes of the above-mentioned types.

The research reported in this paper was carried out under contract with the "Netherlands Civil Aviation Department" upon a recommendation made by the "Netherlands Committee for Structural Strength Requirements for Civil Aircraft". Although some preliminary remarks have been made with regard to existing airworthiness requirements, no particular attention has yet been given to the desirability of revising such requirements in view of the results of the present work and other recent investigations (e.g. ref. 6). This matter will form the subject of further study by the said committee.

## 2 Assumptions.

2.1 The general problem of the response to longitudinal control involves the solution of three simultaneous differential equations (e.g. chapter 10 of ref. 2). The variables in these equations are the airplane velocity  $V$ , pitch angle  $\theta$  and angle of attack  $\alpha$ . The solution gives a very slow oscillation (phugoid mode) with poor damping of the speed  $V$ , pitch angle  $\theta$  (each with relatively large amplitudes) and angle of attack (small amplitude).

Another oscillation with a short period and heavy damping involves mainly the change in angle of attack. During this short period mode, the change in airspeed is very small and the assumption of constant airspeed for a study of the initial response is justified.

The accuracy achieved in this way is reasonable for structural design purposes and depends largely on the achievable accuracy in determining the stability derivatives.

2.2 It is assumed that the initial change of the pitch angle is very small; therefore the change of the component of weight perpendicular to the flight-path has been neglected.

2.3 The calculated stick forces balance the aerodynamic hinge moments only. Stick forces due to angular acceleration of the elevator, down springs and bobweights of the control system, are not taken into account. The control system is assumed to be frictionless and its components to be rigid. The influence of the rotational inertia of the elevator may become important at very large rates of increase of the stick force; in such cases a springtab will deflect first and the elevator deflection can have a considerable lag.

2.4. Aeroelastic effects are neglected (*rigid airplane*).

2.5 The variation of the downwash angle due to engine slipstream effects during the manoeuvre is neglected.

2.6 The aerodynamic derivatives are assumed to be constant during the manoeuvre.

2.7 Aerodynamic lag is neglected.

Some remarks on the limitations imposed by these simplifying assumptions can be found in sec. 4 of ref. 7.

## 3 Derivation of equations.

According to the assumption of constant speed during the initial response to elevator deflection, one of the three differential equations can be eliminated. The remaining two equations refer to equilibrium of forces in vertical direction and equilibrium of moments with respect to the centre of gravity.

In fig. 2 the adopted axes, sign conventions and positive directions are shown.

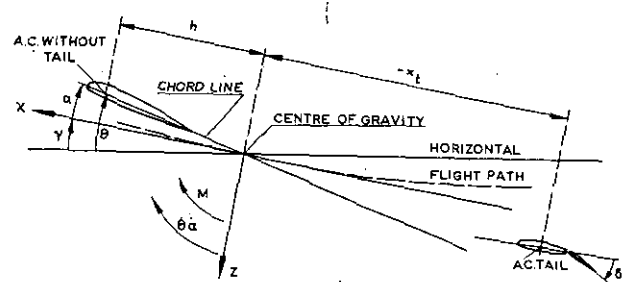


Fig. 2. Adopted axes and positive directions.

In the following the words "force", "angle" etc. mean the variation of these quantities from the values in unaccelerated symmetrical flight; thus  $\Delta\alpha$  is abbreviated to  $\alpha$  (etc.), where  $\Delta\alpha$  is the variation from the initial value. Assuming that there is no loss in speed, summation of forces along the Z-axis gives:

$$m \frac{d\gamma}{dt} V - \frac{dC_L}{d\alpha} aqS - \left( \frac{dC_L}{d\delta} \right)_t \delta\eta q S_t + \left( \frac{dC_L}{d\alpha} \right)_t \frac{d\theta}{dt} \frac{x_t}{V} \frac{1}{\eta} \eta q S_t - \left( \frac{dC_L}{d\alpha} \right)_t \frac{d\alpha}{dt} \frac{(-x_t + h)}{V} \frac{d\epsilon}{d\alpha} \eta q S_t = 0. \quad (1)$$

The first term on the left-hand side represents the mass force. The second term gives the aerodynamic force of the airplane with undeflected elevator, which can be written as:

$$\frac{dC_L}{d\alpha} aqS = \left\{ \left( \frac{dC_L}{d\alpha} \right)_w + \left( \frac{dC_L}{d\alpha} \right)_t \frac{S_t}{S} \left( 1 - \frac{d\epsilon}{d\alpha} \right) \eta \right\} aqS \quad (2)$$

where  $\left( \frac{dC_L}{d\alpha} \right)_w$  refers to the airplane without tail.

The next terms are the force due to elevator deflection, pitching velocity effect of the tailplane and the effect of time lag in downwash at the tail, respectively.

The moment equation is:

$$\begin{aligned} & \left( \frac{dC_L}{d\alpha} \right)_w \alpha q h S + \left( \frac{dC_L}{d\alpha} \right)_t \alpha \eta q S_t \left( 1 - \frac{d\varepsilon}{d\alpha} \right) x_t + \\ & + \left( \frac{dC_L}{d\alpha} \right)_t \frac{d\alpha}{dt} \frac{(-x_t + h)}{V} \frac{d\varepsilon}{d\alpha} \eta q S_t x_t - \\ & - \left( \frac{dC_L}{d\alpha} \right)_t \frac{d\theta}{dt} \frac{x_t}{V} K \sqrt{\eta} q S_t x_t + \\ & + \left( \frac{dC_L}{d\alpha} \right)_t \left( \frac{d\alpha}{d\delta} \right)_t \delta \eta q S_t x_t + \\ & + \left( \frac{dC_M}{d\delta} \right)_t \eta q \frac{S_t^2}{b_t} \delta - m k_v^2 \frac{d^2\theta}{dt^2} = 0. \quad (3) \end{aligned}$$

The first term refers to the pitching moment of the airplane without tail with respect to the centre of gravity:

$$\begin{aligned} M_{CG} &= -\frac{dC_{M_{CG}}}{d\alpha} \cdot \alpha q \frac{S^2}{b} = \left[ \frac{hb}{S} \left( \frac{dC_L}{d\alpha} \right)_w \right] \alpha q \frac{S^2}{b} = \\ &= \left( \frac{dC_L}{d\alpha} \right)_w \alpha q h S \quad (4) \end{aligned}$$

where  $h$  is the distance from the aerodynamic centre of the airplane without tail to the centre of gravity.

The third term represents a correction for the time lag effect in the downwash angle at the tail. The factor  $K$  in the fourth term denotes the ratio of damping moment of the complete airplane to the damping moment due to the tail alone. The meaning of the remaining terms will be evident.

With the aid of the relation (fig. 2)

$$\theta = \alpha + \gamma \quad (5)$$

it is possible to eliminate  $\gamma$  and  $\theta$  from the equations (1), (3) and (5), which yields an equation of the form

$$\frac{d^2\alpha}{dt^2} + K_1 \frac{d\alpha}{dt} + K_2 \alpha = K_3 \delta + K_4 \frac{d\delta}{dt} \quad (6)$$

The coefficients  $K_i$  in this equation for a (damped) oscillation contain the speed  $V$ . In order to reduce computational work it is convenient to introduce a nondimensional time  $\tau$ , originally suggested by GLAUERT:

$$\tau = \frac{\rho g S V}{W} t. \quad (7)$$

With  $\tau$  as a new independent variable equation (6) can be rewritten:

$$\ddot{\alpha} + K_1' \dot{\alpha} + K_2' \alpha = K_3' \delta + K_4' \dot{\delta} \quad (8)$$

where the dots denote differentiations with respect to  $\tau$  (cf. ref. 3).

The coefficients  $K_i'$  of eq. (8) are independent of speed and contain aerodynamic and geometric constants ( $K_i'$  are written out in appendix A, cf. ref. 4).

The possibility of neglecting the part  $K_4' \dot{\delta}$  of

the forcing function in eq. (8) is considered in ref. 4; it appears that this part is in general negligible, except in the case of a very fast elevator deflection.

Starting from the forcing function  $K_3' \delta(\tau)$  (neglecting  $K_4' \dot{\delta}$ ) shaped as an unequal-sided triangle (see  $\delta(\tau)$  in fig. 1), the response of the airplane as well as the stick force required to perform this prescribed elevator motion can be determined.

### 3.1 Airplane response.

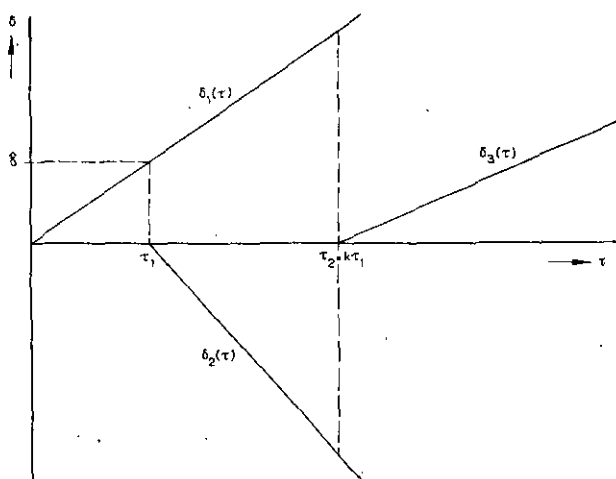
Since the equation

$$\ddot{\alpha} + K_1' \dot{\alpha} + K_2' \alpha = K_3' \delta(\tau) \quad (9)$$

(with  $\delta(\tau)$  according to fig. 1) is linear, the solution can be obtained by superposition of the solutions of three similar equations

$$\ddot{\alpha} + K_1' \dot{\alpha} + K_2' \alpha = K_3' \delta_i(\tau) \quad (i = 1, 2, 3) \quad (10)$$

each with a forcing function  $K_2' \delta_i(\tau) = \lambda K_2' \frac{\hat{\delta}}{\tau_1} \tau$ ; the meaning of  $\lambda$  is explained in fig. 3.



Superposition of  $\delta_1(\tau)$ ,  $\delta_2(\tau)$  and  $\delta_3(\tau)$  gives  $\delta(\tau)$  of fig. 1.

$$\delta_1(\tau) = \frac{\hat{\delta}}{\tau_1} \tau \quad \rightarrow \lambda = 1$$

$$\delta_2(\tau) = \frac{\hat{\delta}}{\tau_1} \frac{k}{k-1} (\tau - \tau_1) \quad \rightarrow \lambda = \frac{-k}{k-1} \quad (\tau < \tau_1, \delta_2(\tau) \equiv 0)$$

$$\delta_3(\tau) = \frac{\hat{\delta}}{k-1} \left[ \frac{\tau}{\tau_1} - k \right] \quad \rightarrow \lambda = \frac{1}{k-1} \quad (\tau < \tau_2, \delta_3(\tau) \equiv 0)$$

$K_3' \delta_i(\tau)$  are the forcing functions of the three equations (10).

Fig. 3. The component parts  $\delta_i(\tau)$  of the elevator motion of fig. 1.

In practice this superposition is performed by superimposing the response of the airplane due to  $\delta_2(\tau)$  for  $\tau \geq \tau_1$  on that due to  $\delta_1(\tau)$ ; the response due to  $\delta_3(\tau)$  is superimposed for  $\tau \geq \tau_2$ .

The above-mentioned responses are obtained from the solution of (9) with  $\delta(\tau) = \frac{\hat{\delta}}{\tau_1} \tau$  and the initial conditions  $\tau = 0 \rightarrow \alpha = \dot{\alpha} = 0$  (unaccelerated flight), which can be shown to be

$$\alpha = \frac{K_3'}{K_2'} \frac{\hat{\delta}}{\tau_1} \left[ \tau - \frac{K_1'}{K_2'} + e^{-\frac{K_1'}{2}\tau} \left\{ \frac{K_1'}{K_2'} \cos \omega\tau + \frac{K_1'^2 - 2K_2'}{2\omega K_2'} \sin \omega\tau \right\} \right] \quad (11)$$

where

$$\omega = + \sqrt{K_2' - \left(\frac{K_1'}{2}\right)^2}$$

Hence:

$$\dot{\alpha} = \frac{K_3'}{K_2'} \frac{\hat{\delta}}{\tau_1} \left[ 1 - e^{-\frac{K_1'}{2}\tau} \right] \cos \omega\tau + \frac{K_1'}{2\omega} \sin \omega\tau \quad (12)$$

and

$$\ddot{\alpha} = \frac{K_3'}{\omega} \frac{\hat{\delta}}{\tau_1} e^{-\frac{K_1'}{2}\tau} \sin \omega\tau.$$

The results of the superposition referred to above will be denoted by  $\bar{\alpha}$ ,  $\bar{\alpha}$ , etc.

### 3.1.1 Increment of aerodynamic tail load.

The increment of the angle of attack of the tailplane due to downwash, pitching velocity and elevator deflection can be written

$$\alpha_t = \alpha \left( 1 - \frac{d\varepsilon}{d\alpha} \right) + \frac{(-x_t + h)}{V} \frac{d\alpha}{dt} \frac{d\varepsilon}{d\alpha} - \frac{x_t}{V} \frac{d\theta}{dt} + \left( \frac{d\alpha}{d\delta} \right)_t \delta. \quad (13)$$

Substituting  $\frac{d\theta}{dt}$  from (1) and (5) in (13) and inserting  $\alpha_t$  in the equation of the increment of the tail load  $\Delta L$  (positive downwards),

$$\Delta L = - \left( \frac{dC_L}{d\alpha} \right)_t \alpha_t \eta q S_t$$

this tail load increment becomes:

$$\Delta L = \psi [\phi_1 \bar{\alpha} + \phi_2 \bar{\alpha} + \phi_3 \delta]. \quad (14)$$

The coefficients  $\psi$  and  $\phi_i$  are written out in Appendix B.

### 3.1.2 Load factor.

The airplane load factor  $\Delta n$  can be computed from  $\bar{\alpha}$  and  $\Delta L$

$$\Delta n = \alpha \left( \frac{dC_L}{d\alpha} \right)_w \frac{\rho V^2 S}{2W} - \frac{\Delta L}{W}. \quad (15)$$

### 3.1.3 Pitching acceleration.

The pitching acceleration  $\frac{d^2\theta}{dt^2}$  can be expressed in terms of  $\bar{\alpha}$  and  $\bar{\alpha}$  by eliminating  $\gamma$  from (1) and (5)

$$\frac{d^2\theta}{dt^2} = \frac{\left( \frac{\rho g S V}{W} \right)^2}{1 + \left( \frac{dC_L}{d\alpha} \right)_t x_t \sqrt{\frac{\rho g S_t}{2W}}} \left[ \left\{ 1 + \left( \frac{dC_L}{d\alpha} \right)_t (-x_t + h) \frac{d\varepsilon}{d\alpha} \eta \frac{\rho g S_t}{2W} \right\} \bar{\alpha} + \frac{1}{2} \left\{ \left( \frac{dC_L}{d\alpha} \right)_w + \left( \frac{dC_L}{d\alpha} \right)_t \left( 1 - \frac{d\varepsilon}{d\alpha} \right) \eta \frac{S_t}{S} \right\} \bar{\alpha} \right]. \quad (16)$$

### 3.1.4 Increment of total tail load.

The increment of the total load of the tail  $\Delta S$  (positive downwards) is composed of the aerodynamic load increment  $\Delta L$  (eq. 14) and inertia components due to pitching acceleration and load factor increment:

$$\Delta S = \Delta L + x_t \frac{d^2\theta}{dt^2} \frac{W_t}{g} + \Delta n W_t \quad (17)$$

where  $W_t$  is the weight of the tail plane.

### 3.2 Stick force.

In this report only the stick force required to balance the aerodynamic hinge moment during the prescribed elevator motion (fig. 1) will be considered.

The general expression for the increment of the stick force  $F$  (from the trimmed configuration) is:

$$F = m_e q S_e c_e (b_1 \alpha_t + b_2 \delta + b_3 \delta_t) \quad (18)$$

where  $q S_e c_e (b_1 \alpha_t + b_2 \delta + b_3 \delta_t)$  is the hinge moment.

In the case of airplane A (see chapter 1) the control column is directly connected with the elevator and no spring tab or servo tab are fitted. In this case the "aerodynamic" stick force becomes

$$F = m_e q S_e c_e (b_1 \alpha_t + b_2 \delta). \quad (19)$$

The elevator of airplane B is fitted with a spring tab (fig. 4). Up to a stick force  $F_1$  the tab will

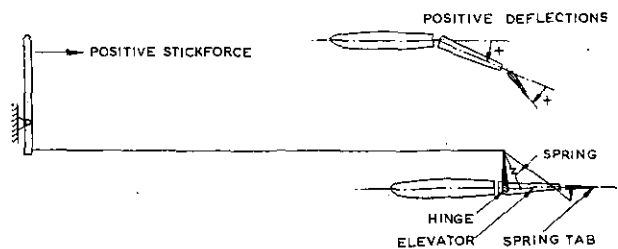


Fig. 4. Schematic diagram of a spring tab; positive deflections.

not deflect due to preloading of the spring. If  $F > F_1$  the tab deflection with respect to the elevator is a function of the stick force alone (neglecting the hinge moment of the tab itself):

$$\delta_t = C(F - F_1) \quad F_1 > 0 \quad (20)$$

where  $C$  is a spring constant. Substitution of (20) into (18) gives the stick force in the case of a deflected spring tab (equation (22)).

Finally, if the tab reaches its maximum deflection  $\delta_{t_{\max}}$ , the elevator acts as a control surface with a deflected trimtab.

Summarizing, the undermentioned equations are valid in the three ranges ( $F \geq -F_1$ )

$$F = m_e q S_e c_e (b_1 \alpha_t + b_2 \delta) - F_1 \leq F \leq F_1 \quad (21)$$

(tab undeflected)

$$F = \frac{m_e q S_e c_e (b_1 \alpha_t + b_2 \delta - b_3 C F_1)}{1 - m_e q C S_e c_e b_3} F \geq F_1 \quad (22)$$

(tab deflected)  $\delta_t < \delta_{t_{\max}}$

$$F = m_e q S_e c_e (b_1 \alpha_t + b_2 \delta + b_3 \delta_{t_{\max}}),$$

$$\delta_t = \delta_{t_{\max}} \quad (23)$$

(constant tab deflection)

In the case of negative stick forces and  $F < -F_1$  equation (20) becomes

$$\delta_t = C (F + F_1) \quad (20')$$

and the required stick force with deflected spring tab is

$$F = \frac{m_e q S_e c_e (b_1 \alpha_t + b_2 \delta + b_3 C F_1)}{1 - m_e q C S_e c_e b_3} F < -F_1$$

$$|\delta_t| < |\delta_{t_{\min}}| \quad (22')$$

or (maximum negative tab deflection)

$$F = m_e q S_e c_e (b_1 \alpha_t + b_2 \delta - b_3 |\delta_{t_{\min}}|)$$

$$\delta_t = \delta_{t_{\min}} \quad (23')$$

#### 4 Numerical data.

The data of airplanes A and B, used in the computations, are compiled in table 1.\*

All manoeuvres have been calculated for sea-level air density at the design manoeuvring speed  $V_A$ , the design cruising speed  $V_C$  and the design dive speed  $V_D$ .

In all cases the elevator will be deflected upwards ( $\delta$  negative) introducing a pull-up of the aircraft; downward elevator deflection changes all signs of the load increments.

### 5 Results.

#### 5.1 Introduction.

In order to facilitate the understanding of the results, the airplane loads, pitching acceleration and required stick force as a function of time are given in an arbitrary case in figs. 5 and 6; this case is a checked manoeuvre with airplane B and  $k=5$  (fig. 1) at speed  $V_C$ .

It appears, that both the increment of the aerodynamic tail load and the increment of the total tail load have two extreme values.

The first extreme value is called *the first maximum* ( $\Delta L_1$ ) of the tail load. This maximum occurs in many cases at the instant of maximum elevator deflection, but at high speed and/or large  $\tau_1$  this first maximum occurs earlier.

This first maximum arises as a result of the downward load due to the deflected elevator and the increasing upward load due to increment of the angle of attack of the tail.

After the elevator has reached its maximum deflection, the effect of the increasing angle of attack of the tail  $\alpha_t$  is dominant, hence  $\Delta L$  decreases and changes sign ( $\tau \approx 0,28$  in fig. 5).

After  $\Delta L$  has reversed its direction the angle of attack of the tail reaches a maximum (in the example of fig. 5 at  $\tau \approx 0,42$ ) and its upward effect has a maximum at that time. Due to the fact that the other component (a downward load as a result of elevator deflection) is still decreasing, an extreme value of the resulting aerodynamic tail load  $\Delta L$ , however, occurs at a later moment. This extreme value will be called *the second maximum* ( $\Delta L_2$ ).

It should be emphasized that the character of the tail plane load at the moments of the first and second maximum is quite different. At the first maximum the elevator is deflected (aft centre of pressure) and at the second maximum the elevator deflection is considerably decreased or zero. In the latter case the loading is comparable with a gust loading.

The total load increment  $\Delta S$  differs from  $\Delta L$  due to mass loads (eq. 17). The maximum values  $\Delta S_1$  and  $\Delta S_2$  (fig. 5) are in all cases smaller than the corresponding values  $\Delta L_1$  and  $\Delta L_2$ .

The computed stick force  $F$  (fig. 6) required to produce the prescribed elevator deflection-time history of fig. 5 is *related to the aerodynamic hinge moment only*; so the computed stick force does not contain the force required to balance the moment due to rotational acceleration of the elevator, mass accelerations of parts of the control system, possible downsprings and bobweights. Such additional parts of the stick force can increase the computed one considerably.

In the case of airplane A (control column directly connected with elevator) the shape of the stick force-time history is the same as the shape of the assumed  $\delta - t$  diagram, as the coefficient  $b_1 = 0$  (table 1, eq. (19)).

Airplane B, however, is fitted with a spring tab; up to a stick force  $F_1 = 7.6$  kg the tab is not deflected and the stick force-deflection ratio is large. If the spring tab deflects ( $F > F_1$ ), this ratio decreases considerably.

Eqs. (21) and (22) can be rewritten

$$F = Aa \quad (24)$$

and

$$F = B(a + D) \quad (25)$$

respectively, where  $a = b_1 \alpha_t + b_2 \delta$  and  $A$ ,  $B$  and  $D$  are constants,  $A \gg B$ .

The two components of  $a$  are given schematically as function of time in fig. 7a and  $a$  itself in fig. 7b. The known preload  $F_1$  determines the

\* The moment of inertia  $I$  ( $\text{kg m sec}^2$ ) is given in terms of  $I' = I g$  ( $\text{kg m}^2$ ), so that  $k_y^2 = \frac{I'}{W}$  ( $\text{m}^2$ ).

value  $a = a_{F_1}$  at which eq. (24) ceases to be valid and in this way the  $F - \tau$  diagram of fig. 7c and fig. 6 can be constructed.

In the graphs in this report sometimes large values of  $\Delta n_{\max}$  occur. In fact, the value of  $\Delta n_{\max}$  is limited by *stalling of the airplane*. In many graphs this "stalling limit" is indicated; the airplane response beyond this limit has to be reduced to this additional  $\Delta n_{\max}$ -limitation. The computed "stalling limit" is based on the static  $C_{L_{\max}}$  but in fast manoeuvres the dynamic  $C_{L_{\max}}$  can increase this stalling limit.

### 5.2 Variation of the centre of gravity (other parameters constant).

A checked manoeuvre with both airplane types has been investigated where the location of the centre of gravity varied in the ranges indicated in table 1. In all cases  $k=2$  and  $t_1=0.3$  sec.

The values of  $\Delta L_1$ ,  $\Delta L_2$  and  $\Delta n$  as functions of the centre of gravity location with  $\hat{\delta} = -0.436$  rad (fig. 1), or a maximum deflection such that the maximum stick force does not exceed a chosen value of 100 kg, are given in figures 8 and 9. The said manoeuvre was investigated, because it was desired to calculate the behaviour of the airplanes when no account is taken of a  $\Delta n$ -limitation. The results may give an impression of the action the pilot might take in an emergency condition and this manoeuvre has therefore been called an "emergency manoeuvre". In the airworthiness requirements it is assumed that the pilot will be able to restrict the load factor to the value corresponding to manoeuvring limit load:  $n=2.5$ . Therefore, the results of the computations were also reduced to  $\Delta n_{\max} = 1.5$  this manoeuvre being called a "normal manoeuvre". In figures 10 and 11 the loads in these manoeuvres are given.

The effect of centre of gravity variation for equal elevator deflections ( $\hat{\delta} = \delta_{\max}$  or  $F_{\max} = 100$  kg) on the first maximum is small (figs. 8 and 9); in the case of equal  $\Delta n_{\max}$  (figs. 10 and 11) the effect is somewhat larger and a forward centre of gravity yields the largest  $\Delta L$ , except at speed  $V_A$ .

In all cases the largest second maximum  $\Delta L_2$  appears at an aft centre of gravity.

The value of the acceleration increment  $\Delta n_{\max}$  due to checked manoeuvres with equal elevator deflection ( $\hat{\delta} = \delta_{\max}$  or  $F_{\max} = 100$  kg) increases with a rearward shift of the centre of gravity.

### 5.3 Variation of airplane weight (other parameters constant).

The effect of airplane weight is investigated by means of a checked manoeuvre with both airplane types ( $k=2$ ) and weights as specified in table 1. As in par. 5.2 the manoeuvre is performed by means of a maximum elevator deflection  $\hat{\delta} = \delta_{\max}$  or, if the required stick force exceeds 100 kg, a deflection such that  $F_{\max} = 100$  kg. Again, this

manoeuvre is reduced such that  $\Delta n_{\max} = 1.5$ . The results are shown in figs 12, 13, 14 and 15.

The change of the first maximum  $\Delta L_1$  as a function of weight is not large if  $\hat{\delta} = \delta_{\max}$  (or  $F_{\max} = 100$  kg); a small airplane weight results in a somewhat larger change (figs 12 and 13). If the manoeuvre is reduced such that  $\Delta n_{\max} \leq 1.5$  a large weight is critical (figs 14 and 15) especially for airplane B (the last-mentioned effect is due to a strong dependence of  $\Delta n_{\max}$  on aircraft weight, fig. 13).

In all cases the second maximum  $\Delta L_2$  is critical for large aircraft weight.

The value of the maximum acceleration increment during a manoeuvre where  $\hat{\delta} = \delta_{\max}$  or  $F_{\max} = 100$  kg increases at decreasing airplane weight.

### 5.4 Variation of moment of inertia (other parameters constant).

The dependence of maximum tail load increments and acceleration increments on the moment of inertia with respect to the  $y$ -axis, is determined with a checked manoeuvre ( $k=2$ ). Again the maximum deflection of the elevator is  $\delta_{\max} = -0.436$  rad (or reduced such that  $F_{\max} = 100$  kg), whereas this "emergency manoeuvre" has been reduced to  $\Delta n_{\max} = 1.5$  as well. The moment of inertia is varied in the range indicated in table 1.

In all cases (figs 16, 17, 18 and 19) the first maximum is critical at a large moment of inertia. This effect of increasing  $\Delta L_1$  with increasing  $I_y$  is relatively strong.

In manoeuvres where  $\hat{\delta} = \delta_{\max}$  or  $F_{\max} = 100$  kg the second maximum is critical at a small moment of inertia. Due to reduction of this manoeuvre to  $\Delta n_{\max} = 1.5$  a large moment of inertia yields the largest  $\Delta L_2$ , except at speed  $V_A$  (figs 18 and 19), but in this case the effect is small.

The maximum acceleration increment ( $\hat{\delta} = \delta_{\max}$  or  $F_{\max} = 100$  kg) is critical at a small value of the moment of inertia.

### 5.5 Combined variation of centre of gravity, weight and moment of inertia.

The qualitative results of par. 5.2 up to and including 5.4, are summarized in table 2.

In order to determine most critical manoeuvre loads in practice, it appears that the trends shown in table 2 do not define immediately the most adverse weight configuration.

It should be emphasized that the equilibrium (or balancing) tail load (the tail load before the initiation of the manoeuvre) must be taken into account in determining the critical load. This equilibrium tail load changes with centre of gravity position and weight. For example, a forward centre of gravity causes a large downward balancing load and in spite of the fact that  $\Delta L_1$  (downward) due to a checked manoeuvre at  $V_A$  is critical at an aft centre of gravity (figs 10 and 11), the total aerodynamic tail load has its maximum value at a forward centre of gravity.

### 5.6 Variation of elevator deflection-time history.

The assumed triangular elevator deflection-time history has been changed by:

1. variation of the ratio  $k = \frac{\tau_2}{\tau_1}$  (fig. 1) with constant  $\tau_1$  ( $t_1 = 0.3$  sec).
2. variation of the "control time"  $\tau_1$  with constant  $k$  ( $k = 2$ ).

#### 5.6.1 Variation of $k = \frac{\tau_2}{\tau_1}$ .

The extreme values of the increments of the tail load  $\Delta L_1$  and  $\Delta L_2$  and the maximum acceleration increment  $\Delta n_{\max}$  at speeds  $V_A$ ,  $V_C$  and  $V_D$  for both airplanes A and B, were computed for elevator motions with different values of the parameter  $k$ . The control time  $t_1$  was 0.3 sec in all cases.

Again two types of manoeuvres were investigated:

1. an "emergency case"  $\hat{\delta} = \delta_{\max} = -0.436$  rad or a value of  $\hat{\delta}$  such that  $F_{\max} = 100$  kg.
2. a "normal case" where  $\hat{\delta}$  is such that  $\Delta n_{\max} = 1.5$ .

The results in the "emergency case" are shown in figs 20 up to 25 inclusive.

It will be evident that  $\Delta L_1$  is independent of  $k$ .

As can be expected the value of  $\Delta n_{\max}$  is increasing with  $k$  ( $k = \infty$  corresponds to an unchecked manoeuvre).

A remarkable effect can be noted in the graphs concerning  $\Delta L_2$ . At relatively low values of  $k$  the graphs of  $\Delta L_2$  show a maximum ( $\Delta L_{2\max}$ ) and at larger values of  $k$ ,  $\Delta L_2$  increases again (airplane A) or is still decreasing (airplane B).

The effect can be explained by the fact that for large values of  $k$  at the instant of the second maximum the elevator has not yet returned to neutral. (See for instance the example of fig. 5.) According to equation (14), in figure 26  $\Delta L_2$  has been split up in three components:

$$\begin{aligned} \Delta L &= \psi [\phi_1 \bar{\alpha} + \phi_2 \bar{\alpha} + \phi_3 \delta] \\ &= \Delta L_{\bar{\alpha}} + \Delta L_{\bar{\alpha}} + \Delta L_{\delta} \end{aligned}$$

in the case of airplane A and speed  $V_A$ . It can be seen that above a certain value of  $k$  a downward component  $\Delta L_{\delta}$  exists at the instant of the second maximum (in the example of fig. 26 this effect is amplified by the component  $\Delta L_{\bar{\alpha}}$  for low values of  $k$ ). This non-zero value of  $\Delta L_{\delta}$  explains the origin of a maximum of  $\Delta L_2$  as a function of  $k$ .

At each speed a value of  $\Delta n_{\max}$  can be computed where the airplane is stalling (defined by  $C_{L\max}$ ). In fact, this phenomenon introduces at each speed a  $\Delta n_{\max}$ -limitation at low values of  $k$ . The results of this  $\Delta n_{\max}$ -limitation are analogous to the results of the reduction to  $\Delta n_{\max} = 1.5$ , discussed in this report as the "normal case".

It can be concluded that in order to determine extreme values of the tail load increment  $\Delta L_2$  in

the emergency case (maximum elevator deflection of maximum stick force) the investigation can be confined to low values of  $k$ .

The tail load increments  $\Delta L_1$  and  $\Delta L_{2\max}$  as functions of airspeed (fig. 27) are analogous of both aircraft A and B if  $\hat{\delta} = \delta_{\max}$ . In the case of airplane A a stick force restriction occurs at  $V = 95$  m sec<sup>-1</sup> ( $F_{\max} = 100$  kg) and at higher speeds the incremental tail loads are reduced considerably.

The results in the "normal case" ( $\hat{\delta}$  such that  $\Delta n_{\max} = 1.5$ ) are shown in figs 28 up to 33 inclusive.

Extreme values of  $\Delta L_1$ ,  $\Delta L_2$  and  $F_{\max}$  as functions of  $k$  arise at the smallest possible  $k$  or (for  $\Delta L_2$  at  $V_A$ ) at such  $k$  that  $\Delta n_{\max} = 1.5$  and  $\hat{\delta} = \delta_{\max}$ .

It was tried to plot tail load increments and stick forces as functions of speed for distinct values of  $k$ , but this did not lead to results, which could add to a better understanding of the effect of speed on the tail loads occurring during the "normal case" pull ups. The different curves appeared to cross each other in a rather confusing way, which did not permit any useful conclusion. Moreover, the graphs for the two aircraft considered did not show similar trends.

The maximum stick forces required to perform the manoeuvres for aircraft B, noted in the graphs (figs 23 up to 25 incl. and 31 up to 33 incl.) are very small. Again it should be stressed, that  $F_{\max}$  contains only the stick force required to balance the aerodynamic hinge moment (see also par. 5.1.5); this part of the actual stick force is indicated as " $F_{\max}$  (aerodyn)" in all graphs. Aircraft B is fitted with a bobweight at the control column. The stick force required to balance the bobweight ( $F_{bw}$ ) is derived in Appendix C and the example of this appendix shows that the real stick force can be considerably larger than  $F_{\max}$  (aerodyn). As the pitch angle  $\theta$  is required to obtain  $F_{bw}$  and  $\theta$  was not computed,  $F_{bw}$  is not available.

Aircraft A is not fitted with a bobweight.

In order to compare the computed maximum tail loads with the loads according to present airworthiness requirements the latter are computed with the aid of the "Civil Air Regulations" § 4b.213 (c).

The unchecked pull-up load at speed  $V_A$  (CAR § 4b.213 (c) (1)) is determined by means of an approximate "rational" analysis, as often used by U. S. aircraft firms.

The checked manoeuvre loads at  $V_A$  and  $V_D$  (§ 4b.213 (c) (2) and (3)) are calculated assuming that the pitching moment due to the additional tail load is balanced by the pitching moment of inertia of the airplane.

Balancing tail loads are determined in the 1 g-condition (CAR cases  $A_1$  and  $D_1$ ) and 2.5 g-condition (CAR cases  $A_2$  and  $D_2$ ). These balancing loads are added to the manoeuvre loads (according to CAR) in order to obtain the total tail loads.

The balancing tail load in the 1 g-condition,

of course, is used to determine the total tail load obtained by means of the rational analysis used in this report.

The comparison is made in figs 34 and 35 at speeds  $V_A$  and  $V_D$  respectively. The results of the rational analysis are the same as those of figs 31 and 33.

It is shown in figs 34 and 35 that the checked manoeuvre-CAR loads correspond to values of  $k$  which are rather large if these requirements are intended to cover emergency conditions as well. Especially the first maximum total tail load  $L_1$  at speed  $V_D$  is much too small.

The total tail loads for two arbitrary selected values of  $k$  ( $k=2$  and  $k=5$ ) as functions of airspeed are compared with the CAR values in fig. 36.

From the figs 34 to 36 incl. it can be concluded, that the checked manoeuvre loads derived from the pitching accelerations prescribed by CAR are not realistic for emergency conditions (often characterized by  $k=2$ ), even if the restriction  $\Delta n_{\max}=1.5$  would be acceptable in this case.

In order to obtain the total aerodynamic tail load, the *balancing tail load* must be taken into account. This balancing load varies with speed. In fig. 37 the total aerodynamic tail loads  $L_1$  and  $L_{2\max}$  and the balancing load are shown as functions of speed. This figure is taken from fig. 27 by adding the balancing load at each speed.

It can be concluded that, apart from gust loads, the extreme value of the second maximum is critical for bending and shear of the tailplane at all speeds; this conclusion for the airplanes A and B need not be true for other airplanes.

#### 5.6.2 Variation of the control time $\tau_1$ .

As stated in par. 5.6, the elevator deflection-time history can be varied in a second way by means of the "control time"  $\tau_1$ . Manoeuvres with different  $\tau_1$  and constant  $k$  ( $k=2$ ) were investigated for both airplanes A and B (figs 38 up to fig. 43 inclusive). The loads of airplane A for different values of  $\tau_1$  are obtained from ref. 5 and are reproduced here.

In the "emergency case" ( $\hat{\delta}=\delta_{\max}$  or  $F_{\max}=100$  kg) it appears that the first maximum of the tail load is critical for the smallest possible value of  $\tau_1$  (aerodynamic lag neglected). The second maximum of the tail load  $\Delta L_2$  and the maximum acceleration increment  $\Delta n_{\max}$  are critical for finite and non-zero values of  $\tau_1$ . Hence there exist "optimum control times" for  $\Delta L_2$  and  $\Delta n_{\max}$  (ref. 5). The optimum control time  $\tau_1$  does not show a significant dependence on the flight speed, hence the real optimum control time  $t_1$  decreases with increasing airspeed. The "stalling limit" referred to in par. 5.1, however, in some cases, causes an optimum control time  $\tau_1$  at the (first) intersection of the curves  $\Delta L_2$  ( $\hat{\delta}=\delta_{\max}$ ) and  $\Delta L_2$  ( $\Delta n_{\max\text{stall}}$ ). The last-mentioned curve is not indicated in the graphs. In the case of airplane A the "stalling limit" is not important, for the restriction  $F_{\max}=100$  kg (speeds  $V_C$  and  $V_D$ )

reduces the manoeuvre to  $\Delta n_{\max} < \Delta n_{\max\text{stall}}$  (figs 39 and 40).

In the "normal case" ( $\Delta n_{\max}=1.5$  according to the present airworthiness requirements) the first maximum  $\Delta L_1$  is still critical for the smallest possible  $\tau_1$ . The second maximum  $\Delta L_2$ , however, is critical at the value of  $\tau_1$  which belongs to the (first) intersection of the curves  $\Delta L_2$  ( $\hat{\delta}=\delta_{\max}$ ) and  $\Delta L_2$  ( $\Delta n_{\max}=1.5$ ); this optimum  $\tau_1$  will in general be smaller than the optimum  $\tau_1$  in the "emergency case".

Incremental tail loads for arbitrary values of  $t_1$  ( $t_1=0.15$  sec, 0.30 sec, 1.20 sec) as functions of airspeed are shown in fig. 44 where the manoeuvre is restricted by  $\Delta n_{\max} \leq 1.5$ ; tail load increments derived from CAR are shown as well.

It appears that the manoeuvre loads according to CAR are in general small: they belong (in the case of airplane B) to a manoeuvre with a control time  $t_1$  of 1.0 to 1.3 seconds, which is relatively "slow".

#### 5.7 Discussion.

In practical rational analyses the design tail loads are often calculated supposing a checked manoeuvre with  $t_1=0.3$  sec,  $k=2$  and  $\Delta n_{\max}=1.5$ . It is possible to test this procedure by means of the results of this report (figs 28 up to 33 incl. and figs 38 up to 43 incl.) for the two airplanes investigated. Concerning the assumption  $k=2$  it appears that a smaller value of  $k$  is more critical, apart from the fact whether  $k < 2$  will be realistic. The assumption  $t_1=0.3$  sec appears to be rational for the second maximum at speed  $V_A$ , but at higher speeds the tail load increments are larger at a smaller control time. Especially the first maximum is very sensitive at small  $t_1$  and this maximum roughly doubles for  $t_1=0.15$  sec with respect to  $t_1=0.3$  sec at  $V_C$  and  $V_D$ . A control time  $t_1=0.15$  sec is not unthinkable according to ref. 6.

On the other hand, in "emergency manoeuvres" (this case with  $\hat{\delta}=\delta_{\max}$  or pilot effort limitation, is not included in present requirements) the tail loads are much larger than in the "normal cases" (compare figs 20 up to 25 incl. with figs 28 up to 33 incl. for parameter  $k$  and see figs 38 up to 43 incl. for parameter  $t_1$ ). The assumptions  $k=2$  and  $t_1=0.3$  sec. for  $\Delta L_{2\max}$  appear to be rational at  $V_D$ ; this speed is critical for airplane B (no pilot effort limitation, fig. 37) but not for airplane A.

It can be concluded that the critical manoeuvre for actual design must be chosen by means of rational investigation of the critical elevator deflection-time history for each airplane configuration in normal cases ( $\Delta n_{\max}=1.5$ ).

Moreover attention has to be paid to the need of an "emergency case" (limited by pilot effort and airplane stalling) to be inserted in structural airworthiness requirements.

#### 6 Conclusions.

6.1 Starting from a prescribed triangular elevator deflection-time history, checked manoeuvres with

two airplanes of quite different sizes were calculated. The parameters varied were the control time  $t_1$  (the time in which the elevator reaches its maximum deflection) and the ratio  $k$  between the time after which the elevator has returned to its initial position and  $t_1$ . The calculations were carried out for two airplanes at different speeds and weight configurations.

Two types of manoeuvres are discussed throughout this report: a so-called "emergency case", where the pilot deflects the elevator due to a sudden event in a very short time (limited by maximum pilot effort) and a "normal case" according to present airworthiness requirements.

6.2 In most respects similar results were obtained for both airplane types investigated.

6.3 In "emergency cases" ( $\hat{\delta} = \delta_{\max}$  or  $F_{\max} = 100$  kg) the second maximum of the tail load increment has critical values both in the case of variation of  $\tau_1$  and in the case of variation of  $k$ , for finite and non-zero values of  $\tau_1$  and  $k$  respectively. The first maximum of the tail load increment is critical for  $\tau_1 = 0$ , that is to say for the smallest possible  $\tau_1$  (neglecting aerodynamic lag).

The maximum normal acceleration increment is critical for a finite and non-zero  $\tau_1$  and  $k = \infty$  (unchecked manoeuvre).

6.4 In "normal cases" ( $\Delta n_{\max} \leq 1.5$ ) both the first and second maximum of tail load increment are critical for the smallest possible  $k$ , except the second maximum at low speeds ( $k > 1$ ). The first maximum is critical at the smallest possible  $\tau_1$ , the second one again at a finite and non-zero  $\tau_1$ .

6.5 The pitching accelerations in the "normal cases" as functions of speed are compared with those prescribed by CAR. 4b. It appears that the CAR-values are related to relatively slow elevator movements, not resulting in critical tail loads.

6.6 For both airplane types investigated the second maximum of the tail load (including the equilibrium load) was larger than the first maximum (absolute values) at all speeds, but this fact need not necessarily be true for other airplanes.

The loading of the tail plane due to the first maximum is different from that of the second maximum (in some cases comparable with a gust loading).

6.7 The required stick forces are quite different for both airplanes (no servo or booster and fitted with spring tab respectively). The stick forces required to balance the aerodynamic hinge moment were very small in the case of the spring tab; additional stick forces due to a bobweight fitted in this airplane can be considerable, but have not been computed.

6.8 It is recommendable to choose the manoeuvre loads in the case  $\Delta n \leq 1.5$  by means of a rational determination of the critical elevator-time deflection history for each airplane configuration.

Moreover it is concluded that attention has to be paid to the need of an "emergency case" (limited by pilot effort) to be inserted in structural airworthiness requirements.

## 7 References.

1. KOEHLER, R. K. The structural tail load problem-theory, tests and criteria; Cornell Aeronautical Laboratory. Report No. CAL-49.
2. PERKINS, C. D. and HAGE, R. E. Airplane performance, stability and control; John Wiley and Sons, New York, 1950.
3. PEARSON, H. A. Derivation of charts for determining the horizontal tail load variation with any elevator motion; NACA Report No. 759, 1943.
4. VAN HOOFF, W. J. Tail loads due to manoeuvres and engine failure; Report SA intern 2, N.V. Koninklijke Nederlandse Vliegtuigenfabriek "Fokker", Amsterdam, oktober 1955 (in Dutch).
5. VAN HOOFF, W. J. Optimum control time in checked and unchecked manoeuvres with different airplanes; Report S.A. intern 7, N.V. Koninklijke Nederlandse Vliegtuigenfabriek "Fokker" Amsterdam, june 1956 (in Dutch).
6. OVERBEEK, J. L. Measurements of the control force-time relations for sudden movements of the controls; Report V.1816, Nationaal Luchtvaartlaboratorium, Amsterdam, December 1958.
7. CZAYKOWSKI, T. Loading conditions of tailed aircraft in longitudinal manoeuvres; Reports and Memoranda No. 3001, London, February 1955.

APPENDIX A.

The coefficients  $K_i'$  of equation (8).

$$K_1' = \frac{W}{pgS} \left( \frac{dC_L}{d\alpha} \right)_w + \left( 1 - \frac{de}{d\alpha} \right) \eta \frac{S_i}{S} \left( \frac{dC_L}{d\alpha} \right)_i + \frac{KX_i^2}{k_{ij}^2} V^- \frac{S_i}{\eta S} \left( \frac{dC_L}{d\alpha} \right)_i - \frac{(-X_i + h)X_i}{k_{ij}^2} \frac{de}{d\alpha} \eta \frac{S_i}{S} \left( \frac{dC_L}{d\alpha} \right)_i \left[ 1 - (K-1) \frac{pgSX_i}{2W} V^- \frac{S_i}{\eta S} \left( \frac{dC_L}{d\alpha} \right)_i \right] \\ + \frac{2W}{pgS} + (-X_i + h) \frac{de}{d\alpha} \eta \frac{S_i}{S} \left( \frac{dC_L}{d\alpha} \right)_i$$

$$K_2' = \left( \frac{W}{pgS} \right)^2 \frac{pgS}{2W} \frac{(h - KX_i)X_i}{k_{ij}^2} \left( \frac{dC_L}{d\alpha} \right)_w V^- \frac{S_i}{\eta S} \left( \frac{dC_L}{d\alpha} \right)_i - \frac{X_i}{k_{ij}^2} \left( 1 - \frac{de}{d\alpha} \right) \eta \frac{S_i}{S} \left( \frac{dC_L}{d\alpha} \right)_i \left[ 1 - (K-1) \frac{pgSX_i}{2W} V^- \frac{S_i}{\eta S} \left( \frac{dC_L}{d\alpha} \right)_i \right] - \frac{h}{k_{ij}^2} \left( \frac{dC_L}{d\alpha} \right)_w \\ + \frac{2W}{pgS} + (-X_i + h) \frac{de}{d\alpha} \eta \frac{S_i}{S} \left( \frac{dC_L}{d\alpha} \right)_i$$

$$K_3' = \left( \frac{W}{pgS} \right)^2 \frac{X_i}{k_{ij}^2} \eta \frac{S_i}{S} \left( \frac{dC_L}{d\alpha} \right)_i \left[ 1 - (K-1) \frac{pgSX_i}{2W} V^- \frac{S_i}{\eta S} \left( \frac{dC_L}{d\alpha} \right)_i \right] + \frac{S_i}{b_i k_{ij}^2} \eta \frac{S_i}{S} \left( \frac{dC_m}{d\delta} \right)_i \left[ 1 + \frac{pgSX_i}{2W} V^- \frac{S_i}{\eta S} \left( \frac{dC_L}{d\alpha} \right)_i \right] \\ + \frac{2W}{pgS} + (-X_i + h) \frac{de}{d\alpha} \eta \frac{S_i}{S} \left( \frac{dC_L}{d\alpha} \right)_i$$

$$K_4' = \frac{W}{pgS} \frac{-\eta \frac{S_i}{S} \left( \frac{dC_L}{d\delta} \right)_i}{2W} + (-X_i + h) \frac{de}{d\alpha} \eta \frac{S_i}{S} \left( \frac{dC_L}{d\alpha} \right)_i$$



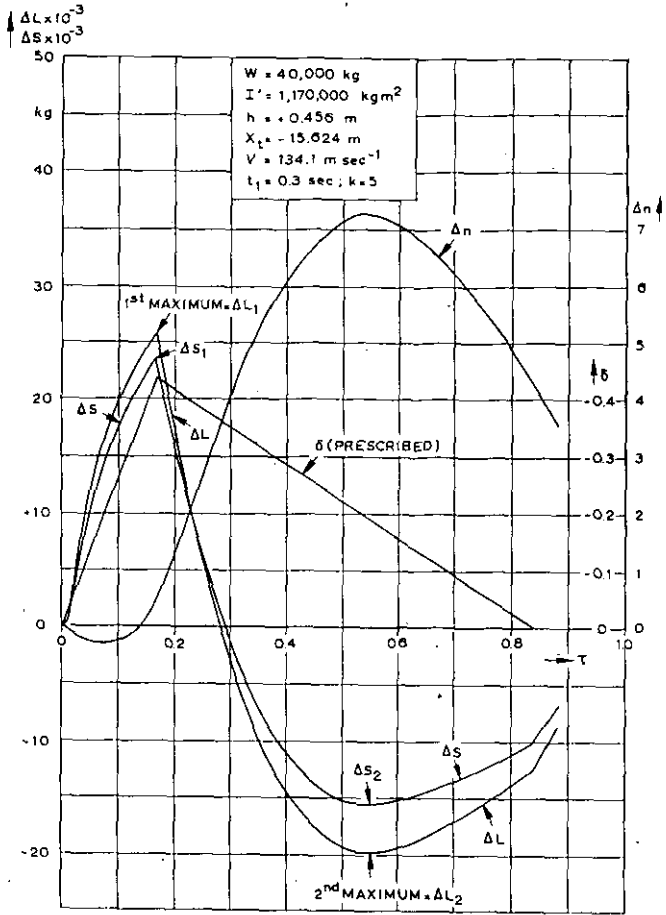


Fig. 5. Example of airplane response. Airplane B,  $k=5$ ; speed  $V_C$ .

Airplane B  $\rightarrow a = b_1 \alpha_t + b_2 \delta = -0.117 \alpha_t + 0.119 |\delta|$  ( $\delta \leq 0$ )

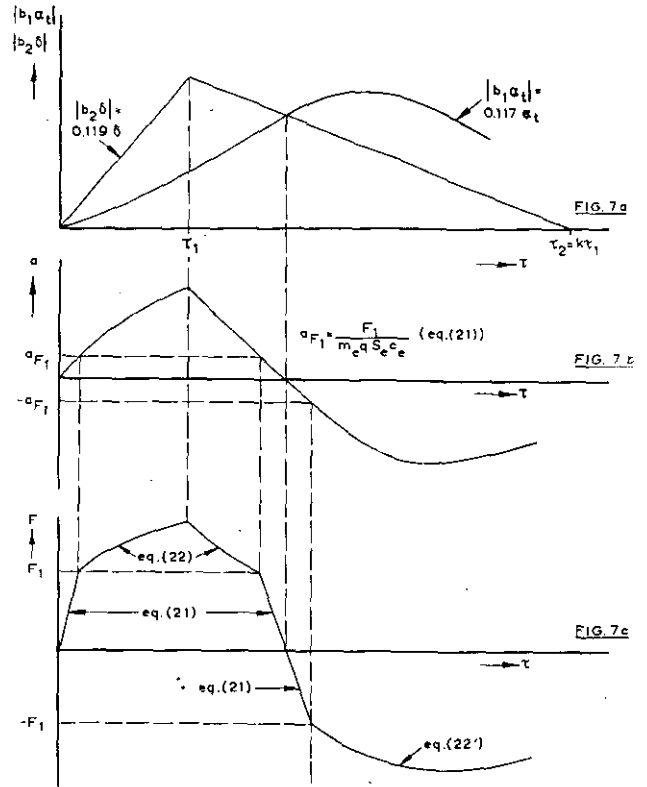


Fig. 7. Structure of the stick force-time diagram of fig. 6.

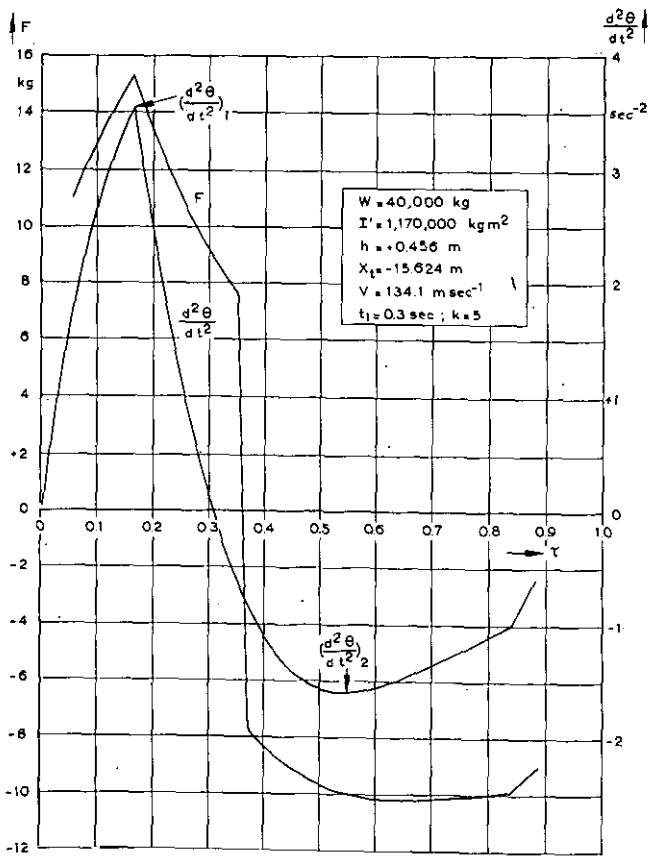


Fig. 6. Example of airplane response (cont.) and required stick force. Airplane B,  $k=5$ ; speed  $V_C$ .

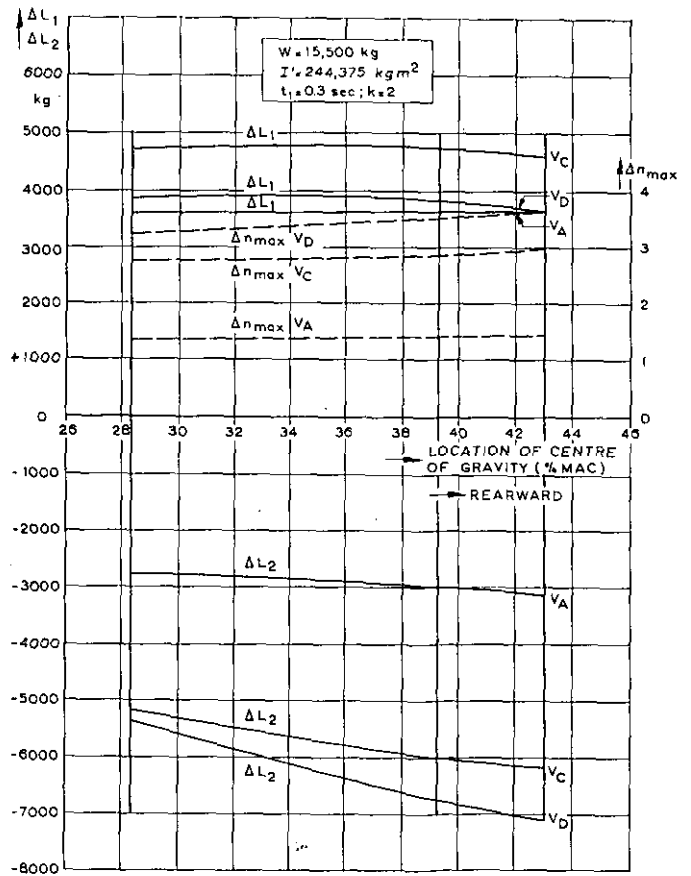


Fig. 8. Airplane A.  $\Delta L_1$ ,  $\Delta L_2$  and  $\Delta n_{\max}$  as functions of centre of gravity location ( $\delta = \delta_{\max} = -0.436$  rad or  $F_{\max} = 100$  kg).

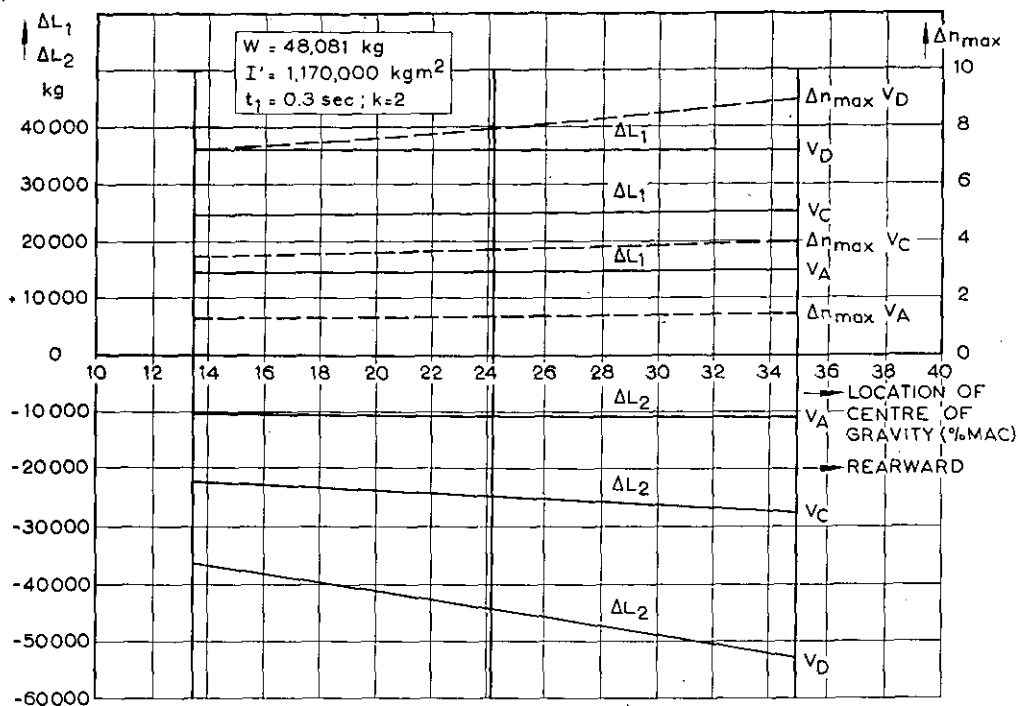


Fig. 9. Airplane B,  $\Delta L_1$ ,  $\Delta L_2$  and  $\Delta n_{\max}$  as functions of centre of gravity location  $\delta = \delta_{\max} = -0.436 \text{ rad}$  or  $F_{\max} = 100 \text{ kg}$ .

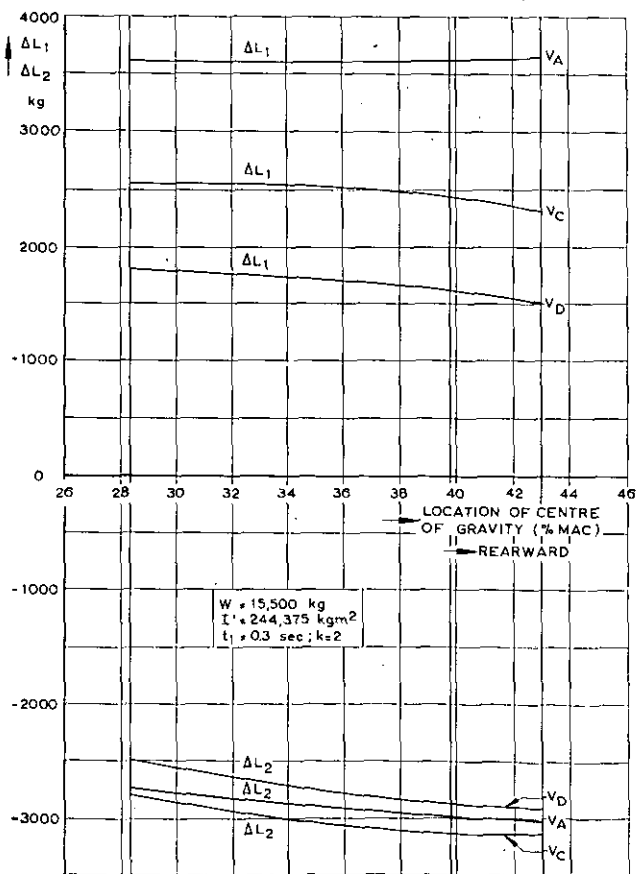


Fig. 10. Airplane A,  $\Delta L_1$  and  $\Delta L_2$  as functions of centre of gravity location ( $\Delta n_{\max} \leq 1.5$ ).

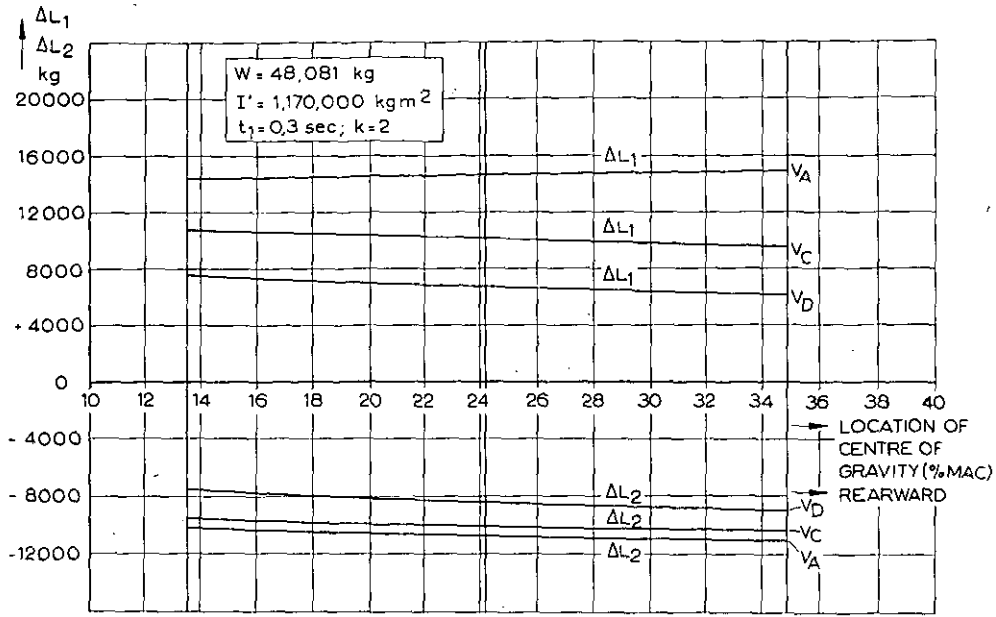


Fig. 11. Airplane B.  $\Delta L_1$  and  $\Delta L_2$  as functions of gravity location ( $\Delta n_{max} \leq 1.5$ ).

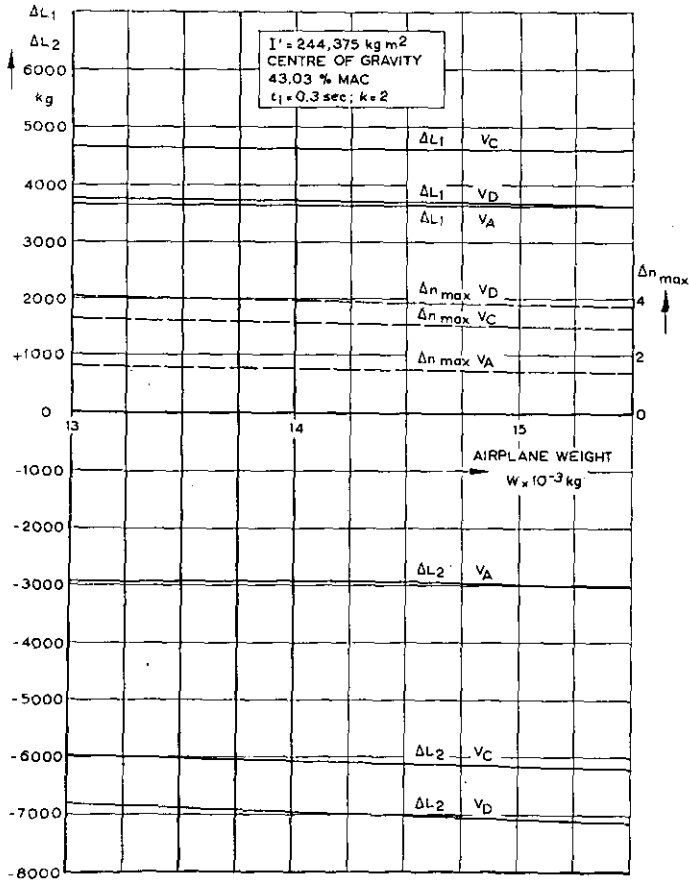


Fig. 12. Airplane A.  $\Delta L_1$ ,  $\Delta L_2$  and  $\Delta n_{max}$  as functions of airplane weight ( $\delta = \delta_{max} = -0.436$  rad or  $F_{max} = 100$  kg).

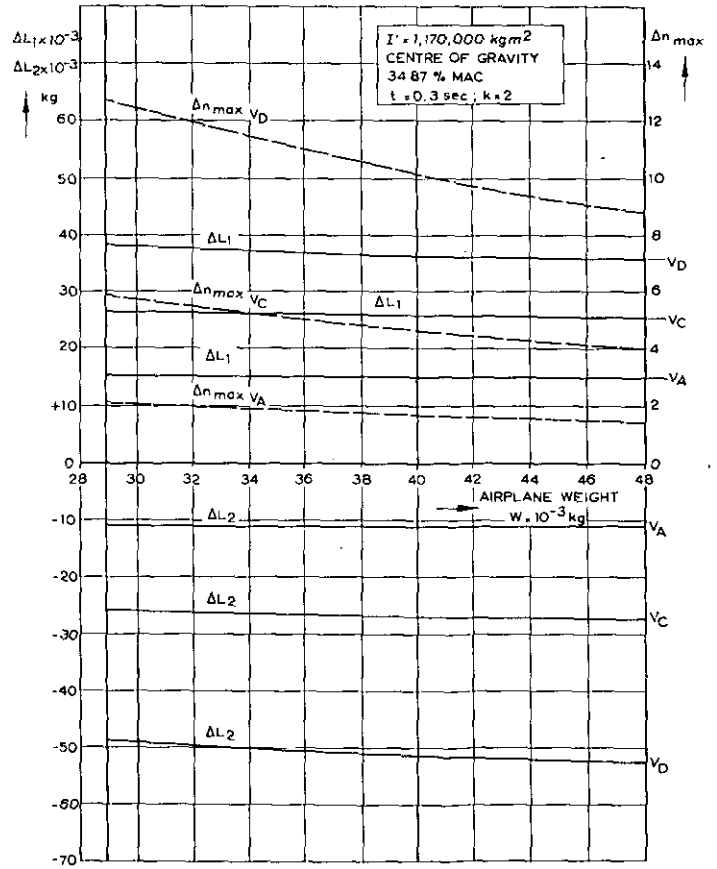


Fig. 13. Airplane B.  $\Delta L_1$ ,  $\Delta L_2$  and  $\Delta n_{max}$  as functions of airplane weight ( $\delta = \delta_{max} = -0.436$  rad or  $F_{max} = 100$  kg).

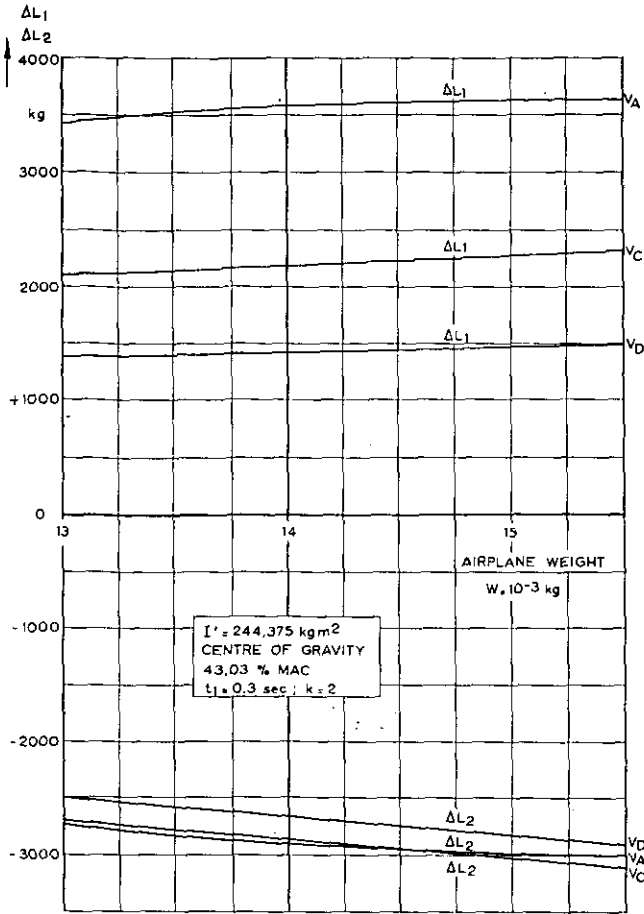


Fig. 14. Airplane A  $\Delta L_1$  and  $\Delta L_2$  as functions of airplane weight ( $\Delta n_{max} \leq 1.5$ ).

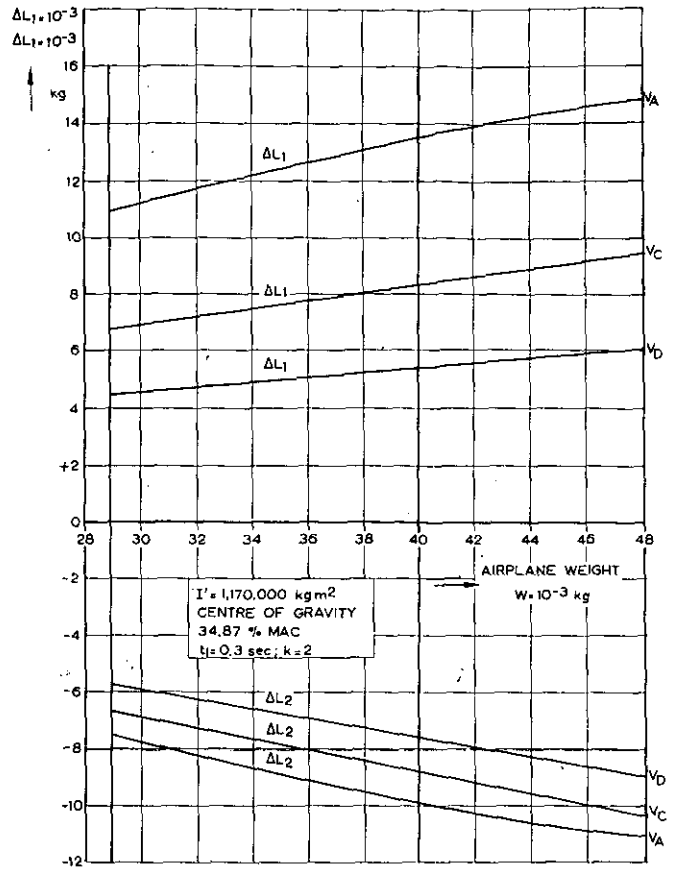


Fig. 15. Airplane B.  $\Delta L_1$  and  $\Delta L_2$  as functions of airplane weight ( $\Delta n_{max} \leq 1.5$ ).

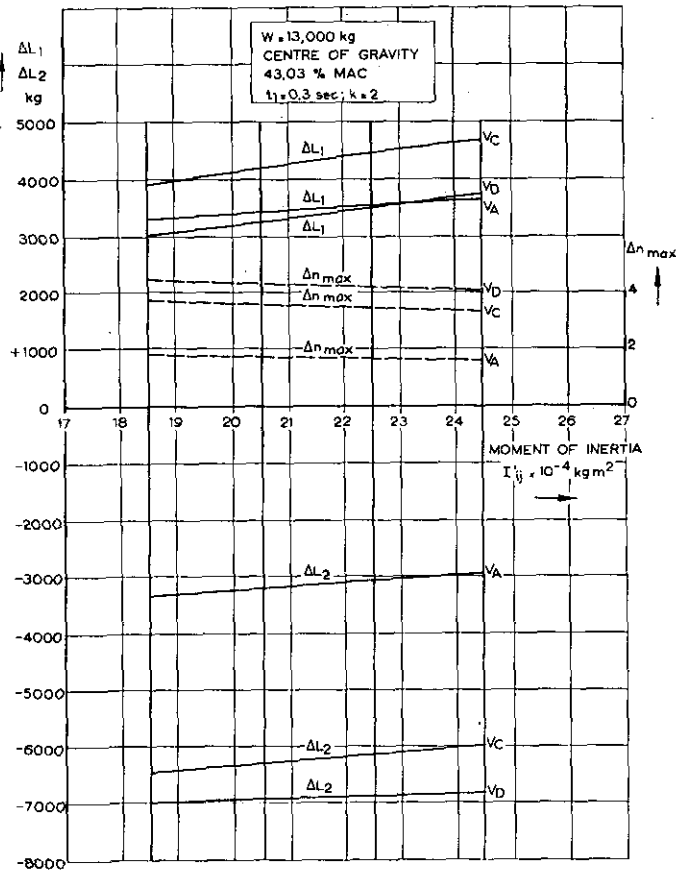


Fig. 16. Airplane A.  $\Delta L_1$ ,  $\Delta L_2$  and  $\Delta n_{max}$  as functions of the moment of inertia ( $\delta = \delta_{max} = -0.436$  rad or  $F_{max} = 100$  kg).

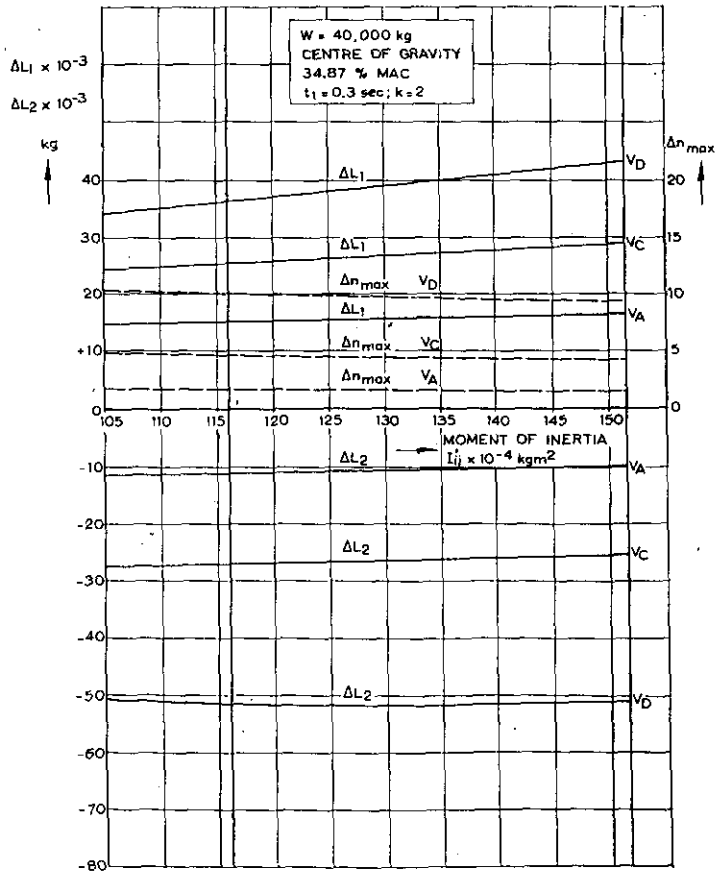


Fig. 17. Airplane B.  $\Delta L_1$ ,  $\Delta L_2$  and  $\Delta n_{max}$  as functions of the moment of inertia ( $\delta = \delta_{max} = -0.436$  rad or  $F_{max} = 100$  kg).

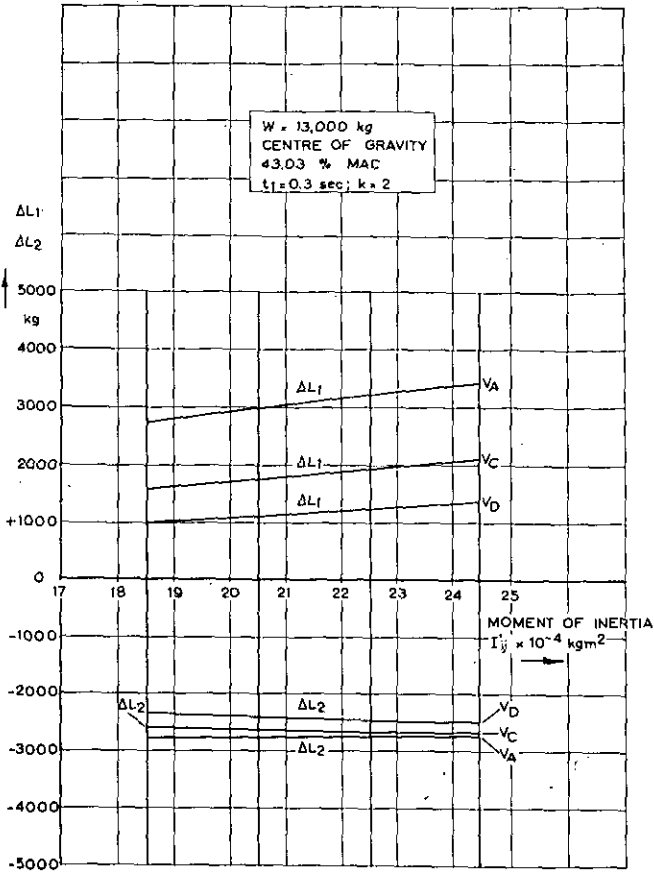


Fig. 18. Airplane A.  $\Delta L_1$  and  $\Delta L_2$  as functions of the moment of inertia ( $\Delta n_{\max} \leq 1.5$ ).

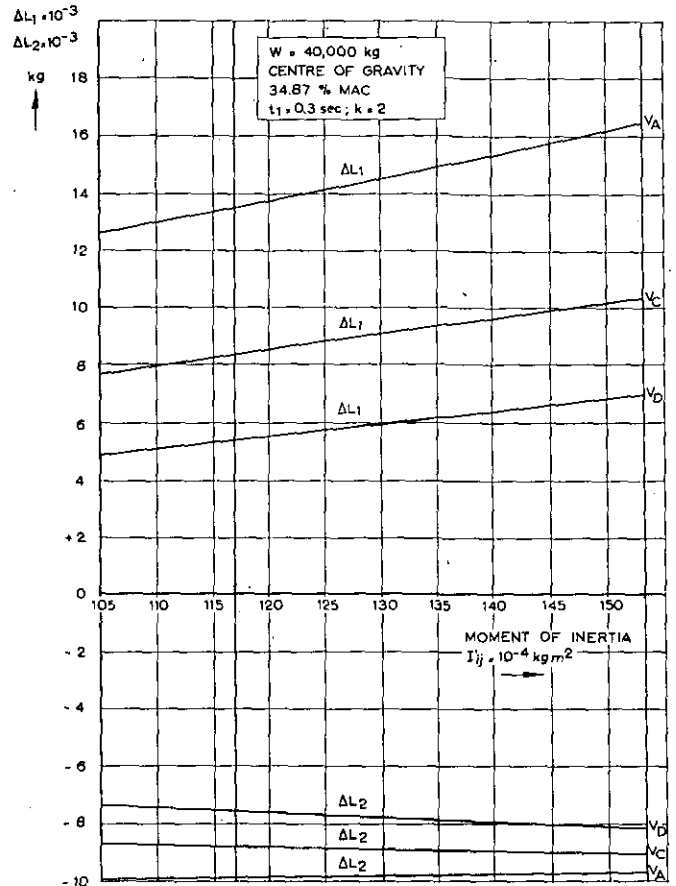


Fig. 19. Airplane B.  $\Delta L_1$  and  $\Delta L_2$  as functions of the moment of inertia ( $\Delta n_{\max} \leq 1.5$ ).

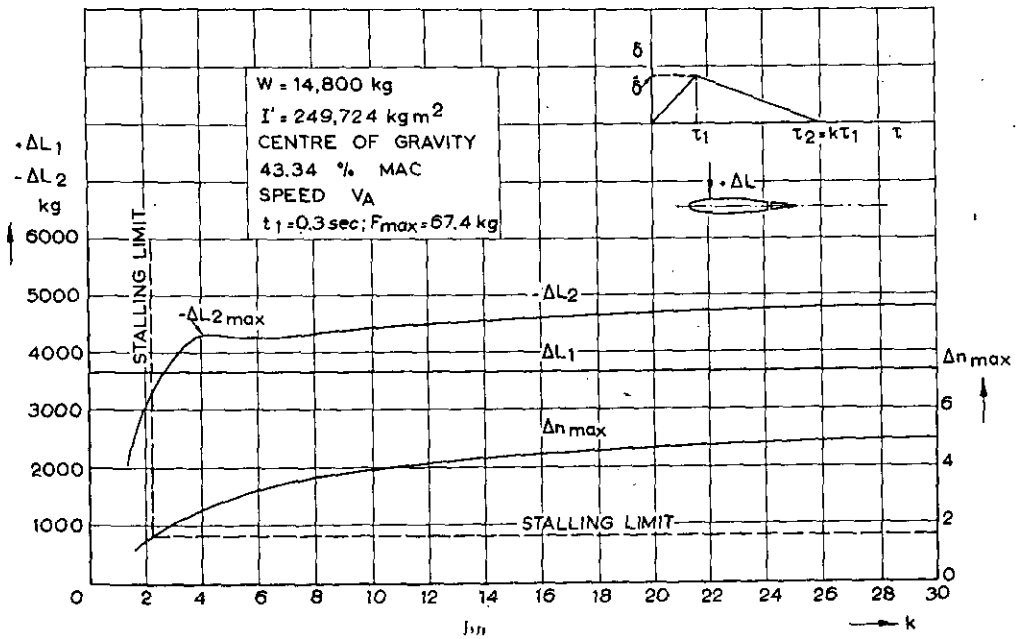


Fig. 20. Airplane A.  $\Delta L_1$ ,  $\Delta L_2$  and  $\Delta n_{\max}$  as functions of  $k = \frac{\tau_2}{\tau_1}$  ( $\hat{\delta} = \delta_{\max} = -0.436 \text{ rad}$ ). Speed  $V$ .

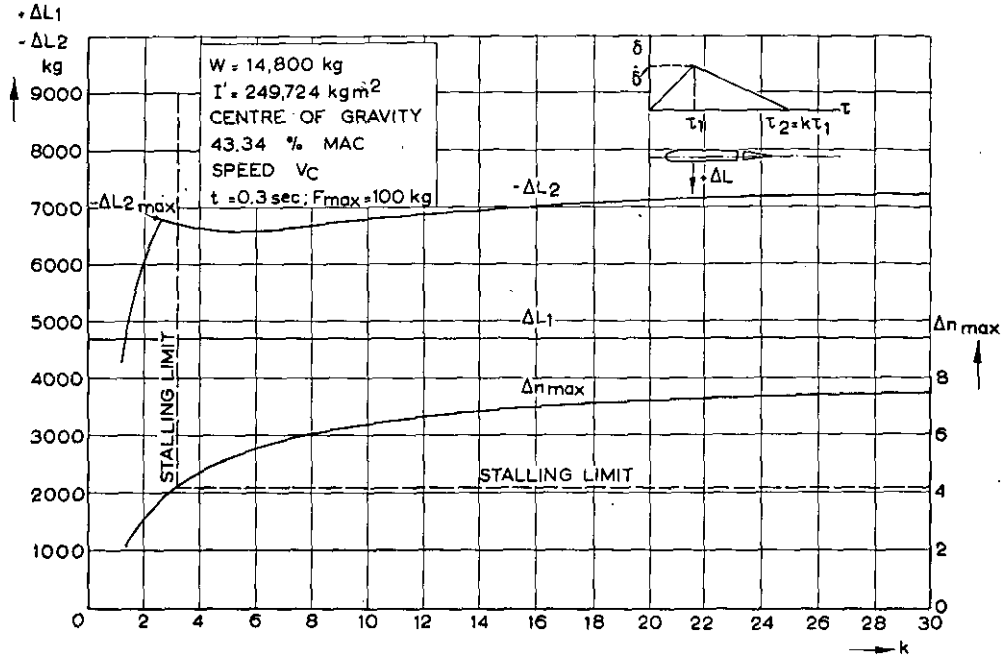


Fig. 21. Airplane A.  $\Delta L_1$ ,  $\Delta L_2$  and  $\Delta n_{\text{max}}$  as functions of  $k = \frac{\tau_2}{\tau_1}$  ( $F_{\text{max}} = 100 \text{ kg}, \hat{\delta} < \delta_{\text{max}}$ ). Speed  $V_C$ .

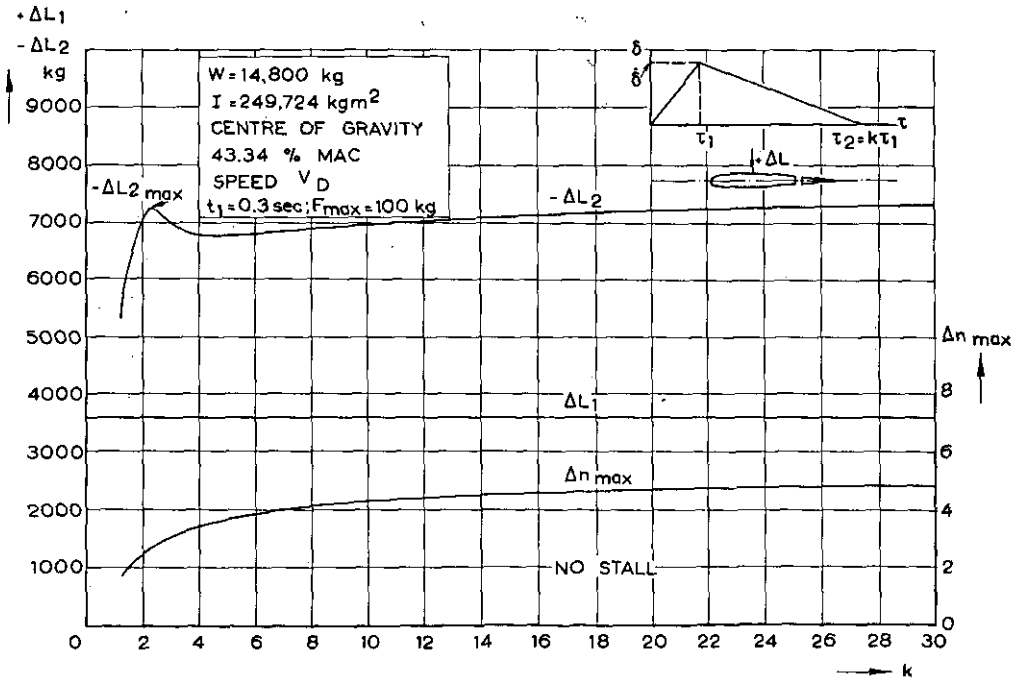


Fig. 22. Airplane A.  $\Delta L_1$ ,  $\Delta L_2$  and  $\Delta n_{\text{max}}$  as functions of  $k = \frac{\tau_2}{\tau_1}$  ( $F_{\text{max}} = 100 \text{ kg}, \hat{\delta} < \delta_{\text{max}}$ ). Speed  $V_D$ .

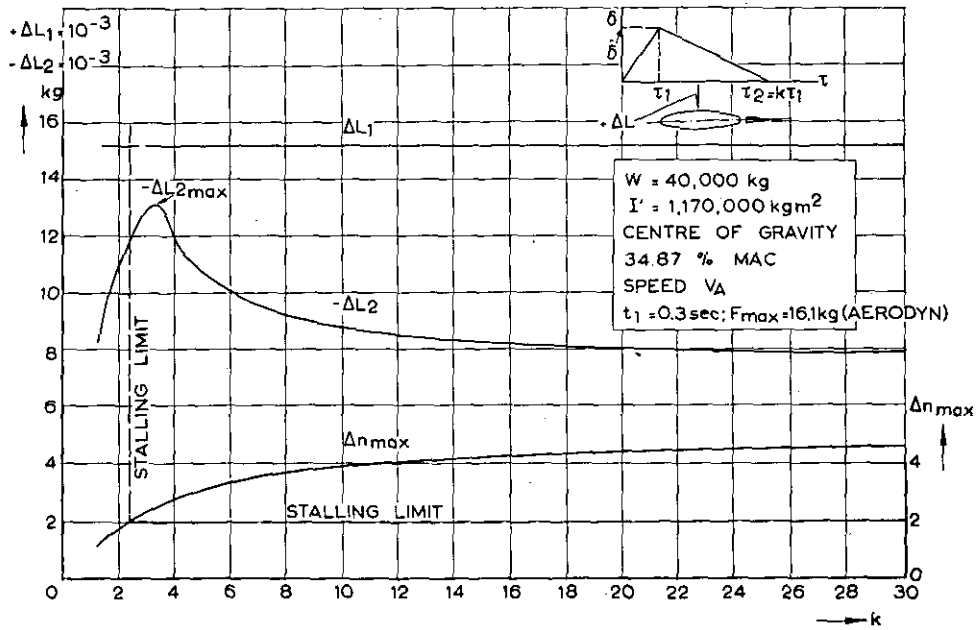


Fig. 23. Airplane B.  $\Delta L_1$ ,  $\Delta L_2$  and  $\Delta n_{max}$  as functions of  $k =$

$$\frac{\tau_2}{\tau_1} (\hat{\delta} = \delta_{max} = -0.436 \text{ rad}). \text{ Speed } V_A.$$

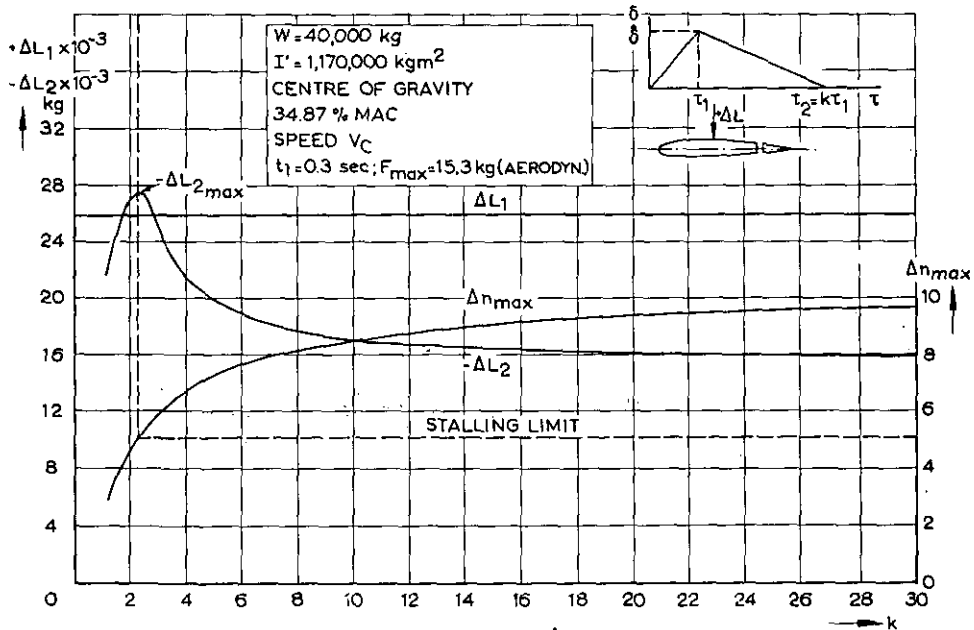


Fig. 24. Airplane B.  $\Delta L_1$ ,  $\Delta L_2$  and  $\Delta n_{max}$  as functions of  $k =$

$$\frac{\tau_2}{\tau_1} (\hat{\delta} = \delta_{max} = -0.436 \text{ rad}). \text{ Speed } V_C.$$

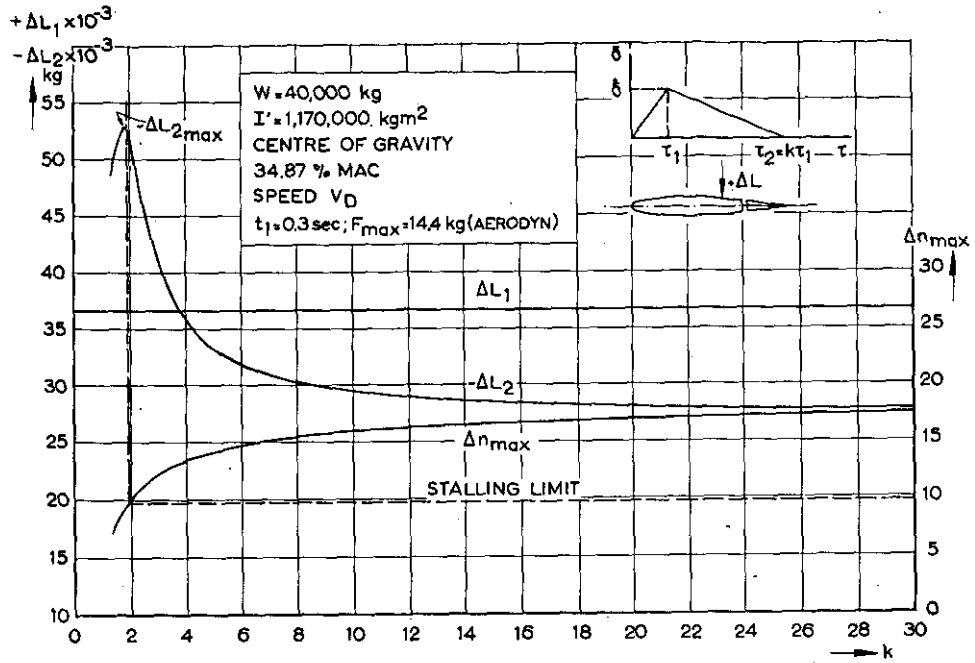


Fig. 25. Airplane B.  $\Delta L_1$ ,  $\Delta L_2$  and  $\Delta n_{max}$  as functions of  $k =$

$$\frac{\tau_2}{\tau_1} (\hat{\delta} = \delta_{max} = -0.436 \text{ rad}). \text{ Speed } V_D.$$

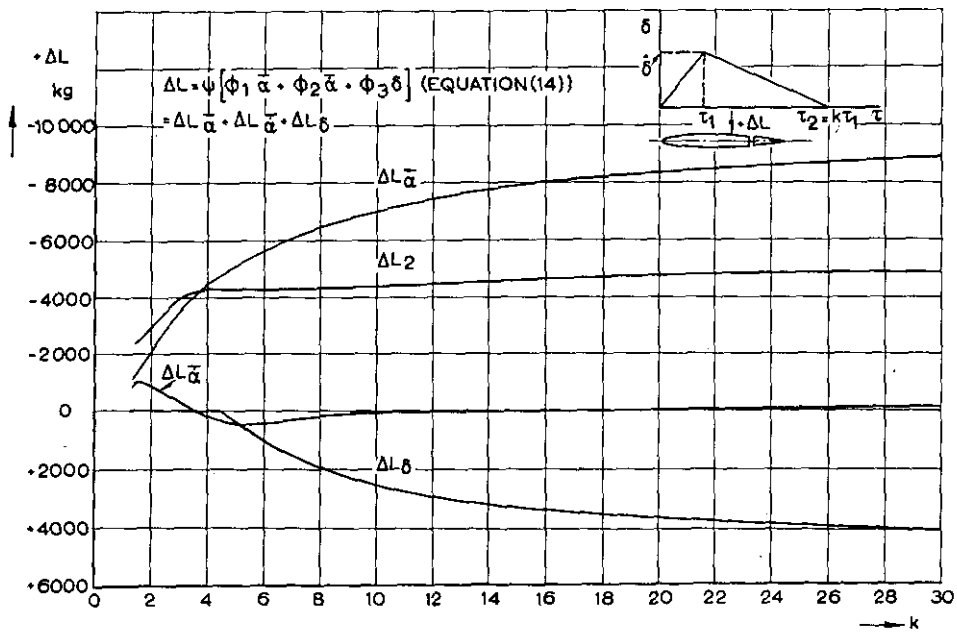


Fig. 26. Component parts of  $\Delta L_2 = \Delta L_{\bar{\alpha}} + \Delta L_{\bar{\alpha}} + \Delta L_{\delta}$  as functions of  $k =$

$$\frac{\tau_2}{\tau_1} (\hat{\delta} = \delta_{max} = -0.436 \text{ rad}). \text{ Airplane A; Speed } V_A.$$



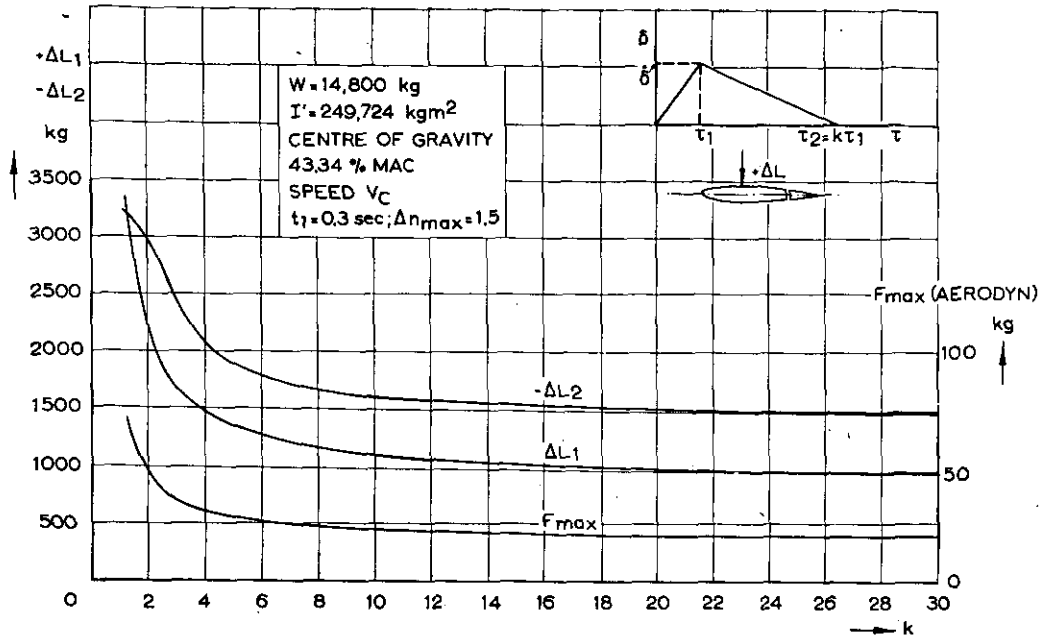


Fig. 29. Airplane A.  $\Delta L_1$ ,  $\Delta L_2$  and  $F_{\max}$  as functions of  $k = \frac{\tau_2}{\tau_1} \Delta n_{\max} = 1.5$ . Speed  $V_C$ .

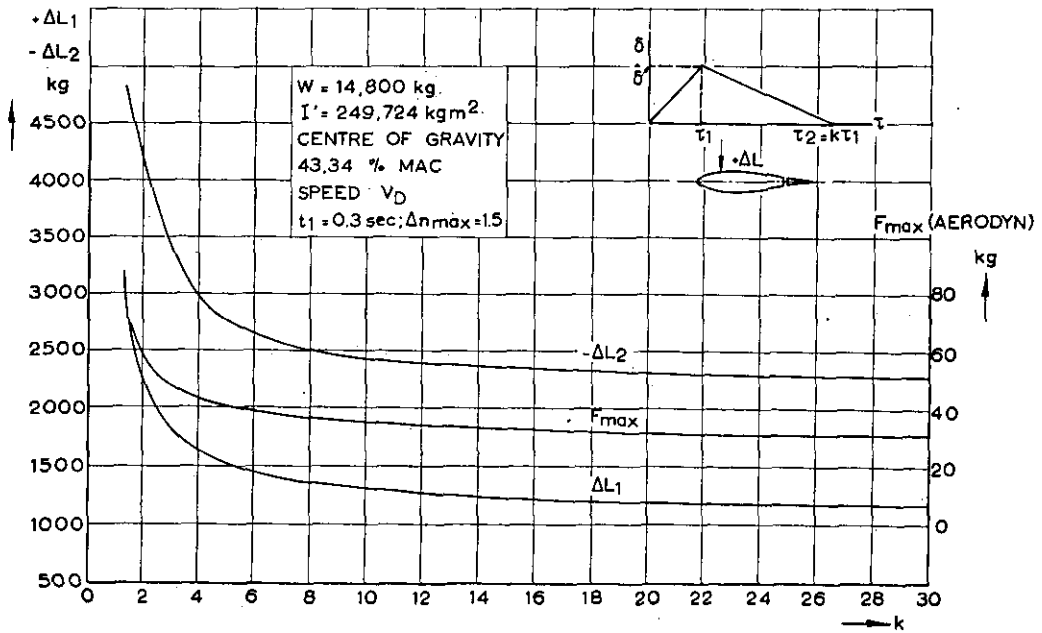


Fig. 30. Airplane A.  $\Delta L_1$ ,  $\Delta L_2$  and  $F_{\max}$  as functions of  $k = \frac{\tau_2}{\tau_1} (\Delta n_{\max} = 1.5)$ . Speed  $V_D$ .

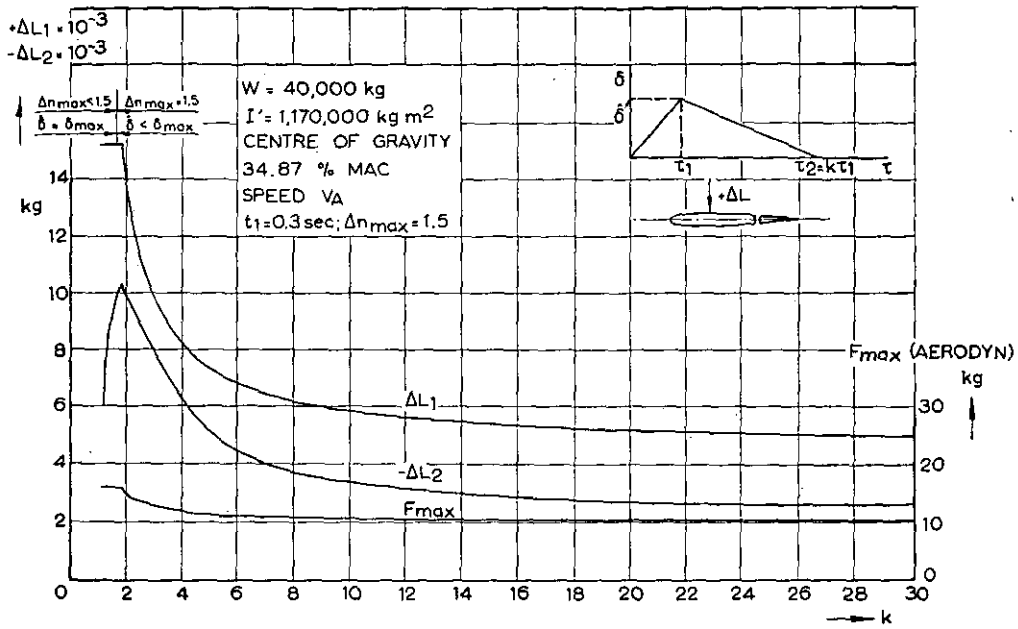


Fig. 31. Airplane B.  $\Delta L_1$ ,  $\Delta L_2$  and  $F_{max}$  as functions of  $k = \frac{\tau_2}{\tau_1}$  ( $\Delta n_{max} = 1.5$ ). Speed  $V_A$ .

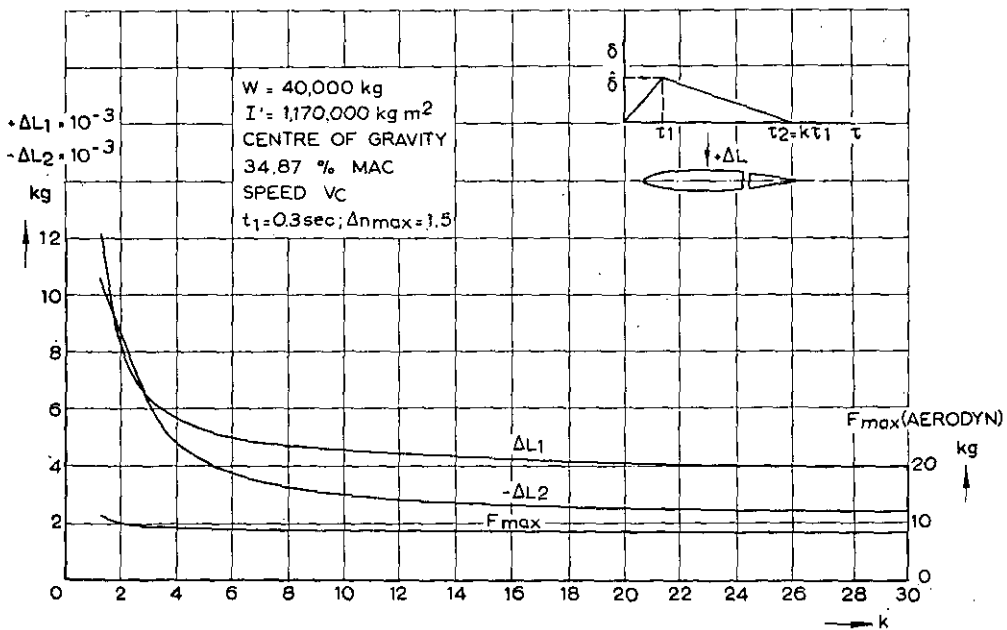


Fig. 32. Airplane B.  $\Delta L_1$ ,  $\Delta L_2$  and  $F_{max}$  as functions of  $k = \frac{\tau_2}{\tau_1}$  ( $\Delta n_{max} = 1.5$ ). Speed  $V_C$ .

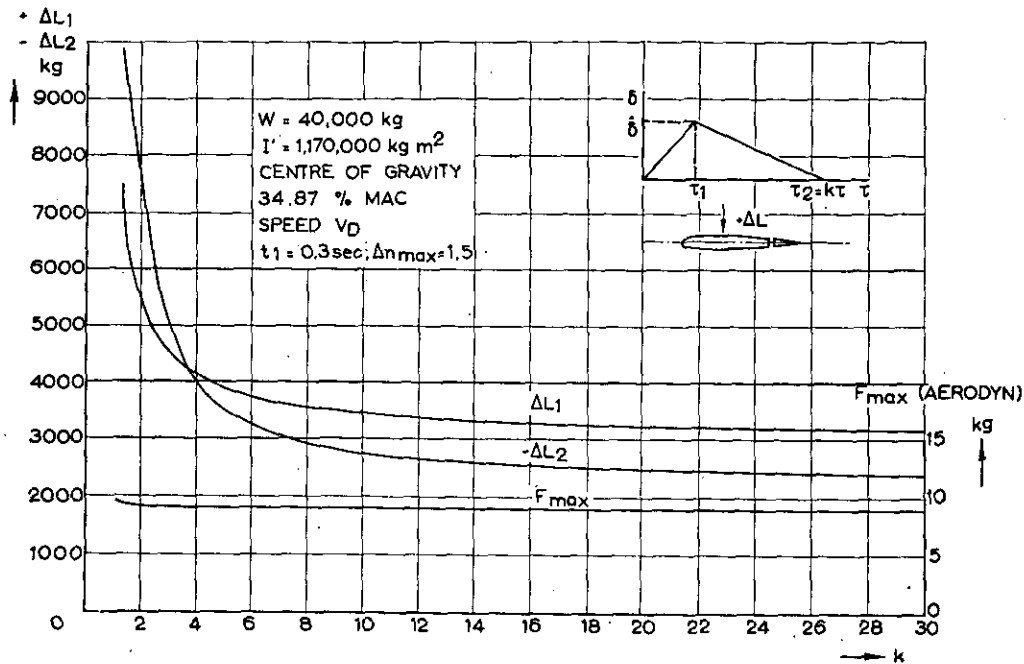


Fig. 33. Airplane B.  $\Delta L_1$ ,  $\Delta L_2$  and  $F_{\text{max}}$  as functions of  $k = \frac{\tau_2}{\tau_1}$  ( $\Delta n_{\text{max}} = 1.5$ ). Speed  $V_D$ .

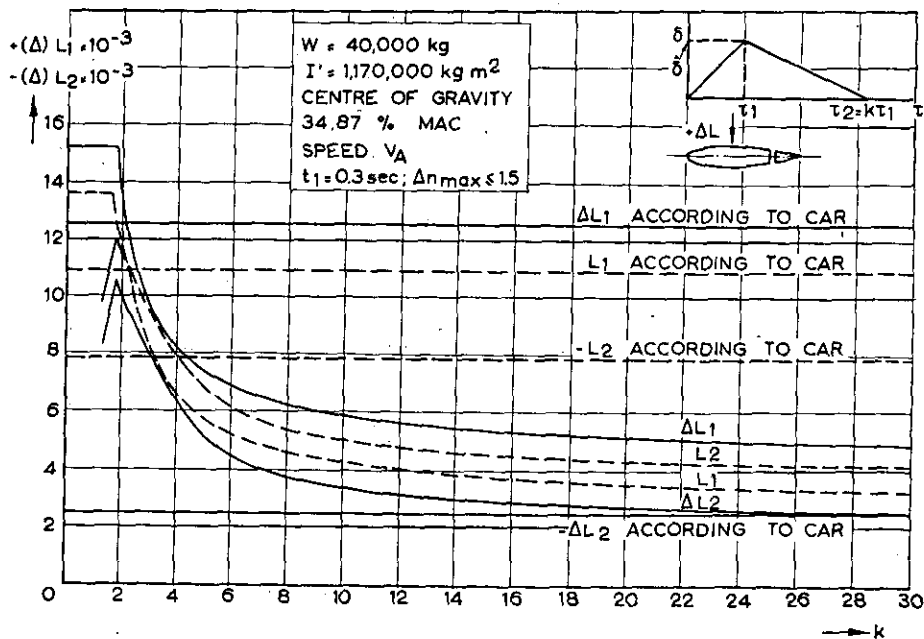


Fig. 34. Airplane B. Comparison of computed tail loads (as functions of  $k$ ) with those according to CAR. Speed  $V_A$ .

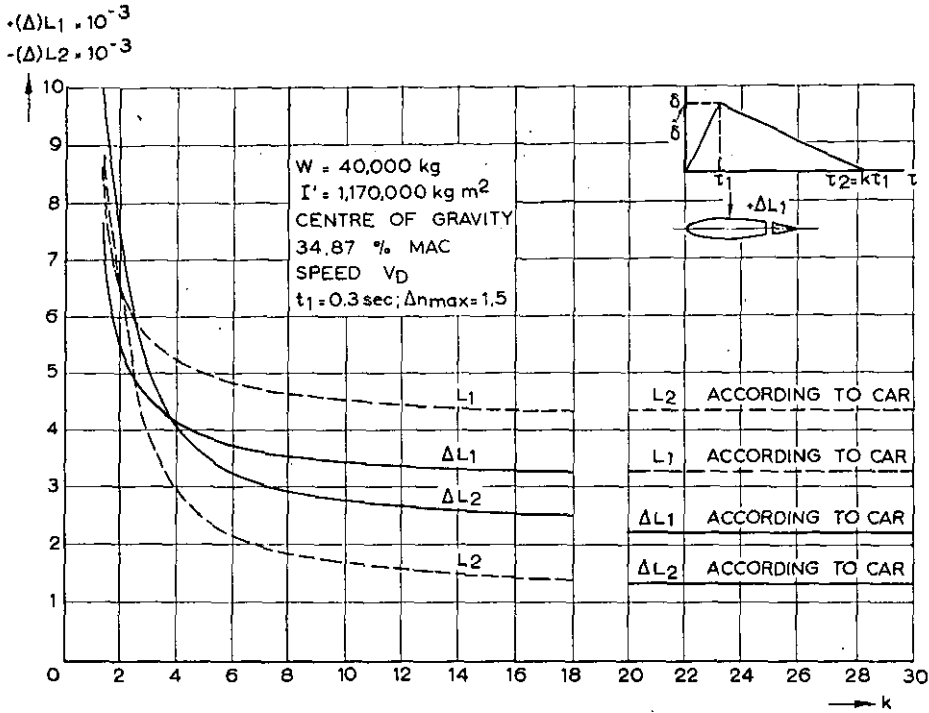


Fig. 35. Airplane B. Comparison of computed tail loads (as functions of  $k$ ) with those according to CAR. Speed  $V_D$ .

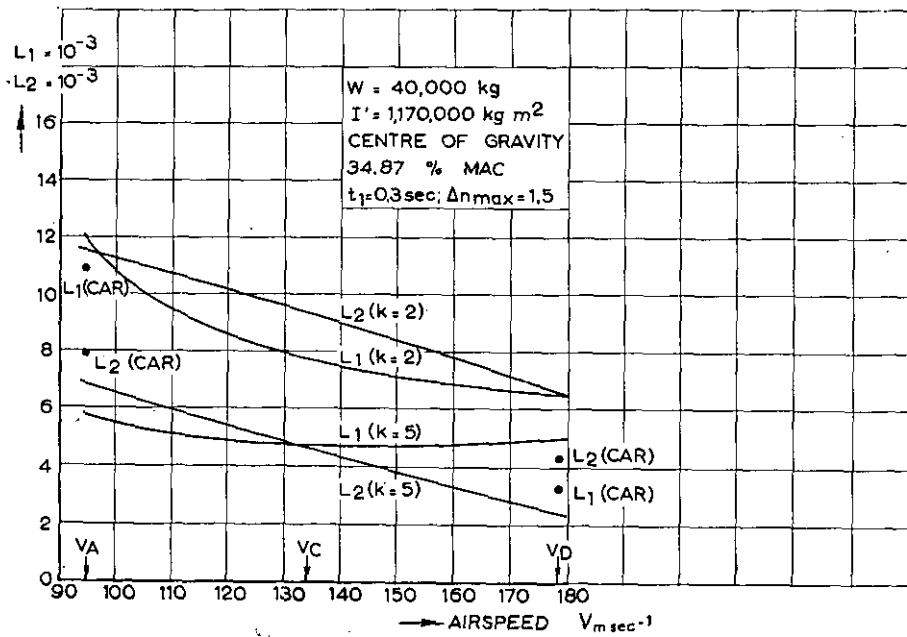


Fig. 36. Airplane B.  $L_1$  and  $L_2$  as functions of airspeed for  $k=2$  and  $k=5$  ( $\Delta n_{\text{max}} = 1.5$ ).

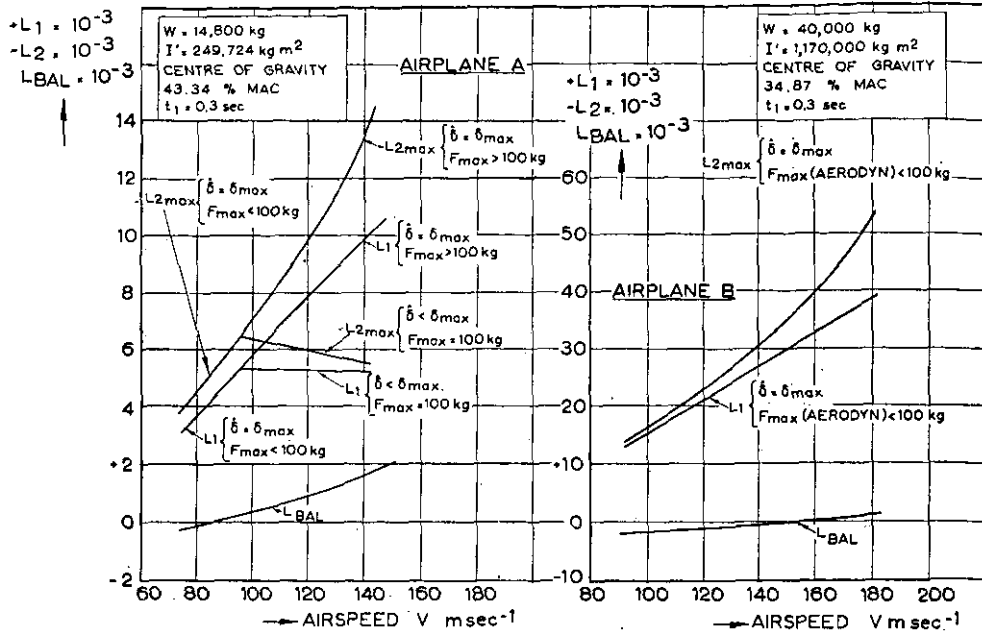


Fig. 37. Airplane A and B.  $L_1$ ,  $L_2$  and the balancing load as functions of airspeed.

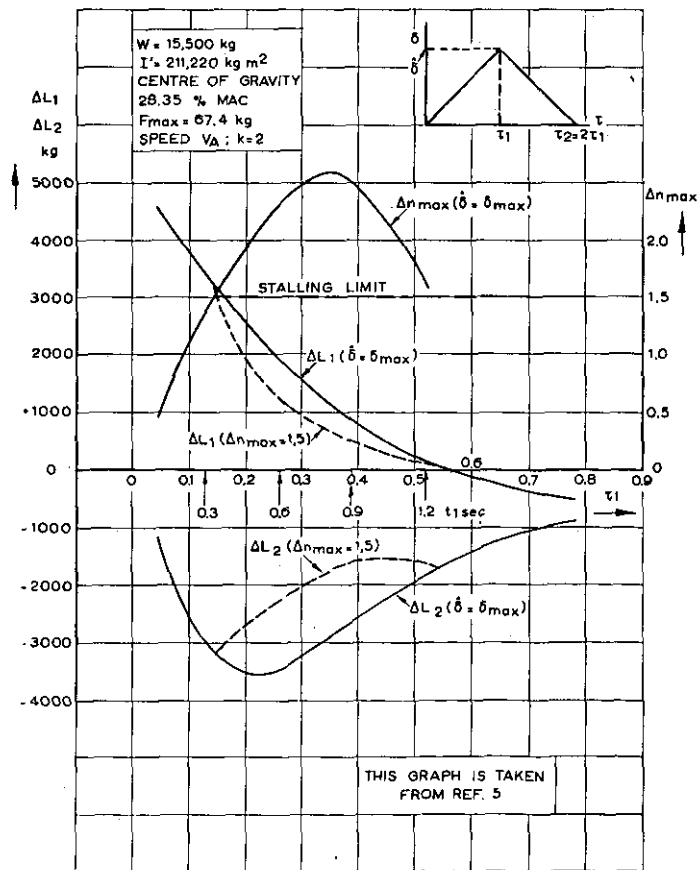


Fig. 38. Airplane A.  $\Delta L_1$ ,  $\Delta L_2$  and  $\Delta n_{max}$  as functions of the "control time"  $\tau_1$  ( $k=2$ ). Speed  $V_A$ .

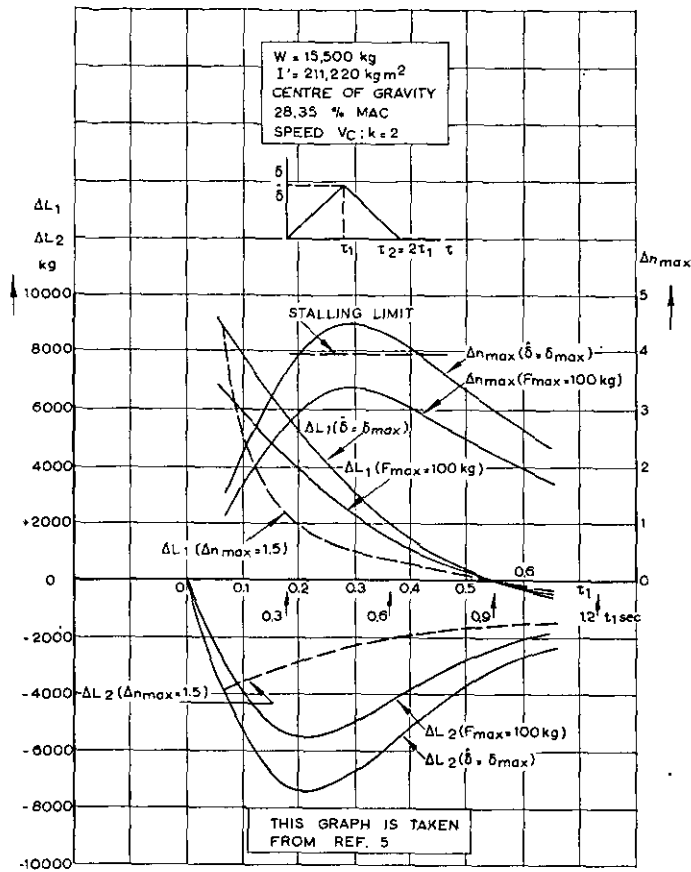


Fig. 39. Airplane A.  $\Delta L_1$ ,  $\Delta L_2$  and  $\Delta n_{max}$  as functions of the "control time"  $\tau_1$  ( $k = 2$ ). Speed  $V_C$ .

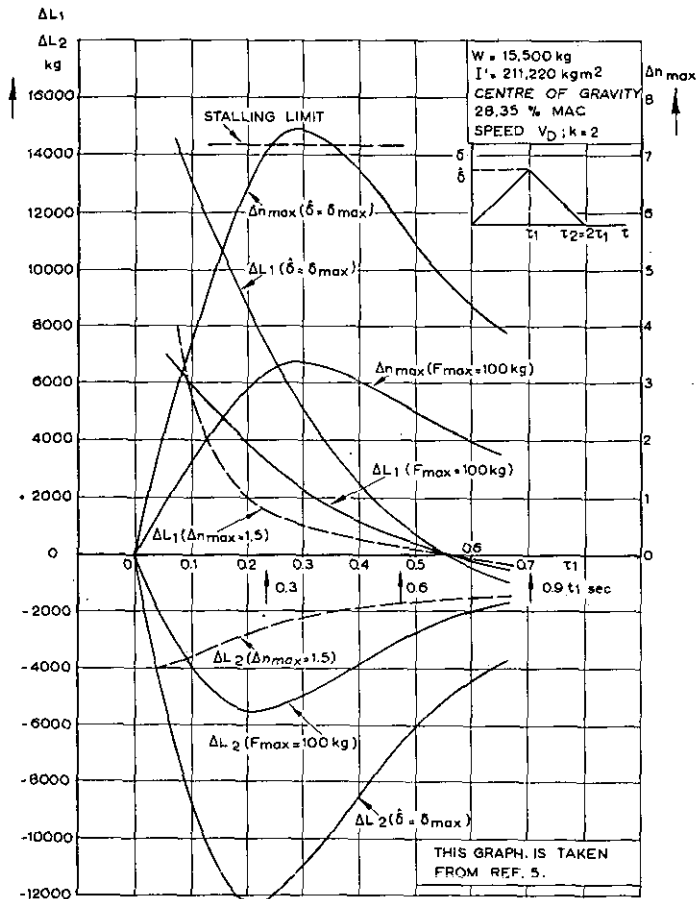


Fig. 40. Airplane A.  $\Delta L_1$ ,  $\Delta L_2$  and  $\Delta n_{max}$  as functions of the "control time"  $\tau_1$  ( $k = 2$ ). Speed  $V_D$ .

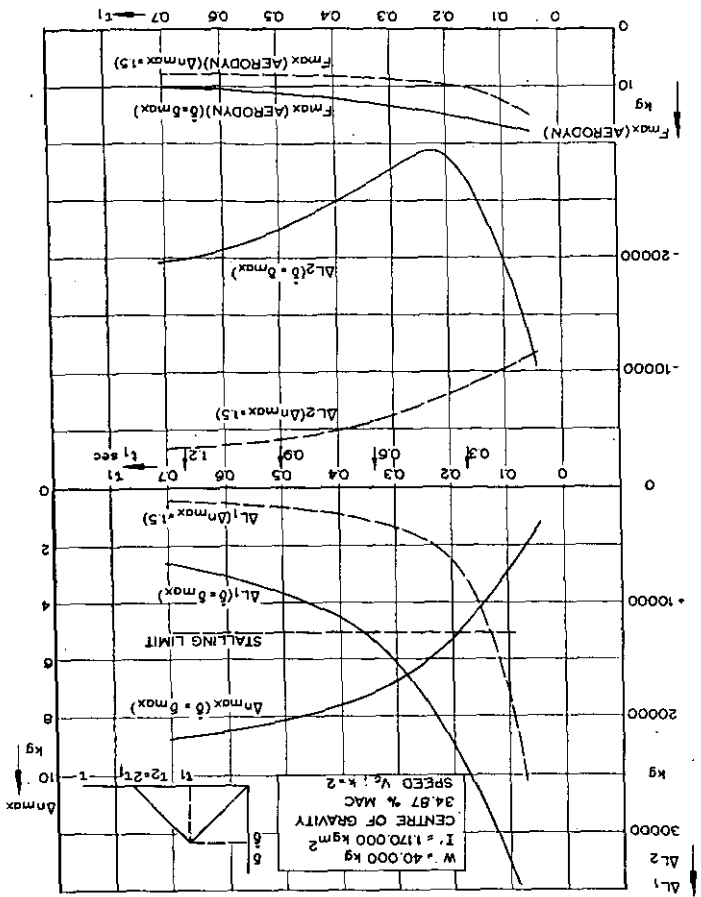


Fig. 41. Airplane B.  $\Delta L_1$ ,  $\Delta L_2$ ,  $\Delta n_{\max}$  and  $F_{\max}$  as functions of the "control time"  $\tau_1$ . Speed  $V_A$ .

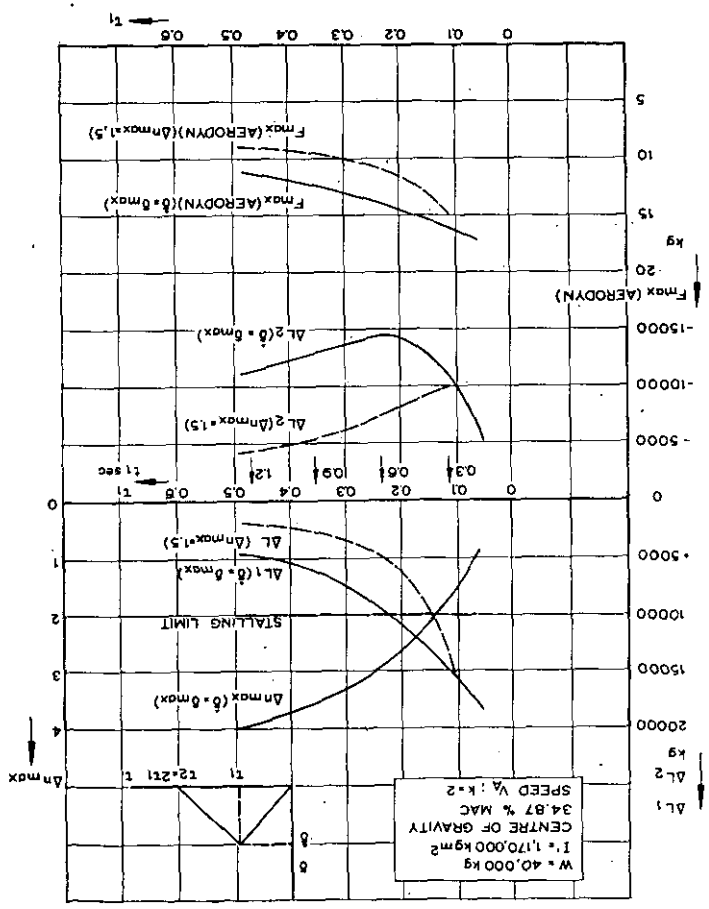


Fig. 42. Airplane B.  $\Delta L_1$ ,  $\Delta L_2$ ,  $\Delta n_{\max}$  and  $F_{\max}$  as functions of the "control time"  $\tau_1$ . Speed  $V_A$ .

Fig. 43. Airplane B.  $\Delta L_1$ ,  $\Delta L_2$ ,  $\Delta n_{max}$  and  $F_{max}$  as functions of the "control time"  $\tau_1$ . Speed  $V_D$ .

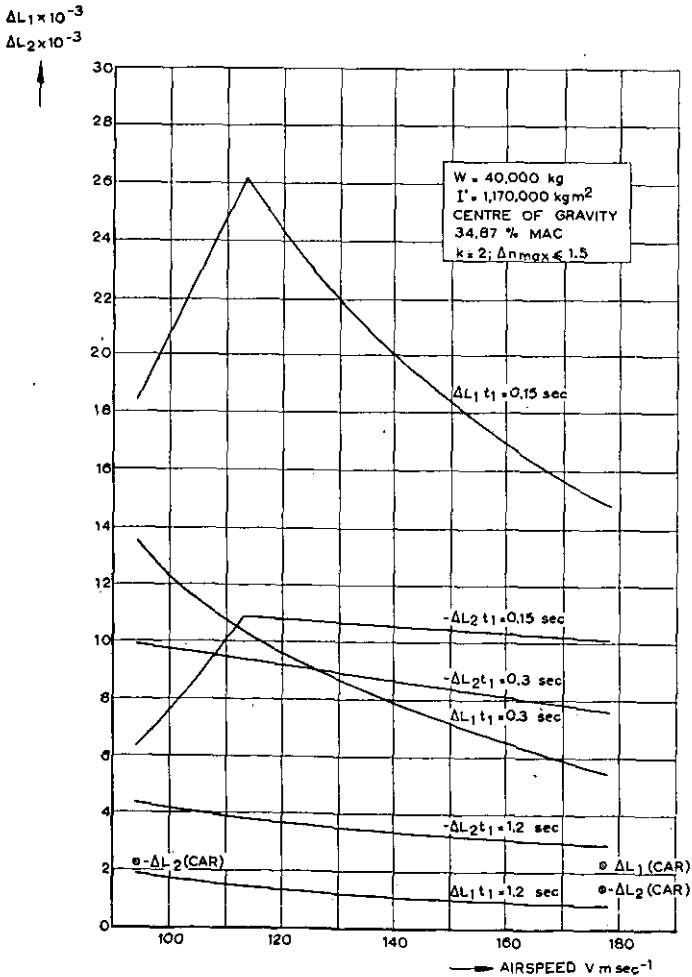
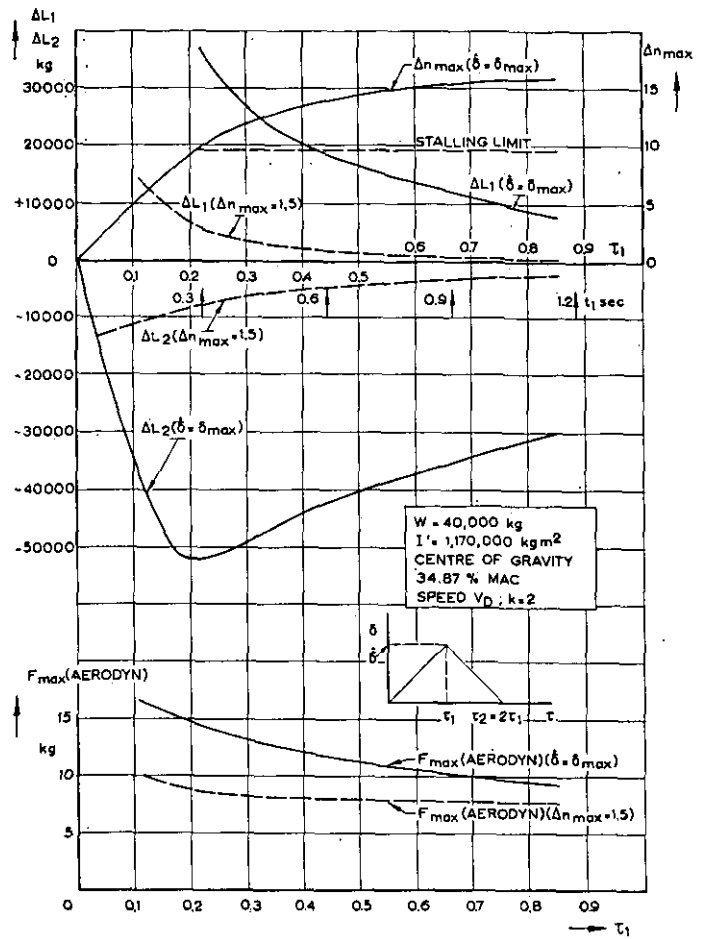


Fig. 44. Airplane B.  $\Delta L_1$  and  $\Delta L_2$  as functions of airspeed ( $\Delta n_{max} \leq 1.5$ ).

TABLE 1.

Numerical data.

	Airplane A	Airplane B			Airplane A	Airplane B	
$S$	70	135.7	$m^2$	$\eta$ (speed $V_A$ )	0.95	1.00	—
$S_t$	16	33.7	$m^2$	$\eta$ (speed $V_C$ and $V_D$ )	1.00	1.00	—
$-x_t + h$	10.892	16.080	m	$V_A$	78.0	94.3	$m \text{ sec}^{-1}$
$b_t$	9.127	14.173	m	$V_C$	110.0	134.1	$m \text{ sec}^{-1}$
$\frac{d\epsilon}{d\alpha}$	0.360	0.395	—	$V_D$	141.4	178.4	$m \text{ sec}^{-1}$
$K$	1.1	1.1	—	$b_1 = \frac{dC_H}{d\alpha_t}$	0	-0.117	$\text{rad}^{-1}$
$\left(\frac{dC_L}{d\alpha}\right)_w$	5.680	4.699	$\text{rad}^{-1}$	$b_2 = \frac{dC_H}{d\delta}$	-0.19	-0.119	$\text{rad}^{-1}$
$\left(\frac{dC_L}{d\alpha}\right)_t$	4.10	3.50	$\text{rad}^{-1}$	$b_3 = \frac{dC_H}{d\delta_t}$	—	-0.175	$\text{rad}^{-1}$
$\left(\frac{dC_L}{d\delta}\right)_t$	2.00	2.58	$\text{rad}^{-1}$	$m_e$	1.89	2.09	$m^{-1}$
$\left(\frac{dC_m}{d\delta}\right)_t$	-0.50	-0.416	$\text{rad}^{-1}$	$S_e$	3.182	10.12	$m^2$
$\rho$	0.12492		$\text{kg sec}^2 m^{-4}$	$c_e$	0.356	0.808	m
$g$	9.8067		$m \text{ sec}^{-2}$	$C$	—	0.02604	$\text{rad kg}^{-1}$
				Airplane A		Airplane B	
Weight variation			15,500 kg $\longleftrightarrow$ 13,000 kg			48,081 kg $\longleftrightarrow$ 28,900 kg	
Moment of inertia variation			249,700 $\text{kgm}^2 \longleftrightarrow$ 185,000 $\text{kgm}^2$			1,170,000 $\text{kgm}^2 \longleftrightarrow$ 1,051,794 $\text{kgm}^2$	
Centre of gravity variation			28.35 % MAC $\longleftrightarrow$ 43.03 % MAC			13.50 % MAC $\longleftrightarrow$ 34.87 % MAC	
<i>Elevator and spring tab deflections:</i>							
$\delta_{\max} = \pm 0.436 \text{ rad } (\pm 25^\circ) \text{ (Airplane A and B)}$							
$\delta_{t \max} = + 0.349 \text{ rad } (+ 20^\circ) \text{ (Airplane B)}$							
$\delta_{t \min} = - 0.140 \text{ rad } (- 8^\circ) \text{ (Airplane B)}$							

TABLE 2.

Critical conditions for  $\Delta L_1$ ,  $\Delta L_2$  and  $\Delta n_{\max}$ .

	kind of manoeuvre	critical condition		
		centre of gravity	weight	moment of inertia
$\Delta L_1$	$\hat{\delta} = \delta_{\max}$ or $F_{\max} = 100$ kg	—*)	—*)	large
	$\Delta n_{\max} = 1.5$	forward (except at $V_A$ )	large	large
$\Delta L_2$	$\hat{\delta} = \delta_{\max}$ or $F_{\max} = 100$ kg	aft	large	small
	$\Delta n_{\max} = 1.5$	aft	large	—*)
$\Delta n_{\max}$	$\hat{\delta} = \delta_{\max}$ or $F_{\max} = 100$ kg	aft	small	small

\*) — means that the effect is small.



REPORT NLR-TR S. 542

# A stress diffusion problem for a wedge-shaped plate with three stiffeners

by

J. P. BENTHEM and J. VAN DER VOOREN.

## Summary.

The isotropic wedge has two edge-stiffeners of equal normal rigidity and a stiffener along the bisector of the wedge. A force acts at the vertex in the direction of the latter stiffener. Methods, previously used by the authors for wedges with one stiffener, are extended for the present case.

The method involves use of the Mellin transform and the numerical solution of two simultaneous singular integral equations of the Cauchy type.

Applications are given for a half wedge angle  $\alpha = 90^\circ$ , i.e. for the half plane with an edge-stiffener and a stiffener normal to the edge, for different stiffness ratios of the stiffeners.

This investigation has been performed under contract with the Netherlands Aircraft Development Board (N.I.V.).

## Contents.

- 1 Introduction.
- 2 Stress-strain relations and expressions for the stress flows in oblique coordinates.
- 3 The boundary conditions and the application of the Mellin transform.
- 4 The position of the poles of  $T_I[s]$  and  $T_{II}[s]$  in the complex  $s$ -plane.
- 5 Evaluation of expansions for  $\hat{t}_I[x]$  and  $t_{II}[y]$ .
- 6 Application of the inverse Mellin transform to the functional equations.
- 7 Determination of the functions  $h_{11}\left[\frac{x}{\xi}\right]$ ,  $f_{12}\left[\frac{x}{\eta}\right]$ ,  $f_{21}\left[\frac{y}{\xi}\right]$  and  $h_{22}\left[\frac{y}{\eta}\right]$ .
- 8 Solution of the problem for  $\alpha = \pi/2$ .
  - 8.1 The expansions for the functions  $\hat{t}_I[x] = t_I[x]$  and  $t_{II}[y]$ .
    - 8.1.1 Small values of  $x$  and  $y$ .
    - 8.1.2 Large values of  $x$  and  $y$ .
      - 8.1.2.1 Expansion for  $t_I[x]$ .
      - 8.1.2.2 Expansion for  $t_{II}[y]$ .
  - 8.2 Determination of the functions  $h_{11}\left[\frac{x}{\xi}\right]$ ,  $f_{12}\left[\frac{x}{\eta}\right]$ ,  $f_{21}\left[\frac{y}{\xi}\right]$ ,  $h_{22}\left[\frac{y}{\eta}\right]$  in case  $\alpha = \pi/2$ .
  - 8.3 Final solutions for  $t_I[x]$  and  $t_{II}[y]$  by means of the integral equations.
9. Way to solution for some other cases.
10. References.

Appendix A — The relation between  $f_{12}\left[\frac{x}{\eta}\right]$  and  $f_{21}\left[\frac{y}{\xi}\right]$ , respectively  $a_{12}[s]$  and  $a_{21}[s]$ .

Appendix B — Analytical integration of some terms in eqs. (8.41) and (8.42) with the aid of (8.43).

6 tables.

14 figures.

## Notations.<sup>1)</sup>

I, II	suffices referring to stiffeners, see fig. 1.
$x, y$	oblique coordinates, defined in fig. 2.
$\alpha$	angle between coordinate axes, or the constant defined in table 2.
$\bar{u}, u_x, u_y, \bar{u}_y$	displacements defined in fig. 3.
$\varepsilon_x, \varepsilon_y, \gamma$	oblique straincomponents, defined in (2.1).
$A_{ij}$	symmetrical matrix, defined in (2.2).
$s_x, s_y, t$	oblique stressflowcomponents, see fig. 2.
$f_i, g_i$	functions of the complex variable $[x + \lambda_i y]$ .
$g_i'$	first derivative of $g_i$ with respect to $[x + \lambda_i y]$ .
$\lambda_i$	roots of eq. (2.4).
$N$	normal force in stiffener.

<sup>1)</sup> Some quantities are replaced by dimensionless quantities with the aid of formula (3.5), without (ultimately) altering their notation (the indication "dl" is dropped again).

$E$	Young's modulus of the wedge material.
$\nu$	Poisson's ratio of the wedge material (0.3).
$h$	plate thickness of the wedge.
$E_s$	Young's modulus of a stiffener.
$A_s$	cross-sectional area of a stiffener.
$P$	load at the vertex, see fig. 1.
$t_I$	oblique stressflow component $t$ along stiffener I.
$t_{II}$	oblique stressflow component $t$ along stiffener II.
$\hat{t}_I$	$t_I + s_{\nu I} \cos \alpha$ , see eq. (3.16).
$H[s]$	Mellin transform of $h[z]$ , according to $H[s] = \int_0^{\infty} h[z] z^{s-1} dz$
	where $s$ is a complex variable.
$\beta P$	normal force in the edge-stiffener at the vertex, see eq. (4.1).
$c$	$(E_s A_s)_I / (E_s A_s)_{II}$ , ratio of normal stiffnesses of the stiffeners I and II.
$\xi$	oblique coordinate, synonymous to $x$ .
$\eta$	oblique coordinate, synonymous to $y$ .
$f_{ij}$ , $i, j=1, 2$	functions, defined in eqs. (6.11) ... (6.14).
$h_{11} \left[ \frac{x}{\xi} \right], h_{22} \left[ \frac{y}{\eta} \right]$	functions, defined in eqs. (6.20), (6.21).
$P_I, P_{II} (= \beta P)$	normal forces in the stiffeners I and II at the vertex.
$\zeta$	symbol, replacing $\eta$ and $\xi$ .
$g_1 \left[ \frac{x}{\zeta} \right]$ $g_2 \left[ \frac{x}{\zeta} \right]$ $g_3 \left[ \frac{x}{\zeta} \right]$	functions, defined in eqs. (8.44) ... (8.46).
$t_I^*[\zeta], t_{II}^*[\zeta]$	
$t_I^{**}[\zeta], t_{II}^{**}[\zeta]$	expansions for $t_I[\zeta]$ and $t_{II}[\zeta]$ in case $\zeta \ll 1$ , see eqs. (8.43).
	expansions for $t_I[\zeta]$ and $t_{II}[\zeta]$ in case $\zeta \gg 1$ , see eqs. (8.43).

## 1 Introduction.

In ref. 1, KORTER solved the problem of the diffusion of a load from a semi-infinite edge-stiffener into an isotropic half plane. The shear flow acting from the stiffener on the half plane is  $t[x]$ . Its Mellin transform is

$$T[s] = \int_0^{\infty} t[x] x^{s-1} dx. \quad (1.1)$$

In ref. 1 a functional equation

$$T[s+1] = -2s T[s] \cot \pi s \quad (1.2)$$

is obtained, which is solved. From this solution  $t[x]$  is determined.

In ref. 2 the authors developed a method to deal with wedge-shaped plates with one edge-stiffener and one edge free. Again the shearflow, acting from the stiffener on the wedge, is  $t[x]$ , its Mellin transform  $T[s]$ . A functional equation

$$T[s+1] = Z[s] T[s] \quad (1.3)$$

is obtained, where  $Z[s]$  is a known function. The further solution of the problem could not follow the lines of ref. 1, since these seem only to be applicable for the wedge angle  $\alpha = 180^\circ$  (i.e. the half plane with semi-infinite edge-stiffener).

The method of ref. 2 is not exact but delivers answers of high accuracy, also for the singular behaviour at  $x \rightarrow 0$  and the asymptotic behaviour at  $x \rightarrow \infty$ .

In this paper the method of ref. 2 is further extended for a case where more than one stiffener is involved. An isotropic wedge with two edge-stiffeners of equal normal rigidity and one stiffener along the bisector of the wedge is investigated. The loading force acts at the vertex in the direction of the latter stiffener. Due to the symmetry of the configuration, only half of the wedge needs to be considered. In view of a possible further extension to anisotropic plates, which could be undertaken, oblique coordinates are used instead of polar coordinates (see also ref. 3).

Along the bisector-stiffener there is a shear flow  $t_I[x]$  and along the edge-stiffener a shear flow  $t_{II}[y]$ . Their respective Mellin transforms are

$$T_I[s] = \int_0^{\infty} t_I[x] x^{s-1} dx \quad (1.4)$$

$$T_{II}[s] = \int_0^{\infty} t_{II}[y] y^{s-1} dy.$$

Instead of (1.3) two simultaneous functional equations

$$\begin{aligned} T_I[s+1] &= Z_{11}[s] T_I[s] + Z_{12}[s] T_{II}[s] \\ T_{II}[s+1] &= Z_{21}[s] T_I[s] + Z_{22}[s] T_{II}[s] \end{aligned} \quad (1.5)$$

are obtained.

When the inverse Mellin transform is applied to these functional equations, two simultaneous singular integral equations of the Cauchy type are obtained. These are to be solved numerically.

Applications are given for a half wedge angle  $\alpha = 90^\circ$ , i.e. for the half plane with an edge-stiffener and a stiffener normal to the edge. There proves to be a logarithmic singularity at  $x=0$ ,  $y=0$ .

In ref. 1, 2 and in the present paper the bending stiffness of the edge stiffener is neglected. Calculations where finite bending and shear stiffnesses of this stiffener are taken into account are now under progress.

## 2 Stress-strain relations and expressions for the stress flows in oblique coordinates.

Fig. 1 shows the configuration to be analyzed. As mentioned, only half this configuration (fig. 2) has to be considered. Fig. 2 also shows the choice of the oblique coordinate system as well as the sign conventions used for the stress flows. Finally, fig. 3 gives the definition of the displacements and strains. The stress-strain relations for the isotropic plate will be repeated here for convenience from ref. 2.

$$\begin{aligned}
 \epsilon_x &= \frac{\partial u}{\partial x} = A_{11} s_x + A_{12} s_y + A_{13} t \\
 \epsilon_y &= \frac{\partial v}{\partial y} = A_{21} s_x + A_{22} s_y + A_{23} t \\
 \gamma &= \frac{\partial v}{\partial x} + \frac{\partial u}{\partial y} = A_{31} s_x + A_{32} s_y + A_{33} t
 \end{aligned}
 \tag{21}$$

where the symmetrical matrix  $A_{ij}$  reads

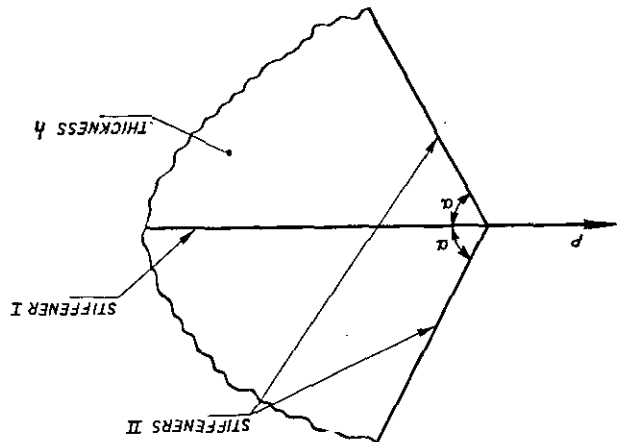


Fig. 1. The configuration to be analyzed.

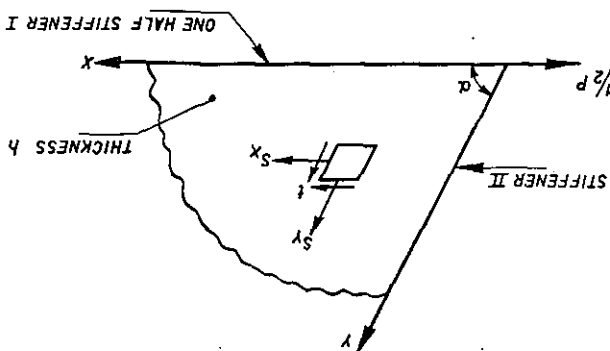


Fig. 2. Definition of the oblique coordinate system and sign convention for the stress flows.

$$\begin{aligned}
 \epsilon_x &= \frac{\partial u}{\partial x} \\
 \epsilon_y &= \frac{\partial v}{\partial y} \\
 \gamma &= \frac{\partial v}{\partial x} + \frac{\partial u}{\partial y}
 \end{aligned}$$

Fig. 3. Definition of the displacement components.

$$\begin{aligned}
 A_{ij} &= \frac{Eh \sin \alpha}{1} \begin{vmatrix} 1 & \cos^2 \alpha - \nu \sin^2 \alpha & 2 \cos \alpha \\ \cos^2 \alpha - \nu \sin^2 \alpha & 1 & 2 \cos \alpha \\ 2 \cos \alpha & 2 \cos \alpha & 2(1 + \cos^2 \alpha + \nu \sin^2 \alpha) \end{vmatrix}
 \end{aligned}
 \tag{22}$$

The expression for the stress flows are (see also ref. 2, or ref. 3)

$$\begin{aligned}
 s_x &= \sum_{i=1}^2 \lambda_i^2 \{ f_i [x + \lambda_i y] - 2 g_i [x + \lambda_i y] + (x - \lambda_i y) g_i' [x + \lambda_i y] \} \\
 s_y &= \sum_{i=1}^2 \{ f_i [x + \lambda_i y] + 2 g_i [x + \lambda_i y] + (x - \lambda_i y) g_i' [x + \lambda_i y] \} \\
 t &= - \sum_{i=1}^2 \lambda_i \{ f_i [x + \lambda_i y] + (x - \lambda_i y) g_i' [x + \lambda_i y] \}
 \end{aligned}
 \tag{23}$$

where the  $\lambda_i$  are two distinct pairs of equal roots of

$$A_{11} \lambda^4 - 2 A_{12} \lambda^3 + (2 A_{13} + A_{23}) \lambda^2 - 2 A_{22} \lambda + A_{22} = 0.
 \tag{24}$$

They are found to be  $\lambda_{1,2} = \exp \pm i\alpha$ .

The  $f_{1,2}$  and  $g_{1,2}$  are analytic functions of the complex variables  $(x + \lambda_{1,2} y)$ .

### 3 The boundary conditions and the application of the Mellin transform.

Along the  $x$ -axis (stiffener I) the two boundary conditions are found from the requirement that the displacement component perpendicular to the concerned stiffener must be zero and from the equilibrium of a stiffener element in  $x$ -direction.

In view of the figs. 3 and 4 these conditions read respectively

$$\bar{u}_{y1} = u_{y1} \sin \alpha - u_{z1} / \tan \alpha = 0
 \tag{31}$$

and

$$\frac{1}{t} \frac{dN_1}{dx} + t_1 + s_{y1} \cos \alpha = 0.
 \tag{32}$$

Along the  $y$ -axis (stiffener II) the boundary conditions are found from the equilibrium of a stiffener element in  $y$ -direction and the direction perpendicular to it. Assuming that stiffener II has only normal rigidity, these conditions read, according to fig. 5,

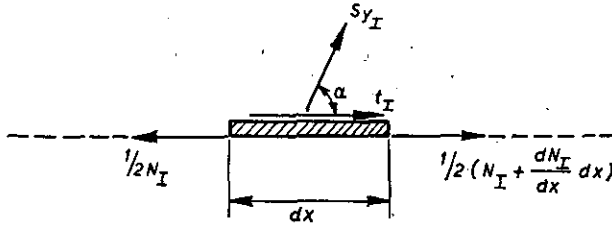


Fig. 4. Equilibrium of an element of the half stiffener I.

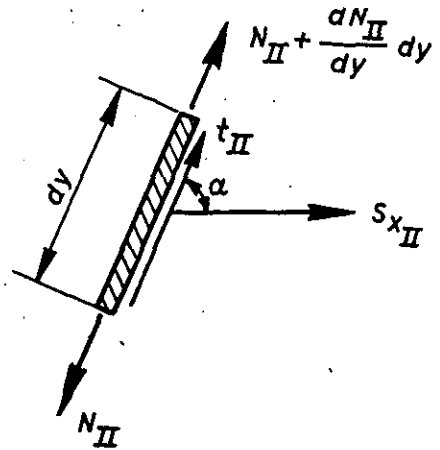


Fig. 5. Equilibrium of an element of stiffener II.

$$\frac{dN_{II}}{dy} + t_{II} + s_{xII} \cos \alpha = 0 \quad (3.3)$$

and

$$s_{xII} \sin \alpha = 0. \quad (3.4)$$

Dimensionless quantities are now introduced by the substitutions

$$\begin{aligned} x &= \frac{(E_s A_s)_{II}}{Eh} x_{aI} & s_x &= \frac{PEh}{(E_s A_s)_{II}} s_{x,aI} & \varepsilon_x &= \frac{P}{(E_s A_s)_{II}} \varepsilon_{x,aI} \\ y &= \frac{(E_s A_s)_{II}}{Eh} y_{aI} & s_y &= \frac{PEh}{(E_s A_s)_{II}} s_{y,aI} & \varepsilon_y &= \frac{P}{(E_s A_s)_{II}} \varepsilon_{y,aI} \\ t &= \frac{PEh}{(E_s A_s)_{II}} t_{aI} & \gamma &= \frac{P}{(E_s A_s)_{II}} \gamma_{aI} \\ f_i &= \frac{PEh}{(E_s A_s)_{II}} f_{i,aI}, & g_i &= \frac{PEh}{(E_s A_s)_{II}} g_{i,aI} \end{aligned} \quad (3.5)$$

When these expressions are substituted into all equations, and if again the notation " $dl$ " is dropped, all equations preserve their original shape, with however

$$P = 1, E = 1, h = 1, E_{sI} = 1, A_{sI} = c \quad (3.6)$$

$$E_{sII} = 1, A_{sII} = 1$$

where

$$c = (E_s A_s)_I / (E_s A_s)_{II}. \quad (3.7)$$

By a twofold differentiation of (3.1) with respect to  $x$  and substitution of the relation

$$\frac{\partial \gamma}{\partial x} = \frac{\partial^2 u_y}{\partial x^2} + \frac{\partial \varepsilon_x}{\partial y}$$

the condition (3.1) can be replaced by eq. (3.8).

The boundary conditions (3.2) and (3.3) are replaced by the eqs. (3.9) and (3.10) after using eq. (3.6), taking into account that the strains in the stiffeners I and II are equal to the strains  $(\varepsilon_x)_{y=0}$  and  $(\varepsilon_y)_{x=0}$  in the plate respectively and taking  $s_{xII} = 0$ , see eq. (3.4).

The boundary conditions thus become

$$\text{for } y = 0: \quad \frac{1}{\sin \alpha} \frac{\partial \gamma}{\partial x} - \frac{1}{\sin \alpha} \frac{\partial \varepsilon_x}{\partial y} - \frac{1}{\text{tg } \alpha} \frac{\partial \varepsilon_x}{\partial x} = 0 \quad (3.8)$$

$$\frac{1}{2} c \frac{d(\varepsilon_x)_{y=0}}{dx} + (t_I + s_y \cos \alpha) = 0 \quad (3.9)$$

$$\text{and for } x = 0: \quad \frac{d(\varepsilon_y)_{x=0}}{dy} + t_{II} = 0 \quad (3.10)$$

$$s_x = 0. \quad (3.11)$$

Substitution of the eqs. (2.1), (2.3), making use of (2.4), finally brings the four boundary conditions into the desired form. They now read successively

$$\begin{aligned} \Sigma [ \{ -A_{11} \lambda_i^2 \cos \alpha + (A_{12} + A_{13} \cos \alpha) \lambda_i - (A_{32} + A_{12} \cos \alpha) + A_{22}/\lambda_i \} f_i'[x] + \\ + \{ (4A_{13} + A_{11} \cos \alpha) \lambda_i^2 - (7A_{12} + 4A_{33} - A_{13} \cos \alpha) \lambda_i + (9A_{32} - 3A_{12} \cos \alpha) - \\ - 3A_{22}/\lambda_i \} g_i'[x] + \{ -A_{11} \lambda_i^2 \cos \alpha + (A_{12} + A_{13} \cos \alpha) \lambda_i - (A_{32} + A_{12} \cos \alpha) + \\ + A_{22}/\lambda_i \} x g_i''[x] ] = 0. \end{aligned} \quad (3.12)$$

$$\begin{aligned} \frac{1}{2} c \Sigma \{ (A_{11} \lambda_i^2 + A_{12} - A_{13} \lambda_i) f_i'[x] + (-A_{11} \lambda_i^2 + 3A_{12} - A_{13} \lambda_i) g_i'[x] + \\ + (A_{11} \lambda_i^2 + A_{12} - A_{13} \lambda_i) x g_i''[x] \} + (t_I + s_y \cos \alpha) = 0. \end{aligned} \quad (3.13)$$

$$\Sigma \{ (A_{22} \lambda_i - A_{23} \lambda_i^2) f_i'[\lambda_i y] + (A_{22} \lambda_i + A_{23} \lambda_i^2) g_i'[\lambda_i y] + (-A_{22} \lambda_i + A_{23} \lambda_i^2) (\lambda_i y) g_i''[\lambda_i y] \} + t_{II} = 0. \quad (3.14)$$

$$\Sigma \lambda_i^2 \{ f_i[\lambda_i y] - 2g_i[\lambda_i y] - (\lambda_i y) g_i'[\lambda_i y] \} = 0. \quad (3.15)$$

Furthermore, expressions for  $(t_I + s_y \cos \alpha)$  and  $t_{II}$  are available from (2.3). They read

$$\hat{t}_I = t_I + s_y \cos \alpha = \Sigma \{ (\cos \alpha - \lambda_i) f_i[x] + (2 \cos \alpha) g_i[x] + (\cos \alpha - \lambda_i) x g_i'[x] \} \quad (3.16)$$

$$t_{II} = -\Sigma \lambda_i \{ f_i[\lambda_i y] - (\lambda_i y) g_i'[\lambda_i y] \} \quad (3.17)$$

where the  $\wedge$  sign denotes a shear stress flow as it is defined in orthogonal coordinates.

Application of the Mellin transforms  $\int_0^\infty \dots x^{s-1} dx$  to (3.12), (3.13), (3.16) and  $\int_0^\infty \dots y^{s-1} dy$  to (3.14), (3.15), (3.17) delivers in accordance with ref. 3, pag. 14, formulas (4.8), (4.9)

$$\begin{aligned} \Sigma [ - \{ -A_{11} \lambda_i^2 \cos \alpha + (A_{12} + A_{13} \cos \alpha) \lambda_i - (A_{32} + A_{12} \cos \alpha) + A_{22}/\lambda_i \} (s-1) F_i[s-1] - \\ \{ (4A_{13} + A_{11} \cos \alpha) \lambda_i^2 - (7A_{12} + 4A_{33} - A_{13} \cos \alpha) \lambda_i + (9A_{32} - 3A_{12} \cos \alpha) - 3A_{22}/\lambda_i \} \\ (s-1) G_i[s-1] + \{ -A_{11} \lambda_i^2 \cos \alpha + (A_{12} + A_{13} \cos \alpha) \lambda_i - (A_{32} + A_{12} \cos \alpha) + \\ + A_{22}/\lambda_i \} s(s-1) G_i[s-1] ] = 0 \end{aligned} \quad (3.18)$$

$$\begin{aligned} \frac{1}{2} c \Sigma \{ - (A_{11} \lambda_i^2 + A_{12} - A_{13} \lambda_i) (s-1) F_i[s-1] - (-A_{11} \lambda_i^2 + 3A_{12} - A_{13} \lambda_i) \\ (s-1) G_i[s-1] + (A_{11} \lambda_i^2 + A_{12} - A_{13} \lambda_i) s (s-1) G_i[s-1] \} + T_I[s] = 0 \end{aligned} \quad (3.19)$$

$$\Sigma \{ - (A_{22} - A_{23} \lambda_i) \lambda_i^{1-s} (s-1) F_i[s-1] - (A_{22} + A_{23} \lambda_i) \lambda_i^{1-s} (s-1) G_i[s-1] + \\ + (-A_{22} + A_{23} \lambda_i) \lambda_i^{1-s} s (s-1) G_i[s-1] \} + T_{II}[s] = 0 \quad (3.20)$$

$$\Sigma \{ \lambda_i^{2-s} F_i[s] - 2 \lambda_i^{2-s} G_i[s] + \lambda_i^{2-s} s G_i[s] \} = 0 \quad (3.21)$$

$$T_I[s] = \Sigma \{ (\cos \alpha - \lambda_i) F_i[s] + 2 \cos \alpha G_i[s] - (\cos \alpha - \lambda_i) s G_i[s] \} \quad (3.22)$$

$$T_{II}[s] = \Sigma \{ -\lambda_i^{1-s} F_i[s] - \lambda_i^{1-s} s G_i[s] \} \quad (3.23)$$

where generally  $H[s] = \int_0^\infty h[z] z^{s-1} dz$ .

After replacement of  $(s-1)$  by  $s$  in eqs. (3.18), (3.19) and (3.20) and dropping the bar again, the six expressions (3.18) ... (3.23) will now be specialized for the isotropic wedge. This is done by inserting the symmetrical matrix  $A_{ij}$  of eq. (2.2), with the factor  $Eh$  replaced by 1, and taking

$$\lambda_{1,2} = \exp \pm i \alpha. \quad (3.24)$$

The result is given in a somewhat different succession in table 1, which contains the formulas (3.25) - (3.28).

In equation (3.27)

$$c = (E_s A_s)_I / (E_s A_s)_{II}. \quad (3.29)$$

From the eqs. (3.23), (3.24), (3.25) and (3.26)  $F_1[s]$ ,  $F_2[s]$ ,  $G_1[s]$  and  $G_2[s]$  can be solved with Cramer's rule, as functions of  $T_I[s]$  and  $T_{II}[s]$ . They read

$$\begin{aligned}
& 4 \{ \sin 2(s-1)\alpha + (s-1) \sin 2\alpha \} F_{1,2} s = [ \{ -s(s-2)(1+\nu) \sin^2 \alpha \\
& -s(1-\nu) \sin \alpha \cos (s-1) \alpha \sin (s-2) \alpha - 2(1-\nu) \cos \alpha \sin (s-1) \alpha \sin (s-2) \alpha \\
& + 2(s-2) \sin \alpha \sin (s-1) \alpha \cos (s-2) \alpha \} \pm i \{ (s(1-\nu) - 2(s-2)) \\
& \sin \alpha \cos (s-1) \alpha \cos (s-2) \alpha + 2(1-\nu) \cos \alpha \cos (s-1) \alpha \sin (s-2) \alpha \\
& + s(1-\nu) \sin \alpha \cos \alpha \} ] T_I[s] + [ 2(s-2) \{ (\cos \alpha \sin (s-2) \alpha \\
& + \sin (s-1) \alpha) \mp i \cos \alpha \cos (s-2) \alpha \} ] T_{II}[s]
\end{aligned} \tag{3.30}$$

and

$$\begin{aligned}
& 4 \{ \sin 2(s-1) \alpha + (s-1) \sin 2\alpha \} G_{1,2} [s] = [ - \{ (2-s(1+\nu)) \sin \alpha \\
& - (1+\nu) \cos (s-1) \alpha \sin (s-2) \alpha \} \mp i \{ (1-\nu) \cos \alpha + (1+\nu) \cos (s-1) \alpha \\
& \cos (s-2) \alpha \} ] T_I[s] + \{ -2 \sin \alpha \cos (s-2) \alpha \mp 2i \cos \alpha \cos (s-2) \alpha \} T_{II}[s].
\end{aligned} \tag{3.31}$$

Inserting of (3.31) and (3.32) into (3.29) and (3.30) delivers, after some tedious but straightforward algebra, the functional equations for  $T_I[s]$  and  $T_{II}[s]$ . They are

$$\begin{aligned}
T_I[s+1] &= -s \frac{c - (1+\nu)(3-\nu) \sin^2(s-1)\alpha - (s-1)^2 (1+\nu)^2 \sin^2 \alpha + 4}{2 \sin 2(s-1)\alpha + (s-1) \sin 2\alpha} T_I[s] \\
&\quad - s \frac{c 2(s-2)(1+\nu) \sin \alpha \sin (s-1)\alpha + 4 \cos (s-2)\alpha}{2 \sin 2(s-1)\alpha + (s-1) \sin 2\alpha} T_{II}[s]
\end{aligned} \tag{3.32}$$

$$\begin{aligned}
T_{II}[s+1] &= -s \frac{2\{s(1+\nu) - 4\} \sin \alpha \sin (s-1)\alpha + 4 \cos (s-2)\alpha}{\sin 2(s-1)\alpha + (s-1) \sin 2\alpha} T_I[s] \\
&\quad - s \frac{-4 \sin^2(s-1)\alpha - 4 \sin^2 \alpha + 4}{\sin 2(s-1)\alpha + (s-1) \sin 2\alpha} T_{II}[s]
\end{aligned} \tag{3.33}$$

from which expansions for  $\hat{t}_I[x]$  and  $t_{II}[y]$  will be developed, for small and large values of  $x, y$  respectively, by means of inverse Mellin transforms.

In a way, similar to that used in ref. 2, it can be proved that  $\hat{t}_I[x]$  and  $t_{II}[y]$  are analytic functions.

#### 4 The position of the poles of $T_I[s]$ and $T_{II}[s]$ in the complex $s$ -plane.

The normal force in the stiffener II at  $y=0$  be

$$P_{II} = \beta P. \tag{4.1}$$

As the stiffeners I and II are connected at the vertex the normal force in stiffener I at  $x=0$  is

$$P_I = (1 - 2\beta \cos \alpha) P. \tag{4.2}$$

In (4.1) and (4.2)  $\beta$  is an unknown constant.

It is now possible to obtain values for  $T_I[1]$  and  $T_{II}[1]$

$$T_I[1] = \int_0^\infty \hat{t}_I dx \tag{4.3}$$

$$T_{II}[1] = \int_0^\infty t_{II} dy \tag{4.4}$$

Introduction of the original coordinates and shear flows with eqs. (3.5) now delivers

$$T_I[1] = \frac{1}{P} \int_0^\infty \hat{t}_I dx = \frac{\frac{1}{2} P_I}{P} = \frac{1}{2} - \beta \cos \alpha \tag{4.5}$$

$$T_{II}[1] = \frac{1}{P} \int_0^\infty t_{II} dy = \frac{P_{II}}{P} = \beta. \tag{4.6}$$

The equations (4.5) and (4.6) express the additional requirement that all stresses vanish at infinity.

From (3.32) and (3.33), in which  $T_I[s]$ ,  $T_I[s+1]$ ,  $T_{II}[s]$  and  $T_{II}[s+1]$  occur, it follows that these four functions must be defined in a strip of the complex  $s$ -plane which is parallel to the imaginary axis and wider than 1. Because the integrals (4.3) and (4.4) are certainly convergent (see 4.5), (4.6)), the point  $s=1$  must lie in the afore mentioned strip.

The integration for the inverse Mellin transform must also take place therein.

Thus

$$\begin{aligned} \operatorname{Re} a_1 &< \operatorname{Re} s < \operatorname{Re} b_1 \\ \operatorname{Re} a_1 &< 1 < \operatorname{Re} b_1 \\ \operatorname{Re} a_1 + 1 &< \operatorname{Re} b_1 \end{aligned} \quad (4.7)$$

In (4.7),  $a_1$  and  $b_1$  (and their complex conjugates  $\bar{a}_1$  and  $\bar{b}_1$ ) are poles of  $T_I[s]$  or  $T_{II}[s]$  or of both of them.

The functional equations (3.32) and (3.33) are now written in the form

$$T_I[s+1] = -\frac{cs}{2N[s]} \begin{vmatrix} T_I[s] & -t_{12}[s] \\ T_{II}[s] & t_{11}[s] \end{vmatrix} \quad (4.8a)$$

$$T_{II}[s+1] = -\frac{s}{N[s]} \begin{vmatrix} T_I[s] & -t_{22}[s] \\ T_{II}[s] & t_{21}[s] \end{vmatrix} \quad (4.8b)$$

or

$$T_I[s-1] = -\frac{2N[s-1]}{c(s-1)} \begin{vmatrix} T_I[s] & \frac{c}{2} t_{12}[s-1] \\ T_{II}[s] & t_{22}[s-1] \\ t_{11}[s-1] & t_{12}[s-1] \\ t_{21}[s-1] & t_{22}[s-1] \end{vmatrix} \quad (4.9a)$$

$$T_{II}[s-1] = -\frac{2N[s-1]}{c(s-1)} \begin{vmatrix} \frac{c}{2} t_{11}[s-1] & T_I[s] \\ t_{21}[s-1] & T_{II}[s] \\ t_{11}[s-1] & t_{12}[s-1] \\ t_{21}[s-1] & t_{22}[s-1] \end{vmatrix} \quad (4.9b)$$

where

$$\begin{aligned} t_{11}[s] &= -(1+\nu)(3-\nu) \sin^2(s-1)\alpha - (s-1)^2(1+\nu)^2 \sin^2\alpha + 4 \\ t_{12}[s] &= 2(s-2)(1+\nu) \sin\alpha \sin(s-1)\alpha + 4 \cos(s-2)\alpha \\ t_{21}[s] &= 2\{s(1+\nu) - 4\} \sin\alpha \sin(s-1)\alpha + 4 \cos(s-2)\alpha \\ t_{22}[s] &= -4 \sin^2(s-1)\alpha - 4 \sin^2\alpha + 4 \\ N[s] &= \sin 2(s-1)\alpha + (s-1) \sin 2\alpha. \end{aligned} \quad (4.10)$$

Furthermore, elaboration of the determinant

$$\Delta[s] = \begin{vmatrix} t_{11}[s] & t_{12}[s] \\ t_{21}[s] & t_{22}[s] \end{vmatrix} \quad (4.11)$$

delivers after substitution of (4.10)

$$\Delta[s] = -(1+\nu) \{ (s-1)^2(1+\nu) \sin^2 2\alpha + (3-\nu) \sin^2 2(s-1)\alpha + 4(s-1) \sin 2\alpha \sin 2(s-1)\alpha \}. \quad (4.12)$$

It appears from (4.9) and (4.11) that  $a_1$  generally is the firstcoming zero of  $s\Delta[s]$  starting from  $\operatorname{Re} s=1$  in negative direction. From (4.8) it may be expected that  $b_1$  is the firstcoming zero of  $N[s-1]$  starting from  $\operatorname{Re} s=1$  in positive direction. It can be proved that, for all values of  $\alpha$ ,  $b_1=2$ .

Analytical continuation of  $T_I[s]$  and  $T_{II}[s]$  outside the strip to the domain  $\operatorname{Re} s > \operatorname{Re} b_1$  is done with the equations (4.8), to the domain  $\operatorname{Re} s < \operatorname{Re} a_1$  with the equations (4.9).

It will be apparent from eqs. (4.8) and (4.9) that any pole of  $T_I[s]$  or  $T_{II}[s]$  in  $s=p$  generally includes poles in  $p+1$ ,  $p+2$ , etc. for  $\operatorname{Re} p > 1$  and in  $p-1$ ,  $p-2$ , etc. for  $\operatorname{Re} p < 1$ .

So there exist series of poles, each starting from a "leading" pole in  $s=p$ . The already mentioned poles at  $s=a_1$  and  $s=b_1(=2)$  are, of course, such "leading" ones.

The situation of any of these poles can be determined from the equations (4.8) and (4.9). The leading poles at  $\operatorname{Re} s < 1$  are, generally, at the zero's of  $s\Delta[s]$ , the leading poles at  $\operatorname{Re} s > 1$  at the zero's of  $N[s-1]$ . The residues of the leading poles, however, generally cannot be solved from these equations directly. The residues of the other poles are known linear functions of the residues of the

leading poles. Multiple poles, which may occur, give some complications but present no essential difficulties. In chapter 8, dealing with the wedge angle  $\alpha = \pi/2$ , it is shown how the relations between the residues of the poles are determined.

### 5 Evaluation of expansions for $\hat{t}_I[x]$ and $t_{II}[y]$ .

Expansions for  $\hat{t}_I[x]$  and  $t_{II}[y]$  can be found by application of the residue theorem in the following manner (see fig. 6).

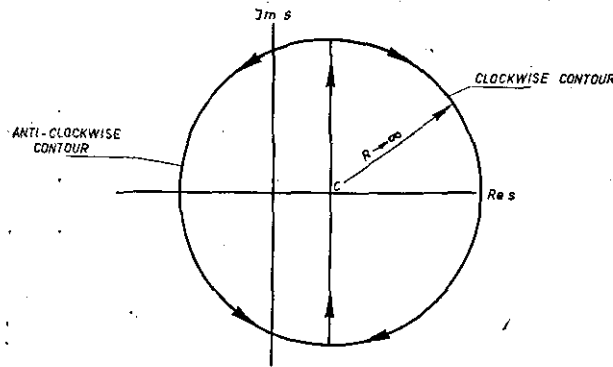


Fig. 6. Integration contours in the complex  $s$ -plane in order to find asymptotic expansions for  $\hat{t}_I[x]$  and  $t_{II}[y]$ .

For small values of  $x, y$  the integration contour  $c - i\infty \rightarrow c + i\infty$  may be closed at infinity, in anti-clockwise direction, thus delivering

$$\hat{t}_I[x] = \frac{1}{2\pi i} \int_{c-i\infty}^{c+i\infty} T_I[s] x^{-s} ds = \sum_{\text{Re } s < 1} \{ \text{residues of poles of } T_I[s] x^{-s} \} \quad (5.1)$$

$$t_{II}[y] = \frac{1}{2\pi i} \int_{c-i\infty}^{c+i\infty} T_{II}[s] y^{-s} ds = \sum_{\text{Re } s < 1} \{ \text{residues of poles of } T_{II}[s] y^{-s} \} \quad (5.2)$$

For large values of  $x, y$  the integration contour  $c - i\infty \rightarrow c + i\infty$  may be closed at infinity in clockwise direction, thus delivering

$$\hat{t}_I[x] = \frac{1}{2\pi i} \int_{c-i\infty}^{c+i\infty} T_I[s] x^{-s} ds = - \sum_{\text{Re } s > 1} \{ \text{residues of poles of } T_I[s] x^{-s} \} \quad (5.3)$$

$$t_{II}[y] = \frac{1}{2\pi i} \int_{c-i\infty}^{c+i\infty} T_{II}[s] y^{-s} ds = - \sum_{\text{Re } s > 1} \{ \text{residues of poles of } T_{II}[s] y^{-s} \} \quad (5.4)$$

### 6 Application of the inverse Mellin transform to the functional equations.

The functional equations (3.32) and (3.33) are rewritten in the simple form

$$\frac{1}{s} T_I[s+1] = \frac{1}{2} c a_{11}[s] T_I[s] + \frac{1}{2} c a_{12}[s] T_{II}[s] \quad (6.1)$$

$$\frac{1}{s} T_{II}[s+1] = a_{21}[s] T_I[s] + a_{22}[s] T_{II}[s] \quad (6.2)$$

where

$$a_{11}[s] = \frac{-(1+\nu)(3-\nu) \sin^2(s-1)\alpha - (s-1)^2(1+\nu)^2 \sin^2 \alpha + 4}{\sin 2(s-1)\alpha + (s-1) \sin 2\alpha} \quad (6.3)$$

$$a_{12}[s] = \frac{2(s-2)(1+\nu) \sin \alpha \sin(s-1)\alpha + 4 \cos(s-2)\alpha}{\sin 2(s-1)\alpha + (s-1) \sin 2\alpha} \quad (6.4)$$

$$a_{21}[s] = \frac{2\{s(1+\nu) - 4\} \sin \alpha \sin(s-1)\alpha + 4 \cos(s-2)\alpha}{\sin 2(s-1)\alpha + (s-1) \sin 2\alpha} \quad (6.5)$$

$$a_{22}[s] = \frac{-4 \sin^2(s-1)\alpha - 4 \sin^2 \alpha + 4}{\sin 2(s-1)\alpha + (s-1) \sin 2\alpha} \quad (6.6)$$

It has already been discussed that the functions  $T_I[s]$  and  $T_{II}[s]$  are defined within the strip

$$\begin{aligned} \operatorname{Re} a_1 < \operatorname{Re} s < 2 \\ \operatorname{Re} a_1 < 1. \end{aligned} \quad (6.7)$$

Thus the functions  $T_I[s+1]$  and  $T_{II}[s+1]$  are defined within the strip

$$\begin{aligned} \operatorname{Re} a_1 - 1 < \operatorname{Re} s < 1 \\ \operatorname{Re} a_1 - 1 < 0. \end{aligned} \quad (6.8)$$

The inverse Mellin transforms  $\frac{1}{2\pi i} \int_{c-i\infty}^{c+i\infty} \dots x^{-s} ds$  and  $\frac{1}{2\pi i} \int_{c-i\infty}^{c+i\infty} \dots y^{-s} ds$  are now applied to the functional equations (6.1) and (6.2) respectively.

The result is

$$P_I/P - 2 \int_0^x \hat{t}_I[\xi] d\xi = c \int_0^\infty \frac{1}{\xi} f_{11} \left[ \frac{x}{\xi} \right] \hat{t}_I[\xi] d\xi + c \int_0^\infty \frac{1}{\eta} f_{12} \left[ \frac{x}{\eta} \right] t_{II}[\eta] d\eta \quad (6.9)$$

$$P_{II}/P - \int_0^y t_{II}[\eta] d\eta = \int_0^\infty \frac{1}{\xi} f_{21} \left[ \frac{y}{\xi} \right] \hat{t}_I[\xi] d\xi + \int_0^\infty \frac{1}{\eta} f_{22} \left[ \frac{y}{\eta} \right] t_{II}[\eta] d\eta \quad (6.10)$$

with

$$f_{12} \left[ \frac{x}{\eta} \right] = \frac{1}{2\pi i} \int_{c-i\infty}^{c+i\infty} a_{12}[s] \left( \frac{x}{\eta} \right)^{-s} ds \quad (6.11)$$

$$f_{21} \left[ \frac{y}{\xi} \right] = \frac{1}{2\pi i} \int_{c-i\infty}^{c+i\infty} a_{21}[s] \left( \frac{y}{\xi} \right)^{-s} ds \quad (6.12)$$

and where  $f_{11} \left[ \frac{x}{\xi} \right]$  and  $f_{22} \left[ \frac{y}{\eta} \right]$  are such that their Mellin transforms are

$$\int_0^\infty f_{11} \left[ \frac{x}{\xi} \right] \left( \frac{x}{\xi} \right)^{s-1} d \left( \frac{x}{\xi} \right) = a_{11}[s] \quad (6.13)$$

and

$$\int_0^\infty f_{22} \left[ \frac{y}{\eta} \right] \left( \frac{y}{\eta} \right)^{s-1} d \left( \frac{y}{\eta} \right) = a_{22}[s]. \quad (6.14)$$

The integrals of (6.13) and (6.14) are Cauchy principal values.

The left-hand sides of (6.9), (6.10) take the given forms for values of  $\operatorname{Re} s > 0$ . This requirement, together with the requirements (6.8), gives for the validity region for  $s$  at the present inversions

$$0 < \operatorname{Re} s < 1. \quad (6.15)$$

The formulas (6.9) ... (6.14) can be verified with ref. 4, page 308 form. (14), page 341 form. (1) and ref. 5, page 43 form. (102) which is a faltung theorem of the Mellin transform.

An attempt to determine  $f_{11} \left[ \frac{x}{\xi} \right]$  and  $f_{22} \left[ \frac{y}{\eta} \right]$ , by application of the inverse Mellin transform to the right-hand sides of (6.13) and (6.14) respectively, fails because these right-hand sides do not tend to zero within their strips of integration (see (6.15)) for  $\operatorname{Im} s \rightarrow \pm \infty$ .

Actually, if  $s = c + iy$ ,  $0 < c < 1$ ,  $y \rightarrow \pm \infty$ ,

$$a_{11}[s] \rightarrow \pm \frac{(3-\nu)(1+\nu)}{2} i \quad (6.16)$$

and

$$a_{22}[s] \rightarrow \pm 2i. \quad (6.17)$$

The function

$$-\frac{(3-\nu)(1+\nu)}{2\pi} \frac{\xi}{\xi-x}$$

has the Mellin transform

$$\begin{aligned} \frac{(3-\nu)(1+\nu)}{2\pi} \int_0^\infty -\frac{1}{1-\frac{x}{\xi}} \left( \frac{x}{\xi} \right)^{s-1} d \left( \frac{x}{\xi} \right) = - \\ -\frac{(3-\nu)(1+\nu)}{2} \cotg \pi s \end{aligned} \quad (6.18)$$

and the function

$$-\frac{2}{\pi} \frac{\eta}{\eta-y}$$

has the Mellin transform

$$\frac{2}{\pi} \int_0^\infty -\frac{1}{1-\frac{y}{\eta}} \left( \frac{y}{\eta} \right)^{s-1} d \left( \frac{y}{\eta} \right) = -2 \cotg \pi s. \quad (6.19)$$

In (6.18) and (6.19), the region of  $s$  is again

$$0 < \operatorname{Re} s < 1$$

and the integrals are Cauchy principal values (ref. 5, page 345, form. (18)).

Within the strip  $0 < \operatorname{Re} s < 1$ , the right-hand sides of (6.18) and (6.19) tend to zero, for  $\operatorname{Im} s \rightarrow \pm \infty$ , in just the same way as do  $a_{11}[s]$  and  $a_{22}[s]$  (compare eqs. (6.16) and (6.17)).

If the function  $h_{11}\left[\frac{x}{\xi}\right]$  and  $h_{22}\left[\frac{y}{\eta}\right]$  are introduced according to

$$h_{11}\left[\frac{x}{\xi}\right] = f_{11}\left[\frac{x}{\xi}\right] + \frac{(3-\nu)(1+\nu)}{2\pi} \frac{\xi}{\xi-x} \quad (6.20)$$

and

$$h_{22}\left[\frac{y}{\eta}\right] = f_{22}\left[\frac{y}{\eta}\right] + \frac{2}{\pi} \frac{\eta}{\eta-y} \quad (6.21)$$

respectively, their Mellin transform are from (6.13), (6.14), (6.18) and (6.19)

$$H_{11}[s] = a_{11}[s] + \frac{(3-\nu)(1+\nu)}{2} \cotg \pi s \quad (6.22)$$

and

$$H_{22}[s] = a_{22}[s] + 2 \cotg \pi s. \quad (6.23)$$

The first terms in the right-hand sides of (6.22) and (6.23) cannot have poles in the region  $0 < \operatorname{Re} s < 1$ , because the second terms do not have one therein.

These functions tend to zero exponentially within the strip of integration for  $\operatorname{Im} s \rightarrow \pm \infty$  and thus their inverse Mellin transforms converge.

With the aid of (6.20) and (6.21), the integral equations (6.9), (6.10) now become

$$P_I/P - 2 \int_0^x \hat{t}_I[\xi] d\xi = c \int_0^x \frac{1}{\xi} h_{11}\left[\frac{x}{\xi}\right] \hat{t}_I[\xi] d\xi - c \frac{(3-\nu)(1+\nu)}{2\pi} \int_0^x \frac{\hat{t}_I[\xi]}{\xi-x} d\xi + c \int_0^y \frac{1}{\eta} f_{12}\left[\frac{x}{\eta}\right] t_{II}[\eta] d\eta \quad (6.24)$$

$$P_{II}/P - \int_0^y t_{II}[\eta] d\eta = \int_0^x \frac{1}{\xi} f_{21}\left[\frac{y}{\xi}\right] \hat{t}_I[\xi] d\xi + \int_0^y \frac{1}{\eta} h_{22}\left[\frac{y}{\eta}\right] t_{II}[\eta] d\eta - \frac{2}{\pi} \int_0^y \frac{t_{II}[\eta]}{\eta-y} d\eta. \quad (6.25)$$

There is another way to set up the integral equations (6.9), (6.10) which is more elaborate. From physical considerations using the original coordinates their form is easily found to be

$$P_I - \int_0^x 2 \hat{t}_I[\xi] d\xi = \frac{(E_s A_s)_I}{Eh} \int_0^x 2 Eh \varepsilon_{11}[x, \xi] \hat{t}_I[\xi] d\xi + \frac{(E_s A_s)_I}{Eh} \int_0^y Eh \varepsilon_{12}[x, \eta] t_{II}[\eta] d\eta \quad (6.26)$$

and

$$P_{II} - \int_0^y t_{II}[\eta] d\eta = \frac{(E_s A_s)_{II}}{Eh} \int_0^x 2 Eh \varepsilon_{21}[y, \xi] \hat{t}_I[\xi] d\xi + \frac{(E_s A_s)_{II}}{Eh} \int_0^y Eh \varepsilon_{22}[y, \eta] t_{II}[\eta] d\eta. \quad (6.27)$$

In (6.26) and (6.27)

$\varepsilon_{11}[x, \xi]$  is the strain along the  $x$ -axis due to the loading force of fig. 7a.

$\varepsilon_{12}[x, \eta]$  is the strain along the  $x$ -axis due to the two loading forces of fig. 7b.

$\varepsilon_{21}[y, \xi]$  is the strain along the  $y$ -axis due to the loading force of fig. 7a.

$\varepsilon_{22}[y, \eta]$  is the strain along the  $y$ -axis due to the two loading forces of fig. 7b.

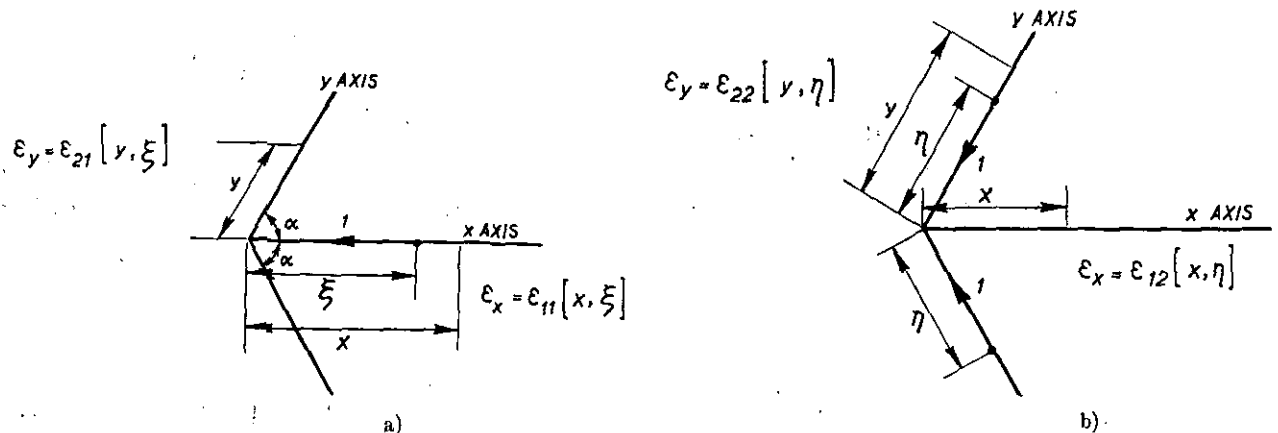


Fig. 7. The wedge without stiffeners with two unit load systems working on it.

The functions  $\varepsilon_{ij}$ ,  $i, j = 1, 2$ , must be determined along the lines of, for example, ref. 3. If these calculations would be carried out, it would appear that, in the original coordinates,

$$\begin{aligned} \frac{1}{\xi} f_{11} \left[ \frac{x}{\xi} \right] &= 2 Eh \varepsilon_{11}[x, \xi] \\ \frac{1}{\eta} f_{12} \left[ \frac{x}{\eta} \right] &= Eh \varepsilon_{12}[x, \eta] \\ \frac{1}{\xi} f_{21} \left[ \frac{y}{\xi} \right] &= 2 Eh \varepsilon_{21}[y, \xi] \\ \frac{1}{\eta} f_{22} \left[ \frac{y}{\eta} \right] &= Eh \varepsilon_{22}[y, \eta]. \end{aligned} \quad (6.28)$$

The function  $\varepsilon_{11}[x, \xi]$  has a singularity at  $x = \xi$ , the character of which is easily detected by noting that in the vicinity of the unit force of fig. 7a the function  $\varepsilon_{11}[x, \xi]$  behaves as if it were acting in an infinite plate. Thus, in the vicinity of  $x = \xi$  (ref. 6, chapter 4, paragraph 38)

$$\varepsilon_{11}[x, \xi] \rightarrow \bar{\varepsilon}_{11}[x, \xi] = -\frac{1}{2 Eh} \frac{(3-\nu)(1+\nu)}{2\pi} \frac{1}{\xi-x}. \quad (6.29)$$

It may now be noted that  $\bar{\varepsilon}_{11}[x, \xi]$  suggests the function that was separated from  $f_{11} \left[ \frac{x}{\xi} \right]$  in (6.20).

The singularity of  $\varepsilon_{22}[y, \eta]$  at  $y = \eta$  is easily detected by recognizing the fact that, in the vicinity of one of the unit forces of fig. 7b, the stress-distribution behaves as if this force were acting on a half plane.

Thus, in the vicinity of  $y = \eta$  (ref. 6, chapter 4, paragraph 33),

$$\varepsilon_{22}[y, \eta] \rightarrow \bar{\varepsilon}_{22}[y, \eta] = -\frac{1}{Eh} \frac{2}{\pi} \frac{1}{\eta-y}. \quad (6.30)$$

It may now be noted that  $\bar{\varepsilon}_{22}[y, \eta]$  suggests the function that was separated from  $f_{22} \left[ \frac{y}{\eta} \right]$  in (6.21).

Because, in view of (6.28), the functions  $f_{12} \left[ \frac{x}{\xi} \right]$  and  $f_{21} \left[ \frac{y}{\eta} \right]$  are related to influence functions, certain symmetry properties may be expected between these functions and their respective Mellin transforms  $a_{12}[s]$  and  $a_{21}[s]$ .

In appendix A, it is proved that these relations are

$$\frac{1}{z} f_{12} \left[ \frac{1}{z} \right] = -z f_{21}[z] \quad (6.31)$$

and

$$-a_{12}[-s+1] = a_{21}[s+1]. \quad (6.32)$$

Indeed, (6.32) proves to be true for (6.4) and (6.5).

## 7 Determination of the functions $h_{11} \left[ \frac{x}{\xi} \right]$ , $f_{12} \left[ \frac{x}{\eta} \right]$ , $f_{21} \left[ \frac{y}{\xi} \right]$ and $h_{22} \left[ \frac{y}{\eta} \right]$ .

The functions concerned are repeated here for convenience

$$\begin{aligned} h_{11} \left[ \frac{x}{\xi} \right] &= \frac{1}{2\pi i} \int_{c-i\infty}^{c+i\infty} \left\{ \frac{(1+\nu)(3-\nu) \sin^2(s-1)\alpha + (s-1)^2(1+\nu)^2 \sin^2\alpha - 4}{\sin 2(s-1)\alpha + (s-1) \sin 2\alpha} + \right. \\ &\quad \left. + \frac{(1+\nu)(3-\nu)}{2} \cotg \pi \xi \left\{ \left( \frac{x}{\xi} \right)^{-s} ds \right. \right. \end{aligned} \quad (7.1)$$

$$f_{12} \left[ \frac{x}{\eta} \right] = \frac{1}{2\pi i} \int_{c-i\infty}^{c+i\infty} -\frac{2(s-2)(1+\nu) \sin \alpha \sin(s-1)\alpha + 4 \cos(s-2)\alpha}{\sin 2(s-1)\alpha + (s-1) \sin 2\alpha} \left( \frac{x}{\eta} \right)^{-s} ds \quad (7.2)$$

$$f_{21} \left[ \frac{y}{\xi} \right] = \frac{1}{2\pi i} \int_{c-i\infty}^{c+i\infty} -\frac{2\{s(1+\nu) - 4\} \sin \alpha \sin(s-1)\alpha + 4 \cos(s-2)\alpha}{\sin 2(s-1)\alpha + (s-1) \sin 2\alpha} \left( \frac{y}{\xi} \right)^{-s} ds \quad (7.3)$$

$$h_{22} \left[ \frac{y}{\eta} \right] = \frac{1}{2\pi i} \int_{c-i\infty}^{c+i\infty} \left\{ \frac{4 \sin^2(s-1)\alpha + 4 \sin^2\alpha - 4}{\sin 2(s-1)\alpha + (s-1) \sin 2\alpha} + 2 \cotg \pi s \right\} \left( \frac{y}{\eta} \right)^{-s} ds. \quad (7.4)$$

In these equations the requirement for  $c$  is that of (6.15)

$$0 < c < 1. \quad (7.5)$$

For values of  $x/\xi$ ,  $x/\eta$ ,  $y/\xi$ ,  $y/\eta < 1$ , the integration line  $c-i\infty \rightarrow c+i\infty$  may be closed at infinity in anti-clockwise direction, like is done in fig. 6, and the integrals are determined as the sum of an infinite series, derived with the aid of the residue theorem. Likewise, for values of  $x/\xi$ ,  $x/\eta$ ,  $y/\xi$ ,  $y/\eta > 1$ , the contour may be closed in clockwise direction and again the residue theorem is applied. Generally, the obtained infinite series cannot be summed into a closed form. However, for  $\alpha = \pi/2$  (see the numerical example) it turns out that the integrals in question, (7.1 ... (7.4), can be given in closed form.

## 8 Solution of the problem for $\alpha = \pi/2$ .

8.1 The expansions for the functions  $\hat{t}_I[x] \equiv t_I[x]$  and  $t_{II}[y]$ .

8.1.1 Small values of  $x$  and  $y$ .

In view of the eqs. (4.8) ... (4.12), the poles of  $T_I[s]$  and  $T_{II}[s]$  in the region  $Re\ s < 1$  may be expected at the zero's of  $(\alpha = \pi/2)$

$$s \sin^2 (s-1) \pi = 0. \quad (8.1)$$

These are  $s = -n$ , where  $n = 0, 1, 2, 3, \dots$

The Laurent expansions of  $T_I[s]$  and  $T_{II}[s]$  for  $s \rightarrow 1$  be  $(\varepsilon \rightarrow 0)$

$$T_I[1 + \varepsilon] = \frac{1}{2} + a_{1,1} \varepsilon + a_{1,2} \varepsilon^2 + a_{1,3} \varepsilon^3 + \dots \quad (8.2a)$$

$$T_{II}[1 + \varepsilon] = \beta + b_{1,1} \varepsilon + b_{1,2} \varepsilon^2 + b_{1,3} \varepsilon^3 + \dots \quad (8.2b)$$

From (4.5) and (4.6) it is determined that the first terms of these expansions must be  $\frac{1}{2}$  and  $\beta$  respectively. The coefficients  $a_{1,1}, a_{1,2} \dots b_{1,1}, b_{1,2} \dots$  are unknown.

With the aid of (4.9) the Laurent expansions for  $T_I[s]$  and  $T_{II}[s]$  in  $s = 0$  are determined from

$$T_I[\varepsilon] = \frac{-2N[\varepsilon]}{c\varepsilon} \frac{\begin{vmatrix} T_I[1 + \varepsilon] & \frac{c}{2} t_{12}[\varepsilon] \\ T_{II}[1 + \varepsilon] & t_{22}[\varepsilon] \end{vmatrix}}{\Delta[\varepsilon]} \quad (8.3a)$$

and

$$T_{II}[\varepsilon] = \frac{-2N[\varepsilon]}{c\varepsilon} \frac{\begin{vmatrix} \frac{c}{2} t_{11}[\varepsilon] & T_I[1 + \varepsilon] \\ t_{21}[\varepsilon] & T_{II}[1 + \varepsilon] \end{vmatrix}}{\Delta[\varepsilon]} \quad (8.3b)$$

According to (4.10), (4.11) and (4.12)

$$N[\varepsilon] \equiv \sin 2(\varepsilon - 1) \frac{\pi}{2} = -\pi\varepsilon + \dots$$

$$t_{11}[\varepsilon] = -(1 + \nu)(3 - \nu) \left( 1 - \frac{\pi^2 \varepsilon^2}{4} + \dots \right) - (s^2 - 2\varepsilon + 1)(1 + \nu^2) + 4 \dots$$

$$t_{12}[\varepsilon] = 2(\varepsilon - 2)(1 + \nu) \left( -1 + \frac{\pi^2 \varepsilon^2}{8} + \dots \right) + 4 \left( -1 + \frac{\pi^2 \varepsilon^2}{8} + \dots \right) \quad (8.4)$$

$$t_{21}[\varepsilon] = 2\{\varepsilon(1 + \nu) - 4\} \left( -1 + \frac{\pi^2 \varepsilon^2}{8} + \dots \right) + 4 \left( -1 + \frac{\pi^2 \varepsilon^2}{8} + \dots \right)$$

$$t_{22}[\varepsilon] = -4 \sin^2(\varepsilon - 1) \frac{\pi}{4} = -4 + \pi^2 \varepsilon^2 + \dots$$

$$\Delta[\varepsilon] = -(1 + \nu)(3 - \nu) \varepsilon^2 \pi^2 + \dots$$

When it is supposed that  $T_I[\varepsilon]$  and  $T_{II}[\varepsilon]$  can be given by the Laurent expansions

$$T_I[\varepsilon] = \dots + \frac{a_{0,-2}}{\varepsilon^2} + \frac{a_{0,-1}}{\varepsilon} + a_{0,0} + a_{0,1} \varepsilon + \dots \quad (8.5a)$$

$$T_{II}[\varepsilon] = \dots + \frac{b_{0,-2}}{\varepsilon^2} + \frac{b_{0,-1}}{\varepsilon} + b_{0,0} + b_{0,1} \varepsilon + \dots \quad (8.5b)$$

it can be found from (8.2) ... (8.5) that

$$a_{0,-n} = 0 \quad \text{for } n = 3, 4, \dots \quad (8.6)$$

$$a_{0,-2} = \frac{4 \left( \frac{1}{c} + \nu\beta \right)}{(1 + \nu)(3 - \nu)\pi} \quad (8.7)$$

$$a_{0,-1} = \frac{-2\beta}{(3-\nu)\pi} + a_{1,1} \frac{8}{c} \frac{1}{(1+\nu)(3-\nu)\pi} + b_{1,1} \frac{4\nu}{(1+\nu)(3-\nu)\pi} \quad (8.8)$$

and

$$b_{0,-n} = 0 \quad \text{for } n=3, 4, \dots \quad (8.9)$$

$$b_{0,-2} = \frac{4 \left( \frac{1}{c} + \nu\beta \right)}{(1+\nu)(3-\nu)\pi} \quad (8.10)$$

$$b_{0,-1} = \frac{-2\beta(1+\nu)}{(3-\nu)\pi} - \frac{1}{c} \frac{2}{(3-\nu)\pi} + a_{1,1} \frac{8}{c} \frac{1}{(1+\nu)(3-\nu)\pi} + b_{1,1} \frac{4\nu}{(1+\nu)(3-\nu)\pi} \quad (8.11)$$

It may thus be concluded that the poles of  $T_I[s]$  and  $T_{II}[s]$  in  $s=0$  are of order 2. Application of the residue theorem, like is done in (5.1), (5.2), and remembering that

$$x^{-s} = x^{-\varepsilon} = e^{-\varepsilon \ln x} = 1 - \varepsilon \ln x + \frac{(\varepsilon \ln x)^2}{2!} + \dots \quad (8.12)$$

and

$$y^{-s} = y^{-\varepsilon} = e^{-\varepsilon \ln y} = 1 - \varepsilon \ln y + \frac{(\varepsilon \ln y)^2}{2!} + \dots \quad (8.13)$$

delivers, when only the poles in  $s=0$  are taken into account,

$$t_I[x] = -a_{0,-2} \ln x + a_{0,-1} \quad (8.14a)$$

$$t_{II}[y] = -b_{0,-2} \ln y + b_{0,-1} \quad (8.14b)$$

With the aid of (8.7), (8.8), (8.10) and (8.11), introducing the unknown

$$A = \frac{-2\beta}{(3-\nu)\pi} + a_{1,1} \frac{8}{c} \frac{1}{(1+\nu)(3-\nu)\pi} + b_{1,1} \frac{4\nu}{(1+\nu)(3-\nu)\pi},$$

the eqs. (8.14) become

$$t_I[x] = -\frac{4 \left( \frac{1}{c} + \nu\beta \right)}{\pi(1+\nu)(3-\nu)} \ln x + A \quad (8.15a)$$

$$t_{II}[y] = -\frac{4 \left( \frac{1}{c} + \nu\beta \right)}{\pi(1+\nu)(3-\nu)} \ln y - \frac{2 \left( \frac{1}{c} + \nu\beta \right)}{\pi(3-\nu)} + A. \quad (8.15b)$$

## 8.1.2 Large values of $x$ and $y$ .

### 8.1.2.1 Expansion for $t_I[x]$ .

In view of equations (4.8) and (4.10) the poles of  $T_I[s]$  and  $T_{II}[s]$  in the region  $\text{Re } s > 1$  may be expected at the zero's of

$$\sin(s-2)\pi = 0.$$

They are  $s=2+n$ , where  $n=0, 1, 2, 3, \dots$ .

With the aid of (4.8) the Laurent expansions for  $T_I[s]$  and  $T_{II}[s]$  in  $s=2$  are determined from

$$T_I[2+\varepsilon] = - \frac{c(1+\varepsilon)}{2N[1+\varepsilon]} \left| \begin{array}{cc} T_I[1+\varepsilon] & -t_{12}[1+\varepsilon] \\ T_{II}[1+\varepsilon] & t_{11}[1+\varepsilon] \end{array} \right| \quad (8.16a)$$

and

$$T_{II}[2+\varepsilon] = - \frac{1+\varepsilon}{N[1+\varepsilon]} \left| \begin{array}{cc} T_I[1+\varepsilon] & -t_{22}[1+\varepsilon] \\ T_{II}[1+\varepsilon] & t_{21}[1+\varepsilon] \end{array} \right|. \quad (8.16b)$$

According to (4.10)

$$\begin{aligned} t_{11}[1+\varepsilon] &= -(1+\nu)(3-\nu)\varepsilon^2 \frac{\pi^2}{4} + 4 - \varepsilon^2(1+\nu)^2 + \dots \\ t_{12}[1+\varepsilon] &= 2(-1+\varepsilon)(1+\nu)\varepsilon \frac{\pi}{2} + 4\varepsilon \frac{\pi}{2} + \dots \varepsilon^3 + \dots \\ t_{21}[1+\varepsilon] &= 2\{(1+\varepsilon)(1+\nu) - 4\}\varepsilon \frac{\pi}{2} + 4\varepsilon \frac{\pi}{2} + \dots \varepsilon^3 + \dots \\ t_{22}[1+\varepsilon] &= -\pi^2 \varepsilon^2 + \dots \varepsilon^4 + \dots \\ N[1+\varepsilon] &= \varepsilon\pi + \dots \end{aligned} \quad (8.17)$$

The Laurent expansions for  $T_I[1 + \varepsilon]$  and  $T_{II}[1 + \varepsilon]$  have already been given in (8.2). When for  $T_I[2 + \varepsilon]$  and  $T_{II}[2 + \varepsilon]$  Laurent expansions are assumed in the form

$$T_I[2 + \varepsilon] = \dots + \frac{a_{2,-1}}{\varepsilon} + a_{2,0} + a_{2,1} \varepsilon + \dots \quad (8.18a)$$

$$T_{II}[2 + \varepsilon] = \dots + \frac{b_{2,-1}}{\varepsilon} + b_{2,0} + b_{2,1} \varepsilon + \dots \quad (8.18b)$$

it can be found from (8.16)... (8.18) that

$$a_{2,-n} = 0 \text{ for } n = 2, 3, \dots \quad (8.19)$$

$$a_{2,-1} = -c/\pi \quad (8.20)$$

$$b_{2,-n} = 0 \text{ for } n = 1, 2, \dots \quad (8.21)$$

From (8.21) it is seen that  $T_{II}[s]$  has no pole at  $s=2$ .

Application of the residue theorem, like is done in (5.4), and remembering that

$$x^{-2-\varepsilon} = x^{-2} (1 - \varepsilon \ln x + \dots)$$

delivers, when from  $T_I[s]$  only the simple pole in  $s=2$  is taken into account,

$$t_I[x] = \frac{c}{\pi} x^{-2}. \quad (8.22)$$

### 8.1.1.2 Expansion for $t_{II}[y]$ .

For this purpose the coefficients  $a_{2,0}$  and  $b_{2,0}$  in (8.18) are computed. They read

$$a_{2,0} = -\frac{c}{2\pi} \{2 + 4a_{1,1} + \pi\beta(1 - \nu)\} \quad (8.23)$$

$$b_{2,0} = \frac{1 - \nu}{2}. \quad (8.24)$$

With the aid of (4.8b) the Laurent expansion for  $T_{II}[s]$  in  $s=3$  is determined from

$$T_{II}[3 + \varepsilon] = -\frac{2 + \varepsilon}{N[2 + \varepsilon]} \begin{vmatrix} T_I[2 + \varepsilon] & -t_{22}[2 + \varepsilon] \\ T_{II}[2 + \varepsilon] & t_{21}[2 + \varepsilon] \end{vmatrix} \quad (8.25)$$

where

$$t_{21}[2 + \varepsilon] = 4\nu + 2\varepsilon(1 + \nu) - \frac{\pi^2\nu}{2} \varepsilon^2 + \dots$$

$$t_{22}[2 + \varepsilon] = -4 + \pi^2 \varepsilon^2 + \dots$$

$$N[2 + \varepsilon] = -\pi\varepsilon \left[ 1 + \frac{\pi^2\varepsilon^2}{6} + \dots \right] \quad (8.26)$$

$$\frac{1}{N[2 + \varepsilon]} = -\left[ \frac{1}{\pi\varepsilon} + \frac{\pi\varepsilon}{6} + \dots \right]$$

When the Laurent expansion for  $T_I[3 + \varepsilon]$  is supposed to be

$$T_I[3 + \varepsilon] = \dots + \frac{b_{3,-2}}{\varepsilon^2} + \frac{b_{3,-1}}{\varepsilon} + b_{3,0} + b_{3,1}\varepsilon + \dots \quad (8.27)$$

it can be found from (8.25) ... (8.27) that

$$b_{3,-n} = 0 \text{ for } n = 3, 4, \dots \quad (8.28)$$

$$b_{3,-2} = \frac{8}{\pi} \nu a_{2,-1} = -\frac{8c}{\pi^2} \nu \quad (8.29)$$

$$b_{3,-1} = -\frac{8}{\pi} b_{2,0} + \frac{4\nu}{\pi} a_{2,-1} + \frac{8\nu}{\pi} a_{2,0}. \quad (8.30)$$

In (8.30)  $b_{2,0}$  is given in (8.24),  $a_{2,-1}$  in (8.20), but  $a_{2,0}$  remains unknown, in spite of (8.23), thus also  $b_{3,-1}$ .

Application of the residue theorem, like is done in (5.4), and remembering that

$$y^{-3-\varepsilon} = y^{-3} (1 - \varepsilon \ln y + \dots)$$

delivers, when from  $T_{II}[s]$  only the double pole in  $s=3$  is taken into account,

$$t_{II}[y] = b_{3,-2} y^{-3} \ln y - b_{3,-1} y^{-3} \quad (8.31)$$

or with (8.29) and (8.30)

$$t_{II}[y] = -\frac{8c}{\pi^2} \nu y^{-3} \ln y + B y^{-3} \quad (8.32)$$

where the coefficient  $B$  remains unknown.

8.2 Determination of the functions  $h_{11} \left[ \frac{x}{\xi} \right]$ ,  $f_{12} \left[ \frac{x}{\eta} \right]$ ,  $f_{21} \left[ \frac{y}{\xi} \right]$  and  $h_{22} \left[ \frac{y}{\eta} \right]$  in case  $\alpha = \pi/2$ .

In this special case,  $\alpha = \pi/2$ , these functions read from (7.1) ... (7.4)

$$h_{11} \left[ \frac{x}{\xi} \right] = \frac{1}{2\pi i} \int_{c-i\infty}^{c+i\infty} \left\{ -\frac{1}{2} (1+\nu)(3-\nu) \cotg \frac{\pi s}{2} - \frac{s(s+1)(1+\nu)^2}{\sin \pi s} + \frac{3s(1+\nu)^2}{\sin \pi s} - \frac{(1+\nu)^2 - 4}{\sin \pi s} + \frac{(1+\nu)(3-\nu)}{2} \cotg \pi s \right\} \left( \frac{x}{\xi} \right)^{-s} ds \quad (8.33)$$

$$f_{21} \left[ \frac{y}{\xi} \right] = \frac{1}{2\pi i} \int_{c-i\infty}^{c+i\infty} \frac{2-s(1+\nu)}{\sin \frac{\pi s}{2}} \left( \frac{y}{\xi} \right)^{-s} ds. \quad (8.34)$$

The function  $f_{12} \left[ \frac{x}{\eta} \right]$  is not mentioned here explicitly because it can easily be found from  $f_{21} \left[ \frac{y}{\xi} \right]$  with the expression (see appendix A, eq. (A.6))

$$\frac{1}{z} f_{21} \left[ \frac{1}{z} \right] = -Z f_{12}[z] \quad (8.35)$$

by taking  $\frac{\eta}{x} = \frac{y}{\xi} = z$ .

Furthermore,

$$h_{22} \left[ \frac{y}{\eta} \right] = \frac{1}{2\pi i} \int_{c-i\infty}^{c+i\infty} \left\{ -\frac{2+2\cos s\pi}{\sin s\pi} + 2 \cotg \pi s \right\} \left( \frac{y}{\eta} \right)^{-s} ds. \quad (8.36)$$

The integrations (8.33), (8.34) and (8.36), where according to chapter 7  $0 < c < 1$ , can be carried out in a direct way, without use of the residue theorem, with the aid of ref. 4, chapter VII. This delivers

$$h_{11} \left[ \frac{x}{\xi} \right] = \frac{(\nu^2 - 2\nu + 5)(x/\xi)^2 + (4\nu^2 + 12)(x/\xi) + (-\nu^2 - 6\nu + 3)}{2\pi \{1 + (x/\xi)\}^2} \quad (8.37)$$

$$f_{12} \left[ \frac{x}{\eta} \right] = \frac{4}{\pi} \frac{\nu - (x/\eta)^2}{\{1 + (x/\eta)^2\}^2} \quad (8.38)$$

$$f_{21} \left[ \frac{y}{\xi} \right] = \frac{4}{\pi} \frac{1 - \nu(y/\xi)^2}{\{1 + (y/\xi)^2\}^2} \quad (8.39)$$

$$h_{22} \left[ \frac{y}{\eta} \right] = -\frac{2}{\pi} \frac{1}{1 + y/\eta}. \quad (8.40)$$

The functions (8.37) ... (8.40) are identical with those already derived by Melan, ref. 7, for the half plane.

8.3 Final solutions for  $t_I[x]$  and  $t_{II}[y]$  by means of the integral equations.

In the integral equations (6.24) and (6.25), the quantities  $\xi$  and  $\eta$  may be replaced by any other symbol. Introduction of the symbol  $\zeta$  in both equations and substitution of (8.37) ... (8.40), (4.1) and (4.2), delivers, when additionally (6.24) is divided by  $c$ ,

$$\begin{aligned} \frac{2}{c} \int_0^\infty t_I[\zeta] d\zeta + \frac{1}{2\pi} \int_0^\infty \frac{1}{\zeta} \frac{(\nu^2 - 2\nu + 5)(x/\zeta)^2 + (4\nu^2 + 12)(x/\zeta) + (-\nu^2 - 6\nu + 3)}{\{1 + (x/\zeta)\}^2} t_I[\zeta] d\zeta \\ - \frac{(1+\nu)(3-\nu)}{2\pi} \int_0^\infty \frac{1}{\zeta} \frac{t_I[\zeta]}{1-x/\zeta} d\zeta + \frac{4}{\pi} \int_0^\infty \frac{1}{\zeta} \frac{\nu - (x/\zeta)^2}{\{1 + (x/\zeta)^2\}^2} t_{II}[\zeta] d\zeta = 1/c \end{aligned} \quad (8.41)$$

$$-\beta + \int_0^y t_{II}[\zeta] d\zeta + \frac{4}{\pi} \int_0^\infty \frac{1}{\zeta} \frac{1 - \nu(y/\zeta)^2}{\{1 + (y/\zeta)^2\}^2} t_I[\zeta] d\zeta - \frac{2}{\pi} \int_0^\infty \frac{1}{\zeta} \frac{t_{II}[\zeta]}{1 + y/\zeta} d\zeta - \frac{2}{\pi} \int_0^\infty \frac{1}{\zeta} \frac{t_{II}[\zeta]}{1 - y/\zeta} d\zeta = 0, \quad (8.42)$$

where according to the eqs. (8.15), (8.22), (8.32)

$$t_I^*[\zeta] = A - \frac{4 \left( \frac{1}{c} + \nu\beta \right)}{\pi(1 + \nu)(3 - \nu)} \ln \zeta$$

$$t_{II}^*[\zeta] = A - \frac{2 \left( \frac{1}{c} + \nu\beta \right)}{\pi(3 - \nu)} - \frac{4 \left( \frac{1}{c} + \nu\beta \right)}{\pi(1 + \nu)(3 - \nu)} \ln \zeta \quad (8.43)$$

$$t_I^{**}[\zeta] = \frac{c}{\pi} \zeta^{-2}$$

$$t_{II}^{**}[\zeta] = B\zeta^{-3} - \frac{8c}{\pi^2} \nu \zeta^{-3} \ln \zeta = 0.$$

The single asterisk stands for small, the double for large values of  $\zeta$ .

Since  $t_{II}[\zeta]$  tends very rapidly to zero for large values of  $\zeta$ , as compared with  $t_I[\zeta]$ , it was considered allowable to put  $t_{II}^{**}[\zeta] = 0$  for values of  $\zeta$  greater than a suitably chosen large value of  $\zeta$ .

The functions

$$\frac{(\nu^2 - 2\nu + 5)(x/\zeta)^2 + (4\nu^2 + 12)(x/\zeta) + (-\nu^2 - 6\nu + 3)}{\{1 + (x/\zeta)^2\}^2} = g_1[x/\zeta] \quad (8.44)$$

$$\frac{\nu - (x/\zeta)^2}{\{1 + (x/\zeta)^2\}^2} = g_2[x/\zeta] \quad (8.45)$$

$$\frac{1 - \nu(y/\zeta)^2}{\{1 + (y/\zeta)^2\}^2} = g_3[y/\zeta] \quad (8.46)$$

are given, as far as necessary, in table 3 for the value  $\nu = 0.3$ . Some of the integrands, occurring in (8.41) and (8.42), can be considerably simplified in the ranges for small, respectively large values of  $\zeta$  (see appendix B).

As both integral equations (8.41) and (8.42) are of the same type as that, given in ref. 2, eq. (5.11), the method for numerical evaluation, given in chapter 5 and table 1 of that reference, is applicable here, but for one additional requirement. When  $t_I^*$ ,  $t_{II}^*$ ,  $t_I^{**}$  and  $t_{II}^{**}$  (see eq. (8.43)) introduce respectively  $n_{1,I}$ ,  $n_{1,II}$ ,  $n_{2,I}$  and  $n_{2,II}$  unknowns, whereas the numbers of unknown values of  $t_I$  and  $t_{II}$ , at moderate values of  $x$  and  $y$ , are respectively  $n_{3,I}$  and  $n_{3,II}$ , the total number of unknowns in each of the equations (8.41) and (8.42) can be denoted

$$(n_{1,I} + n_{1,II}) + (n_{2,I} + n_{2,II}) + (n_{3,I} + n_{3,II}) = q + 2. \quad (8.47)$$

Assuming, that for the necessary relations between the unknowns a number of  $q_I + 1$  is delivered by the  $(q_I + 1)$ -fold application of eq. (8.41) and a number of  $q_{II} + 1$  by the  $(q_{II} + 1)$ -fold application of eq. (8.42) the relation

$$q_I + q_{II} = q \quad (8.48)$$

must hold. This does not necessarily imply that  $q_I = q_{II}$ . However, as the expansions  $t_I^*[x]$  and  $t_{II}^*[y]$  contain the same unknown coefficients and consist of the same number of terms (see eqs. (8.43)), whereas the expansions  $t_I^{**}[x]$  and

$t_{II}^{**}[y]$  are both known (see again eqs. (8.43)), it seems advisable to take in this case

$$n_{3,I} = n_{3,II} \quad (8.49)$$

and

$$q_I = q_{II}$$

in order to obtain an equal degree of accuracy in the solutions for  $t_I[x]$  and  $t_{II}[y]$ .

The scheme of evaluation for both integral equations, in order to separate the necessary system of linear relations between the unknowns into two basic equations, is given in table 2 (this table is the same as table 1 of ref. 2, but for some minor alterations).

As the evaluation schemes for both integral equations will be taken alike, only one of them will be determined here.

From the eqs. (8.43) two conclusions can be drawn, namely

$$(n_{1,I} + n_{1,II}) = 2, \quad (8.50)$$

and

$$(n_{2,I} + n_{2,II}) = 0.$$

Hence, see eqs. (8.47), (8.48) and (8.49),

$$n_{3,I} = q_I = q/2 \quad (8.51)$$

so  $q$  must be an even number.

Taking the value  $q = 18$ , which means from eq. (8.47) a system of 20 linear equations, delivers

$$n_{3,I} = q_I = q. \quad (8.52)$$

When, for  $p_I$  is assumed the value

$$p_I = 11 \quad (8.53)$$

it can directly be concluded from table 2, that

$$r_1 = 21 \quad (8.54)$$

and

$$z_1 = 12.$$

With the expression  $x_n = \delta \alpha^{n-1}$  (see table 2) the values of  $x_{p_1}$  and  $y_{r_1}$  become with  $\alpha = 2$

$$\begin{aligned} x_{p_1} &= \delta 2^{10} = 1024 \delta \\ x_{r_1} &= \delta 2^{20} = 1048576 \delta. \end{aligned} \quad (8.55)$$

For  $\delta$  is, for some values of the stiffness ratio  $c$ , taken the value  $\frac{1}{2} \cdot 10^{-4}$ , hence

$$\begin{aligned} x_n &= 10^{-4} 2^{n-2} \text{ for } n \geq 1 \\ x_0 &= 0 \end{aligned} \quad (8.56)$$

and the values of  $x_{p_1}$  and  $x_{r_1}$  become

$$\begin{aligned} x_{p_1} &= 0.0512 \\ x_{r_1} &= 52.4288. \end{aligned} \quad (8.57)$$

It will be obvious from table 2 that, for use of the Simpson rule,

$$O = \frac{1}{3} h (1 x_1 + 4 x_2 + 2 x_3 + \dots + 4 x_{n-1} + 1 x_n),$$

in that region where the integrations are carried

out numerically, the quantities  $z_1 - w_1$  and  $s_1 - w_1$  have to be even numbers. Together with the information, given in table 2, that  $w_1 \geq 1$  and  $s_1 \geq r_1$  it follows that

$$w_1 = 2, 4, 6, \dots \quad (8.58)$$

and

$$s_1 = 22, 24, 26, \dots \quad (8.59)$$

In view of the further requirements for  $w_1$  and  $s_1$ , mentioned in table 2, the choice

$$\begin{aligned} w_1 &= 2 \\ s_1 &= 24 \end{aligned} \quad (8.60)$$

is reliable, as then

$$x_{w_1}/x_{z_1} = x_2/x_{12} = 2^{-10} = 0.000977 \quad (8.61)$$

and

$$x_{s_1}/x_{z_1} = x_{12}/x_{24} = 2^{-12} = 0.000244$$

which is small enough.

With the aid of the eqs. (8.44) ... (8.46), (8.52) ... (8.60), appendix B and the introduction of the logarithmic coordinates

$$\begin{aligned} \zeta &= e^{\xi^*} \\ x &= e^{x^*} \\ y &= e^{y^*} \end{aligned} \quad (8.62)$$

the integral equations (8.41) and (8.42) become

$$\begin{aligned} &\left(\frac{2}{c} + \frac{4}{\pi x_{12+n}}\right) \int_0^{x_{2+n}^*} t_1^*[\zeta] d\zeta + \frac{2}{c} \int_{x_{2+n}^*}^{x^*} t_1[\zeta^*] e^{\xi^*} d\xi^* + \\ &+ \frac{1}{2\pi} \int_{x_{2+n}^*}^{x_{24+n}^*} g_1[x^*, \zeta^*] t_1[\zeta^*] d\xi^* - \frac{(3-\nu)(1+\nu)}{2\pi} \int_{x_{2+n}^*}^{x_{24+n}^*} \frac{t_1[\zeta^*]}{1 - e^{x_{12+n}^* - \zeta^*}} d\xi^* + \\ &+ \frac{3-6\nu-\nu^2}{2\pi} \int_{x_{24+n}^*}^{\infty} \frac{t_1^{**}[\zeta]}{\zeta} d\zeta - \frac{(3-\nu)(1+\nu)}{2\pi} \int_{x_{24+n}^*}^{\infty} \frac{t_1^{**}[\zeta]}{\zeta - x_{12+n}} d\zeta + \\ &- \frac{4}{\pi x_{12+n}^2} \int_0^{y_{2+n}} \zeta t_{II}^*[\zeta] d\zeta + \frac{4}{\pi} \int_{y_{2+n}^*}^{y_{24+n}^*} g_2[x^*, \zeta^*] t_{II}[\zeta^*] d\xi^* = \frac{1}{c} \end{aligned} \quad (8.63)$$

where  $n = 0 \dots 9$ , and

$$\begin{aligned} &-\beta - \frac{4\nu}{\pi y_{12+n}^2} \int_0^{x_{2+n}} \zeta t_1^*[\zeta] d\zeta + \frac{4}{\pi} \int_{x_{2+n}^*}^{x_{24+n}^*} g_3[y^*, \zeta^*] t_1[\zeta^*] d\xi^* + \\ &+ \frac{4}{\pi} \int_{x_{24+n}^*}^{\infty} \frac{t_1^{**}[\zeta]}{\zeta} d\zeta + \int_0^{y_{2+n}} t_{II}^*[\zeta] d\zeta + \int_{y_{2+n}^*}^{y_{12+n}^*} t_{II}[\zeta^*] e^{\xi^*} d\xi^* + \\ &- \frac{2}{\pi} \int_{y_{2+n}^*}^{y_{24+n}^*} \frac{t_{II}[\zeta^*]}{1 + e^{y_{12+n}^* - \zeta^*}} d\xi^* - \frac{2}{\pi} \int_{y_{2+n}^*}^{y_{24+n}^*} \frac{t_{II}[\zeta^*]}{1 - e^{y_{12+n}^* - \zeta^*}} d\xi^* = 0 \end{aligned} \quad (8.64)$$

where again,  $n = 0 \dots 9$ .

In (8.63) and (8.64) only the integrals, containing  $t_I^*$ ,  $t_{II}^*$ ,  $t_I^{**}$  and  $t_{II}^{**}$ , are solved analytically. The other terms are numerically evaluated with the aid of Simpson's rule. Those involving a Cauchy principal value are numerically evaluated with the aid of the special rule that is developed in ref. 2, appendix C. The so derived basic equations, stemming from (8.63) and (8.64), are given in tables 4 and 5. Further calculations were performed on the N.L.R. digital computer ZEBRA and results were obtained for the stiffness ratios  $c = 1/8, 1/4, 1/2, 1, 2, 4, 8$ . In all these cases in (8.55) the value of  $\delta$  was  $1/2 \cdot 10^{-4}$ .

Figures 8...14 give curves of  $\frac{(E_s A_s)_I}{PEh} t_I[x]$  and  $\frac{(E_s A_s)_I}{PEh} t_{II}[y]$  as functions of  $\frac{Eh}{(E_s A_s)_I} x$  and  $\frac{Eh}{(E_s A_s)_I} y$  respectively. In these figures  $t_I[x]$  and  $t_{II}[y]$  are actual shearflows and  $x$  and  $y$  actual coordinates (shearflows and coordinates with "dimensions"). The way of (3.5) to make quantities dimensionless with  $(E_s A_s)_{II}$  is less suitable to compare the figures 8...14, since the stiffness  $(E_s A_s)_I$  proved to be a more important parameter than the stiffness  $(E_s A_s)_{II}$ . In the figures 8...14, the curves for  $\frac{(E_s A_s)_I}{PEh} t_I[x]$  differ very little. This means that the stiffness of the stiffer II  $((E A_s)_{II})$  is of little influence

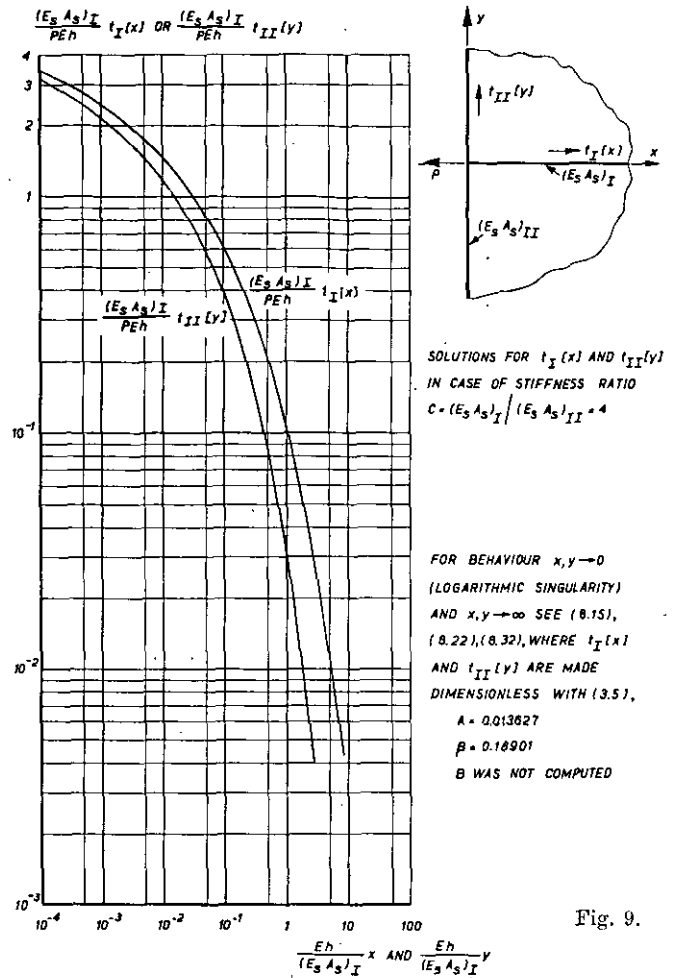


Fig. 9.

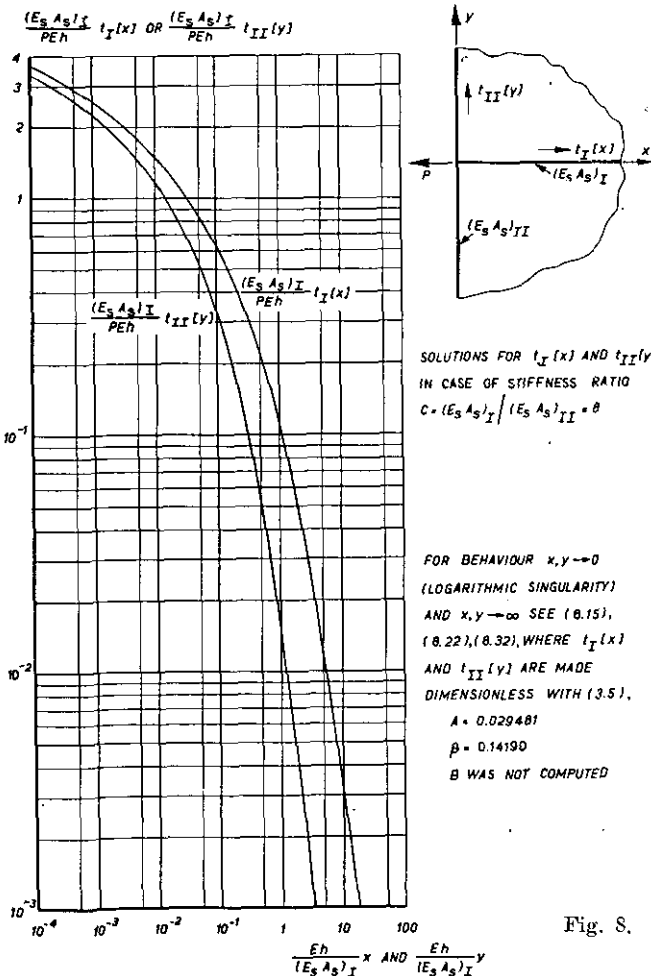


Fig. 8.

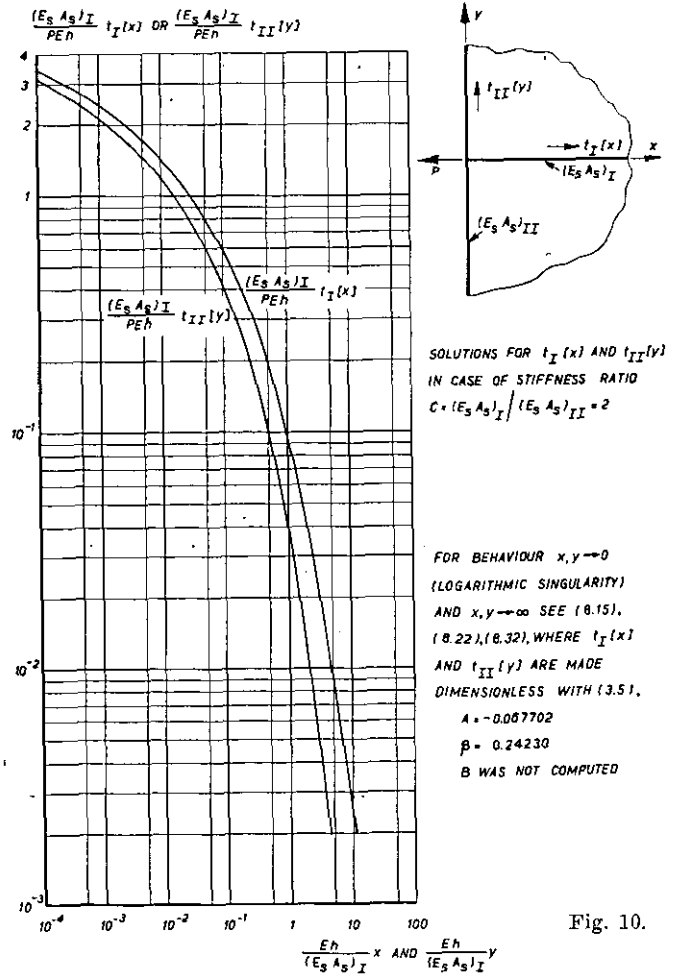
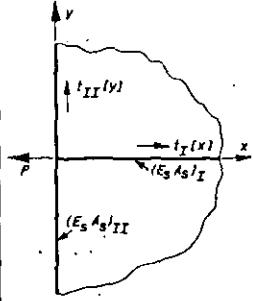
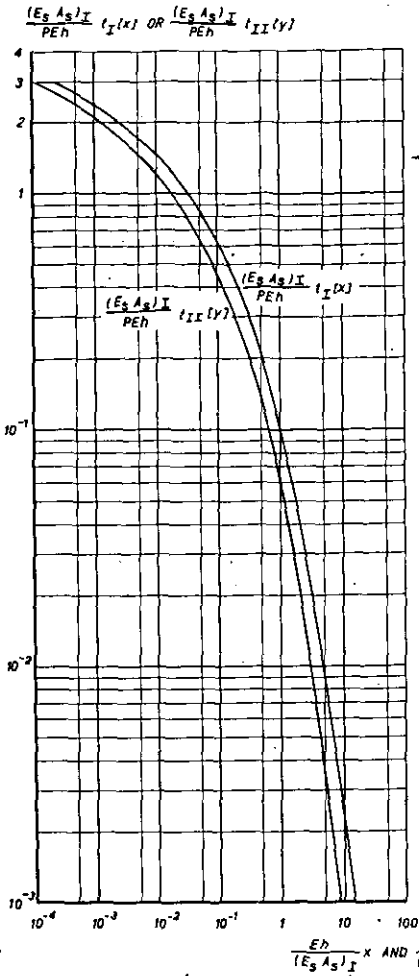


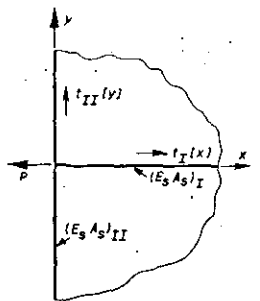
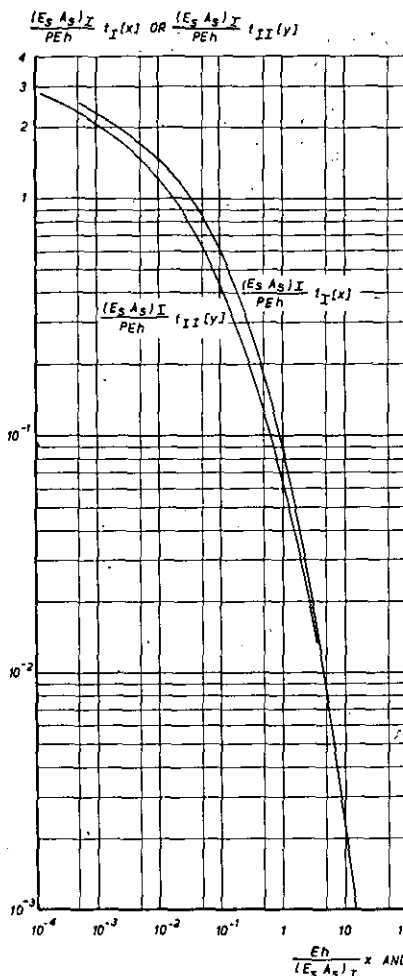
Fig. 10.



SOLUTIONS FOR  $t_I(x)$  AND  $t_{II}(y)$   
IN CASE OF STIFFNESS RATIO  
 $C = (E_s A_s)_I / (E_s A_s)_{II} = 1$

FOR BEHAVIOUR  $x, y \rightarrow 0$   
(LOGARITHMIC SINGULARITY)  
AND  $x, y \rightarrow \infty$  SEE (8.15),  
(8.22), (8.32), WHERE  $t_I(x)$   
AND  $t_{II}(y)$  ARE MADE  
DIMENSIONLESS WITH (3.5),  
 $A = -0.33243$   
 $\beta = 0.29572$   
B WAS NOT COMPUTED

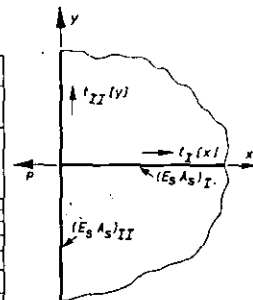
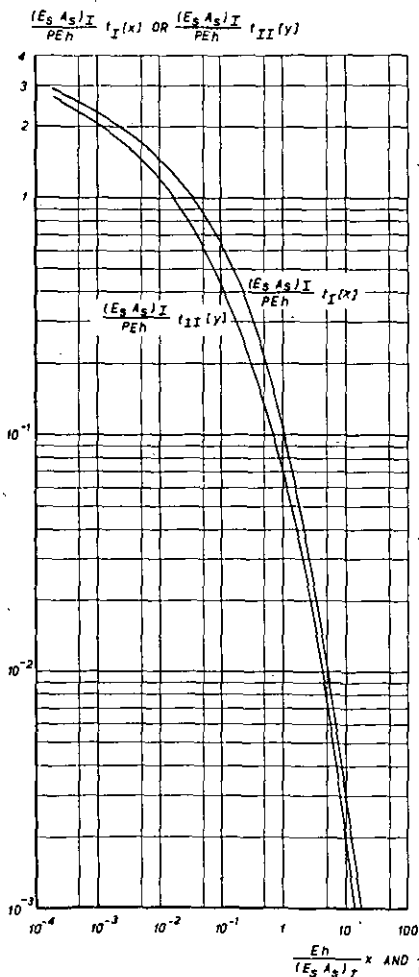
Fig. 11.



SOLUTIONS FOR  $t_I(x)$  AND  $t_{II}(y)$   
IN CASE OF STIFFNESS RATIO  
 $C = (E_s A_s)_I / (E_s A_s)_{II} = 1/4$

FOR BEHAVIOUR  $x, y \rightarrow 0$   
(LOGARITHMIC SINGULARITY)  
AND  $x, y \rightarrow \infty$  SEE (8.15),  
(8.22), (8.32), WHERE  $t_I(x)$   
AND  $t_{II}(y)$  ARE MADE  
DIMENSIONLESS WITH (3.5),  
 $A = -2.8723$   
 $\beta = 0.32593$   
B WAS NOT COMPUTED

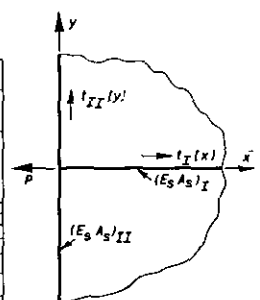
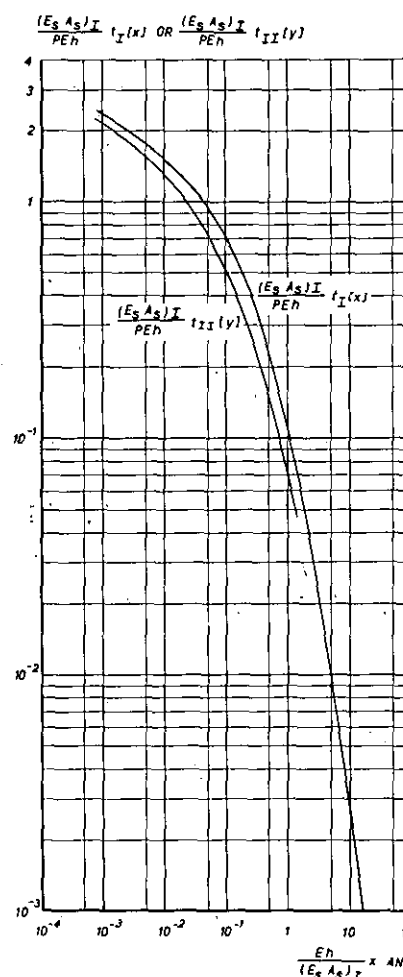
Fig. 13.



SOLUTIONS FOR  $t_I(x)$  AND  $t_{II}(y)$   
IN CASE OF STIFFNESS RATIO  
 $C = (E_s A_s)_I / (E_s A_s)_{II} = 1/2$

FOR BEHAVIOUR  $x, y \rightarrow 0$   
(LOGARITHMIC SINGULARITY)  
AND  $x, y \rightarrow \infty$  SEE (8.15),  
(8.22), (8.32), WHERE  $t_I(x)$   
AND  $t_{II}(y)$  ARE MADE  
DIMENSIONLESS WITH (3.5),  
 $A = -1.05891$   
 $\beta = 0.33477$   
B WAS NOT COMPUTED

Fig. 12.



SOLUTIONS FOR  $t_I(x)$  AND  $t_{II}(y)$   
IN CASE OF STIFFNESS RATIO  
 $C = (E_s A_s)_I / (E_s A_s)_{II} = 1/8$

FOR BEHAVIOUR  $x, y \rightarrow 0$   
(LOGARITHMIC SINGULARITY)  
AND  $x, y \rightarrow \infty$  SEE (8.15),  
(8.22), (8.32), WHERE  $t_I(x)$   
AND  $t_{II}(y)$  ARE MADE  
DIMENSIONLESS WITH (3.5),  
 $A = -7.0756$   
 $\beta = 0.19614$   
B WAS NOT COMPUTED

Fig. 14.

on the shear flow along stiffener I. At large values of  $x$  for all cases<sup>1)</sup>

$$\frac{(E_s A_s)_I}{PEh} t_I[x] = \frac{1}{\pi} \left\{ \frac{Eh}{(E_s A_s)_I} x \right\}^{-2} \quad (8.65)$$

For  $c=1$ , values of  $t_I[x]$  and  $t_{II}[y]$  are given in table 6.

### 9 Way to solution for some other cases.

The formulas of section 8 ( $\alpha = \pi/2$ ) are not applicable to the cases  $c=0$  and  $c=\infty$ . The case  $c=\infty$  (no edge stiffener present) requires a separate treatment, using similar methods. However, for that problem KOTTER and HENS (ref. 8) already gave a solution with the aid of another method, which seems not to be applicable to the case  $c \neq \infty$ .

The case  $c=0$  (only an edge stiffener is present along the boundary of the half plane) was already dealt with by MELAN (ref. 9).

If the loading force, acting at  $x=0$ ,  $y=0$ , is directed in the direction of the edge stiffener, the stiffener normal to the edge remains unstrained. Then again the problem is reduced to that of MELAN (ref. 9).

### 10 References.

1. KOTTER, W. T. On the diffusion of load from a stiffener into a sheet. *Quart. Journ. of Mech. and Appl. Math.* Volume VIII, Part 2, June 1955.
2. BENTHEM, J. P. and v. D. VOOREN, J. On the diffusion of a load from an edge-stiffener into a wedge-shaped plate. NLL-TN S. 541, 1959.
3. BENTHEM, J. P. and v. D. VOOREN, J. On the stress problem of anisotropic wedges. NLL-TN S. 537.
4. ERDÉLYI, A. Tables of integral transforms. Volume I. Mc Graw-Hill Book Comp., New York, 1954.
5. SNEDDON, I. N. Fourier transforms. Mc Graw-Hill Book Comp., New York, 1951.
6. TIMOSHENKO, S. and GOODIER, J. N. Theory of Elasticity. Mc Graw-Hill Book Comp., New York, 1951.
7. MELAN, E., Der Spannungszustand der durch eine Einzelkraft im innern beanspruchten Halbscheibe. *Zeitschrift für angewandte Mathematik und Mechanik*, Band 12, Seite 343, 1932.
8. KOTTER, W. T. and HENS, A. M., The diffusion of a load from a stiffener into a semi-infinite plate. (in Dutch). Unpublished Paper of the Lab. Appl. Mech. of the Techn. Univ., Delft, 1957.
9. MELAN, E., Ein Beitrag zur Theorie geschweisster Verbindungen. *Ingenieur-Archiv*, Band III, Seite 123, 1932.

### APPENDIX A.

The relation between  $f_{12} \left[ \frac{x}{\eta} \right]$  and  $f_{21} \left[ \frac{y}{\xi} \right]$ , respectively  $a_{12}[s]$  and  $a_{21}[s]$ .

For the free wedge, loaded by the systems of figs. 7a and 7b, the following theorem is valid.

The work done by the loading system of fig. 7a due to the displacements stemming from the loading system of fig. 7b is equal to the work done by the loading system of fig. 7b due to the displacements stemming from the loading system of fig. 7a.

Using the notations of figs. 7a and 7b and assuming that at infinity the displacements along the edges and the bisector are zero, this theorem reads in formula

$$\int_{\xi}^{\infty} \epsilon_{12}[x, \eta] dx = 2 \int_{\eta}^{\infty} \epsilon_{21}(y, \xi) dy. \quad (A.1)$$

With eqs. (6.28) this can be rewritten in the form

$$\int_{\xi/\eta}^{\infty} f_{12} \left[ \frac{x}{\eta} \right] d \left( \frac{x}{\eta} \right) = \int_{\eta/\xi}^{\infty} f_{21} \left[ \frac{y}{\xi} \right] d \left( \frac{y}{\xi} \right) \quad (A.2)$$

As  $\left( \frac{y}{\xi} \right)$  and  $\left( \frac{x}{\eta} \right)$  may be replaced by any other symbol, (A.2) is rewritten in the form

$$\int_{1/q}^{\infty} f_{12}[z] dz = \int_0^q f_{12} \left[ \frac{1}{z} \right] \frac{1}{z^2} dz = \int_q^{\infty} f_{21}[z] dz. \quad (A.3)$$

Taking  $q=0$  in (A.3) it is obvious that

$$\int_0^{\infty} f_{21}[z] dz = 0. \quad (A.4)$$

Hence, from (A.3) and (A.4)

$$\int_0^q f_{12} \left[ \frac{1}{z} \right] \frac{1}{z^2} dz = - \int_0^q f_{21}[z] dz \quad (A.5)$$

and as  $q$  is variable

<sup>1)</sup> This follows from (8.22), where  $t_I[x]$ , and  $x$  are dimensionless accordingly (8.35).

$$\frac{1}{z} f_{12} \left[ \frac{1}{z} \right] = -z f_{21}[z]. \quad (\text{A.6})$$

Application of the Mellin transform

$$\int_0^{\infty} \dots z^{s-1} dz \text{ on both sides of (A.6)}$$

delivers, according to ref. 4, chapter VI, form. (3) and (4)

$$a_{12}[-s+1] = -a_{21}[s+1] \quad (\text{A.7})$$

or, replacing  $s$  by  $-s$

$$a_{12}[s+1] = -a_{21}[-s+1]. \quad (\text{A.8})$$

## APPENDIX B.

Analytical integration of some terms in eqs. (8.41) and (8.42) with the aid of (8.43).

In eq. (8.42) the two terms

$$-\frac{2}{\pi} \int \frac{1}{\xi} \frac{t_{11}[\xi]}{1+y/\xi} d\xi - \frac{2}{\pi} \int \frac{1}{\xi} \frac{t_{11}[\xi]}{1-y/\xi} d\xi \quad (\text{B.1})$$

may be simplified to

$$-\frac{2}{\pi y} \int t_{11}^*[\xi] d\xi + \frac{2}{\pi y} \int t_{11}^*[\xi] d\xi = 0 \quad (\text{B.2})$$

when  $\xi$  is small with respect to  $y$ .

Under the same assumption the term

$$\frac{4}{\pi} \int \frac{1}{\xi} \frac{1-\nu(y/\xi)^2}{\{1+(y/\xi)^2\}^2} t_{11}[\xi] d\xi \quad (\text{B.3})$$

of (8.42) may be simplified to

$$-\frac{4\nu}{\pi y^2} \int \xi t_{11}^*[\xi] d\xi. \quad (\text{B.4})$$

When, on the other hand,  $\xi$  is large with respect to  $y$ , (B.3) can satisfactorily be replaced by

$$\frac{4}{\pi} \int \frac{t_{11}^{**}[\xi]}{\xi} d\xi. \quad (\text{B.5})$$

Next, the last three terms in the left hand side of eq. (8.41) will be considered.

The integral

$$\frac{4}{\pi} \int \frac{1}{\xi} \frac{\nu - (x/\xi)^2}{\{1+(x/\xi)^2\}^2} t_{11}[\xi] d\xi \quad (\text{B.6})$$

may be replaced by

$$-\frac{4}{\pi x^2} \int \xi t_{11}^*[\xi] d\xi, \text{ when } (x/\xi) \text{ is large} \quad (\text{B.7})$$

and by

$$\frac{4\nu}{\pi} \int \frac{t_{11}^{**}[\xi]}{\xi} d\xi, \text{ when } (x/\xi) \text{ is small.} \quad (\text{B.8})$$

In just the same way the integral

$$\frac{1}{2\pi} \int \frac{1}{\xi} \frac{(\nu^2 - 2\nu + 5)(x/\xi)^2 + (4\nu^2 + 12)(x/\xi) + (-\nu^2 - 6\nu + 3)}{\{1+(x/\xi)^2\}^3} t_{11}[\xi] d\xi \quad (\text{B.9})$$

may be replaced by

$$\frac{(\nu^2 - 2\nu + 5)}{2\pi x} \int t_1^*[\zeta] d\zeta, \text{ when } (x/\zeta) \text{ is large} \quad (\text{B.10})$$

and by

$$\frac{(-\nu^2 - 6\nu + 3)}{2\pi} \int \frac{t_1^{**}[\zeta]}{\zeta} d\zeta, \text{ when } (x/\zeta) \text{ is small.} \quad (\text{B.11})$$

Finally, when  $\zeta$  is small with respect to  $x$ , the integral

$$\frac{(1 + \nu)(3 - \nu)}{2\pi} \int \frac{1}{\zeta} \frac{t_1[\zeta]}{1 - x/\zeta} d\zeta \quad (\text{B.12})$$

may be replaced by

$$\frac{(1 + \nu)(3 - \nu)}{2\pi x} \int t_1^*[\zeta] d\zeta. \quad (\text{B.13})$$

TABLE 1.

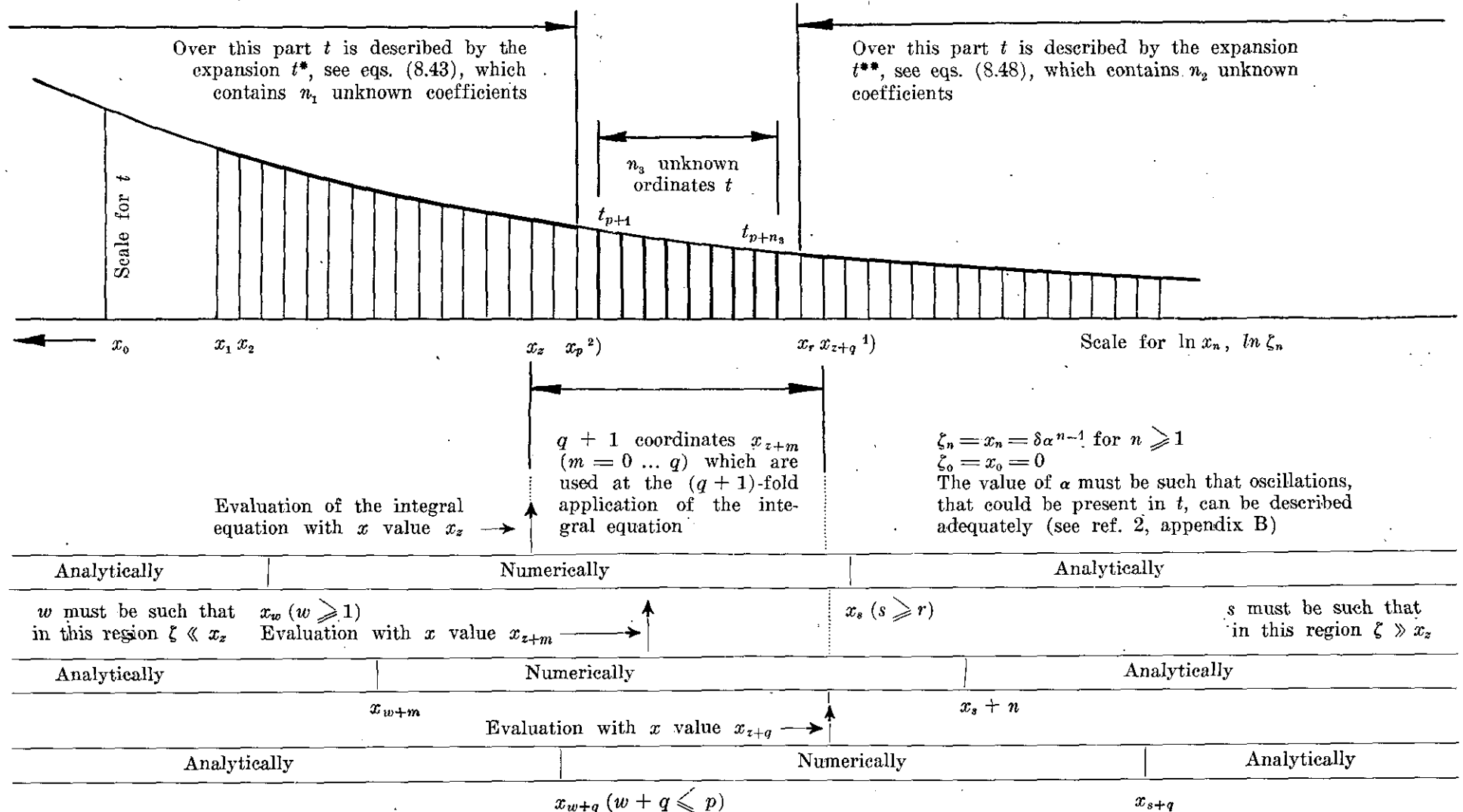
Formules (3.25) ... (3.28).

$\dots\dots F_1[s]$	$+$	$\dots\dots F_3[s]$	$+$	$\dots\dots G_1[s]$	$+$	$\dots\dots G_2[s]$	$=$	r. h. s.	eq.
$+ i(1 + \nu) \sin \alpha$		$-i(1 + \nu) \sin \alpha$		$2(1 - \nu) \cos \alpha$ $+ i\{4 - s(1 + \nu)\} \sin \alpha$		$2(1 - \nu) \cos \alpha$ $- i\{4 - s(1 + \nu)\} \sin \alpha$		0	(3.23)
$\exp(2 - s) i\alpha$		$\exp - (2 - s) i\alpha$		$(s - 2) \exp(2 - s) i\alpha$		$(s - 2) \exp - (2 - s) i\alpha$		0	(3.24)
$- \exp(1 - s) i\alpha$		$- \exp - (1 - s) i\alpha$		$-s \exp(1 - s) i\alpha$		$-s \exp - (1 - s) i\alpha$		$T_{II}[s]$	(3.25)
$-i \sin \alpha$		$i \sin \alpha$		$2 \cos \alpha + is \sin \alpha$		$2 \cos \alpha - is \sin \alpha$		$T_I[s]$	(3.26)
$(1 + \nu) \sin \alpha$		$(1 + \nu) \sin \alpha$		$- \{ (s - 2)(1 + \nu) + 4 \} \sin \alpha$ $+ 4i \cos \alpha$		$- \{ (s - 2)(1 + \nu) + 4 \} \sin \alpha$ $- 4i \cos \alpha$		$\frac{2}{-cs} T_I[s + 1]$	(3.27)
$\cos(s - 2)\alpha - i \sin(s - 2)\alpha$		$\cos(s - 2)\alpha + i \sin(s - 2)\alpha$		$\{ s \cos(s - 2)\alpha - 2 \cos s\alpha \}$ $+ i\{ -s \sin(s - 2)\alpha + 2 \sin s\alpha \}$		$\{ s \cos(s - 2)\alpha - 2 \cos s\alpha \}$ $- i\{ -s \sin(s - 2)\alpha + 2 \sin s\alpha \}$		$\frac{1}{s} T_{II}[s + 1] \sin \alpha$	(3.28)

TABLE 2.

Scheme for the numerical evaluation of an integral equation of the type

$$A + B \int_0^x t[\xi] \alpha \xi + C \int_0^\infty \frac{1}{\xi} h_1[x/\xi] t[\xi] d\xi + D \int_0^\infty \frac{1}{\xi} h_2[x/\xi] g[\xi] d\xi + E \int_0^\infty \frac{1}{\xi} \frac{t[\xi]}{1-x/\xi} d\xi + F \int_0^\infty \frac{1}{\xi} \frac{t[\xi]}{1+x/\xi} d\xi = 0.$$



1) Experience has shown that if  $z + q < r$  the method of solution leads to divergent results. If  $z + q = r$  the results are convergent. With  $z + q > r$  no experience has yet been obtained.  
 2) There is however no objection against  $z > p$ .  
 3) In eq. (8.42)  $x$  is to be replaced by  $y$ ,  $t[\xi] = t_{II}[\xi]$ ,  $g[\xi] = t_I[\xi]$ ,  $C = 0$ .  
 In eq. (8.41)  $t[\xi] = t_I[\xi]$ ,  $g[\xi] = t_{II}[\xi]$ ,  $F = 0$ .

TABLE 3.

Functions  $g_1$ ,  $g_2$  and  $g_3$  of (8.44) ... (8.46).

$x/\xi, y/\xi$	$g_1 [x/\xi]$	$g_2 [x/\xi]$	$g_3 [y/\xi]$
$2^{18}$	+ 0.0000171280	- 0.000000000145519	- 0.0000000000436557
$2^{17}$	+ 0. 342559	- 0. 582076	- 0. 174623
$2^{16}$	+ 0. 685117	- 0. 232831	- 0. 698494
$2^{15}$	+ 0. 137023	- 0. 931324	- 0. 279397
$2^{14}$	+ 0. 274044	- 0. 372529	- 0. 111759
$2^{13}$	+ 0. 548079	- 0. 149012	- 0. 447035
$2^{12}$	+ 0. 109613	- 0. 596046	- 0. 178814
$2^{11}$	+ 0. 219212	- 0. 238418	- 0. 715255
$2^{10}$	+ 0. 438370	- 0. 953675	- 0. 286102
$2^9$	+ 0. 876521	- 0. 381466	- 0. 114439
$2^8$	+ 0. 175216	- 0. 152582	- 0. 457726
$2^7$	+ 0. 350062	- 0. 610266	- 0. 183046
$2^6$	+ 0. 698523	- 0. 244004	- 0. 731469
$2^5$	+ 0.138976	- 0. 974372	- 0. 291446
$2^4$	+ 0.274437	- 0. 387137	- 0. 114763
$2^3$	+ 0.531344	- 0. 150769	- 0. 430769
$2^2$	+ 0.979120	- 0. 543253	- 0. 131488
$2$	+ 1.62185	- 0.148000	- 0. 800000
$1$	+ 2.24500	- 0.175000	+ 0.175000
$2^{-1}$	+ 2.49259	+ 0.0320000	+ 0.592000
$2^{-2}$	+ 2.29408	+ 0.210380	+ 0.869204
$2^{-3}$	+ 1.91396	+ 0.275692	+ 0.964923
$2^{-4}$	+ 1.58407	+ 0.293793	+ 0.991071
$2^{-5}$	+ 1.36830	+ 0.298440	+ 0.997756
$2^{-6}$	+ 1.24495	+ 0.299610	+ 0.999439
$2^{-7}$	+ 1.17899	+ 0.299902	+ 0.999860
$2^{-8}$	+ 1.14488	+ 0.299976	+ 0.999965
$2^{-9}$	+ 1.12754	+ 0.299994	+ 0.999991
$2^{-10}$	+ 1.11879	+ 0.299998	+ 0.999998
$2^{-11}$	+ 1.11441	+ 0.300000	+ 1.00000
$2^{-12}$	+ 1.11220	+ 0.300000	+ 1.00000
$2^{-13}$	+ 1.11110	+ 0.300000	+ 1.00000
$2^{-14}$	+ 1.11055	+ 0.300000	+ 1.00000
$2^{-15}$	+ 1.11027	+ 0.300000	+ 1.00000
$2^{-16}$	+ 1.11014	+ 0.300000	+ 1.00000
$2^{-17}$	+ 1.11007	+ 0.300000	+ 1.00000
$2^{-18}$	+ 1.11003	+ 0.300000	+ 1.00000

TABLE 4.

Evaluation of integral equation (8.63) into a system of ten linear relations between the unknowns.

term	coefficient
$A$	$+0.0002 \cdot 2^n \cdot 1/c + 0.00124279$
$\beta$	$-0.0000150862 \cdot 2^n \cdot n \cdot 1/c + 0.000222226 \cdot 2^n \cdot 1/c - 0.0000937451 n + 0.00138097$
$t_{1 \ 2+n}$	$+0.0000462100 \cdot 2^n \cdot 1/c + 0.000287371$
$t_{1 \ 3+n}$	$+0.000369680 \cdot 2^n \cdot 1/c + 0.00229963$
$t_{1 \ 4+n}$	$+0.000369680 \cdot 2^n \cdot 1/c + 0.00230097$
$t_{1 \ 5+n}$	$+0.00147872 \cdot 2^n \cdot 1/c + 0.00921437$
$t_{1 \ 6+n}$	$+0.00147872 \cdot 2^n \cdot 1/c + 0.00923486$
$t_{1 \ 7+n}$	$+0.00591488 \cdot 2^n \cdot 1/c + 0.0370966$
$t_{1 \ 8+n}$	$+0.00591488 \cdot 2^n \cdot 1/c + 0.0373932$
$t_{1 \ 9+n}$	$+0.0236596 \cdot 2^n \cdot 1/c + 0.151912$
$t_{1 \ 10+n}$	$+0.0236596 \cdot 2^n \cdot 1/c + 0.127023$
$t_{1 \ 11+n}$	$+0.0946380 \cdot 2^n \cdot 1/c + 1.00313$
$t_{1 \ 12+n}$	$+0.0473190 \cdot 2^n \cdot 1/c + 0.0360373$
$t_{1 \ 13+n}$	$-0.914223$
$t_{1 \ 14+n}$	$-0.144438$
$t_{1 \ 15+n}$	$-0.308519$
$t_{1 \ 16+n}$	$-0.158853$
$t_{1 \ 17+n}$	$-0.331679$
$t_{1 \ 18+n}$	$-0.170682$
$t_{1 \ 19+n}$	$-0.346936$
$t_{1 \ 20+n}$	$-0.174956$
$t_{1 \ 21+n}$	$-0.351449$
$t_{1 \ 22+n}$	$-0.176115$
$t_{1 \ 23+n}$	$-0.352622$
$t_{1 \ 24+n}$	$-0.0882052$

TABLE 4.

term	coefficient
$t_{II\ 2+n}$	-0.000000280554
$t_{II\ 3+n}$	-0.00000448882
$t_{II\ 4+n}$	-0.00000897738
$t_{II\ 5+n}$	-0.0000718117
$t_{II\ 6+n}$	-0.000143563
$t_{II\ 7+n}$	-0.00114657
$t_{II\ 8+n}$	-0.00227777
$t_{II\ 9+n}$	-0.0177414
$t_{II\ 10+n}$	-0.0319631
$t_{II\ 11+n}$	-0.174156
$t_{II\ 12+n}$	-0.102964
$t_{II\ 13+n}$	+0.0376523
$t_{II\ 14+n}$	+0.123780
$t_{II\ 15+n}$	+0.324414
$t_{II\ 16+n}$	+0.172857
$t_{II\ 17+n}$	+0.351183
$t_{II\ 18+n}$	+0.176280
$t_{II\ 19+n}$	+0.352903
$t_{II\ 20+n}$	+0.176495
right hand side	$(1/c)(0.0000502874 \cdot 2^n \cdot n \cdot 1/c - 0.000740754 \cdot 2^n \cdot 1/c + 0.000312484 \cdot n + 0.995395)$ $+ c (0.000000345648 \cdot 2^{-2n})$

In this basic equation  $n=0 \dots 9$ .

$$t_{I_p}^* = A - (1/c + 0.3\beta)(0.251437 p - 3.84389)$$

when  $p = 2 \dots 11$

$$t_{I_p}^* = 509295818 \cdot c \cdot 2^{-2p}$$

when  $p = 21 \dots 33$

$$t_{II_p}^* = A - 0.235785(1/c + 0.3\beta) - (1/c + 0.3\beta)(0.251437 p - 3.84389)$$

when  $p = 2 \dots 11$

$$t_{II_p}^{**} = 0$$

when  $p = 21 \dots 31$

The unknowns are  $A, \beta, t_{I_{12}} \dots t_{I_{20}}, t_{II_{12}} \dots t_{II_{20}}$ .

TABLE 5.

Evaluation of integral equation (8.64) into a system of ten linear relations between the unknowns.

term	coefficient
$A$	$+ 0.0001 \cdot 2^n - 0.000000182138$
$\beta$	$- 0.00000754312 \cdot 2^n \cdot n + 0.000104039 \cdot 2^n + 0.0000000137389 n - 1$
$t_{1 \ 2+n}$	$- 0.0000000841661$
$t_{1 \ 3+n}$	$- 0.00000134664$
$t_{1 \ 4+n}$	$- 0.00000269310$
$t_{1 \ 5+n}$	$- 0.0000215395$
$t_{1 \ 6+n}$	$- 0.0000430370$
$t_{1 \ 7+n}$	$- 0.000342953$
$t_{1 \ 8+n}$	$- 0.000675224$
$t_{1 \ 9+n}$	$- 0.00506898$
$t_{1 \ 10+n}$	$- 0.00773628$
$t_{1 \ 11+n}$	$- 0.00941382$
$t_{1 \ 12+n}$	$+ 0.102964$
$t_{1 \ 13+n}$	$+ 0.696623$
$t_{1 \ 14+n}$	$+ 0.511408$
$t_{1 \ 15+n}$	$+ 1.13545$
$t_{1 \ 16+n}$	$+ 0.583111$
$t_{1 \ 17+n}$	$+ 1.17409$
$t_{1 \ 18+n}$	$+ 0.588034$
$t_{1 \ 19+n}$	$+ 1.17656$
$t_{1 \ 20+n}$	$+ 0.588343$
$t_{1 \ 21+n}$	$+ 1.17672$
$t_{1 \ 22+n}$	$+ 0.588363$
$t_{1 \ 23+n}$	$+ 1.17673$
$t_{1 \ 24+n}$	$+ 0.294182$

TABLE 5.

term	coefficient
$t_{II\ 2+n}$	$+ 0.0000231050 \cdot 2^n + 0.000000280550$
$t_{II\ 3+n}$	$+ 0.000184840 \cdot 2^n + 0.00000448890$
$t_{II\ 4+n}$	$+ 0.000184840 \cdot 2^n + 0.00000897780$
$t_{II\ 5+n}$	$+ 0.000739360 \cdot 2^n + 0.0000718262$
$t_{II\ 6+n}$	$+ 0.000739360 \cdot 2^n + 0.000143679$
$t_{II\ 7+n}$	$+ 0.00295744 \cdot 2^n + 0.00115027$
$t_{II\ 8+n}$	$+ 0.00295744 \cdot 2^n + 0.00230731$
$t_{II\ 9+n}$	$+ 0.0118298 \cdot 2^n + 0.0186782$
$t_{II\ 10+n}$	$+ 0.0118298 \cdot 2^n + 0.00385651$
$t_{II\ 11+n}$	$+ 0.0473190 \cdot 2^n + 0.675185$
$t_{II\ 12+n}$	$+ 0.0236596 \cdot 2^n - 0.294182$
$t_{II\ 13+n}$	$- 1.85191$
$t_{II\ 14+n}$	$- 0.592220$
$t_{II\ 15+n}$	$- 1.19541$
$t_{II\ 16+n}$	$- 0.590671$
$t_{II\ 17+n}$	$- 1.17788$
$t_{II\ 18+n}$	$- 0.588508$
$t_{II\ 19+n}$	$- 1.17680$
$t_{II\ 20+n}$	$- 0.588373$
right hand side	$(1/c)(0.0000251438 \cdot 2^n \cdot n - 0.000346798 \cdot 2^n - 0.000000457964 n + 0.000000641563)$ $- c(0.00000115189 \cdot 2^{-2n})$

In this basic equation  $n = 0 \dots 9$ .

$$t_{I_p}^* = A - (1/c + 0.3\beta)(0.251437 p - 3.84389) \quad \text{when } p = 2 \dots 11$$

$$t_{I_p}^{**} = 509295818 \cdot c \cdot 2^{-2p} \quad \text{when } p = 21 \dots 33$$

$$t_{II_p}^* = A - 0.235785(1/c + 0.3\beta) - (1/c + 0.3\beta)(0.251437 p - 3.84389) \quad \text{when } p = 2 \dots 11$$

$$t_{II_p}^{**} = 0 \quad \text{when } p = 21 \dots 31$$

The unknowns are  $A, \beta, t_{I_{12}} \dots t_{I_{20}}, t_{II_{12}} \dots t_{II_{20}}$

TABLE 6.

Solutions for  $t_I[x]$  and  $t_{II}[y]$  in dimensionless form in case of stiffness ratio  $c = (E_s A_s)_I / (E_s A_s)_{II} = 1$ .

$p$	$x$ or $y = 10^{-4} \cdot 2^{p-2}$	$t_I[x]$	$t_{II}[y]$
1	0.00005	3.5787	3.3220
2	0.0001	3.3050	3.0483
3	0.0002	3.0313	2.7745
4	0.0004	2.7575	2.5008
5	0.0008	2.4838	2.2271
6	0.0016	2.2100	1.9533
7	0.0032	1.9363	1.6796
8	0.0064	1.6625	1.4058
9	0.0128	1.3888	1.1321
10	0.0256	1.1150	0.85834
11	0.0512	0.84130	0.58460
12	0.1024	0.62190	0.42904
13	0.2048	0.42356	0.28553
14	0.4096	0.25452	0.16395
15	0.8192	0.13178	0.080568
16	1.6384	0.056618	0.031575
17	3.2768	0.020167	0.0096511
18	6.5536	0.0061195	0.0021176
19	13.1072		0.00034843
20	26.2144		0.000041670

For relations between quantities without and with dimensions see formulas (3.5).

For behaviour  $x, y \rightarrow 0$  and  $x, y \rightarrow \infty$  see (8.15), (8.22) and (8.32).

$A = -0.33243$ ,  $\beta = 0.29572$ ,  $B$  was not computed.

NLR-TR W. 3

# Oscillating rectangular wings in supersonic flow with arbitrary bending and torsion mode shapes.

## Part I. Development of the theory

by

E. M. DE JAGER.

### Summary.

The pressure distribution at the surface of rectangular harmonically oscillating wings at supersonic speeds is determined by aid of Gardner's method for the solution of the potential equation. The solution is valid for arbitrary normal velocity distributions prescribed at the surface of the wing.

Lift and moment have been calculated for arbitrary bending and torsion mode shapes.

The aerodynamic derivatives are given in the form of the sum of some terms each of which consists of two factors, one being a function of the reduced frequency and the Mach number only, the other one containing the bending or the torsion mode shape in a very simple way.

### Contents.

- List of symbols.
- 1 Introduction.
  - 2 The fundamental equations and their solution.
    - 2.1 The boundary value problem.
    - 2.2 Gardner's method for solving the boundary value problem.
    - 2.3 The solution of the problem for  $\sigma(X, Y, T, \xi)$ .
    - 2.4 The derivation of the velocity potential on the wing.
  - 3 Determination of the pressure distribution on the wing.
    - 3.1 The downwash on the wing.
    - 3.2 The pressure distribution in the region of the wing, not influenced by the tips.
    - 3.3 The pressure distribution in the region of the wing tips.
  - 4 Determination of lift and moment.
    - 4.1 Definitions and notations.
    - 4.2 Determination of lift and moment.
    - 4.3 Recapitulation of the results.
  - 5 References.
- Appendices.
- A. Derivation of equation (2.13).
  - B. Derivation of the velocity potential at the wing in the region  $Y > X$ .
    - B.1 The case of translation (bending).
    - B.2 The case of pitch (torsion).
  - C. Derivation of the velocity potential at the wing in the region  $0 < Y < X$ .
    - C.1 The case of translation (bending).
    - C.2 The case of pitch (torsion).

C.3 The approximation  $\varphi\left(\frac{l}{\beta} Y\right) = T_1 + T_3 \frac{Y^2}{\beta^2}$

- D. Derivation of formulae for lift due to translation and pitch.
    - D.1 The lift due to translation
    - D.2 The lift due to pitch.
  - E. Derivation of formulae for the aerodynamic moment due to translation and pitch.
    - E.1 The aerodynamic moment due to translation.
    - E.2 The aerodynamic moment due to pitch.
- This investigation has been performed by order of the Netherlands Aircraft Development Board (N.I.V.).

### List of symbols.

$c$	velocity of sound.
$g(X, Y, T)$	$\frac{l}{\beta} w(x, y, t)$
$h$	amplitude of translation.
$k$	reduced frequency.
$l$	wing chord.
$p(X, Y)$	pressure distribution at the wing outside the Mach waves from leading edge tips.
$p_{tip}(X, Y)$	pressure distribution at the wing inside the Mach waves from leading edge tips.
$\Delta p(X, Y)$	edge correction of the pressure distribution at the wing.
$s$	wingspan.
$t$	time.
$w(x, y, t)$	downwash distribution at the wing.
$x, y, z$	physical coordinates.

$x_e$	$x$ coordinate of elastic axis.
$\mathcal{L}$	total lift.
$\mathcal{M}$	total moment.
$A$	aspect ratio.
$B(y)$	bending mode shape.
$B_i$	coefficients of polynomial approximation of the bending mode shape.
$C_L$	lift coefficient.
$C_M$	moment coefficient.
$L(Y)$	lift per unit span outside the Mach waves from the leading edge tips.
$\Delta L(Y)$	edge correction of the lift per unit span.
$\bar{L}$	lift, not corrected for the influence of the side edges of the wing.
$\Delta \bar{L}$	edge correction of the lift; $\mathcal{L} = \bar{L} + \Delta \bar{L}$ .
$M(Y)$	moment per unit span outside the Mach waves from the leading edge tips.
$\Delta M(Y)$	edge correction of the moment per unit span.
$\bar{M}$	moment, not corrected for the influence of the side edges of the wing.
$\Delta \bar{M}$	edge correction of the moment $\mathcal{M} = \bar{M} + \Delta \bar{M}$ .
$M$	Mach number.
$S$	wing area.
$T_i$	coefficients of polynomial approximation of the torsion mode shape.
$U$	velocity of the undisturbed flow.
$X, Y, Z, T$	Lorentz' transformed coordinates.
$X_e$	$X$ coordinate of elastic axis.
$\beta$	$\sqrt{M^2 - 1}$ .
$\kappa$	$\frac{2kM}{\beta^2}$ .
$\nu$	circular frequency.
$\rho$	density.
$\varphi(X, Y, 0, T)$	velocity potential at the wing outside Mach waves from leading edge tips.
$\varphi_{tip}(X, Y, 0, T)$	velocity potential at the wing inside Mach waves from leading edge tips.
$\Delta \varphi(X, Y, 0, T)$	edge correction of velocity potential at the wing.
$\varphi$	amplitude of rotation.
Subscript $B$	quantities associated with bending of the wing.
Subscript $T$	quantities associated with torsion of the wing.

## 1 Introduction.

The problem of the harmonically oscillating rectangular airfoil at supersonic-speeds has been investigated by many authors using various methods of approach.

Assuming the Mach waves from the leading edge wing tips do not intersect the opposite side

edges, the problem has been solved by Stewartson, Goodman, Rott et. al. for the case that the normal velocity, prescribed at the wing, is independent of the spanwise coordinate (see resp. lit. 1, 2 and 3).

In particular Stewartson solved the problem by using the Laplace transform of the velocity potential, Goodman by aid of Gardner's method for solving the potential equation (lit. 4) and Rott by following a method of Lamb (lit. 5) in his treatment of Sommerfeld's diffraction problem.

A solution in the form of a frequency expansion has been furnished by Watkins and Nelson (lit. 6 and 7); these expansions, however, are only valid in a restricted range of the frequency, viz. for an expansion up to the seventh power of the frequency the range of validity is  $0 \leq k \leq \frac{M^2 - 1}{M^2}$  where  $k$  denotes the reduced frequency and  $M$  the Mach number (see lit. 7).

All these solutions exhibit the disadvantage of being only valid for wings which do not deform in spanwise direction. However, Miles presented in lit. 8 a general solution by aid of the Wiener-Hopf technique; this solution is also valid for a normal velocity distribution varying in spanwise direction.

For a survey of all these theories the reader is referred to lit. 9. In this report a solution is presented which is also valid for normal velocity distributions varying in spanwise direction, the theory is a generalization of Goodman's method (lit. 2). The resulting formulae for the pressure distribution at the wing are rather complicated, which is also the case in Miles' theory. However, after integrating this pressure distribution over the wing surface, simple formulae for lift and moment have been obtained. It appears that it is possible to give a good approximation of the lift and the moment by expressing them in a number of terms each of which consists of two factors, one being a function of the frequency and Mach number only and the other one containing in a very simple way the variation of the downwash distribution in spanwise direction.

This report contains the development of the theory and formulae are given for lift and moment due to translation and pitch; the amplitude of the oscillation may be an arbitrary function of the spanwise coordinate.

The numerical results will be presented in a subsequent paper, ref. 13.

The author wishes to thank Prof. Dr. A. I. van der Vooren and Prof. Dr. E. van Spiegel for their helpful suggestions and their valuable criticism in the preparation of the report; he is also obliged to the members of the computational section of the National Aeronautical Research Institute.

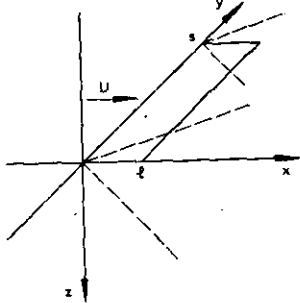
## 2 The fundamental equations and their solution.

### 2.1 The boundary value problem.

The linearized equation for the disturbance velocity potential  $\varphi$  in unsteady non-viscous irrotational compressible flow is given by:

$$(M^2 - 1)\varphi_{xx} - \varphi_{yy} - \varphi_{zz} + 2\frac{M}{c}\varphi_{xt} + \frac{1}{c^2}\varphi_{tt} = 0, \quad (2.1)$$

where  $x$ ,  $y$  and  $z$  are rectangular coordinates in streamwise, spanwise and vertical direction respectively,  $t$  is the time,  $M$  the Mach number and  $c$  the speed of sound (see sketch a).



Sketch a

The problem of calculating the pressure distribution on a given rectangular wing in supersonic flow without interfering tips is essentially the same as that for the quarter infinite wing, since the flow field behind the rectangular wing does not influence the flow field at the wing and the edge effect of one corner is the same as the effect of the other one due to symmetry.

Therefore we shall consider for the present only the quarter infinite wing. In keeping with the concepts of linearized theory the boundary conditions pertaining to equation (2.1) become now:

- (1) the normal velocity, positive in downward direction, is given on the wing; this means  $\varphi_z(x, y, 0, t) = w(x, y, t)$  for

$$0 < x < \infty, \quad 0 < y < \infty.$$

- (2) the disturbances are propagated downstream and they must vanish forward of the Mach waves originating at the leading edge of the airfoil; hence they are upstream of the envelope of the Mach cones with apices along the leading edge of the wing  $\varphi(x, y, z, t) \equiv 0$ .

- (3) the pressure must vanish off the airfoil, since it is asymmetric with respect to  $z$  and only the airfoil is capable of supporting a discontinuity in pressure; hence  $\frac{D\varphi}{Dt} = U \frac{\partial \varphi}{\partial x} + \frac{\partial \varphi}{\partial t} = 0$  for  $0 < -\beta y < x, z = 0$ , where  $U$  is the velocity of the undisturbed flow and  $\beta = \sqrt{M^2 - 1}$ .

By aid of the second boundary condition we can reduce the last condition to a somewhat simpler form, viz.:

$$\varphi(x, y, 0, t) = 0 \text{ for } 0 < -\beta y < x.$$

Equation (2.1) can be simplified by using the well-known Lorentz transformation, viz.:

$$\begin{aligned} X &= \frac{x}{l}, \quad Y = \frac{\beta}{l}y, \quad Z = \frac{\beta}{l}z, \\ T &= \frac{\beta^2 ct - Mx}{l}, \end{aligned} \quad (2.2)$$

where  $l$  is a representative length.

The transformed equation becomes

$$\varphi_{XX} - \varphi_{YY} - \varphi_{ZZ} - \varphi_{TT} = 0 \quad (2.3)$$

and the boundary conditions, pertaining to this equation, may be written as:

- (1)  $\varphi_z(X, Y, +0, T) = g(X, Y, T)$  for  $0 < X < \infty$ ,  $0 < Y < \infty$ , where

$$g(X, Y, T) = \frac{l}{\beta} w(x, y, t) \quad (2.4)$$

- (2)  $\varphi(X, Y, +0, T) = 0$  for  $X < 0$  and for  $Y < 0$ .

This boundary value problem will be solved by Gardner's method.

## 2.2 Short description of Gardner's method for solving the boundary value problem.

The essence of Gardner's method consists in splitting the four dimensional boundary value problems into two three dimensional problems.

For this purpose we introduce the auxiliary independent variable  $\xi$  and the quantities  $\sigma$  and  $\Omega$ .

With a slight modification of Gardner's method it is assumed that the function  $\sigma(X, Y, T, \xi)$  satisfies the partial differential equation

$$\sigma_{XX} - \sigma_{TT} - \sigma - \sigma_{\xi\xi} = 0, \quad (2.5)$$

and is submitted to the boundary conditions:

$$\begin{aligned} \sigma_{\xi}(X, Y, T, \xi) &= g(X, Y, T) \\ \text{for } \xi &= \pm 0, X > 0, \end{aligned} \quad (2.6)$$

and

$$\sigma(X, Y, T, \xi) \equiv 0 \text{ for } X < 0, \quad (2.7)$$

whereas the function  $\Omega(X, Y, Z, T, \xi)$  is a solution of the equation

$$\Omega_{\xi\xi} - \Omega_{YY} - \Omega_{ZZ} = 0, \quad (2.8)$$

and is subjected to the conditions

$$\begin{aligned} \Omega_Z(X, Y, Z, T, \xi) &= \sigma_{\xi}(X, Y, T, \xi) \\ \text{for } Z &= \pm 0, Y > 0, \end{aligned} \quad (2.9)$$

$$\left. \begin{aligned} \Omega(X, Y, Z, T, \xi) &\equiv 0 \\ \text{for } \xi &> X \\ \Omega(X, Y, Z, T, \xi) &\equiv 0 \\ \text{for } Z &= \pm 0, Y < 0, \end{aligned} \right\} \quad (2.10)$$

After the solution of these two boundary value problems the perturbation velocity potential is obtained by putting  $\xi = 0$  in the expression derived for the function  $\Omega(X, Y, Z, T, \xi)$ ; hence

$$\Omega(X, Y, Z, T, 0) = \varphi(X, Y, Z, T). \quad (2.11)$$

It would carry us too far to prove here that this function  $\varphi(X, Y, Z, T)$  really satisfies the boundary value problem pertaining to equation (2.3); see ref. (4).

Hence we may conclude that the time dependent boundary value problem in four variables is reduced to two boundary value problems in three variables, each of which is equivalent to a well-known problem in steady supersonic flow, which can be solved by means of Evvard's theory (ref. 10).





$$\begin{aligned} \varphi(X, Y, +0, T) = & -\frac{1}{\pi} \int_0^X \int_{Y-\xi_1}^{Y+\xi_1} \frac{\sigma_{\xi}(X, Y_1, T, \xi_1)}{\sqrt{\xi_1^2 - (Y - Y_1)^2}} dY_1 d\xi_1 + \\ & + \frac{1}{\pi} \int_Y^X \int_{Y-\xi_1}^{-Y+\xi_1} \frac{\sigma_{\xi}(X, Y_1, T, \xi_1)}{\sqrt{\xi_1^2 - (Y - Y_1)^2}} dY_1 d\xi_1, \quad \text{with } Y < X \end{aligned}$$

or after substituting  $Y - Y_1 = \bar{Y}$

$$\begin{aligned} \varphi(X, Y, +0, T) = & -\frac{1}{\pi} \int_0^X \int_{-\xi_1}^{+\xi_1} \frac{\sigma_{\xi}(X, Y - \bar{Y}, T, \xi_1)}{\sqrt{\xi_1^2 - \bar{Y}^2}} d\bar{Y} d\xi_1 + \\ & + \frac{1}{\pi} \int_Y^X \int_{2Y-\xi_1}^{+\xi_1} \frac{\sigma_{\xi}(X, Y - \bar{Y}, T, \xi_1)}{\sqrt{\xi_1^2 - \bar{Y}^2}} d\bar{Y} d\xi_1, \quad \text{with } Y < X. \end{aligned} \quad (2.17)$$

Comparing equations (2.16) and (2.17) we see at once, that the first term of (2.17) has the same form as the right-hand side of equation (2.16); hence the second term of (2.17) represents the edge effect of the wing.

### 3 Determination of the pressure distribution.

$$w(x, y) = \frac{\partial z}{\partial t} + U \frac{\partial z}{\partial x} = iv B(y) e^{ivt}, \quad (3.3)$$

#### 3.1 The boundary conditions on the wing.

The theory of the preceding chapter will now be applied to harmonically translating and pitching wings. Apart from some restrictions, which will be made later on, the amplitude of the oscillations are assumed to vary arbitrarily in the direction of the wing span, viz. the direction of  $y$ .

The wing surface  $z = z(x, y, t)$  is for the case of translation given by

$$z = z(x, y, t) = B(y) e^{ivt}, \quad (3.1)$$

where the bending mode shape  $B(y)$  is an arbitrary function of  $y$ . Since the bending moment is zero along the edge of the wing,  $\frac{d^2 B}{dy^2}$  must vanish there and hence

$$\left( \frac{d^2 B}{dy^2} \right)_{y=0} = 0. \quad (3.2)$$

Since the flow is supposed not to separate from the wing surface, the downwash on the wing is given by

and according to (2.4) the function  $g(X, Y, T)$  becomes:

$$\begin{aligned} g_B(X, Y, T) = & iv \frac{l}{\beta} B \left( \frac{l}{\beta} Y \right) e^{iv} \frac{iT + lMX}{\beta^2 c} \\ = & ikc\beta B \left( \frac{l}{\beta} Y \right) e^{ix(T+MX)}. \end{aligned} \quad (3.4)$$

For the case of pitching the wing surface will be given by the equation

$$z(x, y, t) = \varphi(y) (x - x_e) e^{ivt}, \quad (3.5)$$

where  $x_e$  is the  $x$ -coordinate of the elastic axis, which is assumed to be parallel with the leading edge of the wing. The torsion mode shape  $\varphi(y)$  is again assumed to be an arbitrary function of  $y$ . Since the torsion moment is zero along the wing tip,  $\frac{d\varphi}{dy}$  must vanish there and hence

$$\left( \frac{d\varphi}{dy} \right)_{y=0} = 0. \quad (3.6)$$

The downwash is now given by the expression

$$w(x, y) = \frac{\partial z}{\partial t} + U \frac{\partial z}{\partial x} = \varphi(y) \{ iv(x - x_e) + U \} e^{ivt}, \quad (3.7)$$

and hence according to (2.4) the function  $g(X, Y, T)$  becomes for the case of torsion:

$$\begin{aligned} g_T(X, Y, T) = & iv \frac{l^2}{\beta} \varphi \left( \frac{l}{\beta} Y \right) \left( X - X_e + \frac{1}{2ik} \right) e^{ix(T+MX)} \\ = & ikc\beta l X \varphi \left( \frac{l}{\beta} Y \right) e^{ix(T+MX)} \\ & - ikc\beta l \left( X_e + \frac{i}{2k} \right) \varphi \left( \frac{l}{\beta} Y \right) e^{ix(T+MX)}. \end{aligned} \quad (3.8)$$

Substitution of the functions  $g_B(X, Y, T)$  and  $g_T(X, Y, T)$  in formula (2.14) yields expressions for the function  $\sigma(X, Y, T, \xi)$  and when we insert consecutively these expressions into formulae (2.16) and (2.17) we get the velocity potential at the wing.

### 3.2 The pressure distribution in the region of the wing not influenced by the tips.

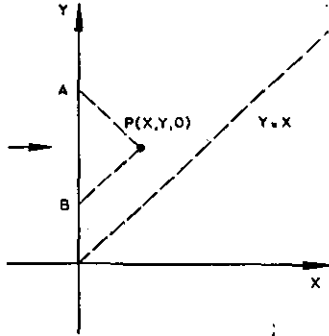
The pressure jump  $p$  over the wing, positive in upward direction, can be determined by aid of the formula:

$$\frac{p}{\frac{1}{2} \rho U^2} = \frac{4}{\text{LMU}} \left\{ M \frac{\partial \varphi(X, Y, +0, T)}{\partial X} - \frac{\partial \varphi(X, Y, +0, T)}{\partial T} \right\}, \quad (3.9)$$

where  $\rho$  denotes the density.

The region of the wing, which is not influenced by the wing tip, i.e. the region  $Y > X$ , will be considered first. The velocity potential in the point  $(X, Y, Z)$  is only determined by the points of the wing lying within the forward Mach cone with  $(X, Y, Z)$  as apex.

Hence the velocity potential at the wing in the point  $P(X, Y, 0)$  is only influenced by the points of the wing lying within the triangle  $ABP$  (see sketch e).



Sketch e

The bending mode shape  $B\left(\frac{l}{\beta} Y\right)$  and the torsion mode shape  $\varphi\left(\frac{l}{\beta} Y\right)$  will be approximated within this triangle by a polynomial of degree  $n$  with coefficients which depend on the spanwise coordinate of the point  $P$ .

The method of calculation is not limited with respect to the value of  $n$  and consequently the results of the calculations can always be improved by using polynomials of higher degree.

When the aspect ratio of the wing is not small and the Mach number of the undisturbed flow is sufficiently large, the triangle  $ABP$  will occupy a relatively small part of the wing surface. In this case the bending mode shape  $B$  and the torsion mode shape  $\varphi$  will be approximated fairly well by using polynomials of the second degree.

Hence we may write

$$B\left(\frac{l}{\beta} Y\right) = l \left( B_1 + B_2 \frac{Y}{\beta} + B_3 \frac{Y^2}{\beta^2} \right) \quad (3.10)$$

$$\varphi\left(\frac{l}{\beta} Y\right) = \left( T_1 + T_2 \frac{Y}{\beta} + T_3 \frac{Y^2}{\beta^2} \right)$$

with dimensionless coefficients which may vary from point to point in spanwise direction.

From the formulae (2.14), (3.4) and (3.10) it follows that the function  $\sigma(X, Y, T, \xi)$  in the case of translation can be written as

$$\sigma_B(X, Y, T, \xi) = i\kappa c \beta l \left( B_1 + B_2 \frac{Y}{\beta} + B_3 \frac{Y^2}{\beta^2} \right) e^{i\kappa T} \bar{\sigma}_B(X, \xi), \quad (3.11)$$

with

$$\bar{\sigma}_B(X, \xi) = - \int_{\xi}^X e^{i\kappa M(X-\bar{X})} J_0(\kappa \sqrt{X^2 - \xi^2}) d\bar{X} \quad \text{and } \xi > 0. \quad (3.12)$$

In the same way it follows from (2.14), (3.8) and (3.10) that the function  $\sigma(X, Y, T, \xi)$  in the case of pitch can be written as:

$$\begin{aligned} \sigma_T(X, Y, T, \xi) = & + i\kappa c \beta l \left( T_1 + T_2 \frac{Y}{\beta} + T_3 \frac{Y^2}{\beta^2} \right) e^{i\kappa T} \bar{\sigma}_T(X, \xi) - \\ & - i\kappa c \beta l \left( X_e + \frac{i}{2k} \right) \left( T_1 + T_2 \frac{Y}{\beta} + T_3 \frac{Y^2}{\beta^2} \right) e^{i\kappa T} \bar{\sigma}_B(X, \xi), \end{aligned} \quad (3.13)$$

with

$$\bar{\sigma}_T(X, \xi) = - \int_{\xi}^X (X - \bar{X}) e^{i\kappa M(X-\bar{X})} J_0(\kappa \sqrt{X^2 - \xi^2}) d\bar{x} \quad \text{and } \xi > 0. \quad (3.14)$$

Inserting (3.11) resp. (3.13) into the expression (2.16) we get the velocity potential at the wing. After some calculations which are performed in appendix B we obtain for the case of translation (bending):

$$\varphi_B(X, Y, +0, T) = -i\kappa c\beta l e^{i\kappa T} \left[ \left( B_1 + B_2 \frac{Y}{\beta} + B_3 \frac{Y^2}{\beta^2} \right) \int_0^X e^{i\kappa M(X-\bar{X})} J_0(\kappa\bar{X}) d\bar{X} - \frac{B_3}{\beta^2} \left\{ \frac{1}{\kappa^2} X J_0(\kappa X) - \frac{1}{\kappa^2} \int_0^X e^{i\kappa M(X-\bar{X})} J_0(\kappa\bar{X}) d\bar{X} + i \frac{M}{\kappa} \int_0^X e^{i\kappa M(X-\bar{X})} \bar{X} J_0(\kappa\bar{X}) d\bar{X} \right\} \right], \quad (3.15)$$

and for the case of pitch (torsion)

$$\begin{aligned} \varphi_T(X, Y, +0, T) = \varphi_B \left\{ X, Y, +0, T; B_h = - \left( X_e + \frac{i}{2k} \right) T_h \right\} - \\ - i\kappa c\beta l e^{i\kappa T} \left[ \left( T_1 + T_2 \frac{Y}{\beta} + T_3 \frac{Y^2}{\beta^2} \right) \int_0^X e^{i\kappa M(X-\bar{X})} (X-\bar{X}) J_0(\kappa\bar{X}) d\bar{X} + \right. \\ \left. + \frac{T_3}{\beta^2} \left\{ + i \frac{M}{x} \int_0^X e^{i\kappa M(X-\bar{X})} \bar{X}^2 J_0(\kappa\bar{X}) d\bar{X} - \frac{1}{\kappa^2} (i\kappa M X + 2) \int_0^X e^{i\kappa M(X-\bar{X})} \bar{X} J_0(\kappa\bar{X}) d\bar{X} + \right. \right. \\ \left. \left. + \frac{X}{\kappa^2} \int_0^X e^{i\kappa M(X-\bar{X})} J_0(\kappa\bar{X}) d\bar{X} \right\} \right], \quad (3.16) \end{aligned}$$

where  $\varphi_B \left\{ X, Y, +0, T; B_h = - \left( X_e + \frac{i}{2k} \right) T_h \right\}$  denotes the velocity potential (3.15) for the bending wing, where the coefficients  $B_h$  are replaced by  $- \left( X_e + \frac{i}{2k} \right) T_h$ ,  $h=1, 2, 3$ .

Using equation (3.9) we get finally the pressure on the wing in the region  $Y > X$ ; for the case of translation:

$$\begin{aligned} \frac{p_B(X, Y)}{\frac{1}{2} \rho U^2} = -4i \frac{\beta}{M^2} \kappa e^{i\kappa T} \left[ \left( B_1 + B_2 \frac{Y}{\beta} + B_3 \frac{Y^2}{\beta^2} \right) \left\{ M J_0(\kappa X) + i\kappa\beta^2 \int_0^X e^{i\kappa M(X-\bar{X})} J_0(\kappa\bar{X}) d\bar{X} \right\} + \right. \\ \left. + \frac{B_3}{\beta^2} \left\{ -i \frac{\beta^2}{\kappa} X J_0(\kappa X) + \frac{M}{\kappa} X J_1(\kappa X) + i \frac{\beta^2}{\kappa} \int_0^X e^{i\kappa M(X-\bar{X})} J_0(\kappa\bar{X}) d\bar{X} + \right. \right. \\ \left. \left. + \beta^2 M \int_0^X e^{i\kappa M(X-\bar{X})} \bar{X} J_0(\kappa\bar{X}) d\bar{X} \right\} \right], \quad (3.17) \end{aligned}$$

and for the case of pitch:

$$\begin{aligned} \frac{p_T(X, Y)}{\frac{1}{2} \rho U^2} = \frac{p_B}{\frac{1}{2} \rho U^2} \left\{ B_h = - \left( X_e + \frac{i}{2k} \right) T_h \right\} + \\ + 4i \frac{\beta}{M^2} \kappa e^{i\kappa T} \left[ + i\kappa\beta^2 \left( T_1 + T_2 \frac{Y}{\beta} + T_3 \frac{Y^2}{\beta^2} \right) \int_0^X e^{i\kappa M(X-\bar{X})} \bar{X} J_0(\kappa\bar{X}) d\bar{X} - \right. \\ - (M + i\kappa\beta^2 X) \left( T_1 + T_2 \frac{Y}{\beta} + T_3 \frac{Y^2}{\beta^2} \right) \int_0^X e^{i\kappa M(X-\bar{X})} J_0(\kappa\bar{X}) d\bar{X} + \frac{T_3}{\beta^2} \left[ \frac{M}{\kappa^2} X J_0(\kappa X) - \right. \\ \left. - \frac{1}{\kappa^2} (M + i\kappa\beta^2 X) \int_0^X e^{i\kappa M(X-\bar{X})} J_0(\kappa\bar{X}) d\bar{X} + \right. \\ \left. + \frac{i}{\kappa} \{ M^2 + \beta^2 (i\kappa M X + 2) \} \int_0^X e^{i\kappa M(X-\bar{X})} \bar{X} J_0(\kappa\bar{X}) d\bar{X} + \right. \\ \left. + M\beta^2 \int_0^X e^{i\kappa M(X-\bar{X})} \bar{X}^2 J_0(\kappa\bar{X}) d\bar{X} \right]. \quad (3.18) \end{aligned}$$

The integrals  $\int_0^X e^{i\kappa(MX-\bar{X})} \bar{X}^n J_0(\kappa\bar{X}) d\bar{X}$  are tabulated by Vera Huckel in ref. (11).

### 3.3 The pressure distribution in the region of the wing tips.

We shall now consider the region of the wing tip, i.e. the region where  $0 < Y < X$ .

The velocity potential in this region is given by equation (2.17). The first term of the right-hand side of this equation is exactly the same expression as the right-hand side of equation (2.16).

The velocity potential  $\varphi_{tip}$  in the region  $0 < Y < X$  can thus be splitted into two parts, viz. one part  $\varphi$  corresponding with the velocity potential in the region  $Y > X$  and the other part  $\Delta\varphi$ , which represents the correction of  $\varphi$  due to the presence of the edge of the wing, or in formula:

$$\varphi_{tip}(X, Y, +0, T) = \varphi(X, Y, +0, T) + \Delta\varphi(X, Y, +0, T), \quad (3.19)$$

where  $\varphi(X, Y, +0, T)$  is given by equation (2.16) and  $\Delta\varphi(X, Y, +0, T)$  by

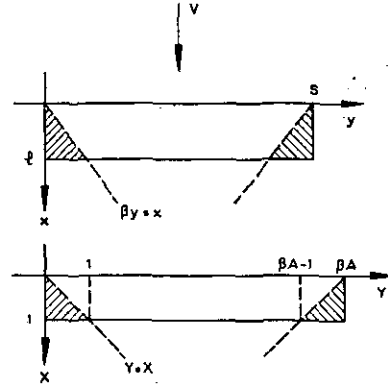
$$\begin{aligned} \Delta\varphi(X, Y, +0, T) = \\ + \frac{1}{\pi} \int_Y^X \int_{2Y-\xi}^{+\xi} \frac{\sigma_{\xi}(X, Y-\bar{Y}, T, \xi)}{\sqrt{\xi^2 - \bar{Y}^2}} d\bar{Y} d\xi, \\ 0 < Y < X. \end{aligned} \quad (3.20)$$

The pressure distribution  $p_{tip}(X, Y)$  in the region of the wing tip can accordingly be written as:

$$p_{tip}(X, Y) = p(X, Y) + \Delta p(X, Y), \quad (3.21)$$

where  $p(X, Y)$  is given by eq. (3.17) or (3.18) and  $\Delta p(X, Y)$  represents the influence of the edge on the pressure distribution. The latter has now to be determined for the cases of translation and pitch.

The bending mode shape  $B(y)$  has a vanishing second derivative for  $y=0$  and therefore this function will be approximated by  $l \left( B_1 + B_2 \frac{Y}{\beta} \right)$  for  $0 < Y < X$  with  $B_1$  and  $B_2$  as constant coefficients. When  $\beta A$  ( $A$  is the aspect ratio of the wing) is sufficiently large, the region influenced by the tip is relatively small in comparison with the whole surface of the wing (see sketch f), and



Sketch f

hence the error introduced by the rather rough approximation of  $B(y)$  for  $0 < Y < X$  will not give rise to large errors in the final results.

Moreover it is in principle possible to approximate the function  $B(y)$  for  $0 < Y < X$  by a polynomial of the third or even higher degree.

Henceforth we shall assume that the quantity  $\beta A$  is large enough in order to be justified to use the approximation  $l \left( B_1 + B_2 \frac{Y}{\beta} \right)$  for the bending mode shape in the region  $0 < Y < X$  of the wing.

The function  $\sigma(X, Y, T, \xi)$  becomes:

$$\sigma_B(X, Y, T, \xi) = i\kappa c \beta l \left( B_1 + B_2 \frac{Y}{\beta} \right) e^{i\kappa T} \bar{\sigma}_B(X, \xi), \quad \xi > 0, 0 < Y < X, \quad (3.22)$$

and this has now to be inserted into equation (3.20).

The result becomes (see appendix C.1):

$$\Delta\varphi_B(X, Y, +0, T) = i\kappa c \beta l e^{i\kappa T} \left[ \left( B_1 + \frac{B_2}{\beta} Y \right) \int_Y^X e^{i\kappa M(X-\bar{X})} I_1(\bar{X}, Y) d\bar{X} - \frac{B_2}{\beta} Y \int_Y^X e^{i\kappa M(X-\bar{X})} I_0(\bar{X}, Y) d\bar{X} \right], \quad (3.23)$$

with

$$I_0(\bar{X}, Y) = \frac{1}{\pi \sqrt{Y}} \int_Y^{\bar{X}} J_0(\kappa \sqrt{\bar{X}^2 - \xi_1^2}) \frac{d\xi_1}{\sqrt{\xi_1 - Y}}. \quad (3.24)$$

$$I_1(\bar{X}, Y) = \frac{\sqrt{Y}}{\pi} \int_Y^{\bar{X}} J_0(\kappa \sqrt{\bar{X}^2 - \xi_1^2}) \frac{d\xi_1}{\xi_1 \sqrt{\xi_1 - Y}}. \quad (3.25)$$

By aid of the equations (3.19), (3.15) and (3.23) the potential  $\varphi_{Btip}(X, Y, +0, T)$  is easily obtained, and using (3.9) and (3.21) the pressure distribution  $p_{Btip}$  due to translation becomes:

$$\frac{p_{Btip}(X, Y)}{\frac{1}{2} \rho U^2} = \frac{p_B(X, Y)}{\frac{1}{2} \rho U^2} + \frac{\Delta p_B(X, Y)}{\frac{1}{2} \rho U^2}; \quad 0 < Y < X, \quad (3.26)$$

where  $\frac{p_B(X, Y)}{\frac{1}{2} \rho U^2}$  is given by equation (3.17) and  $\frac{\Delta p_B(X, Y)}{\frac{1}{2} \rho U^2}$  by the formula:

$$\begin{aligned} \frac{\Delta p_B(X, Y)}{\frac{1}{2} \rho U^2} = & + 4i \frac{\beta}{M^2} \kappa e^{i\kappa T} \left[ M \left( B_1 + \frac{B_2}{\beta} Y \right) I_1(X, Y) - M \frac{B_2}{\beta} Y I_0(X, Y) + \right. \\ & \left. + i\kappa\beta^2 \left( B_1 + \frac{B_2}{\beta} Y \right) \int_Y^X e^{i\kappa M(X-\bar{X})} I_1(\bar{X}, Y) d\bar{X} - i\kappa\beta^2 \frac{B_2}{\beta} Y \int_Y^X e^{i\kappa M(X-\bar{X})} I_0(\bar{X}, Y) d\bar{X} \right], \end{aligned} \quad (3.27)$$

with  $0 < Y < X$ .

In order to determine the pressure distribution on the wing tip the integrals  $I_h(X, Y)$  and  $\int_Y^X e^{i\kappa M(X-\bar{X})} I_h(\bar{X}, Y) d\bar{X}$  ( $h = 0, 1$ ) have to be evaluated numerically. However, it will appear in the next chapter that the numerical evaluation of these integrals is not necessary, when the investigation is confined only to lift and moment of the wing.

In the case of pitch the torsion mode shape  $\varphi(y)$  has a vanishing first derivative for  $y=0$  and therefore this function should be approximated by the polynomial  $T_1 + T_3 \frac{Y^2}{\beta^2}$  for  $0 < Y < X$  with  $T_1$  and  $T_3$  as constant coefficients. However, this approximation of the torsion mode shape gives rise to such a large amount of calculations (see appendix C.3), that instead of the approximation  $\varphi = T_1 + T_3 \frac{Y^2}{\beta^2}$  the rough approximation  $\varphi = T_1 = \text{constant}$  for  $0 < Y < X$  will be used. The error introduced by taking this rough approximation will become smaller according as the quantity  $\beta A$  will be larger, since the parts of the wing

influenced by the wing tips become relatively smaller, when the aspect ratio of the wing or the Mach number is increased (see sketch f).

Henceforth it will be assumed that the aspect ratio of the wing or the Mach number or both will be sufficiently large in order to be justified to use the approximation  $\varphi \left( \frac{l}{\beta} Y \right) = T_1$  for the torsion mode function in the region  $0 < Y < X$  of the wing.

The function  $\sigma(X, Y, T, \xi)$  can be given immediately by putting  $T_2 = 0$  and  $T_3 = 0$  in eq. (3.13) and the result is:

$$\begin{aligned} \sigma_T(X, Y, T, \xi) = & + i\kappa c \beta l T_1 e^{i\kappa T} \bar{\sigma}_T(X, \xi) - \\ & - i\kappa c \beta l \left( X_e + \frac{i}{2k} \right) T_1 e^{i\kappa T} \bar{\sigma}_B(X, \xi), \end{aligned}$$

with  $\xi > 0$  and  $0 < Y < X$ . (3.28)

In order to obtain  $\Delta\varphi_T$  equation (3.28) has to be substituted into equation (3.20); the second term of (3.28) gives a contribution to  $\Delta\varphi_T$  which can be derived immediately from equation (3.23)

by replacing  $B_1$  by  $-\left(X_e + \frac{i}{2k}\right) T_1$  and putting  $B_2$  equal to zero.

The contribution of the first term of (3.28) to  $\Delta\varphi_T$  is determined in appendix C.2 and it appears that the tip correction for the velocity potential can be written as:

$$\begin{aligned} \Delta\varphi_T(X, Y, +0, T) = & i\kappa c \beta l T_1 e^{i\kappa T} \left[ - \left( X_e + \frac{i}{2k} \right) \int_Y^X e^{i\kappa M(X-\bar{X})} I_1(\bar{X}, Y) d\bar{X} + \right. \\ & \left. + \int_Y^X (X - \bar{X}) e^{i\kappa M(X-\bar{X})} I_1(\bar{X}, Y) d\bar{X} \right]. \end{aligned} \quad (3.29)$$

The addition of (3.29) to  $\varphi_T(X, Y, +0, T)$ , given by equation (3.16), yields the velocity potential  $\varphi_{T, \text{tip}}$  on the wing in the region of the wing tip and by aid of (3.9) and (3.21) we obtain finally the pressure distribution  $p_{T, \text{tip}}$  due to pitch.

$$\frac{p_{T, \text{tip}}(X, Y)}{\frac{1}{2} \rho U^2} = \frac{p_T(X, Y)}{\frac{1}{2} \rho U^2} + \frac{\Delta p_T(X, Y)}{\frac{1}{2} \rho U^2}, \quad 0 < Y < X, \quad (3.30)$$

where  $\frac{p_T(X, Y)}{\frac{1}{2} \rho U^2}$  is given by equation (3.18) and  $\frac{\Delta p_T(X, Y)}{\frac{1}{2} \rho U^2}$  by the formula:

$$\begin{aligned} \frac{\Delta p_T}{\frac{1}{2} \rho U^2} = & - 4i\kappa \frac{\beta}{M^2} T_1 e^{i\kappa T} \left[ + M \left( X_e + \frac{i}{2k} \right) I_1(X, Y) - \right. \\ & \left. - \{ 2M + (X - X_e) i\kappa\beta^2 \} \int_Y^X e^{i\kappa M(X-\bar{X})} I_1(\bar{X}, Y) d\bar{X} + i\kappa\beta^2 \int_Y^X \bar{X} e^{i\kappa M(X-\bar{X})} I_1(\bar{X}, Y) d\bar{X} \right]; \quad 0 < Y < X. \end{aligned} \quad (3.31)$$

In order to calculate the pressure distribution in the region of the wing tip  $0 < Y < X$  the integrals  $I_1$ ,  $\int_Y^X e^{i\kappa M(X-\bar{X})} I_1(\bar{X}, Y) d\bar{X}$  and  $\int_Y^X \bar{X} e^{i\kappa M(X-\bar{X})} I_1(\bar{X}, Y) d\bar{X}$  have to be evaluated numerically. When we restrict, however, our investigation to lift and moment, the numerical evaluation of these integrals can be avoided as will appear in the next chapter.

The formula for the pressure distribution due to pitch in the region  $0 < Y < X$  is given in appendix C.3, wherein the torsion mode shape has been approximated by  $\varphi(y) = T_1 + \frac{T_3}{\beta^2} Y^2$ . It turns out that the amount of calculations to obtain convenient expressions for lift and moment will be increased considerably, when the approximation  $\varphi = T_1 + \frac{T_3}{\beta^2} Y^2$  instead of  $\varphi = \text{constant}$  is used.

#### 4 Determination of lift and moment.

##### 4.1 Definitions and notations.

Expressions for lift and moment can be derived from the formulae for the pressure distribution on the wing.

The lift per unit span due to translation can be written as:

$$L_B(Y) = l \int_0^1 p_B(X, Y) dX \quad \text{for } 1 < Y < \beta A - 1, \quad (4.1)$$

and

$$L_B(Y) + \Delta L_B(Y) = l \int_0^1 p_B(X, Y) dX + l \int_Y^1 \Delta p_B(X, Y) dX \quad \text{for } 0 < Y < 1 \text{ and } \beta A - 1 < Y < \beta A, \quad (4.2)$$

where the second term  $\Delta L_B(Y)$  of the left-hand side equals the second term of the right-hand side.

In the same way the lift per unit span due to pitch is

$$L_T(Y) = l \int_0^1 p_T(X, Y) dX \quad \text{for } 1 < Y < \beta A - 1, \quad (4.3)$$

and

$$L_T(Y) + \Delta L_T(Y) = l \int_0^1 p_T(X, Y) dX + l \int_Y^1 \Delta p_T(X, Y) dX \quad \text{for } 0 < Y < 1 \text{ and } \beta A - 1 < Y < \beta A. \quad (4.4)$$

Quite analogously one obtains for the moments about the leading edge per unit span:

$$M_B(Y) = l^2 \int_0^1 X p_B(X, Y) dX \quad \text{for } 1 < Y < \beta A - 1, \quad (4.5)$$

$$M_B(Y) + \Delta M_B(Y) = l^2 \int_0^1 X p_B(X, Y) dX + l^2 \int_Y^1 X \Delta p_B(X, Y) dX \quad \text{for } 0 < Y < 1 \text{ and } \beta A - 1 < Y < \beta A, \quad (4.6)$$

$$M_T(Y) = l^2 \int_0^1 X p_T(X, Y) dX \quad \text{for } 1 < Y < \beta A - 1, \quad (4.7)$$

$$M_T(Y) + \Delta M_T(Y) = l^2 \int_0^1 X p_T(X, Y) dX + l^2 \int_Y^1 X \Delta p_T(X, Y) dX \quad \text{for } 0 < Y < 1 \text{ and } \beta A - 1 < Y < \beta A. \quad (4.8)$$

Integrating these expressions to  $Y$  and assuming the bending mode shape and the torsion mode shape symmetrical with respect to the midchord of the wing one obtains for the total lift and moment the following expressions:

$$\mathcal{L}_B = \bar{L}_B + \Delta\bar{L}_B = \frac{2l}{\beta} \int_0^{\frac{1}{2}\beta A} L_B(Y) dY + \frac{2l}{\beta} \int_0^1 \Delta L_B(Y) dY, \quad (4.9)$$

$$\mathcal{L}_T = \bar{L}_T + \Delta\bar{L}_T = \frac{2l}{\beta} \int_0^{\frac{1}{2}\beta A} L_T(Y) dY + \frac{2l}{\beta} \int_0^1 \Delta L_T(Y) dY, \quad (4.10)$$

$$\mathcal{M}_B = \bar{M}_B + \Delta\bar{M}_B = \frac{2l}{\beta} \int_0^{\frac{1}{2}\beta A} M_B(Y) dY + \frac{2l}{\beta} \int_0^1 \Delta M_B(Y) dY, \quad (4.11)$$

$$\mathcal{M}_T = \bar{M}_T + \Delta\bar{M}_T = \frac{2l}{\beta} \int_0^{\frac{1}{2}\beta A} M_T(Y) dY + \frac{2l}{\beta} \int_0^1 \Delta M_T(Y) dY, \quad (4.12)$$

where  $\bar{L}_B = \frac{2l}{\beta} \int_0^{\frac{1}{2}\beta A} L_B(Y) dY$ ,  $\Delta\bar{L}_B = \frac{2l}{\beta} \int_0^1 \Delta L_B(Y) dY$  and in the same way for the corresponding terms in the other formulae.

The first terms represent the part of lift or moment, which corresponds with results obtained by strip theory, whereas the second terms represent the correction due to the finite span of the wing.

Substituting the formulae for the pressure distribution (3.17), (3.18), (3.27) and (3.31) one gets finally the desired expressions for lift and moment.

The formulae (3.27) and (3.31) are valid for the case that the Mach waves from the leading edge do not intersect on the surface of the wing, hence for  $\beta A > 2$  (see sketch f). Therefore one might think that the derived expressions for lift and moment will also be valid for  $\beta A > 2$ . However, it can easily be shown that the expressions for lift and moment will be even valid for  $\beta A > 1$ , when the downwash distribution at the wing is symmetrical with respect to the midchord of the wing. The formulae for the pressure distribution are however not valid in the extended range of  $\beta A$ .

Hence our results for lift and moment will be valid as long as the Mach waves from the leading edge tips do not intersect the opposite side edges of the wing.

#### 4.2 Determination of lift and moment.

The determination of the first part of lift and moment viz.  $\bar{L}$  and  $\bar{M}$  can be performed by integrating the formulae (3.17) and (3.18) first to  $X$  and consecutively to  $Y$ .

The integration to  $X$  results into a combination of functions  $f_\lambda(\kappa, M)$  defined by

$$f_\lambda(\kappa, M) = \int_0^1 e^{-i\kappa M X} (\kappa X)^\lambda J_0(\kappa X) dX, \quad (4.13)$$

with  $\lambda = 0, 1, 2, 3, 4$ .

These integrals, of course also occurring in two-dimensional unsteady supersonic flow theory, are tabulated by Vera Huckel in ref. 11. The integration to  $Y$  involves for the case of translation nothing more than the integration into the spanwise direction of the bending mode shape and its second derivative, and correspondingly for the case of pitch the integration of the torsion mode shape and its second derivative. The calculations have been carried out in appendices D.1, D.2, E.1 and E.2 and the results are summarized in the next section.

The determination of the second part of lift and moment viz.  $\Delta\bar{L}$  and  $\Delta\bar{M}$  which represent the influence of the wing edges involves the reduction of the double integrals:

$$\Delta\bar{L} = \frac{2l^2}{\beta} \int_0^1 \left\{ \int_Y^1 \Delta p(X, Y) dX \right\} dY, \quad (4.14)$$

and

$$\Delta\bar{M} = \frac{2l^3}{\beta} \int_0^1 \left\{ \int_Y^1 X \Delta p(X, Y) dX \right\} dY. \quad (4.15)$$

Substituting equations (3.27) and (3.31) into (4.14) and (4.15) and performing the integration to  $X$  gives rise to the occurrence of integrals which to the authors knowledge can only be calculated numerically.

Since this involves much numerical tedious calculations the order of integration will be interchanged and the double integral can then be reduced to integrals which partly can be calculated exactly and partly can be written in the form (4.13).

The reductions have been carried out in appendices D.1, D.2, E.1 and E.2 and the results are again summarized in the next section.

### 4.3 Recapitulation of the results.

In this section we give a review of the results for lift and moment derived in the appendices D and E and make some complementary remarks.

#### a) The lift due to bending of the wing.

The lift coefficient due to bending reads:

$$C_{L_B} = \frac{\mathcal{L}_B}{\frac{1}{2} \rho U^2 S e^{i\omega t}} = \frac{\bar{L}_B}{\frac{1}{2} \rho U^2 S e^{i\omega t}} + \frac{\Delta \bar{L}_B}{\frac{1}{2} \rho U^2 S e^{i\omega t}}, \quad (4.16)$$

where the second term is a correction of the first one due to the finite span of the wing;  $S$  denotes the wing area.

$$\left. \begin{aligned} \frac{\bar{L}_B}{\frac{1}{2} \rho U^2 S e^{i\omega t}} &= F_B(\kappa, M) \frac{\int_0^{\frac{1}{2}\beta A} B\left(\frac{lY}{\beta}\right) dY}{\frac{1}{2} \beta A} + G_B(\kappa, M) \frac{\left\{ \frac{dB(y)}{dy} \right\}_{y=0}}{\beta A}, \\ \frac{\Delta \bar{L}_B}{\frac{1}{2} \rho U^2 S e^{i\omega t}} &= H_B(\kappa, M) \frac{B_1}{\beta A} + K_B(\kappa, M) \frac{B_2}{\beta A}, \end{aligned} \right\} \quad (4.17)$$

where  $B(y) = B\left(\frac{lY}{\beta}\right)$  is the bending mode shape of the wing;  $B_1$  and  $B_2$  are constants such that  $l\left(B_1 + B_2 \frac{Y}{\beta}\right)$  approximates the bending mode shape as well as possible in the region  $0 < Y < X$ .

$$\left. \begin{aligned} F_B(\kappa, M) &= -4i \frac{\beta}{M^2} \kappa \{ (M + i\kappa\beta^2) f_0(\kappa, M) - i\beta^2 f_1(\kappa, M) \}, \\ G_B(\kappa, M) &= +4i \frac{1}{M^2} \frac{1}{\kappa} [-Me^{-i\kappa M} J_0(\kappa) + (M + i\kappa\beta^2) f_0(\kappa, M) - i\{2\beta^2 + \\ &\quad + M(M + i\kappa\beta^2)\} f_1(\kappa, M) - M\beta^2 f_2(\kappa, M)], \\ H_B(\kappa, M) &= +4 \frac{\beta}{M^2} \left[ 1 + \frac{1}{\kappa\beta^2} \{ iM + e^{-i\kappa M} (\sin \kappa - iM \cos \kappa) \} \right], \\ K_B(\kappa, M) &= -\frac{1}{4} G_B(\kappa, M). \end{aligned} \right\} \quad (4.18)$$

#### b) The lift due to torsion of the wing.

The lift coefficient to torsion reads

$$C_{L_T} = \frac{\mathcal{L}_T}{\frac{1}{2} \rho U^2 S e^{i\omega t}} = \frac{\bar{L}_T}{\frac{1}{2} \rho U^2 S e^{i\omega t}} + \frac{\Delta \bar{L}_T}{\frac{1}{2} \rho U^2 S e^{i\omega t}}, \quad (4.19)$$

where the second term again denotes the correction of the first one due to the finite span of the wing.

$$\left. \begin{aligned} \frac{\bar{L}_T}{\frac{1}{2} \rho U^2 S e^{i\omega t}} &= \left\{ F_T(\kappa, M) - \left( X_e + \frac{iM}{\beta^2 \kappa} \right) F_B(\kappa, M) \right\} \frac{\int_0^{\frac{1}{2}\beta A} \varphi\left(\frac{lY}{\beta}\right) dY}{\frac{1}{2} \beta A} + \\ &\quad + \left\{ G_T(\kappa, M) + \beta \left( X_e + \frac{iM}{\beta^2 \kappa} \right) G_B(\kappa, M) \right\} \frac{1}{\beta A} \left\{ \frac{d\varphi\left(\frac{lY}{\beta}\right)}{dY} \right\}_{Y=\frac{1}{2}\beta A}, \\ \frac{\Delta \bar{L}_T}{\frac{1}{2} \rho U^2 S e^{i\omega t}} &= \left\{ H_T(\kappa, M) - \left( X_e + \frac{iM}{\beta^2 \kappa} \right) H_B(\kappa, M) \right\} \frac{T_1}{\beta A}, \end{aligned} \right\} \quad (4.20)$$

where  $\varphi(y) = \varphi\left(l \frac{Y}{\beta}\right)$  denotes the torsion mode shape of the wing;  $T_1$  is the constant which approximates the torsion mode shape as well as possible in the region  $0 < Y < X$ .

$$\begin{aligned}
 F_T(\kappa, M) &= + 2i \frac{\beta}{M^2} \{ -\kappa(2M + i\beta^2\kappa)f_0(\kappa, M) + 2(M + i\kappa\beta^2)f_1(\kappa, M) - i\beta^2f_2(\kappa, M) \}, \\
 G_T(\kappa, M) &= + 2i \frac{\beta}{M^2} \frac{1}{\kappa^2} [ -\kappa(2M + i\beta^2\kappa)f_0(\kappa, M) + \{ 4M + 2i\kappa(3\beta^2 + 1) - \kappa^2\beta^2M \} \cdot \\
 &\quad \cdot f_1(\kappa, M) + \{ -5i\beta^2 - 2i + 2\kappa M\beta^2 \} f_2(\kappa, M) - M\beta^2f_3(\kappa, M) ], \\
 H_T(\kappa, M) &= + \frac{4}{\beta^3M^2} \cdot \frac{1}{\kappa^2} \left[ \{ (1 + M^2) \cos \kappa + 2iM \sin \kappa \} e^{-i\kappa M} - (1 + M^2) + i\kappa M\beta^2 + \frac{\kappa^2\beta^4}{2} \right]
 \end{aligned} \tag{4.21}$$

c) *The aerodynamic moment due to bending of the wing.*

The moment coefficient due to bending reads:

$$C_{M_B} = \frac{\mathfrak{M}_B}{\frac{1}{2} \rho U^2 S l e^{i\omega t}} = \frac{\bar{M}_B}{\frac{1}{2} \rho U^2 S l e^{i\omega t}} + \frac{\Delta \bar{M}_B}{\frac{1}{2} \rho U^2 S l e^{i\omega t}}, \tag{4.22}$$

where the second term is again the correction of the first one due to the finite span of the wing.

$$\begin{aligned}
 \frac{\bar{M}_B}{\frac{1}{2} \rho U^2 S l e^{i\omega t}} &= P_B(\kappa, M) \frac{\int_0^{\frac{1}{2}\beta A} \frac{B\left(\frac{lY}{\beta}\right) dY}{l} + Q_B(\kappa, M) \left\{ \frac{dB(y)}{dy} \right\}_{y=0}}{\frac{1}{2} \beta A}, \\
 \frac{\Delta \bar{M}_B}{\frac{1}{2} \rho U^2 S l e^{i\omega t}} &= R_B(\kappa, M) \frac{B_1}{\beta A} + S_B(\kappa, M) \frac{B_2}{\beta A}.
 \end{aligned} \tag{4.23}$$

$$\begin{aligned}
 P_B(\kappa, M) &= + 2 \frac{\beta}{M^2} \{ \kappa^2\beta^2f_0(\kappa, M) - 2iMf_1(\kappa, M) - \beta^2f_2(\kappa, M) \}, \\
 Q_B(\kappa, M) &= - \frac{2}{M^2} \frac{1}{\kappa^2} \{ 2i\kappa M e^{-i\kappa M} J_0(\kappa) + \kappa^2\beta^2f_0(\kappa, M) - iM(4 + \kappa^2\beta^2) \cdot \\
 &\quad \cdot f_1(\kappa, M) - (5\beta^2 + 2)f_2(\kappa, M) + iM\beta^2f_3(\kappa, M) \}, \\
 R_B(\kappa, M) &= + \frac{2\beta}{M^2} \left[ 1 - \frac{2}{\kappa^2\beta^4} \left\{ (1 + M^2) \cos \kappa + 2iM \sin \kappa + i\kappa M\beta^2 \cos \kappa - \right. \right. \\
 &\quad \left. \left. - \kappa\beta^2 \sin \kappa \right\} e^{-i\kappa M} - (M^2 + 1) \right], \\
 S_B(\kappa, M) &= - \frac{1}{4} Q_B(\kappa, M).
 \end{aligned} \tag{4.24}$$

d) *The aerodynamic moment due to torsion of the wing.*

The moment coefficient due to torsion reads:

$$C_{M_T} = \frac{\mathfrak{M}_T}{\frac{1}{2} \rho U^2 S l e^{i\omega t}} = \frac{\bar{M}_T}{\frac{1}{2} \rho U^2 S l e^{i\omega t}} + \frac{\Delta \bar{M}_T}{\frac{1}{2} \rho U^2 S l e^{i\omega t}}, \tag{4.25}$$

where the second term again denotes the correction of the first one due to the finite span of the wing.

$$\begin{aligned}
 \frac{\bar{M}_T}{\frac{1}{2} \rho U^2 S l e^{i\omega t}} &= \left\{ P_T(\kappa, M) - \left( X_c + \frac{iM}{\kappa\beta^2} \right) P_B(\kappa, M) \right\} \frac{\int_0^{\frac{1}{2}\beta A} \varphi\left(\frac{lY}{\beta}\right) dY}{\frac{1}{2} \beta A} + \\
 &\quad + \left\{ Q_T(\kappa, M) + \beta \left( X_c + \frac{iM}{\kappa\beta^2} \right) Q_B(\kappa, M) \right\} \frac{1}{\beta A} \left\{ \frac{d\varphi\left(\frac{lY}{\beta}\right)}{dY} \right\}_{Y=\frac{1}{2}\beta A} \\
 \frac{\Delta \bar{M}_T}{\frac{1}{2} \rho U^2 S l e^{i\omega t}} &= \left\{ R_T(\kappa, M) - \left( X_c + \frac{iM}{\kappa\beta^2} \right) R_B(\kappa, M) \right\} \frac{T_1}{\beta A}.
 \end{aligned} \tag{4.26}$$

$$\begin{aligned}
P_T(\kappa, M) &= + \frac{2}{3} \frac{i\beta}{\kappa M^2} \{ -\kappa^2(3M + 2i\kappa\beta^2)f_0(\kappa, M) + 3i\kappa^2\beta^2 \cdot f_1(\kappa, M) + \\
&\quad + 3M \cdot f_2(\kappa, M) - i\beta^2 \cdot f_3(\kappa, M) \}, \\
Q_T(\kappa, M) &= + \frac{2}{3} \frac{i\beta}{\kappa^3 M^2} [-\kappa^2(3M + 2i\kappa\beta^2)f_0(\kappa, M) + i\kappa^2 \{ 3(3\beta^2 + 1) + 2i\kappa M\beta^2 \} \cdot \\
&\quad \cdot f_1(\kappa, M) + 3M(3 + \kappa^2\beta^2)f_2(\kappa, M) - i(7\beta^2 + 3)f_3(\kappa, M) - M\beta^2 \cdot f_4(\kappa, M) ], \\
R_T(\kappa, M) &= + \frac{4}{M^2\beta^5} \frac{1}{\kappa^2} [ \{ (4 + 3\beta^2) \sin \kappa - iM(4 + \beta^2) \cos \kappa + 2i\kappa M\beta^2 \sin \kappa + \\
&\quad + \kappa\beta^2(\beta^2 + 2) \cos \kappa \} e^{-iM\kappa} + iM(4 + \beta^2) + \frac{1}{2}iM\kappa^2\beta^4 + \frac{1}{2}\kappa^3\beta^6 ].
\end{aligned}$$

The expressions given in this section for lift and moment are valid for arbitrary bending and torsion mode shapes, provided  $\beta A$  is not too small (see section 3.3) and the Mach waves from the leading edge tips do not intersect the opposite side edges of the wing.

The corrections due to the finite span of the wing appear to be inversely proportional to the effective aspect ratio  $\beta A$ .

For the case of a flat wing translating or pitching harmonically the bending mode shape becomes  $B = h = \text{constant}$  and the torsion mode shape becomes  $\varphi = \alpha = \text{constant}$  and the formulae given in this section become quite exact.

For the case of translation the formulae for the lift and moment derivatives become:

$$\frac{\partial C_L}{\partial h} = \frac{\mathcal{L}_B}{\frac{1}{2}\rho U^2 S h e^{i\omega t}} = F_B(\kappa, M) + \frac{H_B(\kappa, M)}{\beta A}, \quad (4.27)$$

$$\frac{\partial C_M}{\partial h} = \frac{\mathcal{M}_B}{\frac{1}{2}\rho U^2 S h l e^{i\omega t}} = P_B(\kappa, M) + \frac{R_B(\kappa, M)}{\beta A}, \quad (4.28)$$

where  $h$  is the amplitude of the translation.

For the case of pitch one obtains:

$$\frac{\partial C_L}{\partial \varphi} = \frac{\mathcal{L}_T}{\frac{1}{2}\rho U^2 S \varphi e^{i\omega t}} = \left\{ F_T(\kappa, M) - \left( X_e + \frac{iM}{\beta^2 \kappa} \right) F_B(\kappa, M) \right\} + \left\{ \frac{H_T(\kappa, M) - \left( X_e + \frac{iM}{\beta^2 \kappa} \right) H_B(\kappa, M)}{\beta A} \right\}, \quad (4.29)$$

$$\frac{\partial C_M}{\partial \varphi} = \frac{\mathcal{M}_T}{\frac{1}{2}\rho U^2 S l \varphi e^{i\omega t}} = \left\{ P_T(\kappa, M) - \left( X_e + \frac{iM}{\beta^2 \kappa} \right) P_B(\kappa, M) \right\} + \left\{ \frac{R_T(\kappa, M) - \left( X_e + \frac{iM}{\beta^2 \kappa} \right) R_B(\kappa, M)}{\beta A} \right\}. \quad (4.30)$$

The first term of these expressions represents the two dimensional part while the second term yields the correction due to the finite span of the wing.

The numerical results of this report are presented in ref. 13.

## 5 References.

- 1 STEWARTSON, K. On the linearized potential theory of unsteady supersonic motion. *Quart. J. Mech. and Appl. Math.* 3, 182-199 (1950).
- 2 GOODMAN, T. R., The quarter infinite wing oscillating at supersonic speeds. *Quart. Appl. Math.* 10, 189-192 (1952).
- 3 ROY, N. On the unsteady motion of a thin rectangular wing in supersonic flow. *J. A. S.* 18, 775-776, (1951).
- 4 GARDNER, C. Time dependent linearized supersonic flow past planar wings. *Comm. on Pure and Appl. Math.* 3, 33-38 (1950).
- 5 LAMB, H. On Sommerfeld's diffraction problem and on reflection by a parabolic mirror. *Proc. London Math. Soc.* (2), 4, 190-203 (1906).
- 6 WATKINS, C. E. Effect of aspect ratio on the air forces and moments of harmonically oscillating thin rectangular wings in supersonic potential flow. *N. A. C. A. Rep.* 1028, 1951.
- 7 NELSON, H. C., RAINEY, R. A., WATKINS, C. E. Lift and moment coefficients expanded to the seventh power of frequency for oscillating rectangular wings in supersonic flow and applied to a specific flutter problem. *N. A. C. A. Tech. Note* 3076, 1954.
- 8 MILES, J. W. The oscillating rectangular airfoil at supersonic speeds. *Quart. Appl. Math.* 9, 47-65, 1951.
- 9 MILES, J. W. Potential theory of unsteady supersonic flow. *Cambridge monographs on mechanics and appl. math.* Cambridge University Press, 1959.
- 10 EVVARD, J. C. Use of source distribution for evaluating theoretical aerodynamics of thin finite wings at supersonic speeds. *N. A. C. A. Rep.* 951, 1950.
- 11 HUCKEL, VERA. Tabulation of the  $f_A$  functions which occur in the aerodynamic theory of oscillating wings in supersonic flow. *N. A. C. A. Tech. Note* 3606, 1056.
- 12 BATEMAN, H. Higher transcendental functions. Vol. II, pag. 46. *Mc Graw-Hill Book Company Inc.* 1953.
- 13 DE JAGER, E. M. Oscillating rectangular wings in supersonic flow with arbitrary bending and torsion mode shapes. Part II Numerical results. *N. L. L. Report W. 5, National Aeronautical Research Institute, Amsterdam* 1960.

## APPENDIX A

## Derivation of equation (2.13).

Inserting the limits of integration equation (2.12) can be written as:

$$\sigma(X, Y, T, \xi) = -\frac{1}{\pi} \int_0^{X-\xi} \int_{T-\sqrt{(X-X_1)^2-\xi^2}}^{T+\sqrt{(X-X_1)^2-\xi^2}} g(X_1, Y, T_1) \frac{dT_1 dX_1}{\sqrt{(X-X_1)^2 - (T-T_1)^2 - \xi^2}}, \quad \xi > 0. \quad (\text{A.1})$$

For harmonic oscillations we may write:

$$\varphi(X, Y, Z, T) = \Phi(X, Y, Z) e^{i\kappa T}$$

with  $\kappa = \frac{2kM}{\beta^2}$  and  $k$  the reduced frequency.

Hence  $\varphi_z(X, Y, 0, T) = \Phi_z(X, Y, 0) e^{i\kappa T}$  and the function  $g(X, Y, T)$  may be written as  $g(X, Y, T) = G(X, Y) e^{i\kappa T}$ .

Substituting this into equation (A.1) we obtain:

$$\sigma(X, Y, T, \xi) = -\frac{1}{\pi} \int_0^{X-\xi} G(X_1, Y) \left\{ \int_{T-\sqrt{(X-X_1)^2-\xi^2}}^{T+\sqrt{(X-X_1)^2-\xi^2}} \frac{e^{i\kappa T_1} dT_1}{\sqrt{(X-X_1)^2 - (T-T_1)^2 - \xi^2}} \right\} dX_1, \quad \xi > 0.$$

The integration to  $T_1$  is performed by putting

$$T_1 = T - \sqrt{(X-X_1)^2 - \xi^2} \cos \Theta$$

and the result is

$$\begin{aligned} \int_{T-\sqrt{(X-X_1)^2-\xi^2}}^{T+\sqrt{(X-X_1)^2-\xi^2}} \frac{e^{i\kappa T_1} dT_1}{\sqrt{(X-X_1)^2 - (T-T_1)^2 - \xi^2}} &= e^{i\kappa T} \int_0^\pi e^{-i\kappa \sqrt{(X-X_1)^2 - \xi^2} \cos \Theta} d\Theta = \\ &= \pi e^{i\kappa T} J_0 \{ \kappa \sqrt{(X-X_1)^2 - \xi^2} \}. \end{aligned}$$

Hence

$$\sigma(X, Y, T, \xi) = - \int_0^{X-\xi} g(X_1, Y, T) J_0 \{ \kappa \sqrt{(X-X_1)^2 - \xi^2} \} dX_1$$

which is identical to eq. (2.13).

## APPENDIX B

Derivation of the velocity potential on the wing in the region  $Y > X$ .

## B.1 The case of translation (bending).

In the case of translation the function  $\sigma(X, Y, T, \xi)$  introduced in section 2.2 can be written as:

$$\sigma_B(X, Y, T, \xi) = i\kappa c \beta l \left( B_1 + B_2 \frac{Y}{\beta} + B_3 \frac{Y^2}{\beta^2} \right) e^{i\kappa T} \bar{\sigma}_B(X, \xi) \quad (\text{B.1})$$

$$\bar{\sigma}_B(X, \xi) = - \int_{\xi}^X e^{i\kappa M(X-\bar{X})} J_0(\kappa \sqrt{\bar{X}^2 - \xi^2}) d\bar{X} \quad \text{and } \xi > 0. \quad (\text{B.2})$$

According to equation (2.16) the velocity potential becomes

$$\begin{aligned} \varphi_B(X, Y, +0, T) &= -\frac{i\kappa c \beta l}{\pi} e^{i\kappa T} \int_0^X \frac{\partial}{\partial \xi_1} \bar{\sigma}_B(X, \xi_1) \left\{ \int_{\xi_1}^{Y+\xi_1} \frac{B_1 + B_2 \frac{Y_1}{\beta} + B_3 \frac{Y_1^2}{\beta^2}}{\sqrt{\xi_1^2 - (Y-Y_1)^2}} dY_1 \right\} d\xi_1 = \\ &= -\frac{i\kappa c \beta l}{\pi} e^{i\kappa T} \int_0^X \frac{\partial}{\partial \xi_1} \bar{\sigma}_B(X, \xi_1) \left\{ \int_{-\xi_1}^{+\xi_1} \frac{B_1 + B_2 \frac{(Y-\bar{Y})}{\beta} + B_3 \frac{(Y-\bar{Y})^2}{\beta^2}}{\sqrt{\xi_1^2 - \bar{Y}^2}} d\bar{Y} \right\} d\xi_1. \end{aligned}$$

The inner integral equals  $\pi(B_1 + B_2 \frac{Y}{\beta} + B_3 \frac{Y^2}{\beta^2} + 1/2 \frac{B_3}{\beta^2} \xi_1^2)$  and thus the velocity potential can be written as

$$\begin{aligned} \varphi_B(X, Y, +0, T) &= + i\kappa c \beta l e^{i\kappa T} \left[ \left( B_1 + B_2 \frac{Y}{\beta} + B_3 \frac{Y^2}{\beta^2} \right) \bar{\sigma}_B(X, 0) - 1/2 \frac{B_3}{\beta^2} \int_0^X \frac{\partial}{\partial \xi_1} \{ \bar{\sigma}_B(X, \xi_1) \} \xi_1^2 d\xi_1 \right] = \\ &= + i\kappa c \beta l e^{i\kappa T} \left[ \left( B_1 + B_2 \frac{Y}{\beta} + B_3 \frac{Y^2}{\beta^2} \right) \bar{\sigma}_B(X, 0) + \frac{B_3}{\beta^2} \int_0^X \bar{\sigma}_B(X, \xi_1) \xi_1 d\xi_1 \right], \end{aligned}$$

After substitution of (B.2) and interchanging the order of integration we can write:

$$\begin{aligned} \int_0^X \bar{\sigma}_B(X, \xi_1) \xi_1 d\xi_1 &= - \int_0^X e^{i\kappa M(X-\bar{X})} \left\{ \int_0^{\bar{X}} J_0(\kappa \sqrt{\bar{X}^2 - \xi_1^2}) \xi_1 d\xi_1 \right\} d\bar{X} = \\ &= - \int_0^X e^{i\kappa M(X-\bar{X})} \bar{X}^2 \left\{ \int_0^{\frac{\pi}{2}} J_0(\kappa \bar{X} \sin \varphi) \sin \varphi \cos \varphi d\varphi \right\} d\bar{X}. \end{aligned}$$

The inner integral equals  $\frac{J_1(\kappa \bar{X})}{\kappa \bar{X}}$  (see ref. 12) and hence

$$\begin{aligned} \int_0^X \bar{\sigma}_B(X, \xi_1) \xi_1 d\xi_1 &= - \frac{1}{\kappa} \int_0^X e^{i\kappa M(X-\bar{X})} \bar{X} J_1(\kappa \bar{X}) d\bar{X} = \\ &+ \frac{1}{\kappa^2} \int_0^X e^{i\kappa M(X-\bar{X})} \bar{X} \frac{dJ_0(\kappa \bar{X})}{d\bar{X}} d\bar{X} = \frac{1}{\kappa^2} X J_0(\kappa X) - \frac{1}{\kappa^2} \int_0^X e^{i\kappa M(X-\bar{X})} J_0(\kappa \bar{X}) d\bar{X} + \\ &+ i \frac{M}{\kappa} \int_0^X e^{i\kappa M(X-\bar{X})} \kappa J_0(\kappa \bar{X}) d\bar{X}. \end{aligned}$$

Inserting this result into the last expression for the velocity potential we obtain finally:

$$\begin{aligned} \varphi_B(X, Y, +0, T) &= - i\kappa c \beta l e^{i\kappa T} \left\{ \left( B_1 + B_2 \frac{Y}{\beta} + B_3 \frac{Y^2}{\beta^2} \right) \int_0^X e^{i\kappa M(X-\bar{X})} J_0(\kappa \bar{X}) d\bar{X} - \right. \\ &\left. - \frac{B_3}{\beta^2} \frac{1}{\kappa^2} \left[ X J_0(\kappa X) - \int_0^X e^{i\kappa M(X-\bar{X})} J_0(\kappa \bar{X}) d\bar{X} + i\kappa M \int_0^X e^{i\kappa M(X-\bar{X})} \bar{X} J_0(\kappa \bar{X}) d\bar{X} \right] \right\} \quad (B.3) \end{aligned}$$

which expression is the same as expression (3.15).

## B.2 The case of pitch (torsion).

We shall now deduce the expression for the velocity potential for the case of pitch. The function  $\sigma(X, Y, T, \xi)$  is given by equations (3.13) and (3.14) viz.:

$$\begin{aligned} \sigma_T(X, Y, T, \xi) &= + i\kappa c \beta l \left( T_1 + T_2 \frac{Y}{\beta} + T_3 \frac{Y^2}{\beta^2} \right) e^{i\kappa T} \bar{\sigma}_T(X, \xi) - \\ &- i\kappa c \beta l \left( X_e + \frac{i}{2k} \right) \left( T_1 + T_2 \frac{Y}{\beta} + T_3 \frac{Y^2}{\beta^2} \right) e^{i\kappa T} \bar{\sigma}_B(X, \xi) \quad (B.4) \end{aligned}$$

with

$$\bar{\sigma}_T(X, \xi) = - \int_{\xi}^X (X - \bar{X}) e^{i\kappa M(X-\bar{X})} J_0(\kappa \sqrt{\bar{X}^2 - \xi^2}) d\bar{X} \quad \text{with } \xi > 0. \quad (B.5)$$

The second term of the right-hand side of equation (B.4) gives a contribution to the velocity potential on the wing which equals the velocity potential  $\varphi_B(X, Y, +0, T)$  for the case of translation, where however the coefficients  $B_h$  are replaced by  $-\left(X_e + \frac{i}{2k}\right) T_h$ ,  $h=1, 2, 3$ .

This part will be denoted by  $\varphi_B \left\{ X, Y, + 0, T; B_h = - \left( X_e + \frac{i}{2k} \right) T_h \right\}$ .

The contribution of the first term of equation (B.4) to the velocity potential will be denoted by  $\varphi_{T,1}(X, Y, + 0, T)$  and according to equation (2.16) we can write:

$$\begin{aligned} \varphi_{T,1}(X, Y, + 0, T) &= - \frac{i\kappa c\beta l}{\pi} e^{i\kappa T} \int_0^X \frac{\partial \bar{\sigma}_T(X, \xi_1)}{\partial \xi_1} \left\{ \int_{-\xi_1}^{+\xi_1} \frac{T_1 + T_2 \frac{Y - \bar{Y}}{\beta} + T_3 \frac{(Y - \bar{Y})^2}{\beta^2}}{\sqrt{\xi_1^2 - \bar{Y}^2}} d\bar{Y} \right\} d\xi_1 \\ &= + i\kappa c\beta l e^{i\kappa T} \left\{ \left( T_1 + T_2 \frac{Y}{\beta} + T_3 \frac{Y^2}{\beta^2} \right) \bar{\sigma}_T(X, 0) - \frac{1}{2} \frac{T_3}{\beta^2} \int_0^X \xi_1^2 \frac{\partial \bar{\sigma}_T(X, \xi_1)}{\partial \xi_1} d\xi_1 \right\} = \\ &= - i\kappa c\beta l e^{i\kappa T} \left\{ \left( T_1 + T_2 \frac{Y}{\beta} + T_3 \frac{Y^2}{\beta^2} \right) \int_0^X (X - \bar{X}) e^{i\kappa M(X - \bar{X})} J_0(\kappa \bar{X}) d\bar{X} - \frac{T_3}{\beta^2} \int_0^X \bar{\sigma}_T(X, \xi_1) \xi_1 d\xi_1 \right\}. \quad (\text{B.6}) \end{aligned}$$

The integral  $\int_0^X \bar{\sigma}_T(X, \xi_1) \xi_1 d\xi_1$  can be reduced in the same way as  $\int_0^X \bar{\sigma}_B(X, \xi_1) d\xi_1$  and the result becomes

$$\begin{aligned} \int_0^X \bar{\sigma}_T(X, \xi_1) \xi_1 d\xi_1 &= -i \frac{M}{\kappa} \int_0^X e^{i\kappa M(X - \bar{X})} \bar{X}^2 J_0(\kappa \bar{X}) d\bar{X} + \frac{i\kappa M X + 2}{\kappa^2} \int_0^X e^{i\kappa M(X - \bar{X})} \bar{X} \cdot J_0(\kappa \bar{X}) d\bar{X} - \\ &= - \frac{X}{\kappa^2} \int_0^X e^{i\kappa(MX - \bar{X})} J_0(\kappa \bar{X}) d\bar{X}. \end{aligned}$$

Inserting this result into equation (B.6) and adding the contribution  $\varphi_B \left\{ X, Y, + 0, T; \right.$

$B_h = - \left( X_e + \frac{i}{2k} \right) T_h \left. \right\}$  we obtain finally

$$\begin{aligned} \varphi_T(X, Y, + 0, T) &= \varphi_B \left\{ X, Y, + 0, T; B_h = - \left( X_e + \frac{i}{2k} \right) T_h \right\} - \\ &= - i\kappa c\beta l e^{i\kappa T} \left[ \left( T_1 + T_2 \frac{Y}{\beta} + T_3 \frac{Y^2}{\beta^2} \right) \int_0^X (X - \bar{X}) e^{i\kappa M(X - \bar{X})} J_0(\kappa \bar{X}) d\bar{X} + \right. \\ &+ \frac{T_3}{\beta^2} \left\{ + i \frac{M}{\kappa} \int_0^X e^{i\kappa M(X - \bar{X})} \bar{X}^2 J_0(\kappa \bar{X}) d\bar{X} - \frac{2 + i\kappa M X}{\kappa^2} \int_0^X e^{i\kappa M(X - \bar{X})} \bar{X} J_0(\kappa \bar{X}) d\bar{X} + \right. \\ &\left. \left. + \frac{X}{\kappa^2} \int_0^X e^{i\kappa M(X - \bar{X})} J_0(\kappa \bar{X}) d\bar{X} \right\} \right] \quad (\text{B.6}) \end{aligned}$$

which is the same as expression (3.16).

## APPENDIX C.

**Derivation of the velocity potential on the wing in the region  $0 < Y < X$ .**

### C.1 The case of translation (bending).

The velocity potential in the region of the wing tip is denoted by  $\varphi_{B_{tip}}(X, Y, + 0, T)$  and according to eq. (3.19) it can be written as:

$$\varphi_{B_{tip}}(X, Y, + 0, T) = \varphi_B(X, Y, + 0, T) + \Delta\varphi_B(X, Y, + 0, T) \quad (\text{C.1})$$

where  $0 < Y < X$ .

The first term of the right-hand side is already determined in appendix B and is given by equation (B.3) or (3.15).

The second term  $\Delta\varphi_B(X, Y, +0, T)$  is obtained by substitution of

$$\sigma = \sigma_B(X, Y, T, \xi) = i\kappa c\beta l \left( B_1 + B_2 \frac{Y}{\beta} \right) e^{i\kappa T} \bar{\sigma}_B(X, \xi) \quad (3.22)$$

with

$$\bar{\sigma}_B(X, \xi) = - \int_{\xi}^X e^{i\kappa M(X-\bar{X})} J_0(\kappa \sqrt{\bar{X}^2 - \xi^2}) d\bar{X} \quad (3.12)$$

into

$$\Delta\varphi_B = \frac{1}{\pi} \int_Y^X \int_{2Y-\xi_1}^{+\xi_1} \frac{\sigma_{\xi}(X, Y-\bar{Y}, T, \xi_1)}{\sqrt{\xi_1^2 - \bar{Y}^2}} d\bar{Y} d\xi_1. \quad (3.20)$$

Hence  $\Delta\varphi_B$  can be put into the form

$$\Delta\varphi_B = \frac{i\kappa c\beta l e^{i\kappa T}}{\pi} \int_Y^X \left\{ \frac{\partial \bar{\sigma}_B(X, \xi_1)}{\partial \xi_1} \right\} \left\{ \int_{2Y-\xi_1}^{+\xi_1} \frac{B_1 + \frac{B_2}{\beta} (Y-\bar{Y})}{\sqrt{\xi_1^2 - \bar{Y}^2}} d\bar{Y} \right\} d\xi_1. \quad (C.2)$$

The inner integral can be reduced to

$$\left( B_1 + \frac{B_2}{\beta} Y \right) \left( \frac{\pi}{2} - \sin^{-1} \frac{2Y-\xi_1}{\xi_1} \right) - 2 \frac{B_2}{\beta} \sqrt{Y} \cdot \sqrt{\xi_1 - Y}$$

and equation (C.2) can then be written as:

$$\Delta\varphi_B = i\kappa c\beta l e^{i\kappa T} \left[ -\frac{1}{2} \left( B_1 + \frac{B_2}{\beta} Y \right) \bar{\sigma}_B(X, Y) - \frac{1}{\pi} \left( B_1 + \frac{B_2}{\beta} Y \right) \int_Y^X \left\{ \frac{\partial}{\partial \xi_1} \bar{\sigma}_B(X, \xi_1) \right\} \sin^{-1} \frac{2Y-\xi_1}{\xi_1} d\xi_1 - \right. \\ \left. - \frac{2}{\pi} \frac{B_2}{\beta} \sqrt{Y} \int_Y^X \frac{\partial}{\partial \xi_1} \bar{\sigma}_B(X, \xi_1) \sqrt{\xi_1 - Y} d\xi_1 \right]$$

or after partial integration:

$$\Delta\varphi_B = i\kappa c\beta l e^{i\kappa T} \left[ \frac{B_2}{\beta} \frac{\sqrt{Y}}{\pi} \int_Y^X \bar{\sigma}_B(X, \xi_1) \frac{d\xi_1}{\sqrt{\xi_1 - Y}} - \left( B_1 + \frac{B_2}{\beta} Y \right) \frac{\sqrt{Y}}{\pi} \int_Y^X \bar{\sigma}_B(X, \xi_1) \frac{d\xi_1}{\xi_1 \sqrt{\xi_1 - Y}} \right].$$

Substitution of (3.12) into this expression for  $\Delta\varphi_B$  and interchanging the order of integration yields finally:

$$\Delta\varphi_B(X, Y, +0, T) = i\kappa c\beta l e^{i\kappa T} \left[ -\frac{B_2}{\beta} Y \int_Y^X e^{i\kappa M(X-\bar{X})} I_0(\bar{X}, Y) d\bar{X} + \left( B_1 + \frac{B_2}{\beta} Y \right) \int_Y^X e^{i\kappa M(X-\bar{X})} I_1(\bar{X}, Y) d\bar{X} \right] \quad (C.3)$$

where

$$I_0(\bar{X}, Y) = \frac{1}{\pi \sqrt{Y}} \int_Y^{\bar{X}} J_0(\kappa \sqrt{\bar{X}^2 - \xi_1^2}) \frac{d\xi_1}{\sqrt{\xi_1 - Y}} \quad \text{and} \quad I_1(\bar{X}, Y) = \frac{\sqrt{Y}}{\pi} \int_Y^{\bar{X}} J_0(\kappa \sqrt{\bar{X}^2 - \xi_1^2}) \frac{d\xi_1}{\xi_1 \sqrt{\xi_1 - Y}} \quad (C.4)$$

This expression for  $\Delta\varphi_B(X, Y, +0, T)$  is the same as eq. (3.23).

## C.2 The case of pitch (torsion).

The velocity potential in the region of the wing tip is denoted by  $\varphi_{T_{tip}}(X, Y, +0, T)$  and according to (3.19) it can be written as

$$\varphi_{T_{tip}}(X, Y, +0, T) = \varphi_T(X, Y, +0, T) + \Delta\varphi_T(X, Y, +0, T) \quad \text{with} \quad 0 < Y < X. \quad (C.5)$$

The first term of the right-hand side of equation (C.5) represents the part of the velocity potential which is not influenced by the wing edges. This term is already determined in appendix B and is given by the formulae (B.6) or (3.16).

The second term denotes the influence of the edge in the velocity potential and this part of the velocity potential is obtained by substitution of

$$\sigma = \sigma_T(X, Y, T, \xi) = i\kappa c\beta l T_1 e^{i\kappa T} \bar{\sigma}_T(X, \xi) - i\kappa c\beta l \left( X_e + \frac{i}{2k} \right) T_1 e^{i\kappa T} \bar{\sigma}_B(X, \xi) \quad (3.28)$$

with

$$\bar{\sigma}_B(X, \xi) = \frac{1}{\pi} \int_{\xi}^X e^{i\kappa M(X-\bar{X})} J_0(\sqrt{X^2 - \xi^2}) d\bar{X} \quad (3.12)$$

and

$$\bar{\sigma}_T(X, \xi) = - \int_{\xi}^X (X - \bar{X}) e^{i\kappa M(X-\bar{X})} J_0(\kappa \sqrt{X^2 - \xi^2}) d\bar{X} \quad (3.14)$$

into

$$\Delta\varphi = + \frac{1}{\pi} \int_Y^X \int_{2Y-\xi_1}^{+\xi_1} \frac{\sigma_{\xi}(X, Y - \bar{Y}, T, \xi_1)}{\sqrt{\xi_1^2 - \bar{Y}^2}} d\bar{Y} d\xi_1. \quad (3.20)$$

The second term of (3.28) gives a contribution to  $\Delta\varphi_T$  which can be obtained immediately from equation (3.23) or (C.3) by replacing  $B_1$  by  $-\left(X_e + \frac{i}{2k}\right) T_1$  and putting  $B_2$  equal to zero.

Hence  $\Delta\varphi_T$  can be written as:

$$\begin{aligned} \Delta\varphi_T(X, Y, +0, T) &= i\kappa c\beta l T_1 e^{i\kappa T} \left[ -\left(X_e + \frac{i}{2k}\right) \int_Y^X e^{i\kappa M(X-\bar{X})} I_1(\bar{X}, Y) d\bar{X} + \right. \\ &\quad \left. + \frac{1}{\pi} \int_Y^X \left\{ \frac{\partial}{\partial \xi_1} \bar{\sigma}_T(X, \xi_1) \right\} \left\{ \int_{2Y-\xi_1}^{+\xi_1} \frac{d\bar{Y}}{\sqrt{\xi_1^2 - \bar{Y}^2}} \right\} d\xi_1 \right] = \\ &= i\kappa c\beta l T_1 e^{i\kappa T} \left[ -\left(X_e + \frac{i}{2k}\right) \int_Y^X e^{i\kappa M(X-\bar{X})} I_1(\bar{X}, Y) d\bar{X} + \frac{1}{\pi} \int_Y^X \left\{ \frac{\partial}{\partial \xi_1} \bar{\sigma}_T(X, \xi_1) \right\} \left( \frac{\pi}{2} - \sin^{-1} \frac{2Y - \xi_1}{\xi_1} \right) d\xi_1 \right] \\ &= i\kappa c\beta l T_1 e^{i\kappa T} \left[ -\left(X_e + \frac{i}{2k}\right) \int_Y^X e^{i\kappa M(X-\bar{X})} I_1(\bar{X}, Y) d\bar{X} - \frac{1}{\pi} \sqrt{Y} \int_Y^X \bar{\sigma}_T(X, \xi_1) \frac{d\xi_1}{\xi_1 \sqrt{\xi_1^2 - Y}} \right]. \quad (C.6) \end{aligned}$$

Substitution of (3.14) into the second term of (C.6) and interchanging the order of integration yields finally

$$\begin{aligned} \Delta\varphi_T(X, Y, +0, T) &= i\kappa c\beta l T_1 e^{i\kappa T} \left[ -\left(X_e + \frac{i}{2k}\right) \int_Y^X e^{i\kappa M(X-\bar{X})} I_1(\bar{X}, Y) d\bar{X} + \right. \\ &\quad \left. + \int_Y^X (X - \bar{X}) e^{i\kappa M(X-\bar{X})} I_1(\bar{X}, Y) d\bar{X} \right] \quad (C.7) \end{aligned}$$

with

$$I_1(\bar{X}, Y) = \frac{\sqrt{Y}}{\pi} \int_Y^{\bar{X}} J_0(\kappa \sqrt{X^2 - \xi_1^2}) \frac{d\xi_1}{\xi_1 \sqrt{\xi_1^2 - Y}}$$

which is the same expression as the right-hand side of eq. (3.29).

### C.3 The approximation $\varphi\left(\frac{l}{\beta} Y\right) = T_1 + \frac{T_3}{\beta^2} Y^2$ .

In order to get some insight in the amount of calculations necessary for the determination of the pressure distribution in the region of the wing tip, when the torsion mode shape  $\varphi(y)$  is approximated by  $\varphi\left(\frac{l}{\beta} Y\right) = T_1 + \frac{T_3}{\beta^2} Y^2$  instead of by  $\varphi\left(\frac{l}{\beta} Y\right) = \text{constant}$ , we derive here the formula for the pressure distribution.

As the derivation of the formula for the velocity potential on the wing does not involve any difficulty and can be performed in the same way as in appendix C.2, it will be sufficient to give this formula without deduction. Hence

$$\varphi_{T_{tip}}(X, Y, +0, T) = \varphi_T(X, Y, +0, T) + \Delta\varphi_T(X, Y, +0, T); \quad 0 < Y < X \quad (C.8)$$

where  $\varphi_T(X, Y, +0, T)$  is given by equation (B.6) or (3.16) and

$$\begin{aligned} \Delta p_T(X, Y, +0, T) = & + i\kappa\beta l e^{i\kappa T} \left[ - \left( X_e + \frac{i}{2k} \right) \left\{ \left( T_1 + \frac{T_3}{\beta^2} Y^2 \right) \int_Y^X e^{i\kappa M(X-\bar{X})} I_1(\bar{X}, Y) d\bar{X} - \right. \right. \\ & - \frac{T_3}{\beta^2} Y^2 \int_Y^X e^{i\kappa M(X-\bar{X})} H(\bar{X}, Y) d\bar{X} \left. \right\} + \left( T_1 + \frac{T_3}{\beta^2} Y^2 \right) \int_Y^X e^{i\kappa M(X-\bar{X})} (X-\bar{X}) I_1(\bar{X}, Y) d\bar{X} - \\ & \left. - \frac{T_3}{\beta^2} Y^2 \int_Y^X e^{i\kappa M(X-\bar{X})} (X-\bar{X}) H(\bar{X}, Y) d\bar{X} \right] \text{ with } 0 < Y < X \end{aligned} \quad (C.9)$$

where

$$H(\bar{X}, Y) = \frac{3}{2} I_0(\bar{X}, Y) + \frac{3}{2} I_2(\bar{X}, Y) - \frac{\pi}{2} I_3(\bar{X}, Y) + I_4(\bar{X}, Y) - \frac{1}{2} I_5(\bar{X}, Y)$$

and

$$\begin{aligned} I_0(\bar{X}, Y) &= \frac{1}{\pi \sqrt{Y}} \int_Y^{\bar{X}} J_0(\kappa \sqrt{\bar{X}^2 - \xi^2}) \frac{d\xi}{\sqrt{\xi - Y}} \\ I_1(\bar{X}, Y) &= \frac{\sqrt{Y}}{\pi} \int_Y^{\bar{X}} J_0(\kappa \sqrt{\bar{X}^2 - \xi^2}) \frac{d\xi}{\xi \sqrt{\xi - Y}} \\ I_2(\bar{X}, Y) &= \frac{1}{\pi Y^{3/2}} \int_Y^{\bar{X}} J_0(\kappa \sqrt{\bar{X}^2 - \xi^2}) \sqrt{\xi - Y} d\xi \\ I_3(\bar{X}, Y) &= \frac{1}{\pi Y^2} \int_Y^{\bar{X}} J_0(\kappa \sqrt{\bar{X}^2 - \xi^2}) \xi d\xi \\ I_4(\bar{X}, Y) &= \frac{1}{\pi Y^2} \int_Y^{\bar{X}} J_0(\kappa \sqrt{\bar{X}^2 - \xi^2}) \xi \sin^{-1} \left( \frac{2Y - \xi}{\xi} \right) d\xi \\ I_5(\bar{X}, Y) &= \frac{1}{\pi Y^{3/2}} \int_Y^{\bar{X}} J_0(\kappa \sqrt{\bar{X}^2 - \xi^2}) \frac{\xi d\xi}{\sqrt{\xi - Y}} \end{aligned} \quad (C.10)$$

By aid of formula (3.9) we obtain the pressure distribution  $p_{r_{tip}}(X, Y)$  in the region of the wing tip and consequently

$$\frac{p_{r_{tip}}(X, Y)}{\frac{1}{2} \rho U^2} = \frac{p_T(X, Y)}{\frac{1}{2} \rho U^2} + \frac{\Delta p_T(X, Y)}{\frac{1}{2} \rho U^2}; \quad 0 < Y < X \quad (C.11)$$

where  $\frac{p_T(X, Y)}{\frac{1}{2} \rho U^2}$  is given by equation (3.18) and  $\frac{\Delta p_T(X, Y)}{\frac{1}{2} \rho U^2}$  by the formula

$$\begin{aligned} \frac{\Delta p_T(X, Y)}{\frac{1}{2} \rho U^2} = & -4 i\kappa \frac{\beta}{M^2} e^{i\kappa T} \left[ \left( X_e + \frac{i}{2k} \right) \left\{ \left( T_1 + \frac{T_3}{\beta^2} Y^2 \right) \left\{ M I_1(X, Y) + i\kappa \beta^2 \int_Y^X e^{i\kappa M(X-\bar{X})} I_1(\bar{X}, Y) d\bar{X} \right\} - \right. \right. \\ & - \frac{T_3}{\beta^2} Y^2 \left\{ M H(X, Y) + i\kappa \beta^2 \int_Y^X e^{i\kappa M(X-\bar{X})} H(\bar{X}, Y) d\bar{X} \right\} \left. \right] - \\ & - \left( T_1 + \frac{T_3}{\beta^2} Y^2 \right) \left\{ M \int_Y^X e^{i\kappa M(X-\bar{X})} I_1(\bar{X}, Y) d\bar{X} + i\kappa \beta^2 \int_Y^X e^{i\kappa M(X-\bar{X})} (X-\bar{X}) I_1(\bar{X}, Y) d\bar{X} \right\} \\ & + \frac{T_3}{\beta^2} Y^2 \left\{ M \int_Y^X e^{i\kappa M(X-\bar{X})} H(\bar{X}, Y) d\bar{X} + i\kappa \beta^2 \int_Y^X e^{i\kappa M(X-\bar{X})} (X-\bar{X}) H(\bar{X}, Y) d\bar{X} \right\} \end{aligned} \quad (C.12)$$

For the determination of the pressure distribution it is necessary to evaluate numerically all the integrals (C.10) and all the other integrals occurring in equation (C.12).

However, when the investigation is restricted to lift and moment only, these numerical evaluations can be avoided; nevertheless it is seen, that the amount of calculations is increased considerably when the torsion mode shape  $\varphi\left(\frac{l}{\beta} Y\right)$  is approximated by  $\varphi = T_1 + \frac{\beta_2}{T_3} Y^2$  instead of by  $\varphi = \text{constant}$  for  $0 < Y < X$ .

## APPENDIX D.

### Derivation of formulae for lift due to translation and pitch.

#### D.1 The lift due to translation.

The lift due to translation is denoted by  $\mathfrak{L}_B$  which consists of two parts, viz.  $\bar{L}_B$  and  $\Delta\bar{L}_B$ .

$\bar{L}_B$  is defined by:

$$\bar{L}_B = \frac{2l}{\beta} \int_0^{\frac{1}{2}\beta A} L_B(Y) dY \quad (\text{D.1})$$

with  $A$  as aspect ratio of the wing and

$$L_B(Y) = l \int_0^1 p_B(X, Y) dX \quad (\text{D.2})$$

where  $p_B(X, Y)$  is given by equation (3.17).

Regarding the integration to  $X$  we have to bear in mind that  $L_B(Y)$  represents the lift per unit span at some time  $t$  and hence the factor  $e^{ixT}$  has to be written as  $e^{ivt} \cdot e^{-ixMX}$ .

Inserting (3.17) into (D.2) one obtains:

$$\begin{aligned} \frac{L_B(Y)}{\frac{1}{2}\rho U^2 l} = & -4i \frac{\beta}{M^2} \kappa e^{ivT} \left[ \left( B_1 + B_2 \frac{Y}{\beta} + B_3 \frac{Y^2}{\beta^2} \right) \left[ M \int_0^1 e^{-ixMX} J_0(\kappa X) dX + \right. \right. \\ & \left. \left. + i\kappa\beta^2 \int_0^1 \left\{ \int_0^X e^{-ixM\bar{X}} J_0(\kappa\bar{X}) d\bar{X} \right\} dX \right] + \frac{B_3}{\beta^2} \left[ \frac{-i\beta^2}{\kappa} \int_0^1 e^{-ixMX} X J_0(\kappa X) dX + \right. \right. \\ & \left. \left. + \frac{M}{\kappa} \int_0^1 e^{-ixMX} X J_1(\kappa X) dX + \frac{i\beta^2}{\kappa} \int_0^1 \left\{ \int_0^X e^{-ixM\bar{X}} J_0(\kappa\bar{X}) d\bar{X} \right\} dX + \beta^2 M \int_0^1 \left\{ \int_0^X e^{-ixM\bar{X}} \bar{X} J_0(\kappa\bar{X}) d\bar{X} \right\} dX \right] \end{aligned} \quad (\text{D.3})$$

Putting

$$\int_0^1 e^{-ixMX} (\kappa X)^\lambda J_0(\kappa X) dX = f_\lambda(\kappa, M) \quad (\text{D.4})$$

partial integration yields:

$$\int_0^1 e^{-ixMX} (\kappa X) J_1(\kappa X) dX = -e^{-ixM} J_0(\kappa) + f_0(\kappa, M) - iM f_1(\kappa, M) \quad (\text{D.5})$$

$$\int_0^1 \left\{ \int_0^X e^{-ixM\bar{X}} J_0(\kappa\bar{X}) d\bar{X} \right\} dX = f_0(\kappa, M) - \frac{1}{\kappa} f_1(\kappa, M) \quad (\text{D.6})$$

$$\int_0^1 \left\{ \int_0^X e^{-ixM\bar{X}} (\kappa\bar{X}) J_0(\kappa\bar{X}) d\bar{X} \right\} dX = f_1(\kappa, M) - \frac{1}{\kappa} f_2(\kappa, M) \quad (\text{D.7})$$

Hence

$$\frac{L_B(Y)}{\frac{1}{2} \rho U^2 l} = -4i \frac{\beta}{M^2} \kappa e^{i\kappa Y} \left\{ \left( B_1 + B_2 \frac{Y}{\beta} + B_3 \frac{Y^2}{\beta^2} \right) \left\{ (M + i\kappa\beta^2) f_0(\kappa, M) - i\beta^2 f_1(\kappa, M) \right\} + \right. \\ \left. + \frac{B_3}{\kappa^2 \beta^2} \left\{ -M e^{-i\kappa M} J_0(\kappa) + (M + i\kappa\beta^2) f_0(\kappa, M) - i(2\beta^2 + M(M + i\kappa\beta^2)) f_1(\kappa, M) - M\beta^2 f_2(\kappa, M) \right\} \right\} \quad (D. 8)$$

Integrating with respect to  $Y$  gives

$$\frac{\bar{L}_B}{\frac{1}{2} \rho U^2 S} = -4i \frac{\beta}{M^2} \kappa e^{i\kappa Y} \left[ \left\{ (M + i\kappa\beta^2) f_0(\kappa, M) - i\beta^2 f_1(\kappa, M) \right\} \frac{\int_0^{1/2\beta A} B \left( \frac{lY}{\beta} \right) dY}{\frac{1}{2} \beta A} + \right. \\ \left. + \frac{1}{\kappa^2 \beta^2} \left\{ -M e^{-i\kappa M} J_0(\kappa) + (M + i\kappa\beta^2) f_0(\kappa, M) - i(2\beta^2 + M(M + i\kappa\beta^2)) f_1(\kappa, M) - \right. \right. \\ \left. \left. - M\beta^2 \cdot f_2(\kappa, M) \frac{\int_0^{1/2\beta A} B_3(Y) dY}{\frac{1}{2} \beta A} \right\} \right] \quad (D. 9)$$

Since  $B_3(Y)$  can be written as

$$B_3(Y) = \frac{\beta^2}{2l} \frac{d^2 B \left( \frac{lY}{\beta} \right)}{dY^2}$$

and the bending mode shape is assumed symmetrical with respect to the midchord of the wing, the second integral in (D.9) can be simplified to:

$$\frac{\int_0^{1/2\beta A} B_3(Y) dY}{\frac{1}{2} \beta A} = \frac{-\beta}{lA} \left\{ \frac{dB \left( \frac{l}{\beta} Y \right)}{dY} \right\}_{Y=0} = -\frac{1}{A} \left\{ \frac{dB(y)}{dy} \right\}_{y=0}$$

We proceed now to the calculation of the second term  $\Delta \bar{L}_B$  of the lift.  $\Delta \bar{L}_B$  is defined by  $\Delta \bar{L}_B = \frac{2l}{\beta} \int_0^1 \Delta L_B(Y) dY$  with  $\Delta L_B(Y) = l \int_Y^1 \Delta p_B(X, Y) dX$ , where  $\Delta p_B(X, Y)$  is given by equation (3.27).

Hence

$$\Delta \bar{L}_B = \frac{2l^2}{\beta} \int_0^1 \left\{ \int_Y^1 \Delta p_B(X, Y) dX \right\} dY = \frac{2l^2}{\beta} \int_0^1 \left\{ \int_0^X \Delta p_B(X, Y) dY \right\} dX.$$

Substitution of equation (3.27) yields for the inner integral:

$$\int_0^X \frac{\Delta p_B(X, Y)}{\frac{1}{2} \rho U^2} dY = +4i \frac{\beta}{M^2} \kappa e^{i\kappa Y} \left[ MB_1 \int_0^X I_1(X, Y) dY + M \frac{B_2}{\beta} \int_0^X Y I_1(X, Y) dY - \right. \\ \left. - M \frac{B_2}{\beta} \int_0^X Y I_0(X, Y) dY + i\kappa\beta^2 B_1 \int_0^X \left\{ \int_Y^X e^{i\kappa M(X-\bar{X})} I_1(\bar{X}, Y) d\bar{X} \right\} dY + \right. \\ \left. + i\kappa\beta^2 \frac{B_2}{\beta} \int_0^X Y \left\{ \int_Y^X e^{i\kappa M(X-\bar{X})} I_1(\bar{X}, Y) d\bar{X} \right\} dY - i\kappa\beta^2 \frac{B_2}{\beta} \int_0^X Y \left\{ \int_Y^X e^{i\kappa M(X-\bar{X})} I_0(\bar{X}, Y) d\bar{X} \right\} dY \right]. \quad (D. 10)$$

The coefficients  $B_1$  and  $B_2$  are now taken as constant and independent of the spanwise direction  $Y$ ; the integrals  $I_0(X, Y)$  and  $I_1(X, Y)$  are given by equation (C.4) or (3.24) and (3.25).

The substitution of (3.25) gives for instance:

$$\int_0^X I_1(X, Y) dY = \int_0^X \frac{\sqrt{Y}}{\pi} \left\{ \int_Y^X J_0(\kappa \sqrt{X^2 - \xi^2}) \frac{d\xi}{\xi \sqrt{\xi - Y}} \right\} dY$$

or after interchanging the order of integration

$$\int_0^X I_1(X, Y) dY = \frac{1}{2} \int_0^X J_0(\kappa \sqrt{X^2 - \xi^2}) d\xi = \frac{\sin(\kappa X)}{2\kappa} \quad (D.11)$$

In the same way it appears that:

$$\int_0^X Y I_1(X, Y) dY = \frac{3}{8} (\kappa X) \frac{J_1(\kappa X)}{\kappa^2} \quad (D.12)$$

and

$$\int_0^X Y I_0(X, Y) dY = \frac{1}{2} (\kappa X) \frac{J_1(\kappa X)}{\kappa^2} \quad (D.13)$$

The double integrals occurring in equation (D.10) are also reduced by aid of interchanging the order of integration, e. g.

$$\int_0^X \left\{ \int_Y^X e^{i\kappa M(X-\bar{X})} I_1(\bar{X}, Y) d\bar{X} \right\} dY = \int_0^X e^{i\kappa M(X-\bar{X})} \left\{ \int_0^{\bar{X}} I_1(\bar{X}, Y) dY \right\} d\bar{X} = \frac{e^{i\kappa MX}}{2\kappa} \int_0^X e^{-i\kappa M\bar{X}} \sin(\kappa\bar{X}) d\bar{X} = \frac{1}{2\kappa^2\beta^2} \left\{ iM \sin(\kappa X) + \cos(\kappa X) - e^{i\kappa MX} \right\} \quad (D.14)$$

In the same way it can be shown that:

$$\int_0^X Y \left\{ \int_Y^X e^{i\kappa M(X-\bar{X})} I_1(\bar{X}, Y) d\bar{X} \right\} dY = \frac{3}{8} \frac{e^{i\kappa MX}}{\kappa^2} \int_0^X e^{-i\kappa M\bar{X}} (\kappa\bar{X}) J_1(\kappa\bar{X}) d\bar{X}.$$

By aid of partial integration the integral is reduced to the form:

$$\int_0^X e^{-i\kappa M\bar{X}} (\kappa\bar{X}) J_1(\kappa\bar{X}) d\bar{X} = -e^{-i\kappa MX} \cdot X \cdot J_0(\kappa X) + f_0(X; \kappa, M) - iM f_1(X; \kappa, M) \quad (D.15)$$

where

$$\left. \begin{aligned} f_0(X; \kappa, M) &= \int_0^X e^{-i\kappa M\bar{X}} J_0(\kappa\bar{X}) d\bar{X} \\ f_1(X; \kappa, M) &= \int_0^X e^{-i\kappa M\bar{X}} (\kappa\bar{X}) J_0(\kappa\bar{X}) d\bar{X}. \end{aligned} \right\} \quad (D.16)$$

Hence

$$\int_0^X Y \left\{ \int_Y^X e^{i\kappa M(X-\bar{X})} I_1(\bar{X}, Y) d\bar{X} \right\} dY = \frac{3}{8} \frac{1}{\kappa^2} \left[ -X J_0(\kappa X) + e^{i\kappa MX} \left\{ f_0(X; \kappa, M) - iM f_1(X; \kappa, M) \right\} \right] \quad (D.17)$$

Besides, it follows from (D.16) that  $f_0(1; \kappa, M) = f_0(\kappa, M)$  and  $f_1(1; \kappa, M) = f_1(\kappa, M)$  (see eq. (D.4)).

The last double integral of equation (D.10) can be reduced as:

$$\begin{aligned} \int_0^X Y \left\{ \int_Y^X e^{i\kappa M(X-\bar{X})} I_0(\bar{X}, Y) d\bar{X} \right\} dY &= \frac{1}{2} \frac{e^{i\kappa MX}}{\kappa^2} \int_0^X e^{-i\kappa M\bar{X}} (\kappa\bar{X}) J_1(\kappa\bar{X}) d\bar{X} = \\ &= \frac{1}{2} \frac{1}{\kappa^2} \left[ -X J_0(\kappa X) + e^{i\kappa MX} \left\{ f_0(X; \kappa, M) - iM f_1(X; \kappa, M) \right\} \right]. \end{aligned} \quad (D.18)$$

Inserting (D.11)—(D.18) into (D.10) gives finally:

$$\begin{aligned} \int_0^X \frac{\Delta p_B(X, Y)}{\frac{1}{2} \rho U^2} dY &= + 2 \frac{\beta}{M^2} e^{i\kappa T} \left\{ B_1 \left\{ e^{i\kappa MX} - \cos(\kappa X) \right\} + \right. \\ &\left. + \frac{1}{4} B_2 \beta \left[ e^{i\kappa MX} \left\{ f_0(X; \kappa, M) - iM f_1(X; \kappa, M) \right\} - X J_0(\kappa X) - \frac{iM}{\beta^2} X J_1(\kappa X) \right] \right\}. \end{aligned} \quad (D.19)$$

Substituting  $e^{i\kappa T} = e^{i\kappa t} \cdot e^{-i\kappa M X}$  and integrating (D.19) with respect to  $X$  gives by aid of the equations (D.4), (D.15) and (D.16)

$$\begin{aligned} \frac{\Delta \bar{L}_B}{\frac{1}{2} \rho U^2 S} = & \frac{4}{M^2} \frac{e^{i\kappa t}}{A} \left\{ B_1 \left[ 1 + \frac{1}{\kappa \beta^2} \left\{ iM + e^{-i\kappa M} (\sin \kappa - iM \cos \kappa) \right\} \right] - \right. \\ & \left. - \frac{1}{4} \frac{i}{\beta \kappa} B_2 \left[ -Me^{-i\kappa M} J_0(\kappa) + (M + i\kappa \beta^2) f_0(\kappa, M) - i \{ 2\beta^2 + M(M + i\kappa \beta^2) \} f_1(\kappa, M) - M\beta^2 f_2(\kappa, M) \right] \right\}. \end{aligned} \quad (D.20)$$

The lift due to translation can now easily be obtained by adding  $\bar{L}_B$  and  $\Delta \bar{L}_B$ .

## D.2 The lift due to pitch.

The lift due to pitch is denoted by  $\mathcal{L}_T$ , which consists of two parts  $\bar{L}_T$  and  $\Delta \bar{L}_T$ .  $\bar{L}_T$  is defined by the expression:

$$\bar{L}_T = \frac{2l}{\beta} \int_0^{1/2 \beta A} L_T(Y) dY \quad (D.21)$$

with

$$L_T(Y) = l \int_0^1 p_T(X, Y) dX \quad (D.22)$$

where  $p_T(X, Y)$  is given by equation (3.18).

Inserting equation (3.18) into (D.22) yields:

$$\begin{aligned} \frac{L_T(Y)}{\frac{1}{2} \rho U^2 l} = & \frac{L_B \{ \dot{Y}; B_h = - \left( X_0 + \frac{iM}{\beta^2 \kappa} \right) T_h \}}{\frac{1}{2} \rho U^2 \cdot l} + \\ & + 2i \frac{\beta}{M^2} e^{i\kappa t} \left\{ \left\{ -\kappa(2M + i\beta^2 \kappa) f_0(\kappa, M) + 2(M + i\beta^2 \kappa) f_1(\kappa, M) - i\beta^2 f_2(\kappa, M) \right\} \left( T_1 + T_2 \frac{Y}{\beta} + T_3 \frac{Y^2}{\beta^2} \right) + \right. \\ & + \frac{T_3(Y)}{\kappa^2 \beta^2} \left[ -\kappa(2M + i\kappa \beta^2) f_0(\kappa, M) + \{ 4M + 2i\kappa(3\beta^2 + 1) - \kappa^2 \beta^2 M \} f_1(\kappa, M) - \right. \\ & \left. \left. - i(2 + 5\beta^2 + 2i\kappa M \beta^2) f_2(\kappa, M) - M\beta^2 f_3(\kappa, M) \right] \right\} \end{aligned} \quad (D.23)$$

The derivation of this expression runs along the same lines as in the case of translation (see appendix D.1).

Use has been made of the following formulae which are easily checked by aid of partial integration;

$$\int_0^1 \left\{ \int_0^X e^{-i\kappa M \bar{X}} (\kappa \bar{X})^\lambda J_0(\kappa \bar{X}) d\bar{X} \right\} dX = f_\lambda(\kappa, M) - \frac{1}{\kappa} f_{\lambda+1}(\kappa, M) \quad (D.24)$$

with

$$f_\lambda(\kappa, M) = \int_0^1 e^{-i\kappa M X} (\kappa X)^\lambda J_0(\kappa X) dX \quad (D.4)$$

$$\int_0^1 X \left\{ \int_0^X e^{-i\kappa M \bar{X}} J_0(\kappa \bar{X}) d\bar{X} \right\} = \frac{1}{2} \left\{ f_0(\kappa, M) - \frac{1}{\kappa^2} f_2(\kappa, M) \right\} \quad (D.25)$$

$$\int_0^1 X \left\{ \int_0^X e^{-i\kappa M \bar{X}} (\kappa \bar{X}) J_0(\kappa \bar{X}) d\bar{X} \right\} = \frac{1}{2} \left\{ f_1(\kappa, M) - \frac{1}{\kappa^2} f_3(\kappa, M) \right\} \quad (D.26)$$

Integrating eq. (D.23) with respect to  $Y$ , using (D.9) and remembering that the coefficients  $T_1$ ,  $T_2$  and  $T_3$  depend on the spanwise coordinate  $Y$ , one gets finally for the part  $\bar{L}_T$  of the lift due to pitch:

$$\begin{aligned}
\frac{\bar{L}_T}{\frac{1}{2} \rho U^2 S} = & + 2i \frac{\beta}{M^2} e^{i\kappa l} \left\{ 2 \left( \kappa X_e + \frac{iM}{\beta^2} \right) \left[ \left\{ (M + i\kappa\beta^2) f_0(\kappa, M) - i\beta^2 f_1(\kappa, M) \right\} \frac{\int_0^{1/2 \beta A} \varphi \left( \frac{lY}{\beta} \right) dY}{\frac{1}{2} \beta A} + \right. \right. \\
& + \frac{1}{\kappa^2 \beta^2} \left\{ -M e^{-i\kappa M} J_0(\kappa) + (M + i\kappa\beta^2) f_0(\kappa, M) - i(2\beta^2 + M(M + i\kappa\beta^2)) f_1(\kappa, M) - \right. \\
& \left. \left. - M\beta^2 f_2(\kappa, M) \right\} \frac{\int_0^{1/2 \beta A} T_3(Y) dY}{\frac{1}{2} \beta A} \right] \\
& + \left\{ -\kappa(2M + i\beta^2 \kappa) f_0(\kappa, M) + 2(M + i\kappa\beta^2) f_1(\kappa, M) - i\beta^2 f_2(\kappa, M) \right\} \frac{\int_0^{1/2 \beta A} \varphi \left( \frac{lY}{\beta} \right) dY}{\frac{1}{2} \beta A} + \\
& + \frac{1}{\kappa^2 \beta^2} \left[ -\kappa(2M + i\kappa\beta^2) f_0(\kappa, M) + \left\{ 4M + 2i\kappa(3\beta^2 + 1) - \kappa^2 \beta^2 M \right\} f_1(\kappa, M) - i(2 + 5\beta^2 + \right. \\
& \left. + 2i\kappa M \beta^2) f_2(\kappa, M) - M\beta^2 f_3(\kappa, M) \right] \frac{\int_0^{1/2 \beta A} T_3(Y) dY}{\frac{1}{2} \beta A} \left. \right\} \quad (D. 27)
\end{aligned}$$

The integrals of the function  $T_3(Y)$  can again be simplified by putting

$$T_3(Y) = \frac{\beta^2}{2} \frac{d^2 \varphi \left( \frac{lY}{\beta} \right)}{dY^2}.$$

Since the torsion moment is zero along the wing tip,  $\frac{d\varphi \left( \frac{lY}{\beta} \right)}{dY}$  must vanish for  $Y=0$  and hence the integral of the function  $T_3(Y)$  can be reduced to the simple form:

$$\frac{\int_0^{1/2 \beta A} T_3(Y) dY}{\frac{1}{2} \beta A} = \frac{\beta}{A} \left\{ \frac{d\varphi \left( \frac{lY}{\beta} \right)}{dY} \right\}_{Y=1/2 \beta A} = \frac{l}{A} \left( \frac{d\varphi}{dy} \right)_{y=\frac{s}{2}}. \quad (D. 28)$$

We proceed now to the reduction of the second term  $\Delta \bar{L}_T$  of the lift due to pitch.  $\Delta \bar{L}_T$  is defined by

$$\Delta \bar{L}_T = \frac{2l}{\beta} \int_0^1 \Delta L_T(Y) dY \quad (D. 29)$$

with

$$\Delta L_T(Y) = l \int_Y^1 \Delta p_T(X, Y) dX \quad (D. 30)$$

where  $\Delta p_T(X, Y)$  is given by equation (3.31).

After interchanging the order of integration (D. 29) becomes:

$$\Delta \bar{L}_T = \frac{2l^2}{\beta} \int_0^1 \left\{ \int_0^X \Delta p_T(X, Y) dY \right\} dX. \quad (D. 31)$$

Substitution of equation (3.31) yields:

$$\begin{aligned}
\int_0^X \frac{\Delta p_T(X, Y)}{\frac{1}{2} \rho U^2} dY = & -4i\kappa \frac{\beta}{M^2} T_1 e^{i\kappa T} \left[ + M \left( X_e + \frac{iM}{\kappa\beta^2} \right) \int_0^X I_1(X, Y) dY - \right. \\
& - \left\{ 2M + (X - X_e) i\kappa\beta^2 \right\} \int_0^X \int_Y^X e^{i\kappa M(X-\bar{X})} I_1(\bar{X}, Y) d\bar{X} \left\{ dY + i\kappa\beta^2 \int_0^X \int_Y^X \bar{X} e^{i\kappa M(X-\bar{X})} I_1(\bar{X}, Y) d\bar{X} \left\{ dY \right\} \right]
\end{aligned} \quad (D. 32)$$

where  $T_1$  is now taken as a constant.

The first two integrals are already reduced in appendix D.1 and the third integral can easily be reduced by aid of partial integration.

The result is

$$\int_0^X \left\{ \int_Y^X \bar{X} e^{i\kappa M(X-\bar{X})} I_1(\bar{X}, Y) d\bar{X} \right\} dY = \frac{1}{2\kappa^3} \frac{M^2}{\beta^2} \left[ \frac{(\kappa X) \cos(\kappa X)}{M^2} - \frac{(\kappa X) \sin(\kappa X)}{iM} + \left( \frac{2}{\beta^2} - \frac{1}{M^2} \right) \sin(\kappa X) + \frac{2}{iM\beta^2} \cos(\kappa X) - \frac{2 e^{i\kappa M X}}{iM\beta^2} \right] \quad (D.33)$$

Substituting this result and the formulae (D.11) and (D.14) into (D.32) and using  $e^{i\kappa T} = e^{i\kappa t} \cdot e^{-i\kappa M X}$  one obtains:

$$\int_0^X \frac{\Delta p_T(X, Y)}{\frac{1}{2} \rho U^2} dY = + 2 \frac{\beta}{M^2} T_1 e^{i\kappa t} \left\{ \left( X_e + \frac{iM}{\kappa\beta^2} \right) \left\{ e^{-i\kappa M X} \cos(\kappa X) - 1 \right\} - \frac{iM}{\kappa\beta^2} \left\{ \left( -\frac{\sin(\kappa X)}{iM} + \cos(\kappa X) \right) e^{-i\kappa M X} + \frac{i\beta^2}{M} (\kappa X) - 1 \right\} \right\} \quad (D.34)$$

Integrating finally with respect to  $X$  one gets the desired expression for  $\Delta \bar{L}_T$ , viz.:

$$\frac{\Delta \bar{L}_T}{\frac{1}{2} \rho U^2 S} = - \frac{4}{M^2 \beta^2} \frac{T_1}{A} \frac{e^{i\kappa t}}{\kappa} \left\{ \left( X_e + \frac{iM}{\kappa\beta^2} \right) \left\{ (\sin \kappa - iM \cos \kappa) e^{-i\kappa M} + iM + \kappa\beta^2 \right\} - \frac{1}{\kappa\beta^2} \left[ \left\{ (1 + M^2) \cos \kappa + 2 iM \sin \kappa \right\} e^{-i\kappa M} - (1 + M^2) + i\kappa M \beta^2 + \kappa^2 \frac{\beta^4}{2} \right] \right\} \quad (D.35)$$

By adding the expression (D.27) and (D.35) the lift due to pitch is obtained.

## APPENDIX E.

### Derivation of formulae for the aerodynamic moment due to translation and pitch.

#### E.1 The aerodynamic moment due to translation.

The aerodynamic moment due to translation is denoted by  $\mathfrak{M}_B$  where  $\mathfrak{M}_B$  again consists of two parts  $\bar{M}_B$  and  $\Delta \bar{M}_B$ .

$\bar{M}_B$  is defined by

$$\bar{M}_B = \frac{2l}{\beta} \int_0^{\frac{1}{2}\beta A} M_B(Y) dY \quad (E.1)$$

with

$$M_B(Y) = l^2 \int_0^1 X p_B(X, Y) dX \quad (E.2)$$

and  $p_B(X, Y)$  is given by equation (3.17).

Inserting (3.17) into (E.2) one arrives at an expression analogous to equation (D.3), viz.:

$$\begin{aligned} \frac{M_B(Y)}{\frac{1}{2} \rho U^2 l^2} = & - 4 i \frac{\beta}{M^2} \kappa e^{i\kappa t} \left[ \left\{ B_1 + B_2 \frac{Y}{\beta} + B_3 \left( \frac{Y}{\beta} \right)^2 \right\} \left[ M \int_0^1 e^{-i\kappa X M} X J_0(\kappa X) dX + \right. \right. \\ & + i\kappa\beta^2 \int_0^1 X \left\{ \int_0^X e^{-i\kappa M \bar{X}} J_0(\kappa \bar{X}) d\bar{X} \right\} dX \left. \right] + \frac{B_3}{\beta^2} \left[ -i \frac{\beta^2}{x} \int_0^1 e^{-i\kappa M X} X^2 J_0(\kappa X) dX + \right. \\ & + \frac{M}{\kappa} \int_0^1 X^2 e^{-i\kappa M X} J_1(\kappa X) dX + \\ & \left. \left. + \frac{i\beta^2}{\kappa} \int_0^1 X \left\{ \int_0^X e^{-i\kappa M \bar{X}} J_0(\kappa \bar{X}) d\bar{X} \right\} dX + \beta^2 M \int_0^1 X \left\{ \int_0^X e^{-i\kappa M \bar{X}} \cdot \bar{X} J_0(\kappa \bar{X}) d\bar{X} \right\} dX \right] \quad (E.3) \end{aligned}$$

The only integral occurring in this expression and not already determined in appendix D is

$$\int_0^1 (\kappa X)^2 e^{-i\kappa M X} J_1(\kappa X) dX.$$

This integral is easily reduced by aid of partial integration and the result is:

$$\int_0^1 e^{-i\kappa M X} (\kappa X)^2 J_1(\kappa X) dX = -\kappa e^{-i\kappa M} J_0(\kappa) + 2f_1(\kappa, M) - iMf_2(\kappa, M). \quad (\text{E. 4})$$

Using equations (D. 4), (D. 25), (D. 26) and (E. 4) the right-hand side of (E. 3) becomes:

$$\begin{aligned} \frac{M_B(Y)}{\frac{1}{2} \rho U^2 l^2} = & + 2 \frac{\beta}{M^2} e^{i\beta Y} \left[ \{ \kappa^2 \beta^2 f_0(\kappa, M) - 2iMf_1(\kappa, M) - \beta^2 f_2(\kappa, M) \} \frac{B\left(\frac{lY}{\beta}\right)}{l} + \right. \\ & + \frac{B_3(Y)}{\kappa^2 \beta^2} \{ 2i\kappa M e^{-i\kappa M} J_0(\kappa) + \beta^2 \kappa^2 f_0(\kappa, M) - iM(4 + \beta^2 \kappa^2) f_1(\kappa, M) - \\ & \left. - (5\beta^2 + 2)f_2(\kappa, M) + iM\beta^2 f_3(\kappa, M) \} \right] \quad (\text{E. 4}) \end{aligned}$$

Integrating with respect to  $Y$  yields ultimately

$$\begin{aligned} \frac{\bar{M}_B}{\frac{1}{2} \rho U^2 S l} = & + 2 \frac{\beta}{M^2} e^{i\beta Y} \left[ \{ \kappa^2 \beta^2 f_0(\kappa, M) - 2iMf_1(\kappa, M) - \beta^2 f_2(\kappa, M) \} \frac{\int_0^{\frac{1}{2}\beta A} \frac{B\left(\frac{lY}{\beta}\right)}{l} dY}{\frac{1}{2}\beta A} - \right. \\ & + \frac{1}{\kappa^2 \beta^2} \{ 2i\kappa M e^{-i\kappa M} J_0(\kappa) + \beta^2 \kappa^2 f_0(\kappa, M) - iM(4 + \beta^2 \kappa^2) f_1(\kappa, M) + \\ & \left. - (5\beta^2 + 2)f_2(\kappa, M) + iM\beta^2 f_3(\kappa, M) \} \frac{\int_0^{\frac{1}{2}\beta A} B_3(Y) dY}{\frac{1}{2}\beta A} \right] \quad (\text{E. 5}) \end{aligned}$$

We proceed now to the reduction of the second part  $\Delta \bar{M}_B$  of the aerodynamic moment due to translation. This quantity is defined by

$$\Delta \bar{M}_B = \frac{2l}{\beta} \int_0^1 \Delta M_B(Y) dY \quad (\text{E. 6})$$

with

$$\Delta M_B(Y) = l^2 \int_Y^1 X \cdot \Delta p_B(X, Y) dY; \quad (\text{E. 7})$$

and  $\Delta p_B(X, Y)$  is given by equation (3.27).

After interchanging the order of integration  $\Delta \bar{M}_B$  becomes

$$\Delta \bar{M}_B = \frac{2l^3}{\beta} \int_0^1 X \left\{ \int_0^X \Delta p_B(X, Y) dY \right\} dX. \quad (\text{E. 8})$$

The inner integral has been reduced already in appendix D.1 (see formula (D.19)).

Multiplication of this expression with  $X$  and integrating consecutively to  $X$  gives the second part of the aerodynamic moment and the result is:

$$\begin{aligned} \frac{\Delta \bar{M}_B}{\frac{1}{2} \rho U^2 S l} = & + \frac{2}{M^2} \frac{e^{i\beta Y}}{A} \left[ B_1 \left[ 1 - \frac{2}{\kappa^2 \beta^4} \{ (1 + M^2) \cos \kappa + 2iM \sin \kappa + i\kappa M \beta^2 \cos \kappa - \kappa \beta^2 \sin \kappa \} e^{-i\kappa M} - \right. \right. \\ & \left. \left. - (M^2 + 1) \right\] + \frac{1}{4} \frac{B_2}{\beta \kappa^2} [ \kappa^2 \beta^2 f_0(\kappa, M) - iM(4 + \kappa^2 \beta^2) f_1(\kappa, M) - \right. \\ & \left. - 5\beta^2 + 2)f_2(\kappa, M) + iM\beta^2 f_3(\kappa, M) + 2i\kappa M e^{-i\kappa M} J_0(\kappa) \right] \quad (\text{E. 9}) \end{aligned}$$

The aerodynamic moment due to translation can now easily be obtained by adding  $\bar{M}_B$  and  $\Delta \bar{M}_B$ .

## E.2 The aerodynamic moment due to pitch.

The aerodynamic moment due to pitch is denoted by  $\mathfrak{M}_T$ , where  $\mathfrak{M}_T$  consists of the parts  $\overline{M}_T$  and  $\Delta\overline{M}_T$ .

$\overline{M}_T$  is defined by:

$$\overline{M}_T = \frac{2l}{\beta} \int_0^{1/2\beta A} M_T(Y) dY, \quad (\text{E. 10})$$

with

$$M_T(Y) = l^2 \int_0^1 X p_T(X, Y) dX \quad (\text{E. 11})$$

and  $p_T(X, Y)$  is given by equation (3.18).

Substitution of (3.18) into equation (E.11) yields:

$$\begin{aligned} \frac{M_T(Y)}{1/2 \rho U^2 l^2} = & \frac{M_B \left\{ Y; B_h = - \left( X_e + \frac{i}{k} \right) T_h \right\}}{1/2 \rho U^2 l^2} + 4i \frac{\beta}{M^2} \kappa e^{i\kappa Y} \left[ + i\kappa\beta^2 \left( T_1 + T_2 \frac{Y}{\beta} + T_3 \frac{Y^2}{\beta^2} \right) \right. \\ & \int_0^1 X \left\{ \int_0^X e^{-i\kappa M\bar{X}} \cdot \bar{X} \cdot J_0(\kappa\bar{X}) d\bar{X} \right\} dX - M \left( T_1 + T_2 \frac{Y}{\beta} + T_3 \frac{Y^2}{\beta^2} \right) \int_0^1 X \left\{ \int_0^X e^{-i\kappa M\bar{X}} J_0(\kappa\bar{X}) d\bar{X} \right\} dX - \\ & - i\kappa\beta^2 \left( T_1 + T_2 \frac{Y}{\beta} + T_3 \frac{Y^2}{\beta^2} \right) \int_0^1 X^2 \left\{ \int_0^X e^{-i\kappa M\bar{X}} J_0(\kappa\bar{X}) d\bar{X} \right\} dX + \\ & + \frac{T_3(Y)}{\beta^2} \left[ \frac{M}{\kappa^2} \int_0^1 X^2 e^{-i\kappa M X} J_0(\kappa X) dX - \frac{M}{\kappa^2} \int_0^1 X \left\{ \int_0^X e^{-i\kappa M\bar{X}} J_0(\kappa\bar{X}) d\bar{X} \right\} dX - \right. \\ & - \frac{i\beta^2}{\kappa} \int_0^1 X^2 \left\{ \int_0^X e^{-i\kappa M\bar{X}} J_0(\kappa\bar{X}) d\bar{X} \right\} dX + \frac{i}{\kappa} (3\beta^2 + 1) \int_0^1 X \left\{ \int_0^X e^{-i\kappa M\bar{X}} \cdot \bar{X} \cdot J_0(\kappa\bar{X}) d\bar{X} \right\} dX - \\ & \left. - M\beta^2 \int_0^1 X^2 \left\{ \int_0^X e^{-i\kappa M\bar{X}} \cdot \bar{X} \cdot J_0(\kappa\bar{X}) d\bar{X} \right\} dX + M\beta^2 \int_0^1 X \left\{ \int_0^X e^{-i\kappa M\bar{X}} \cdot \bar{X}^2 J_0(\kappa\bar{X}) d\bar{X} \right\} dX \right] \quad (\text{E. 12}) \end{aligned}$$

The only integrals not yet reduced are  $\int_0^1 X^2 \left\{ \int_0^X e^{-i\kappa M\bar{X}} J_0(\kappa\bar{X}) d\bar{X} \right\} dX$ ,

$$\int_0^1 X^2 \left\{ \int_0^X e^{-i\kappa M\bar{X}} \cdot \bar{X} \cdot J_0(\kappa\bar{X}) d\bar{X} \right\} dX \quad \text{and} \quad \int_0^1 X \left\{ \int_0^X e^{-i\kappa M\bar{X}} \cdot \bar{X}^2 J_0(\kappa\bar{X}) d\bar{X} \right\} dX.$$

By aid of partial integration the following formulae can be easily checked:

$$\left. \begin{aligned} \int_0^1 X^2 \left\{ \int_0^X e^{-i\kappa M\bar{X}} J_0(\kappa\bar{X}) d\bar{X} \right\} dX &= 1/3 \left\{ f_0(\kappa, M) - \frac{1}{\kappa^2} f_3(\kappa, M) \right\} \\ \int_0^1 X^2 \left\{ \int_0^X e^{-i\kappa M\bar{X}} (\kappa\bar{X}) J_0(\kappa\bar{X}) d\bar{X} \right\} dX &= 1/3 \left\{ f_1(\kappa, M) - \frac{1}{\kappa^2} f_4(\kappa, M) \right\} \\ \int_0^1 X \left\{ \int_0^X e^{-i\kappa M\bar{X}} (\kappa\bar{X})^2 J_0(\kappa\bar{X}) d\bar{X} \right\} dX &= 1/2 \left\{ f_2(\kappa, M) - \frac{1}{\kappa^2} f_4(\kappa, M) \right\} \end{aligned} \right\} \quad (\text{E. 13})$$

By means of the equations (D. 4), (D. 25), (D. 26) and (E. 13) one obtains after a small calculation:

$$\frac{M_T(Y)}{1/2 \rho U^2 l^2} = \frac{M_B \left\{ Y; B_h = - \left( X_e + \frac{i}{k} \right) T_h \right\}}{1/2 \rho U^2 l^2} +$$

$$+ \frac{2}{3} i \frac{\beta}{M^2} \frac{e^{i\omega t}}{\kappa} \left[ \left\{ -\kappa^2 (3M + 2i\kappa\beta^2) f_0(\kappa, M) + 3i\kappa^2 \beta^2 f_1(\kappa, M) + 3M f_2(\kappa, M) - i\beta^2 f_3(\kappa, M) \right\} \varphi \left( \frac{lY}{\beta} \right) + \right.$$

$$+ \frac{1}{\kappa^2 \beta^2} \left[ -\kappa^2 (3M + 2i\kappa\beta^2) f_0(\kappa, M) + i\kappa^2 \{ 3(1 + 3\beta^2) + 2i\kappa M \beta^2 \} f_1(\kappa, M) + 3M(3 + \kappa^2 \beta^2) f_2(\kappa, M) - \right.$$

$$\left. \left. - i(7\beta^2 + 3) f_3(\kappa, M) - M\beta^2 f_4(\kappa, M) \right] T_3(Y) \right] \quad (E. 14)$$

Integrating with respect to  $Y$  gives finally the first part of the aerodynamic moment due to pitch, viz.:

$$\frac{\bar{M}_T}{1/2 \rho U^2 l S} = -2 \frac{\beta}{M^2} e^{i\omega t} \left( X_e + \frac{iM}{\kappa\beta^2} \right) \left[ \left\{ \kappa^2 \beta^2 f_0(\kappa, M) - 2iM f_1(\kappa, M) - \beta^2 f_2(\kappa, M) \right\} \frac{\int_0^{1/2 \beta A} \varphi \left( \frac{lY}{\beta} \right) dY}{1/2 \beta A} + \right.$$

$$+ \frac{1}{\kappa^2 \beta^2} \left\{ 2i\kappa M e^{-i\kappa M} J_0(\kappa) + \kappa^2 \beta^2 f_0(\kappa, M) - iM(4 + \kappa^2 \beta^2) f_1(\kappa, M) - (5\beta^2 + 2) f_2(\kappa, M) + iM\beta^2 f_3(\kappa, M) \right\} .$$

$$\left. \frac{\int_0^{1/2 \beta A} T_3(Y) dY}{1/2 \beta A} \right] + \frac{2}{3} \frac{i\beta}{M^2} \frac{e^{i\omega t}}{\kappa} \left[ \left\{ -\kappa^2 (3M + 2i\kappa\beta^2) f_0(\kappa, M) + 3i\kappa^2 \beta^2 f_1(\kappa, M) + 3M f_2(\kappa, M) - \right. \right.$$

$$\left. \left. - i\beta^2 f_3(\kappa, M) \right\} \frac{\int_0^{1/2 \beta A} \varphi \left( \frac{lY}{\beta} \right) dY}{1/2 \beta A} + \frac{1}{\kappa^2 \beta^2} \left[ -\kappa^2 (3M + 2i\kappa\beta^2) f_0(\kappa, M) + i\kappa^2 \{ 3(1 + 3\beta^2) + 2i\kappa M \beta^2 \} f_1(\kappa, M) + \right.$$

$$\left. \left. + 3M(3 + \kappa^2 \beta^2) f_2(\kappa, M) - i(7\beta^2 + 3) f_3(\kappa, M) - M\beta^2 f_4(\kappa, M) \right] \frac{\int_0^{1/2 \beta A} T_3(Y) dY}{1/2 \beta A} \right] \quad (E. 15)$$

At last the second part of the aerodynamic moment will be determined.  $\Delta \bar{M}_T$  is defined as:

$$\Delta \bar{M}_T = \frac{2l}{\beta} \int_0^1 \Delta M_T(Y) dY \quad (E. 16)$$

where

$$\Delta M_T(Y) = l^2 \int_Y^1 X \Delta p_T(X, Y) dX \quad (E. 17)$$

and  $\Delta p_T(X, Y)$  is given by the expression (3.31).

Hence

$$\Delta \bar{M}_T = \frac{2l^3}{\beta} \int_0^1 X \left\{ \int_0^X \Delta p_T(X, Y) dY \right\} dX. \quad (E. 18)$$

The inner integral has been reduced already in appendix D.2 (see form. (D. 34)). Multiplying this expression with  $X$  and integrating consecutively to  $X$ , one obtains for the second part of the aerodynamic moment:

$$\begin{aligned}
\frac{\Delta \bar{M}_T}{\frac{1}{2} \rho U^2 l S} = & \frac{4}{M^2} \frac{T_1}{A} \frac{e^{i\nu t}}{\kappa^2 \beta^4} \left[ \left( X_e + \frac{iM}{\kappa \beta^2} \right) [ \{ (2 + \beta^2) \cos \kappa + 2 iM \sin \kappa + i\kappa M \beta^2 \cos \kappa - \kappa \beta^2 \sin \kappa \} e^{-i\kappa M} - \right. \\
& - (\beta^2 + 2) - \frac{1}{2} \cdot \kappa^2 \beta^4 ] + \frac{1}{\kappa \beta^2} [ \{ + \kappa \beta^2 (\beta^2 + 2) \cos \kappa + 2 i\kappa M \beta^2 \sin \kappa - iM (\beta^2 + 4) \cos \kappa + \\
& \left. + (3 \beta^2 + 4) \sin \kappa \} e^{-i\kappa M} + iM (4 + \beta^2) + \frac{1}{2} iM \kappa^2 \beta^4 + \frac{1}{3} \cdot \kappa^3 \beta^6 ] \right] \quad (E. 19)
\end{aligned}$$

The total aerodynamic moment due to pitch is obtained by adding the right-hand sides of eqs. (E.15) and (E.19).



## REPORT TR W. 5.

# Oscillating rectangular wings in supersonic flow with arbitrary bending and torsion mode shapes.

## Part II: Numerical results

by

E. M. DE JAGER.

### Summary.

As has been shown in part I the aerodynamic derivatives can be given in the form of the sum of some terms each of which consists of two factors, one being a function of the reduced frequency and the Mach number, the other one containing the bending or the torsion mode shape.

Tables of the factors containing the reduced frequency  $k$  and the Mach number  $M$  are presented for  $k = 0 (0.1) 1$  and  $M = 1.2 (0.1) 1.6 (0.2) 2 (0.5) 4$ .

In order to show the influence of frequency, Mach number and aspect ratio graphs are given of the aerodynamic derivatives for a translating and pitching flat wing.

They have been plotted as functions of the reduced frequency for different values of aspect ratio and Mach number.

### Contents.

- List of symbols.
- 1 Introduction.
  - 2 Recapitulation of the theoretical results.
  - 3 Application of the theory to a flat wing.
  - 4 References.
- 11 tables.  
24 figures.

### List of symbols.

- |               |   |
|---------------|---|
| $h$           | amplitude of translation                                    |
| $k$           | reduced frequency $\frac{vl}{2U}$                           |
| $l$           | wing chord  |
| $s$           | wing span   |
| $t$           | time  |
| $x, y, z$     | rectangular coordinates                                     |
| $x_e$         | $x$ coordinate of spanwise elastic axis                     |
| $A$           | aspect ratio  |
| $B_{1, 2, 3}$ | coefficients of polynomial approximating bending mode shape |
| $B(y)$        | bending mode shape  |
| $C_L$         | lift coefficient  |
| $C_M$         | moment coefficient  |
| $L_B$         | lift due to bending   |
| $L_T$         | lift due to torsion   |
| $M_B$         | moment due to bending                                       |
| $M_T$         | moment due to torsion                                       |
| $M$           | Mach number   |

- |                |   |
|----------------|---|
| $S$            | wing area   |
| $T_{1, 2, 3}$  | coefficients of polynomial approximating torsion mode shape           |
| $U$            | undisturbed flow velocity   |
| $\beta$        | $\sqrt{M^2 - 1}$  |
| $\kappa$       | $\frac{2kM}{\beta^2}$   |
| $\nu$          | circular frequency  |
| $\rho$         | density   |
| $\varphi$      | amplitude of torsional oscillation                                    |
| $\varphi(y)$   | torsion mode function   |
| $F(\kappa, M)$ | } functions occurring in the formulae for the aerodynamic derivatives |
| $G(\kappa, M)$ |   |
| $H(\kappa, M)$ |   |
| $K(\kappa, M)$ |   |
| $P(\kappa, M)$ |   |
| $Q(\kappa, M)$ |   |
| $R(\kappa, M)$ |   |
| $S(\kappa, M)$ |   |

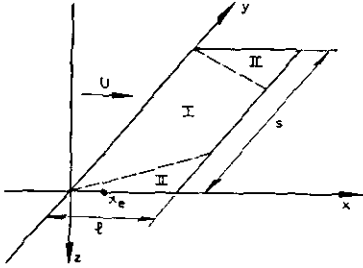
suffix  $B$  denotes quantities associated with bending  
suffix  $T$  denotes quantities associated with torsion

### 1 Introduction.

In N.L.R. report W. 3 (ref. 1) we considered the problem of the harmonically oscillating rectangular wing in supersonic flow. The wing was assumed to execute small torsional oscillations of amplitude  $\varphi(y)$  about some spanwise axis  $x = x_e$  (see sketch) and small vertical translations of amplitude  $B(y)$ , where  $\varphi(y)$  and  $B(y)$  may be arbitrary functions of the spanwise coordinate  $y$ .

Outside the Mach lines from the leading edge tips (region I)  $\varphi(y)$  and  $B(y)$  were locally approximated by polynomials of the second degree, viz.:

$$\begin{aligned}\varphi(y) &= T_1 + T_2 \frac{y}{l} + T_3 \frac{y^2}{l^2} \\ B(y) &= l \left( B_1 + B_2 \frac{y}{l} + B_3 \frac{y^2}{l^2} \right) \quad (1.1)\end{aligned}$$



while in the regions II inside the Mach lines from the leading edge tips  $\varphi(y)$  and  $B(y)$  were approximated by:

$$\begin{aligned}\varphi(y) &= T_1 \\ B(y) &= l \left( B_1 + B_2 \frac{y}{l} \right), \quad (1.2)\end{aligned}$$

(compare lit. 1 sections 3.2 and 3.3). Expressions were given for lift and moment. These expressions consist of a number of terms each of which is composed of two factors, one containing the reduced frequency and the Mach number only, the other one the bending or torsion mode shape  $B(y)$  and  $\varphi(y)$  in a very simple way.

The functions  $\varphi(y)$  and  $B(y)$  were taken symmetrically with respect to the midchord of the wing.

The formulae for lift and moment are valid as long as the Mach waves from the leading edge tips do not intersect the opposite side edges; this means that the effective aspect ratio  $\beta A$  must be larger than 1;  $A$  is the aspect ratio and  $\beta = \sqrt{M^2 - 1}$ .

The theory is so much the more accurate according as the approximations (1.1) and (1.2) for the bending and the torsion mode shape are more accurate.

The rather rough approximations (1.2) for arbitrary bending and torsion mode shapes in the regions II inside the Mach waves from the leading edge tips may be of little value when the regions II occupy a large part of the wing i. e. when the value of  $\beta A$  is close to 1. However, the accuracy of the approximation (1.2) increases when  $\beta A$  becomes larger; moreover the influence of the tips upon lift and moment of the wing decreases for larger values of  $\beta A$ . For a translating and pitching flat wing the formulae for lift and moment are quite exact.

## 2 Recapitulation of the theoretical results.

In this section we give a review of the results derived in ref. 1.

### a) The lift due to bending of the wing.

The lift coefficient (lift positive in upward direction) can be written as:

$$C_{L_B} = \frac{\mathcal{L}_B}{\frac{1}{2} \rho U^2 S e^{i\nu t}} = \frac{\bar{L}_B}{\frac{1}{2} \rho U^2 S e^{i\nu t}} + \frac{\Delta \bar{L}_B}{\frac{1}{2} \rho U^2 S e^{i\nu t}} \quad (2.1)$$

where the second term is the edge correction of the first one due to the finite span of the wing;  $U$  is the undisturbed velocity,  $S$  the wing area,  $\nu$  the circular frequency,  $t$  the time and  $\rho$  the density.

$$\begin{aligned}\frac{\bar{L}_B}{\frac{1}{2} \rho U^2 S e^{i\nu t}} &= F_B(\kappa, M) \frac{\int_0^{\frac{1}{2}s} \frac{B(y)}{l} dy}{\frac{1}{2}s} + G_B(\kappa, M) \left( \frac{dB}{dy} \right)_{y=0} \\ \frac{\Delta \bar{L}_B}{\frac{1}{2} \rho U^2 S e^{i\nu t}} &= H_B(\kappa, M) \frac{B_1}{\beta A} + K_B(\kappa, M) \frac{B_2}{\beta A} \quad (2.2)\end{aligned}$$

where  $\kappa = \frac{2kM}{\beta^2}$ ,  $k$  the reduced frequency  $\frac{\nu l}{2U}$ ,  $l$  the wing chord,  $s$  the wing span,  $M$  the Mach number,  $\beta = \sqrt{M^2 - 1}$  and  $A$  the aspect ratio.  $B(y)$  is the bending mode shape of the wing and  $B_1$  and  $B_2$  are constants such that  $l \left( B_1 + B_2 \frac{y}{l} \right)$  approximates the bending mode shape as close as possible in the  $0 < y < \frac{l}{\beta}$ .

The complex functions  $F_B$ ,  $G_B$ ,  $H_B$  and  $K_B$  are given in section (4.6) of ref. 1;  $K_B = -\frac{1}{4} G_B$  and the functions  $F_B$ ,  $G_B$  and  $H_B$  are tabulated in tables 1—11 for  $k = 0(0.1)1$  and  $M = 1.2(0.1)1.6(0.2)2(0.5)4$ .

b) *The lift due to torsion of the wing.*

The lift coefficient can be written as

$$C_{L_T} = \frac{\mathfrak{L}_T}{\frac{1}{2} \rho U^2 S e^{i\omega t}} = \frac{\bar{L}_T}{\frac{1}{2} \rho U^2 S e^{i\omega t}} + \frac{\Delta \bar{L}_T}{\frac{1}{2} \rho U^2 S e^{i\omega t}} \quad (2.3)$$

where the second term represents the edge correction.

$$\begin{aligned} \frac{\bar{L}_T}{\frac{1}{2} \rho U^2 S e^{i\omega t}} &= \left\{ F_T(\kappa, M) - \left( \frac{x_e}{l} + \frac{iM}{\beta^2 \kappa} \right) F_B(\kappa, M) \right\} \frac{\int_0^{\frac{1}{2}s} \varphi(y) dy}{\frac{1}{2}s} + \\ &+ \left\{ G_T(\kappa, M) + \beta \left( \frac{x_e}{l} + \frac{iM}{\beta^2 \kappa} \right) G_B(\kappa, M) \right\} \frac{l^2}{\beta^2} \left( \frac{d\varphi}{dy} \right)_{y=\frac{1}{2}s} \\ \frac{\Delta \bar{L}_T}{\frac{1}{2} \rho U^2 S e^{i\omega t}} &= \left\{ H_T(\kappa, M) - \left( \frac{x_e}{l} + \frac{iM}{\beta^2 \kappa} \right) H_B(\kappa, M) \right\} \frac{T_1}{\beta A} \end{aligned} \quad (2.4)$$

where  $x_e$  is the  $x$ -coordinate of the elastic axis and  $\varphi(y)$  the torsion mode function.  $T_1$  is the constant, that approximates the torsion mode shape as close as possible in the region  $0 < y < \frac{l}{\beta}$ .

The complex functions  $F_T$ ,  $G_T$  and  $H_T$  are given in section (4.6) of ref. 1 and they are tabulated in tables 1—11.

c) *The aerodynamic moment due to bending of the wing.*

The aerodynamic moment (positive nose-heavy) is taken with respect to the leading edge of the wing; the moment coefficient reads as:

$$C_{M_B} = \frac{\mathfrak{M}_B}{\frac{1}{2} \rho U^2 S l e^{i\omega t}} = \frac{\bar{M}_B}{\frac{1}{2} \rho U^2 S l e^{i\omega t}} + \frac{\Delta \bar{M}_B}{\frac{1}{2} \rho U^2 S l e^{i\omega t}} \quad (2.5)$$

where the second term represents again the edge correction.

$$\begin{aligned} \frac{\bar{M}_B}{\frac{1}{2} \rho U^2 S l e^{i\omega t}} &= P_B(\kappa, M) \frac{\int_0^{\frac{1}{2}s} \frac{B(y)}{l} dy}{\frac{1}{2}s} + Q_B(\kappa, M) \frac{\left( \frac{dB}{dy} \right)_{y=0}}{\beta A} \\ \frac{\Delta \bar{M}_B}{\frac{1}{2} \rho U^2 S l e^{i\omega t}} &= R_B(\kappa, M) \frac{B_1}{\beta A} + S_B(\kappa, M) \frac{B_2}{\beta A} \end{aligned} \quad (2.6)$$

$S_B(\kappa, M) = -\frac{1}{4} \cdot Q_B(\kappa, M)$  and  $P_B$ ,  $Q_B$  and  $R_B$  are given in section (4.6) of ref. 1; they are tabulated in tables 1—11.

d) *The aerodynamic moment due to torsion of the wing.*

The moment (positive nose heavy), is taken with respect to the leading edge of the wing, and the moment coefficient reads as:

$$C_{M_T} = \frac{\mathfrak{M}_T}{\frac{1}{2} \rho U^2 S l e^{i\omega t}} = \frac{\bar{M}_T}{\frac{1}{2} \rho U^2 S l e^{i\omega t}} + \frac{\Delta \bar{M}_T}{\frac{1}{2} \rho U^2 S l e^{i\omega t}} \quad (2.7)$$

where the second term represents again the edge correction.

$$\frac{\bar{M}_T}{\frac{1}{2} \rho U^2 \cdot S \cdot l \cdot e^{i\nu t}} = \left\{ P_T(\kappa, M) - \left( \frac{x_e}{l} + \frac{iM}{\beta^2 \kappa} \right) P_B(\kappa, M) \right\} \frac{\int_0^{\frac{1}{2}s} \varphi(y) dy}{\frac{1}{2}s} +$$

$$+ \left\{ Q_T(\kappa, M) + \beta \left( \frac{x_e}{l} + \frac{iM}{\beta^2 \kappa} \right) Q_B(\kappa, M) \right\} \frac{l^2}{\beta^2} \frac{\left( \frac{d\varphi}{dy} \right)_{y=\frac{1}{2}s}}{s}$$

$$\frac{\Delta \bar{M}_T}{\frac{1}{2} \rho U^2 \cdot S \cdot l \cdot e^{i\nu t}} = \left\{ R_T(\kappa, M) - \left( \frac{x_e}{l} + \frac{iM}{\beta^2 \kappa} \right) R_B(\kappa, M) \right\} \frac{T_1}{\beta A}. \quad (2.8)$$

The functions  $P_T$ ,  $Q_T$  and  $R_T$  are given in section (4.6) of ref. 1; they are tabulated in tables 1—11.

The calculation of the aerodynamic derivatives can now easily be performed for some given bending or torsion mode function by aid of the tables 1—11.

It appears that the correction of lift and moment due to the finite span of the wing is inversely proportional to the effective aspect ratio  $\beta A$ .

### 3 Application of the theory to a flat wing.

For a flat wing, plunging with amplitude  $h$ , the formulae for lift and moment about the leading edge reduce to

$$\frac{\partial C_L}{\partial h} = \frac{L_h}{\frac{1}{2} \rho U^2 \cdot S \cdot h \cdot e^{i\nu t}} = F_B(\kappa, M) + \frac{H_B(\kappa, M)}{\beta A}$$

$$\frac{\partial C_M}{\partial h} = \frac{M_h}{\frac{1}{2} \rho U^2 \cdot S \cdot l \cdot h \cdot e^{i\nu t}} = P_B(\kappa, M) + \frac{R_B(\kappa, M)}{\beta A}. \quad (3.1)$$

For the wing, if pitching with amplitude  $\varphi$  about the spanwise axis  $x=x_e$ , the formulae for lift and moment about the leading edge become:

$$\frac{\partial C_L}{\partial \varphi} = \frac{L_\varphi}{\frac{1}{2} \rho U^2 \cdot S \cdot \varphi \cdot e^{i\nu t}} = \left\{ F_T(\kappa, M) - \left( \frac{x_e}{l} + \frac{iM}{\beta^2 \kappa} \right) F_B(\kappa, M) \right\} + \left\{ \frac{H_T(\kappa, M) - \left( \frac{x_e}{l} + \frac{iM}{\beta^2 \kappa} \right) H_B(\kappa, M)}{\beta A} \right\}$$

$$\frac{\partial C_M}{\partial \varphi} = \frac{M_\varphi}{\frac{1}{2} \rho U^2 \cdot S \cdot l \cdot \varphi \cdot e^{i\nu t}} = \left\{ P_T(\kappa, M) - \left( \frac{x_e}{l} + \frac{iM}{\beta^2 \kappa} \right) P_B(\kappa, M) \right\} +$$

$$+ \left\{ \frac{R_T(\kappa, M) - \left( \frac{x_e}{l} + \frac{iM}{\beta^2 \kappa} \right) R_B(\kappa, M)}{\beta A} \right\}. \quad (3.2)$$

These formulae are essentially the same as those derived by Miles in refs. 2 and 3.

In order to obtain some insight into the variation of the aerodynamic derivatives as functions of the reduced frequency, aspect ratio and Mach number, the absolute value of the aerodynamic derivatives and their phase with respect to the phase of the plunging or pitching motion have been plotted as functions of the reduced frequency for several values of the aspect ratio and for  $M=1.3, 2$  and  $4$ .

These graphs are presented in figs. 1, 1a, 1b, — 8, 8a, 8b; the moments, however, have not been taken with respect to the leading edge of the wing, but with respect to the axis of rotation of the pitching wing; the abscissa of this axis has been chosen as  $x=\frac{1}{2}l$ , viz. the midchord line of the

wing. The range of the reduced frequency is 0—1.0 and the aspect-ratio varies from its minimum value  $A=\frac{1}{\beta}$  to  $\infty$ .

It appears that the absolute value of the aerodynamic derivatives decreases when the Mach number increases. The variation of the magnitude and the phase of the aerodynamic derivatives as functions of the aspect ratio becomes smaller according as the aspect-ratio becomes larger and this effect is in general stronger when the Mach number is increased; this result is in agreement with the fact, that the correction term due to the finite span of the wing is inversely proportional to the effective aspect ratio  $\beta A$ .

There are some values of the reduced frequency where the magnitude of the aerodynamic derivative

or its phase seems to be independent of the aspect ratio; see figs. 4a, 6a, 8a and 8b.

It seems that the curves for different aspect ratio all intersect in one point. Careful calculations, however, have shown that this common point of intersection is not real; nevertheless the variation of the magnitude of the aerodynamic derivative or its phase as function of the aspect ratio is very small in the neighbourhood of these values of the reduced frequency.

Nelson, Rainey and Watkins have also presented a theory for the oscillating flat rectangular wing in supersonic flight (ref. 4). They present amongst others expressions for lift and moment coefficients expanded to the seventh power of the frequency. Their results, however, are only valid

for  $0 \leq k \leq \frac{M^2 - 1}{M^2}$ , whereas the results of this

report are valid for all values of  $k$ .

The numerical results presented here are in good agreement with those of reference 4. Computation of the formulae of ref. 4 has revealed that the numerical results for the moment curve slope and the corresponding phase angle associated

with pitching are not in good agreement with the corresponding graphs in ref. 4.

Since the values computed from the formulae of ref. 4 agree quite well with those derived from the formulae (3.1) and (3.2) of this paper, it may be concluded that a little error has been made in ref. 4 in drawing the graphs for the moment curve slope and the corresponding phase angle associated with pitch.

#### 4 References.

1. DE JAGER, E. M. Oscillating rectangular wings in supersonic flow with arbitrary bending and torsion mode shapes. Part I. N.L.R. report W.3. Nat. Aeronaut. Res. Inst. Amsterdam, 1959.
2. MILES, J. W. The aerodynamic forces on an oscillating airfoil at supersonic speeds. *J. Aeronaut. Sci.* 14, 351-358 (1947).
3. MILES, J. W. The oscillating rectangular airfoil at supersonic speeds. Inyokern, Calif., N.A.V.O.R.D. report 1185, N.O.T.S. 241 (1949).
4. NELSON, H. C., RAINEY, R. A., WATKINS, C. E. Lift and moment coefficients expanded to the seventh power of frequency for oscillating rectangular wings in supersonic flow and applied to a specific flutter problem. N.A.C.A. T.N. 3076, 1954.

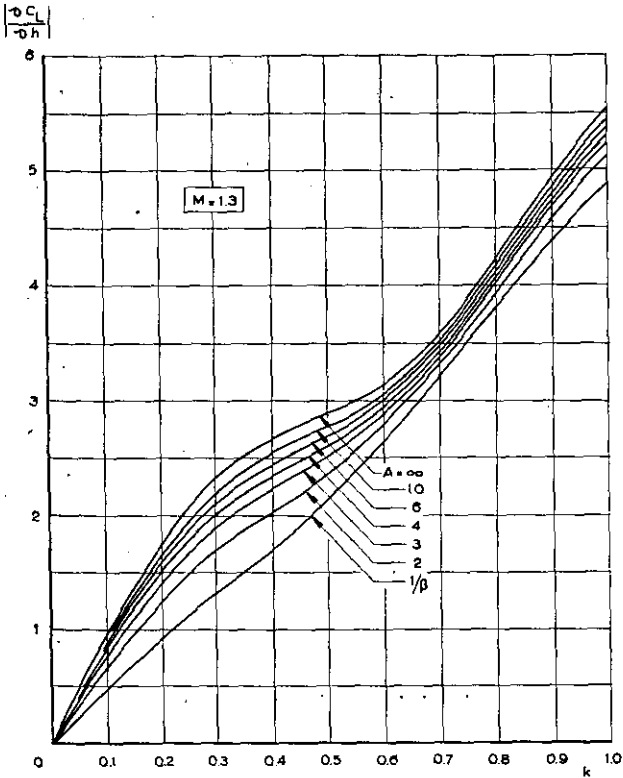


Fig. 1a. Lift curve slopes for translation as a function of reduced frequency for some values of the aspect ratio. Mach number  $M = 1.3$ .

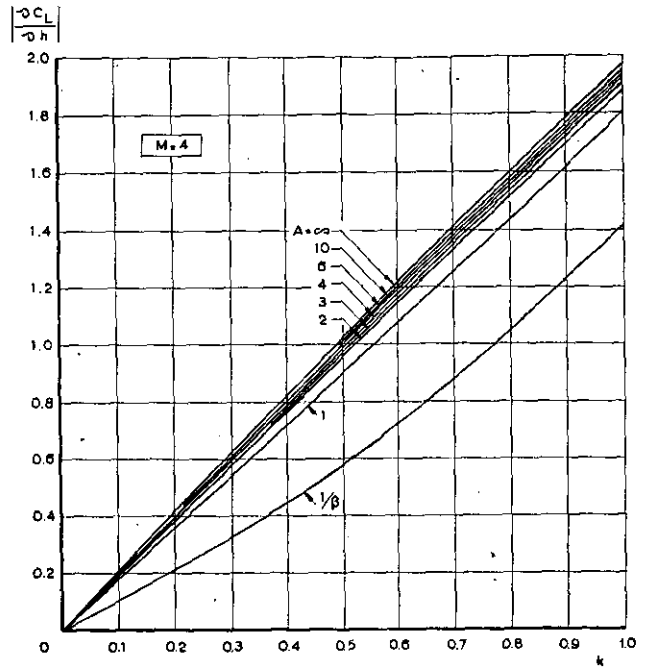


Fig. 1c. Lift curve slopes for translation as a function of reduced frequency for some values of the aspect ratio. Mach number  $M = 4$ .

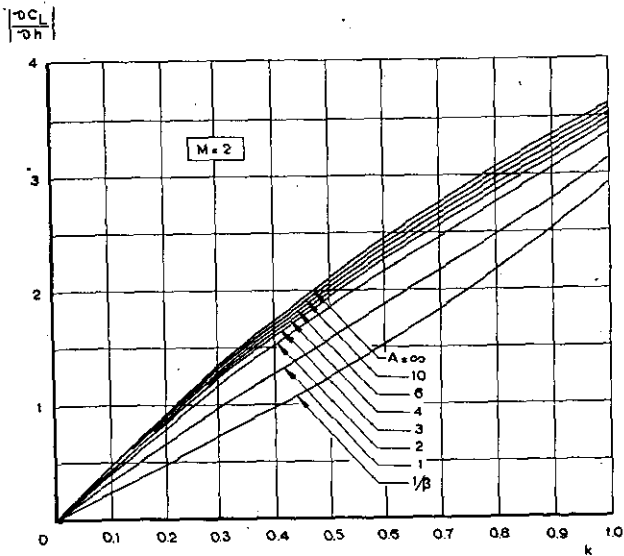


Fig. 1b. Lift curve slopes for translation as a function of reduced frequency for some values of the aspect ratio. Mach number  $M = 2$ .

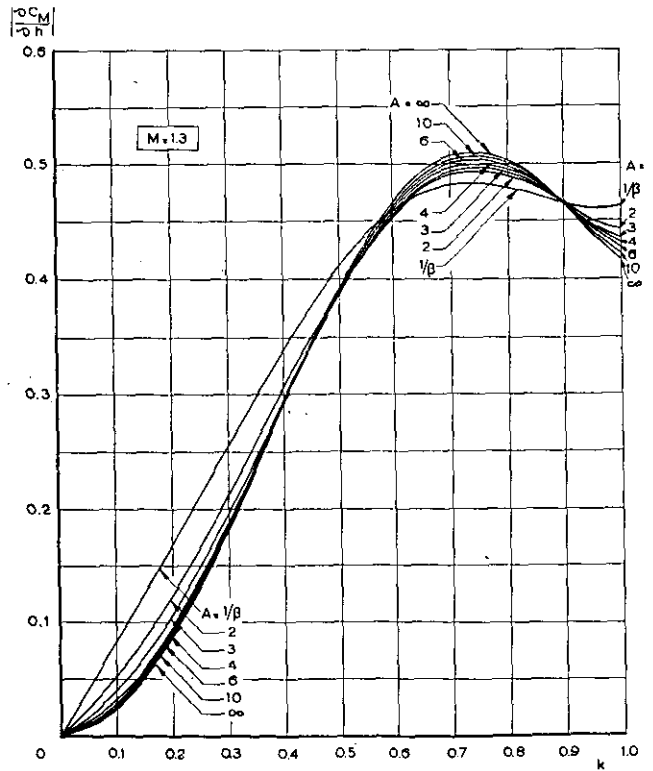


Fig. 2a. Moment curve slopes for translation as a function of reduced frequency for some values of the aspect ratio. The moment is taken with respect to the midchord line of the wing. Mach number  $M = 1.3$ .

Fig. 2c. Moment curve slopes for translation as a function of reduced frequency for some values of the aspect ratio. The moment is taken with respect to the midchord line of the wing. Mach number  $M = 4$ .

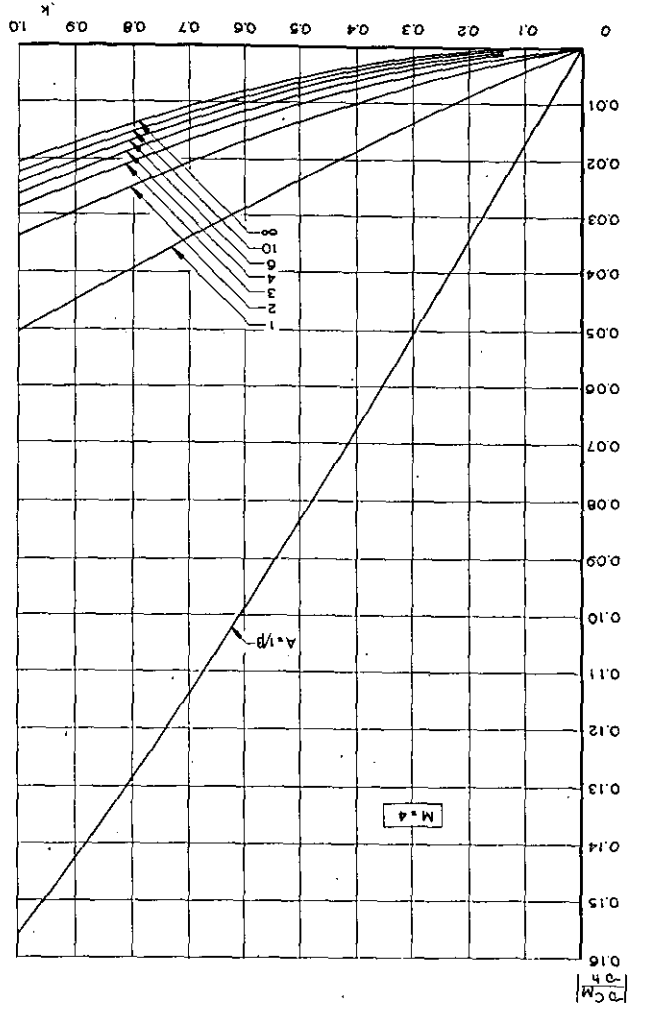


Fig. 2b. Moment curve slopes for translation as a function of reduced frequency for some values of the aspect ratio. The moment is taken with respect to the midchord line of the wing. Mach number  $M = 2$ .

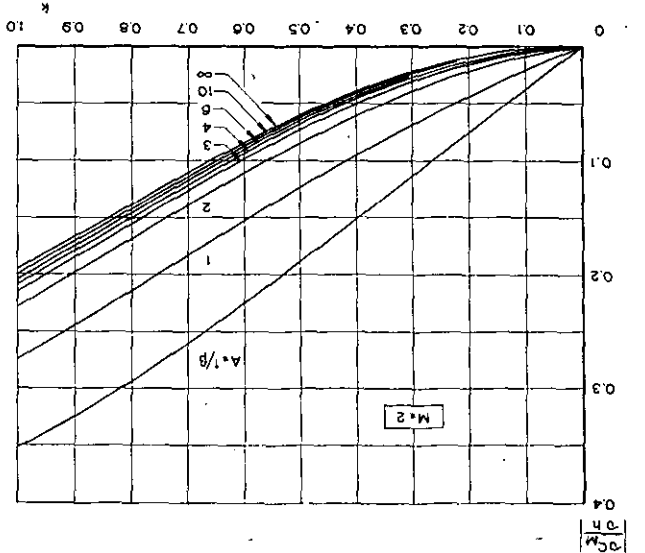


Fig. 3b. Lift curve slopes for pitch as a function of reduced frequency for some values of the aspect ratio. Axis of rotation is midchord line of the wing. Mach number  $M = 2$ .

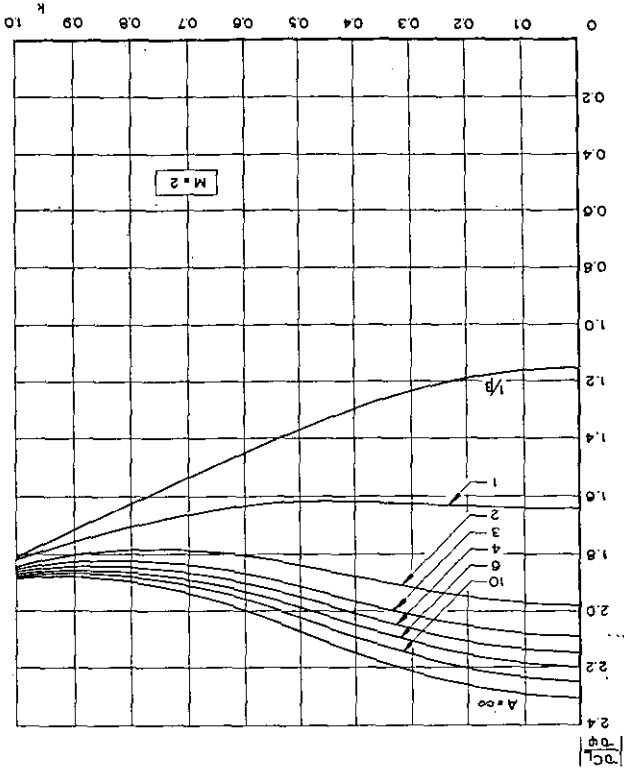
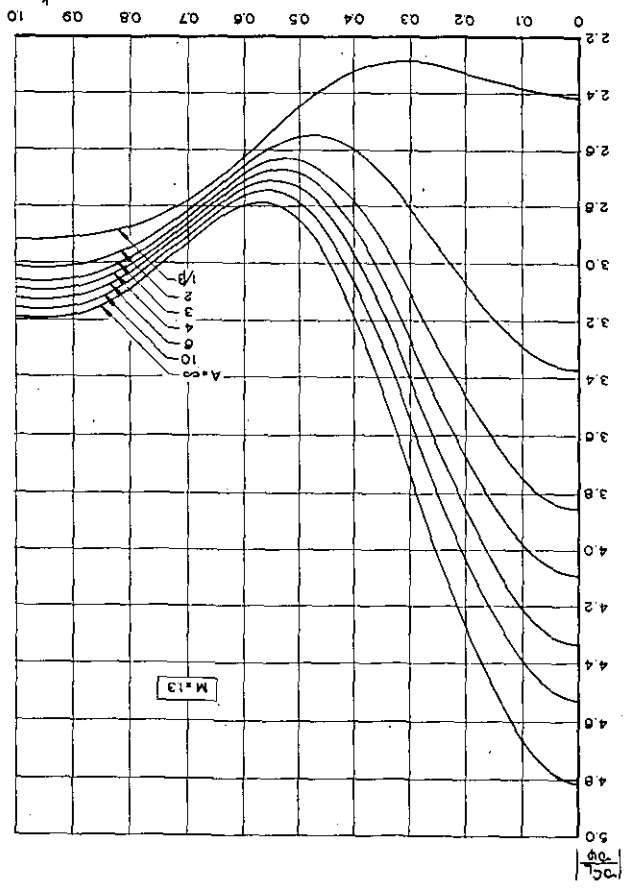


Fig. 3a. Lift curve slopes for pitch as a function of reduced frequency for some values of the aspect ratio. Axis of rotation is midchord line of the wing. Mach number  $M = 1.8$ .



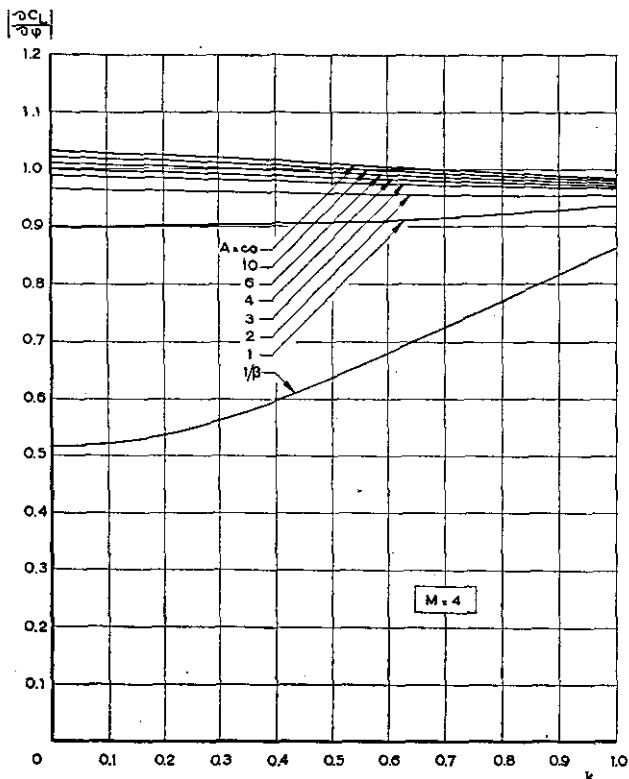


Fig. 3c. Lift curves slopes for pitch as a function of reduced frequency for some values of the aspect ratio. Axis of rotation is midchord line of the wing. Mach number  $M = 4$ .

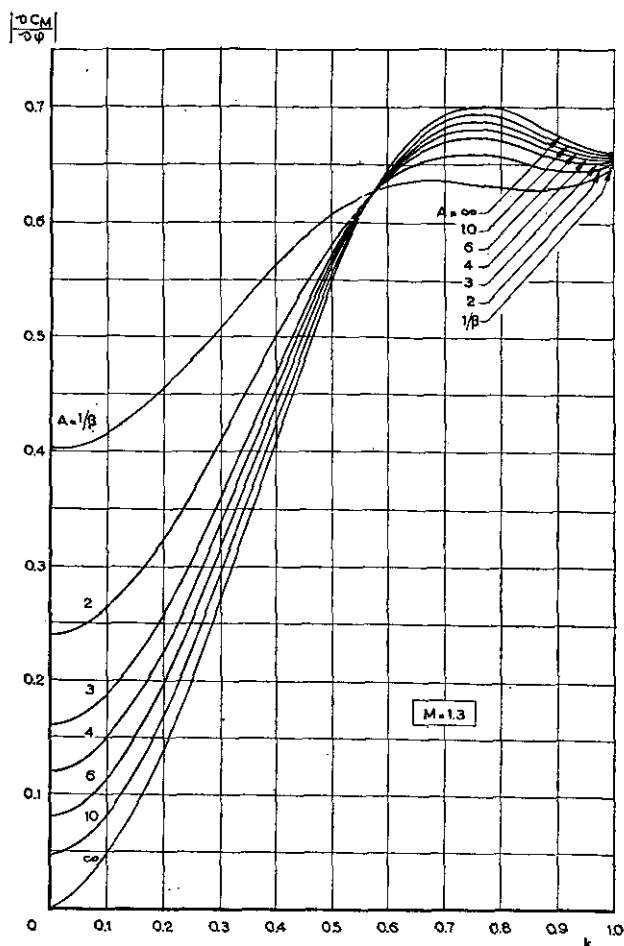


Fig. 4a. Moment curve slopes for pitch as a function of reduced frequency for some values of the aspect ratio. Axis of rotation is midchord line of the wing. The moment is taken with respect to the axis of rotation. Mach number  $M = 1.3$ .

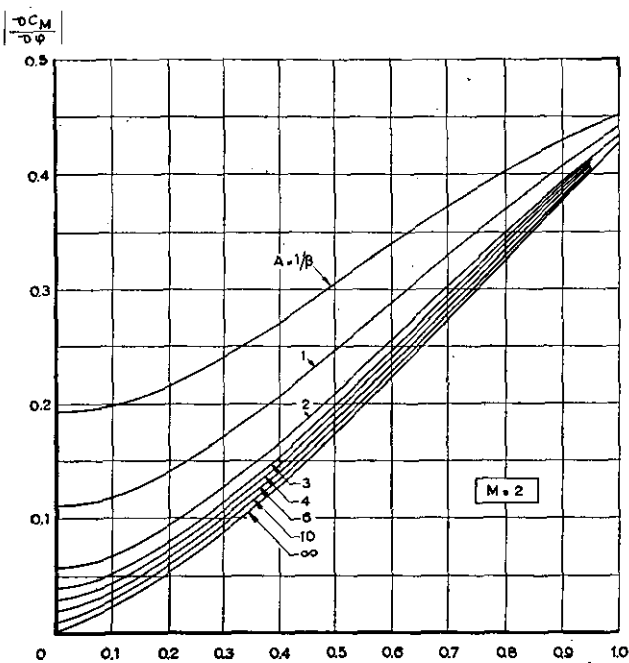


Fig. 4b. Moment curve slopes for pitch as a function of reduced frequency for some values of the aspect ratio. Axis of rotation is midchord line of the wing. The moment is taken with respect to the axis of rotation. Mach number  $M = 2$ .

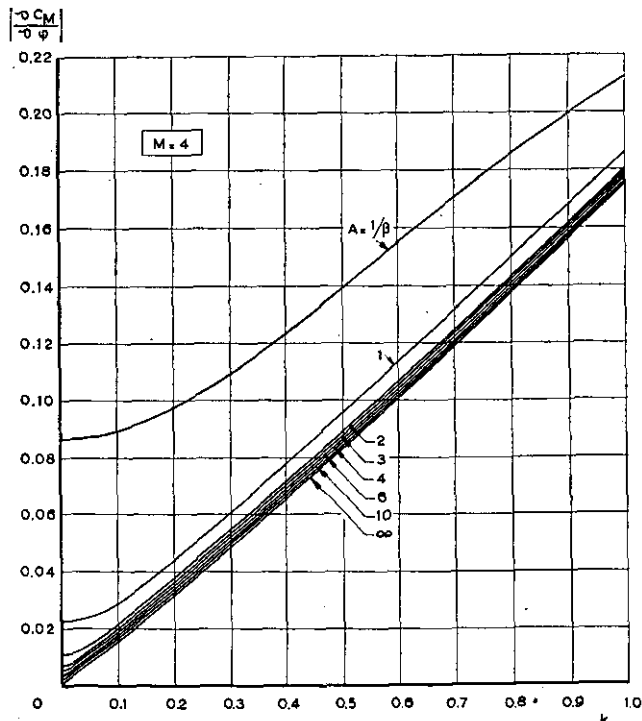


Fig. 4c. Moment curve slopes for pitch as a function of reduced frequency for some values of the aspect ratio. Axis of rotation is midchord line of the wing. The moment is taken with respect to the axis of rotation. Mach number  $M = 4$ .

Fig. 5b. Phase angle in radians between lift vector and angular displacement vector for translation as a function of reduced frequency for some values of the aspect ratio. Mach number  $M = 2$ .

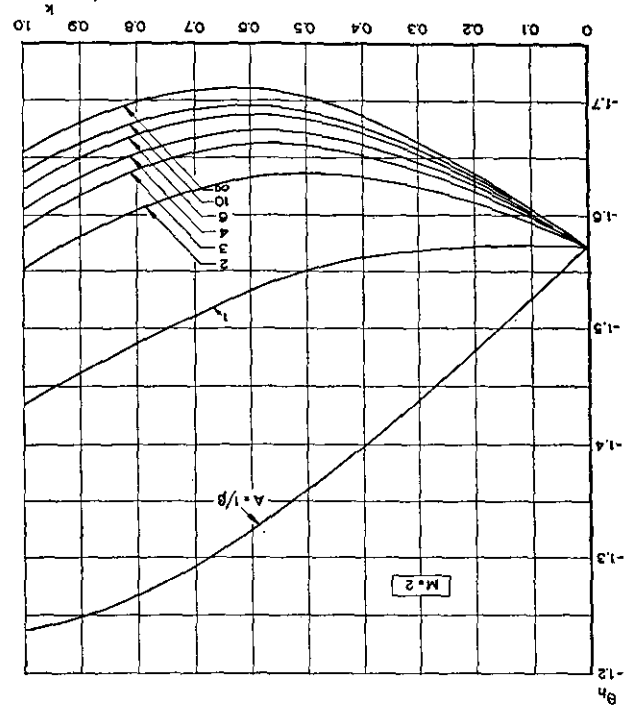


Fig. 5a. Phase angle in radians between lift vector and angular displacement vector for translation as a function of reduced frequency for some values of the aspect ratio. Mach number  $M = 1.3$ .

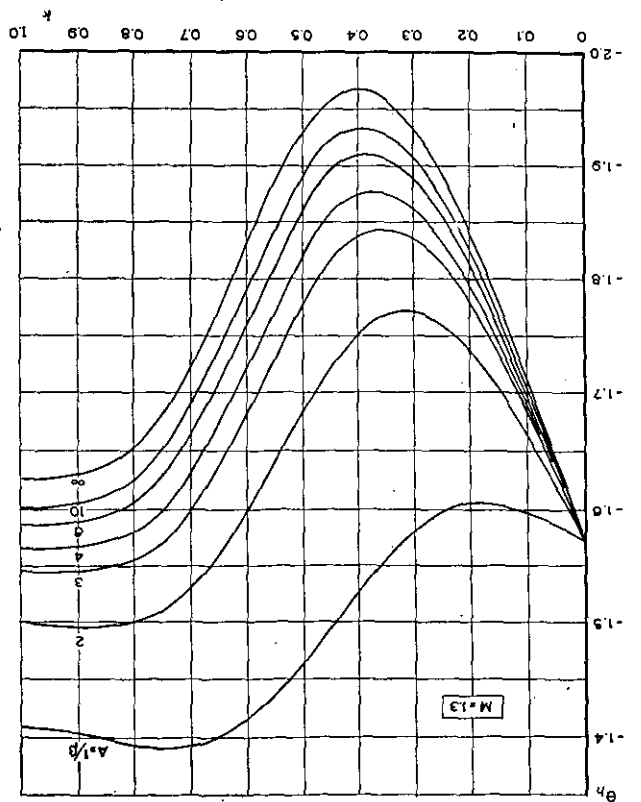


Fig. 6a. Phase angle in radians between moment vector and angular displacement vector for translation as a function of reduced frequency for some values of the aspect ratio. The moment is taken with respect to the midchord line of the wing. Mach number  $M = 1.3$ .

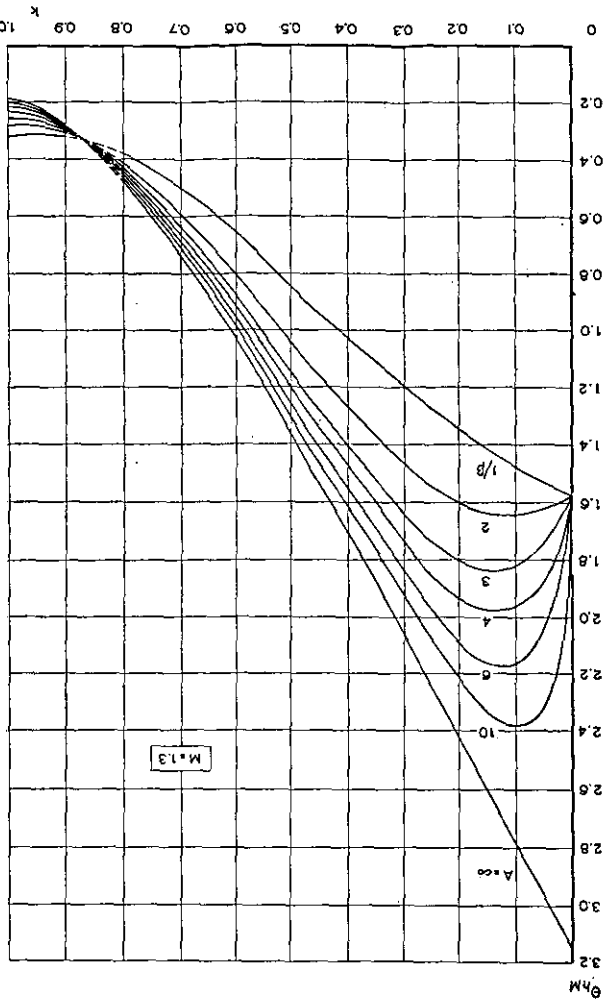
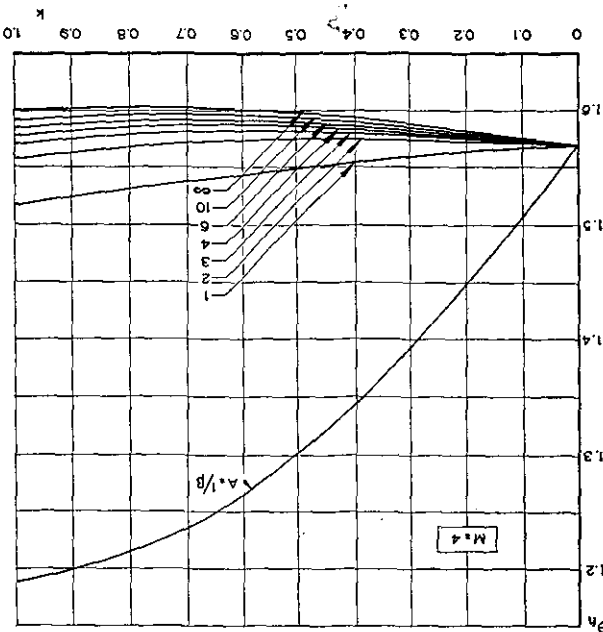


Fig. 5c. Phase angle in radians between lift vector and angular displacement vector for translation as a function of reduced frequency for some values of the aspect ratio. Mach number  $M = 4$ .



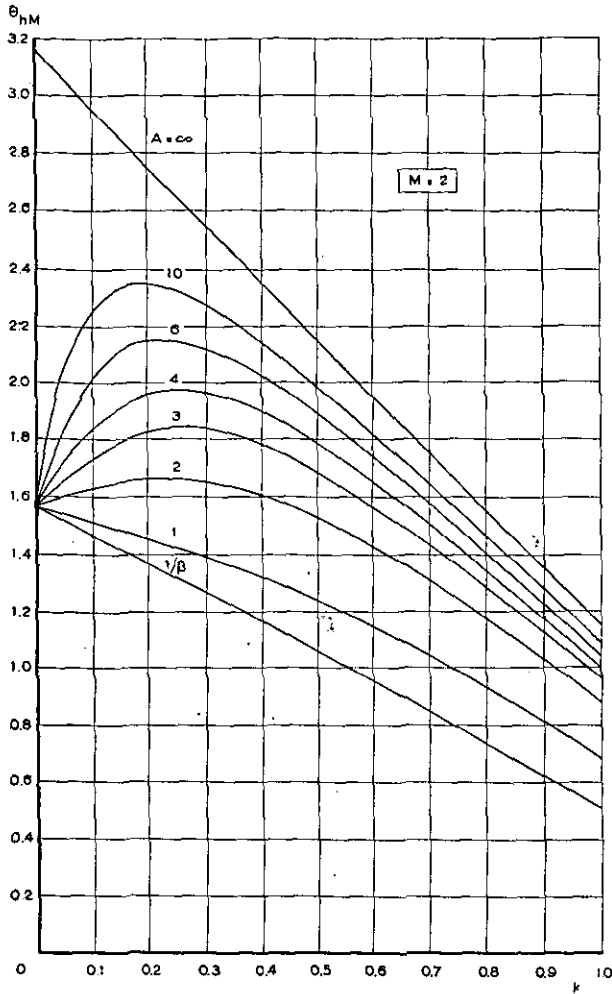


Fig. 6b. Phase angle in radians between moment vector and angular displacement vector for translation as a function of reduced frequency for some values of the aspect ratio. The moment is taken with respect to the midchord line of the wing. Mach number  $M = 2$ .

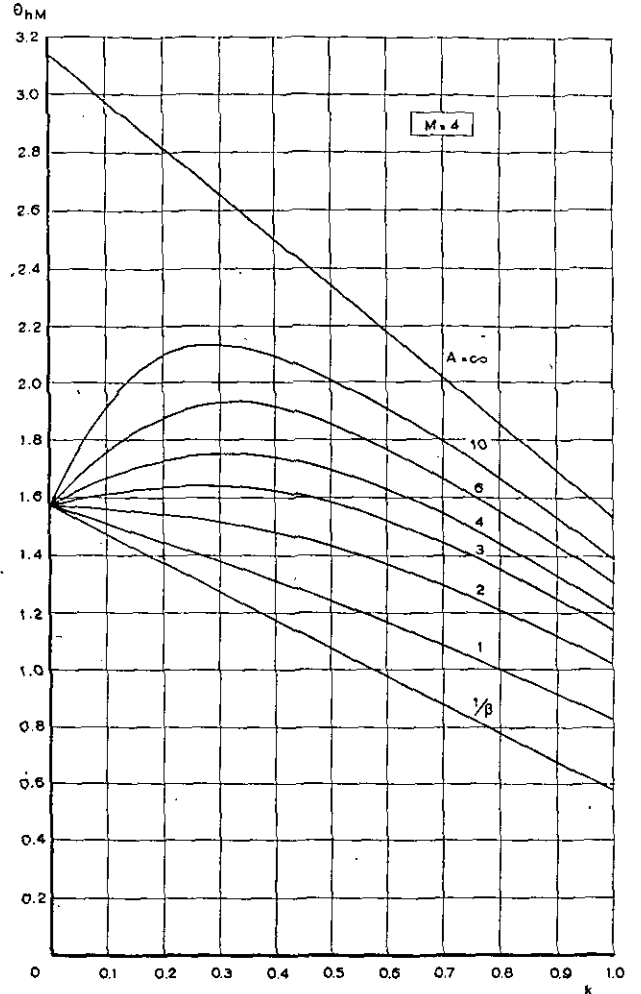


Fig. 6c. Phase angle in radians between moment vector and angular displacement vector for translation as a function of reduced frequency for some values of the aspect ratio. The moment is taken with respect to the midchord line of the wing. Mach number  $M = 4$ .

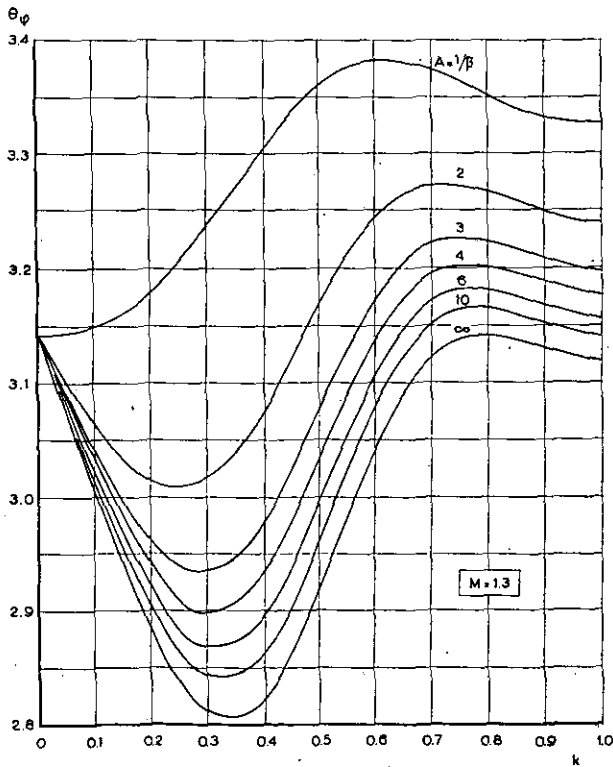


Fig. 7a. Phase angle in radians between lift vector and angular displacement vector for pitch as a function of reduced frequency for some values of the aspect ratio. Axis of rotation is midchord line of the wing. Mach number  $M = 1.3$ .

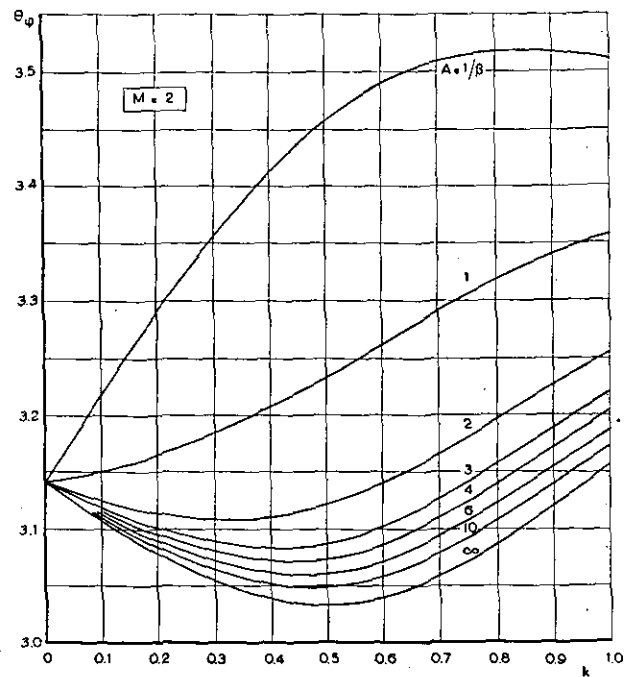


Fig. 7b. Phase angle in radians between lift vector and angular displacement vector for pitch as a function of reduced frequency for some values of the aspect ratio. Axis of rotation is midchord line of the wing. Mach number  $M = 2$ .

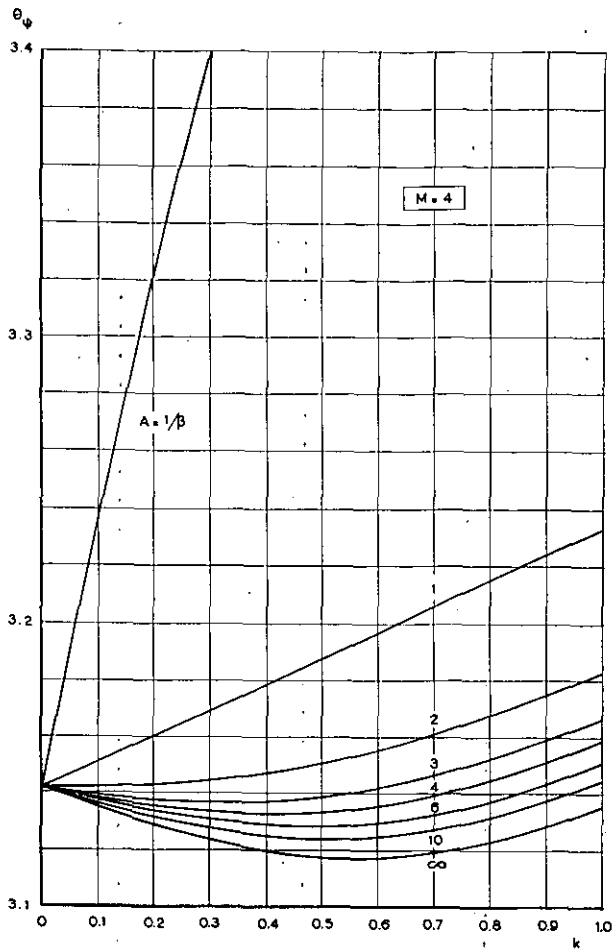


Fig. 7c. Phase angle in radians between lift vector and angular displacement vector for pitch as a function of reduced frequency for some values of the aspect ratio. Axis of rotation is midchord line of the wing. Mach number  $M = 4$ .

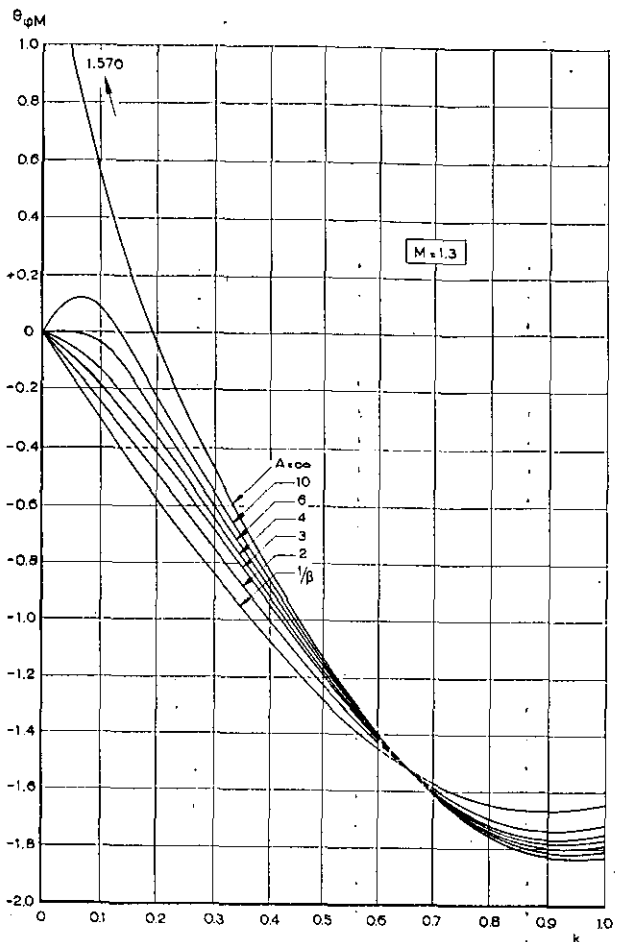


Fig. 8a. Phase angle in radians between moment vector and angular displacement vector for pitch as a function of reduced frequency for some values of the aspect ratio. Axis of rotation is midchord line of the wing. The moment is taken with respect to the axis of rotation. Mach number  $M = 1.3$ .

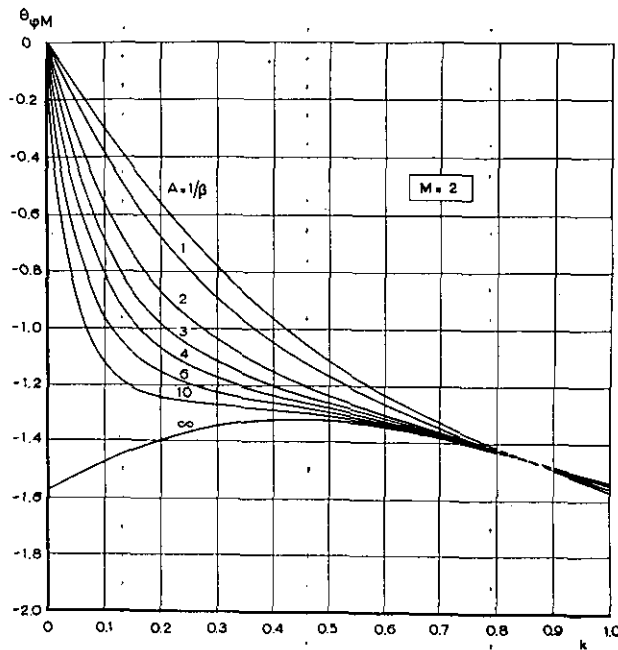


Fig. 8b. Phase angle in radians between moment vector and angular displacement vector for pitch as a function of reduced frequency for some values of the aspect ratio. Axis of rotation is midchord line of the wing. The moment is taken with respect to the axis of rotation. Mach number  $M = 2$ .

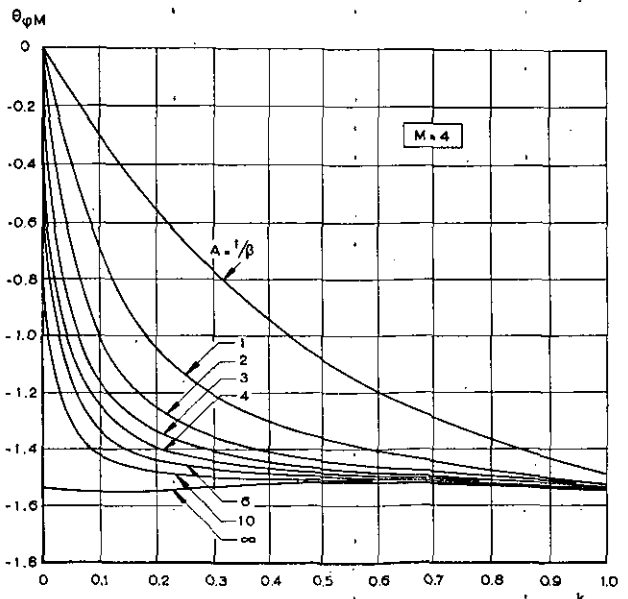


Fig. 8c. Phase angle in radians between moment vector and angular displacement vector for pitch as a function of reduced frequency for some values of the aspect ratio. Axis of rotation is midchord line of the wing. The moment is taken with respect to the axis of rotation. Mach number  $M = 4$ .

TABLE 1.

 $M = + 1.20000.$ 

$k$	$Re F_B$	$Im F_B$	$Re G_B$	$Im G_B$	$Re H_B$	$Im H_B$
0	— 0.00000	— 0.00000	+ 0.00000	+ 0.00000	+ 0.00000	+ 0.00000
0.1	— 0.25199	— 1.12107	+ 0.12465	+ 0.26501	+ 0.20755	+ 0.53974
0.2	— 0.78059	— 1.83371	+ 0.40395	+ 0.33983	+ 0.66929	+ 0.76704
0.3	— 1.13645	— 2.11894	+ 0.63536	+ 0.18686	+ 1.05089	+ 0.63482
0.4	— 1.09199	— 2.32579	+ 0.67684	— 0.06235	+ 1.14144	+ 0.37298
0.5	— 0.82088	— 2.78445	+ 0.54892	— 0.23265	+ 1.00920	+ 0.25121
0.6	— 0.64896	— 3.48975	+ 0.38827	— 0.24969	+ 0.88412	+ 0.34101
0.7	— 0.68709	— 4.18091	+ 0.31297	— 0.17492	+ 0.91452	+ 0.50163
0.8	— 0.75502	— 4.68146	+ 0.33201	— 0.11882	+ 1.05059	+ 0.56760
0.9	— 0.64103	— 5.09127	+ 0.37072	— 0.13261	+ 1.14600	+ 0.51896
1.0	— 0.36149	— 5.63369	+ 0.36434	— 0.18104	+ 1.13464	+ 0.46661
	$Re F_T$	$Im F_T$	$Re G_T$	$Im G_T$	$Re H_T$	$Im H_T$
0	— 0.00000	— 0.00000	— 0.00000	— 0.00000	— 0.00000	— 0.00000
0.1	— 0.08690	— 0.58139	— 0.01687	— 0.04600	+ 0.05315	+ 0.18818
0.2	— 0.29949	— 1.05051	— 0.05819	— 0.06972	+ 0.05315	+ 0.30925
0.3	— 0.52920	— 1.36722	— 0.10236	— 0.06243	+ 0.32990	+ 0.33735
0.4	— 0.68332	— 1.57827	— 0.12954	— 0.03278	+ 0.43142	+ 0.29813
0.5	— 0.73883	— 1.76831	— 0.13293	+ 0.00110	+ 0.47093	+ 0.24321
0.6	— 0.73517	— 1.99458	— 0.11979	+ 0.02425	+ 0.46990	+ 0.21222
0.7	— 0.72370	— 2.25931	— 0.10322	+ 0.03273	+ 0.46276	+ 0.21240
0.8	— 0.72443	— 2.53277	— 0.09233	+ 0.03217	+ 0.46931	+ 0.22670
0.9	— 0.72358	— 2.79403	— 0.08815	+ 0.03054	+ 0.48704	+ 0.23671
1.0	— 0.70199	— 3.04909	— 0.08656	+ 0.03171	+ 0.50355	+ 0.23802
	$Re P_B$	$Im P_B$	$Re Q_B$	$Im Q_B$	$Re R_B$	$Im R_B$
0	— 0.00000	— 0.00000	+ 0.00000	+ 0.00000	+ 0.00000	+ 0.00000
0.1	— 0.16510	— 0.53968	+ 0.09922	+ 0.19566	+ 0.15440	+ 0.35157
0.2	— 0.48110	— 0.78321	+ 0.31623	+ 0.23473	+ 0.48471	+ 0.45778
0.3	— 0.60725	— 0.75171	+ 0.48106	+ 0.09274	+ 0.72098	+ 0.29747
0.4	— 0.40866	— 0.74752	+ 0.48156	— 0.11177	+ 0.71003	+ 0.07484
0.5	— 0.08205	— 1.01614	+ 0.34852	— 0.23099	+ 0.53827	+ 0.00799
0.6	+ 0.08621	— 1.49517	+ 0.20767	— 0.21312	+ 0.41422	+ 0.12879
0.7	+ 0.03660	— 1.92161	+ 0.15736	— 0.12558	+ 0.45176	+ 0.28923
0.8	— 0.03059	— 2.14870	+ 0.19282	— 0.07032	+ 0.58128	+ 0.34090
0.9	+ 0.08255	— 2.29724	+ 0.23783	— 0.08658	+ 0.65896	+ 0.28226
1.0	+ 0.34050	— 2.58459	+ 0.23385	— 0.13323	+ 0.63109	+ 0.22858
	$Re P_T$	$Im P_T$	$Re Q_T$	$Im Q_T$	$Re R_T$	$Im R_T$
0	— 0.00000	— 0.00000	— 0.00000	— 0.00000	+ 0.00000	+ 0.00000
0.1	— 0.06481	— 0.38475	— 0.01402	— 0.03656	+ 0.04237	+ 0.14008
0.2	— 0.21942	— 0.68090	— 0.04799	— 0.05415	+ 0.14560	+ 0.22474
0.3	— 0.37547	— 0.86094	— 0.08323	— 0.04576	+ 0.25536	+ 0.23433
0.4	— 0.46157	— 0.96907	— 1.10301	— 0.01953	+ 0.32470	+ 0.19312
0.5	— 0.46744	— 1.07686	— 0.10240	+ 0.00853	+ 0.34190	+ 0.14588
0.6	— 0.43372	— 1.22703	— 0.08868	+ 0.02590	+ 0.32890	+ 0.12444
0.7	— 0.40560	— 1.41308	— 0.07370	+ 0.03017	+ 0.31653	+ 0.13117
0.8	— 0.39612	— 1.60367	— 0.06501	+ 0.02728	+ 0.32020	+ 0.14812
0.9	— 0.38809	— 1.78005	— 0.06267	+ 0.02456	+ 0.33488	+ 0.15843
1.0	— 0.36234	— 1.95003	— 0.06233	+ 0.02513	+ 0.34781	+ 0.15947

TABLE 2.

 $M = + 1.30000.$ 

$k$	$Re F_B$	$Im F_B$	$Re G_B$	$Im G_B$	$Re H_B$	$Im H_B$
0	-0.00000	-0.00000	+ 0.00000	+ 0.00000	+ 0.00000	+ 0.00000
0.1	-0.13330	-0.92987	+ 0.05917	+ 0.18041	+ 0.12061	+ 0.45548
0.2	-0.46369	-1.68244	+ 0.21260	+ 0.29075	+ 0.43173	+ 0.76956
0.3	-0.82231	-2.17631	+ 0.39807	+ 0.29178	+ 0.80686	+ 0.86717
0.4	-1.03573	-2.46546	+ 0.54605	+ 0.19071	+ 1.10676	+ 0.77077
0.5	-1.01912	-2.70075	+ 0.60838	+ 0.03473	+ 1.24529	+ 0.51830
0.6	-0.81315	-3.03922	+ 0.57794	-0.11361	+ 1.22370	+ 0.42126
0.7	-0.54647	-3.55750	+ 0.48625	-0.20559	+ 1.11727	+ 0.37285
0.8	-0.35087	-4.22019	+ 0.38360	-0.22574	+ 1.02583	+ 0.44395
0.9	-0.28396	-4.91785	+ 0.31305	-0.19291	+ 1.01821	+ 0.57762
1.0	-0.30539	-5.54531	+ 0.29190	-0.14470	+ 1.10143	+ 0.69471
	$Re F_T$	$Im F_T$	$Re G_T$	$Im G_T$	$Re H_T$	$Im H_T$
0	-0.00000	-0.00000	-0.00000	-0.00000	+ 0.00000	+ 0.00000
0.1	-0.04526	-0.47316	-0.00993	-0.03834	+ 0.03053	+ 0.15526
0.2	-0.16674	-0.89975	-0.03679	-0.06669	+ 0.11347	+ 0.28120
0.3	-0.32737	-1.25007	-0.07283	-0.07837	+ 0.22618	+ 0.35837
0.4	-0.48216	-1.52068	-0.10833	-0.07203	+ 0.34052	+ 0.38302
0.5	-0.59508	-1.73262	-0.13486	-0.05159	+ 0.43274	+ 0.36662
0.6	-0.65045	-1.91993	-0.14793	-0.02437	+ 0.49075	+ 0.32976
0.7	-0.65449	-2.11469	-0.14778	+ 0.00186	+ 0.51601	+ 0.29342
0.8	-0.62753	-2.33545	-0.13844	+ 0.02151	+ 0.51994	+ 0.27163
0.9	-0.59191	-2.58387	-0.12550	+ 0.03255	+ 0.51719	+ 0.26817
1.0	-0.56183	-2.84950	-0.11386	+ 0.03631	+ 0.51909	+ 0.27816
	$Re P_B$	$Im P_B$	$Re Q_B$	$Im Q_B$	$Re R_B$	$Im R_B$
0	-0.00000	-0.00000	+ 0.00000	+ 0.00000	+ 0.00000	+ 0.00000
0.1	-0.08804	-0.45671	+ 0.04721	+ 0.13425	+ 0.09009	+ 0.30022
0.2	-0.29605	-0.78270	+ 0.16807	+ 0.21047	+ 0.31826	+ 0.48836
0.3	-0.49494	-0.92625	+ 0.31039	+ 0.19743	+ 0.58068	+ 0.50880
0.4	-0.55358	-0.94478	+ 0.41564	+ 0.10400	+ 0.76623	+ 0.38775
0.5	-0.42404	-0.96813	+ 0.44603	-0.02738	+ 0.81255	+ 0.21467
0.6	-0.16270	-1.11929	+ 0.39985	-0.14295	+ 0.73295	+ 0.09150
0.7	+ 0.10802	-1.44281	+ 0.30834	-0.20334	+ 0.60126	+ 0.07942
0.8	+ 0.27666	-1.88474	+ 0.21695	-0.19984	+ 0.50589	+ 0.17232
0.9	+ 0.30796	-2.33398	+ 0.16196	-0.15372	+ 0.50102	+ 0.30945
1.0	+ 0.25644	-2.96581	+ 0.15483	-0.10099	+ 0.58235	+ 0.41655
	$Re P_T$	$Im P_T$	$Re Q_T$	$Im Q_T$	$Re R_T$	$Im R_T$
0	-0.00000	-0.00000	-0.00000	-0.00000	+ 0.00000	+ 0.00000
0.1	-0.03384	-0.31433	-0.00827	-0.03057	+ 0.02438	+ 0.11602
0.2	-0.12349	-0.59167	-0.03050	-0.05261	+ 0.09013	+ 0.20770
0.3	-0.23841	-0.80938	-0.05996	-0.06051	+ 0.17799	+ 0.25934
0.4	-0.34228	-0.96701	-0.08827	-0.05336	+ 0.26435	+ 0.26880
0.5	-0.40741	-1.08413	-0.10834	-0.03486	+ 0.32988	+ 0.24684
0.6	-0.42412	-1.19006	-0.11661	-0.01152	+ 0.36572	+ 0.21159
0.7	-0.40117	-1.31074	-0.11375	+ 0.00994	+ 0.37477	+ 0.18076
0.8	-0.35832	-1.45918	-0.10366	+ 0.02490	+ 0.36820	+ 0.16529
0.9	-0.31526	-1.63334	-0.09143	+ 0.03203	+ 0.35917	+ 0.16685
1.0	-0.28303	-1.82136	-0.08126	+ 0.03295	+ 0.35714	+ 0.17968

TABLE 3.

 $M = + 1.40000.$ 

$h$	$Re F_B$	$Im F_B$	$Re G_B$	$Im G_B$	$Re H_B$	$Im H_B$
0	-0.00000	-0.00000	+ 0.00000	+ 0.00000	+ 0.00000	+ 0.00000
0.1	-0.08242	-0.79946	+ 0.03477	+ 0.13285	+ 0.08194	+ 0.39412
0.2	-0.29977	-1.50434	+ 0.12966	+ 0.23160	+ 0.30509	+ 0.70887
0.3	-0.57375	-2.05493	+ 0.25935	+ 0.27209	+ 0.60911	+ 0.88963
0.4	-0.80748	-0.44749	+ 0.39043	+ 0.24682	+ 0.91607	+ 0.92259
0.5	-0.92157	-2.73353	+ 0.49145	+ 0.16626	+ 1.15574	+ 0.83659
0.6	-0.88209	-2.99807	+ 0.54188	+ 0.05461	+ 1.28694	+ 0.69062
0.7	-0.70986	-3.32621	+ 0.53712	-0.05842	+ 1.30774	+ 0.55204
0.8	-0.46803	-3.77177	+ 0.48818	-0.14689	+ 1.25146	+ 0.47374
0.9	-0.23418	-4.34027	+ 0.41649	-0.19590	+ 1.17097	+ 0.47843
1.0	-0.06894	-4.99242	+ 0.34601	-0.20452	+ 1.11782	+ 0.55514
	$Re F_T$	$Im F_T$	$Re G_T$	$Im G_T$	$Re H_T$	$Im H_T$
0	-0.00000	-0.00000	-0.00000	-0.00000	+ 0.00000	+ 0.00000
0.1	-0.02782	-0.40396	-0.00686	-0.03303	+ 0.02065	+ 0.13324
0.2	-0.10519	-0.78349	-0.02610	-0.06038	+ 0.07876	+ 0.25024
0.3	-0.21548	-1.12019	-0.05405	-0.07763	+ 0.16381	+ 0.33836
0.4	-0.33606	-1.40588	-0.08557	-0.08251	+ 0.26122	+ 0.39127
0.5	-0.44420	-1.64393	-0.11525	-0.07528	+ 0.35587	+ 0.40985
0.6	-0.52260	-1.84724	-0.13864	-0.05848	+ 0.43551	+ 0.40126
0.7	-0.56292	-2.03391	-0.15306	-0.03612	+ 0.49319	+ 0.37657
0.8	-0.56649	-2.22194	-0.15799	-0.01261	+ 0.52799	+ 0.34755
0.9	-0.54215	-2.42471	-0.15489	+ 0.00825	+ 0.54417	+ 0.32384
1.0	-0.50236	-2.64843	-0.14646	+ 0.02401	+ 0.54906	+ 0.31102
	$Re P_B$	$Im P_B$	$Re Q_B$	$Im Q_B$	$Re R_B$	$Im R_B$
0	-0.00000	-0.00000	+ 0.00000	+ 0.00000	+ 0.00000	+ 0.00000
0.1	-0.05460	-0.39550	+ 0.02777	+ 0.09914	+ 0.06129	+ 0.26088
0.2	-0.19458	-0.72085	+ 0.10302	+ 0.16997	+ 0.22633	+ 0.45863
0.3	-0.35826	-0.93474	+ 0.20419	+ 0.19286	+ 0.44530	+ 0.55127
0.4	-0.47142	-1.04161	+ 0.30310	+ 0.16260	+ 0.65485	+ 0.53132
0.5	-0.47737	-1.08960	+ 0.37382	+ 0.08942	+ 0.79987	+ 0.426674
0.6	-0.35950	-1.15084	+ 0.40038	-0.00508	+ 0.85143	+ 0.28936
0.7	-0.14694	-1.29231	+ 0.38091	-0.09528	+ 0.81454	+ 0.17547
0.8	+ 0.09846	-1.54982	+ 0.32692	-0.15976	+ 0.72346	+ 0.12619
0.9	+ 0.30797	-1.91556	+ 0.25841	-0.18748	+ 0.62680	+ 0.15458
1.0	+ 0.43342	-2.34400	+ 0.19653	-0.18001	+ 0.56875	+ 0.24412
	$Re P_T$	$Im P_T$	$Re Q_T$	$Im Q_T$	$Re R_T$	$Im R_T$
0	-0.00000	-0.00000	-0.00000	-0.00000	+ 0.00000	+ 0.00000
0.1	-0.02082	-0.26874	-0.00571	-0.02637	+ 0.01650	+ 0.09970
0.2	-0.07822	-0.51803	-0.02168	-0.04788	+ 0.06272	+ 0.18589
0.3	-0.15845	-0.73355	-0.04470	-0.06079	+ 0.12969	+ 0.24825
0.4	-0.24300	-0.90968	-0.07031	-0.06326	+ 0.20505	+ 0.28189
0.5	-0.31371	-1.05045	-0.09389	-0.05568	+ 0.7622	+ 0.28815
0.6	-0.35749	-1.16761	-0.11168	-0.04039	+ 0.33329	+ 0.27366
0.7	-0.36912	-1.27677	-0.12157	-0.02097	+ 0.37108	+ 0.24819
0.8	-0.35161	-1.39247	-0.12335	-0.00130	+ 0.38973	+ 0.22179
0.9	-0.31403	-1.52569	-0.11852	+ 0.01542	+ 0.39371	+ 0.20233
1.0	-0.26793	-1.67923	-0.10964	+ 0.02726	+ 0.38994	+ 0.19387

TABLE 4.

 $M = + 1.50000.$ 

$k$	$Re F_B$	$Im F_B$	$Re G_B$	$Im G_B$	$Re H_B$	$Im H_B$
0	— 0.00000	— 0.00000	+ 0.00000	+ 0.00000	+ 0.00000	+ 0.00000
0.1	— 0.05588	— 0.70539	+ 0.02307	+ 0.10325	+ 0.06095	+ 0.34886
0.2	— 0.20784	— 1.35327	+ 0.08767	+ 0.18688	+ 0.23143	+ 0.64676
0.3	— 0.41331	— 1.90222	+ 0.18106	+ 0.23552	+ 0.47746	+ 0.85452
0.4	— 0.61504	— 2.33824	+ 0.28523	+ 0.24121	+ 0.75183	+ 0.95340
0.5	— 0.75725	— 2.67806	+ 0.38102	+ 0.20486	+ 1.00562	+ 0.94853
0.6	— 0.80100	— 2.96358	+ 0.45225	+ 0.13561	+ 1.19964	+ 0.86619
0.7	— 0.73422	— 3.24932	+ 0.48901	+ 0.04829	+ 1.31286	+ 0.74605
0.8	— 0.57359	— 3.58676	+ 0.48931	— 0.04023	+ 1.34582	+ 0.63043
0.9	— 0.35814	— 4.01031	+ 0.45879	— 0.11493	+ 1.31826	+ 0.55371
1.0	— 0.13660	— 4.52906	+ 0.40862	— 0.16574	+ 1.26201	+ 0.53468
	$Re F_T$	$Im F_T$	$Re G_T$	$Im G_T$	$Re H_T$	$Im H_T$
0	— 0.00000	— 0.00000	— 0.00000	— 0.00000	+ 0.00000	+ 0.00000
0.1	— 0.01881	— 0.35522	— 0.00518	— 0.02918	+ 0.01533	+ 0.11747
0.2	— 0.07205	— 0.69571	— 0.01999	— 0.05464	+ 0.05922	+ 0.22457
0.3	— 0.15083	— 1.00949	— 0.04233	— 0.07330	+ 0.12583	+ 0.31265
0.4	— 0.24236	— 1.28946	— 0.06914	— 0.08313	+ 0.20661	+ 0.37614
0.5	— 0.33251	— 1.53452	— 0.09689	— 0.08347	+ 0.29189	+ 0.41329
0.6	— 0.40847	— 1.74929	— 0.12223	— 0.07504	+ 0.37255	+ 0.42620
0.7	— 0.46105	— 1.94284	— 0.14247	— 0.05975	+ 0.44148	+ 0.42003
0.8	— 0.48596	— 2.12648	— 0.15597	— 0.04021	+ 0.49455	+ 0.40185
0.9	— 0.48402	— 2.31138	— 0.16231	— 0.01929	+ 0.53091	+ 0.37911
1.0	— 0.46020	— 2.50645	— 0.16214	— 0.00043	+ 0.55264	+ 0.35828
	$Re P_B$	$Im P_B$	$Re Q_B$	$Im Q_B$	$Re R_B$	$Im R_B$
0	— 0.00000	— 0.00000	+ 0.00000	+ 0.00000	+ 0.00000	+ 0.00000
0.1	— 0.03707	— 0.35017	+ 0.01843	+ 0.07715	+ 0.04562	+ 0.23139
0.2	— 0.13579	— 0.65756	+ 0.06979	+ 0.13801	+ 0.17221	+ 0.42219
0.3	— 0.26248	— 0.89273	+ 0.14319	+ 0.16995	+ 0.35163	+ 0.54187
0.4	— 0.37267	— 1.04878	+ 0.22339	+ 0.16685	+ 0.54522	+ 0.57726
0.5	— 0.42474	— 1.14354	+ 0.29436	+ 0.13021	+ 0.71373	+ 0.53523
0.6	— 0.39253	— 1.21429	+ 0.34293	+ 0.06849	+ 0.82708	+ 0.44000
0.7	— 0.27317	— 1.30649	+ 0.36159	+ 0.00515	+ 0.87137	+ 0.32602
0.8	— 0.08763	— 1.46029	+ 0.34981	+ 0.07620	+ 0.85127	+ 0.22857
0.9	+ 0.12588	— 1.69894	+ 0.31361	— 0.13218	+ 0.13218	+ 0.17460
1.0	+ 0.32361	— 2.02262	+ 0.26359	+ 0.16536	+ 0.70936	+ 0.17640
	$Re P_T$	$Im P_T$	$Re Q_T$	$Im Q_T$	$Re R_T$	$Im R_T$
0	— 0.00000	— 0.00000	— 0.00000	— 0.00000	+ 0.00000	+ 0.00000
0.1	— 0.01408	— 0.23647	— 0.00432	— 0.02330	+ 0.01225	+ 0.08795
0.2	— 0.05369	— 0.46120	— 0.01662	— 0.04344	+ 0.04722	+ 0.16729
0.3	— 0.11144	— 0.66480	— 0.03508	— 0.05776	+ 0.09990	+ 0.23087
0.4	— 0.17682	— 0.84202	— 0.05703	— 0.06459	+ 0.16305	+ 0.27427
0.5	— 0.23840	— 0.99268	— 0.07944	— 0.06346	+ 0.22853	+ 0.29636
0.6	— 0.29609	— 1.12133	— 0.09944	— 0.05510	+ 0.28879	+ 0.29926
0.7	— 0.31308	— 1.23609	— 0.11479	— 0.04124	+ 0.33813	+ 0.28773
0.8	— 0.31688	— 1.34666	— 0.12421	— 0.02423	+ 0.37354	+ 0.26798
0.9	— 0.29931	— 1.46224	— 0.12746	— 0.00658	+ 0.39484	+ 0.24638
1.0	— 0.26561	— 1.58974	— 0.12529	+ 0.00952	+ 0.40438	+ 0.22828

TABLE 5.

 $M = + 1.60000.$ 

$k$	$Re F_B$	$Im F_B$	$Re G_B$	$Im G_B$	$Re H_B$	$Im H_B$
0	— 0.00000	— 0.00000	+ 0.00000	+ 0.00000	+ 0.00000	+ 0.00000
0.1	— 0.04026	— 0.63385	+ 0.01654	+ 0.08330	+ 0.04807	+ 0.31407
0.2	— 0.15169	— 1.22957	+ 0.06356	+ 0.15402	+ 0.18462	+ 0.59240
0.3	— 0.30845	— 1.75767	+ 0.13369	+ 0.20173	+ 0.38820	+ 0.80578
0.4	— 0.71414	— 2.20393	+ 0.21617	+ 0.21989	+ 0.62781	+ 0.93672
0.5	— 0.61011	— 2.57245	+ 0.29875	+ 0.20683	+ 0.86889	+ 0.89222
0.6	— 0.68413	— 2.88439	+ 0.36987	+ 0.16585	+ 1.07988	+ 0.95355
0.7	— 0.67748	— 3.17285	+ 0.42055	+ 0.10438	+ 1.23789	+ 0.87327
0.8	— 0.58858	— 3.47520	+ 0.44579	+ 0.03245	+ 1.33233	+ 0.77010
0.9	— 0.43274	— 3.82464	+ 0.44514	+ 0.08925	+ 1.36594	+ 0.67289
1.0	— 0.23784	— 4.24305	+ 0.42236	+ 0.10128	+ 1.35294	+ 0.60492
$k$	$Re F_T$	$Im F_T$	$Re G_T$	$Im G_T$	$Re H_T$	$Im H_T$
0	— 0.00000	— 0.00000	— 0.00000	— 0.00000	+ 0.00000	+ 0.00000
0.1	— 0.01353	— 0.31858	— 0.00415	— 0.02623	+ 0.01207	+ 0.10551
0.2	— 0.05221	— 0.62745	— 0.01612	— 0.04982	+ 0.04700	+ 0.20378
0.3	— 0.11071	— 0.91834	— 0.03458	— 0.06846	+ 0.10111	+ 0.28850
0.4	— 0.18108	— 1.18569	— 0.05751	— 0.08045	+ 0.16891	+ 0.35513
0.5	— 0.25409	— 1.42735	— 0.08247	— 0.08496	+ 0.24384	+ 0.40137
0.6	— 0.32063	— 1.64477	— 0.10699	— 0.08199	+ 0.31924	+ 0.42736
0.7	— 0.37309	— 1.84252	— 0.12880	— 0.07242	+ 0.38922	+ 0.43543
0.8	— 0.40639	— 1.02733	— 0.14620	— 0.05776	+ 0.44935	+ 0.42961
0.9	— 0.41848	— 2.20710	— 0.15814	— 0.03992	+ 0.49713	+ 0.41489
1.0	— 0.41035	— 2.38915	— 0.16436	— 0.02092	+ 0.53211	+ 0.39640
$k$	$Re P_B$	$Im P_B$	$Re Q_B$	$Im Q_B$	$Re R_B$	$Im R_B$
0	— 0.00000	— 0.00000	+ 0.00000	+ 0.00000	+ 0.00000	+ 0.00000
0.1	— 0.02673	— 0.31527	+ 0.01322	+ 0.06229	+ 0.03600	+ 0.20856
0.2	— 0.09948	— 0.60212	+ 0.05065	+ 0.11413	+ 0.13762	+ 0.38862
0.3	— 0.19774	— 0.83933	+ 0.10600	+ 0.14692	+ 0.28708	+ 0.51728
0.4	— 0.29306	— 1.01825	+ 0.17012	+ 0.15548	+ 0.45890	+ 0.58159
0.5	— 0.35602	— 1.14510	+ 0.23272	+ 0.13881	+ 0.62505	+ 0.58085
0.6	— 0.36351	— 1.23961	+ 0.28422	+ 0.10020	+ 0.76064	+ 0.52620
0.7	— 0.30439	— 1.33032	+ 0.31743	+ 0.04640	+ 0.84867	+ 0.43785
0.8	— 0.18219	— 1.44782	+ 0.32874	— 0.01379	— 0.88299	+ 0.34049
0.9	— 0.01426	— 1.01754	+ 0.31853	— 0.07120	+ 0.86881	+ 0.25800
1.0	+ 0.17251	— 1.85390	+ 0.29077	— 0.11803	+ 0.82083	+ 0.20852
$k$	$Re P_T$	$Im P_T$	$Re Q_T$	$Im Q_T$	$Re R_T$	$Im R_T$
0	— 0.00000	— 0.00000	— 0.00000	— 0.00000	+ 0.00000	+ 0.00000
0.1	— 0.01013	— 0.21217	— 0.00346	— 0.02096	+ 0.00965	+ 0.07903
0.2	— 0.03895	— 0.41658	— 0.01341	— 0.03966	+ 0.03750	+ 0.15203
0.3	— 0.08202	— 0.60674	— 0.02869	— 0.05412	+ 0.08042	+ 0.21381
0.4	— 0.13280	— 0.77843	— 0.04755	— 0.06295	+ 0.13371	+ 0.26068
0.5	— 0.18374	— 0.93035	— 0.06787	— 0.06545	+ 0.19185	+ 0.29093
0.6	— 0.22758	— 1.06417	— 0.08752	— 0.06172	+ 0.24927	+ 0.30491
0.7	— 0.25844	— 1.18413	— 0.10460	— 0.05258	+ 0.30113	+ 0.30488
0.8	— 0.27269	— 1.29622	— 0.11768	— 0.03941	+ 0.34395	+ 0.29447
0.9	— 0.26937	— 1.40702	— 0.12596	— 0.02391	+ 0.37595	+ 0.27806
1.0	— 0.25006	— 1.52265	— 0.12933	— 0.00784	+ 0.39713	+ 0.26003

TABLE 6.

 $M = +1.80000$ .

$k$	$Re F_B$	$Im F_B$	$Re G_B$	$Im G_B$	$Re H_B$	$Im H_B$
0	-0.00000	-0.00000	+0.00000	+0.00000	+0.00000	+0.00000
0.1	-0.02351	-0.53110	+0.00984	+0.05844	+0.03341	+0.26370
0.2	-0.08984	-1.04237	+0.03827	+0.11052	+0.12991	+0.50655
0.3	-0.18718	-1.51732	+0.08211	+0.15065	+0.27887	+0.71045
0.4	-0.29802	-1.94561	+0.13652	+0.17470	+0.46422	+0.86225
0.5	-0.40218	-2.32477	+0.19566	+0.18042	+0.66672	+0.95541
0.6	-0.48011	-2.66059	+0.25335	+0.16771	+0.86657	+0.99054
0.7	-0.51619	-2.96613	+0.30391	+0.13853	+0.04610	+0.97500
0.8	-0.50121	-3.25951	+0.34279	+0.09652	+1.19193	+0.91246
0.9	-0.43382	-3.56090	+0.36708	+0.04654	+1.29654	+0.84589
1.0	-0.32060	-3.88925	+0.37573	-0.00608	+1.35886	+0.76506
	$Re F_T$	$Im F_T$	$Re G_T$	$Im G_T$	$Re H_T$	$Im H_T$
0	-0.00000	-0.00000	-0.00000	-0.00000	+0.00000	+0.00000
0.1	-0.00788	-0.26640	-0.00296	-0.02200	+0.00838	+0.08837
0.2	-0.03069	-0.52778	-0.01158	-0.04240	+0.03289	+0.17254
0.3	-0.06599	-0.77965	-0.02519	-0.05975	+0.07173	+0.24868
0.4	-0.11007	-1.01864	-0.04271	-0.07288	+0.12210	+0.31372
0.5	-0.15836	-1.24274	-0.06280	-0.08097	+0.18050	+0.36558
0.6	-0.20597	-1.45159	-0.08398	-0.08367	+0.24309	+0.40331
0.7	-0.24828	-1.64639	-0.10474	-0.08107	+0.30607	+0.42715
0.8	-0.28139	-1.82972	-0.12374	-0.07366	+0.36604	+0.43838
0.9	-0.30254	-2.00516	-0.13988	-0.06227	+0.42027	+0.43915
1.0	-0.31034	-2.17686	-0.15238	-0.04801	+0.46692	+0.43214
	$Re P_B$	$Im P_B$	$Re Q_B$	$Im Q_B$	$Re R_B$	$Im R_B$
0	-0.00000	-0.00000	+0.00000	+0.00000	+0.00000	+0.00000
0.1	-0.01562	-0.26470	+0.00787	+0.04374	+0.02503	+0.17532
0.2	-0.05916	-0.51459	+0.03053	+0.08218	+0.09702	+0.33402
0.3	-0.12119	-0.73766	+0.06528	+0.11073	+0.20714	+0.46176
0.4	-0.18796	-0.92697	+0.10799	+0.12600	+0.34212	+0.54853
0.5	-0.24382	-1.08203	+0.15369	+0.12632	+0.48622	+0.58983
0.6	-0.27414	-1.20900	+0.19724	+0.11181	+0.62349	+0.58724
0.7	-0.26790	-1.31974	+0.23393	+0.08436	+0.74003	+0.54785
0.8	-0.21982	-1.42979	+0.26011	+0.04731	+0.82589	+0.48307
0.9	-0.13128	-1.55574	+0.27362	+0.00493	+0.87628	+0.40674
1.0	-0.01026	-1.71240	+0.27392	-0.03815	+0.89194	+0.33292
	$Re P_T$	$Im P_T$	$Re Q_T$	$Im Q_T$	$Re R_T$	$Im R_T$
0	-0.00000	-0.00000	-0.00000	-0.00000	+0.00000	+0.00000
0.1	-0.00591	-0.17749	-0.00246	-0.01758	+0.00670	+0.06622
0.2	-0.02292	-0.35096	-0.00964	-0.03380	+0.02626	+0.12894
0.3	-0.04903	-0.51688	-0.02093	-0.04741	+0.05715	+0.18499
0.4	-0.08116	-0.67264	-0.03540	-0.05741	+0.09697	+0.23187
0.5	-0.11557	-0.81680	-0.05188	-0.06315	+0.14275	+0.26792
0.6	-0.14828	-0.94931	-0.06909	-0.06435	+0.19126	+0.29248
0.7	-0.17561	-1.07141	-0.08574	-0.06112	+0.23933	+0.30589
0.8	-0.19456	-1.18549	-0.10070	-0.05395	+0.28416	+0.30940
0.9	-0.20316	-1.29469	-0.11304	-0.04359	+0.32359	+0.30495
1.0	-0.20062	-1.40258	-0.12215	-0.03102	+0.35624	+0.29492

TABLE 7.

 $M = + 2.00000.$ 

$k$	$Re F_B$	$Im F_B$	$Re G_B$	$Im G_B$	$Re H_B$	$Im H_B$
0	-0.00000	-0.00000	+0.00000	+0.00000	+0.00000	+0.00000
0.1	-0.01520	-0.45984	+0.00662	+0.04380	+0.02547	+0.22856
0.2	-0.05854	-0.90779	+0.02588	+0.08377	+0.09969	+0.44311
0.3	-0.12350	-1.33362	+0.05609	+0.11648	+0.21629	+0.63109
0.4	-0.20023	-1.73017	+0.09460	+0.13917	+0.36547	+0.78259
0.5	-0.27690	-2.09437	+0.13810	+0.15002	+0.53503	+0.89135
0.6	-0.34127	-2.42769	+0.18293	+0.14830	+0.71175	+0.95525
0.7	-0.38241	-2.73592	+0.22548	+0.13445	+0.88279	+0.79637
0.8	-0.39214	-3.02847	+0.26247	+0.10990	+1.03695	+0.96052
0.9	-0.36617	-3.31708	+0.29133	+0.07699	+1.16586	+0.91647
1.0	-0.30460	-3.61429	+0.31034	+0.03863	+1.26461	+0.84475
	$Re F_T$	$Im F_T$	$Re G_T$	$Im G_T$	$Re H_T$	$Im H_T$
0	-0.00000	-0.00000	-0.00000	-0.00000	+0.00000	+0.00000
0.1	-0.00509	-0.23043	-0.00230	-0.01906	+0.00638	+0.07650
0.2	-0.01992	-0.45785	-0.00904	-0.03701	+0.02517	+0.15018
0.3	-0.04314	-0.67954	-0.01981	-0.05282	+0.05527	+0.21843
0.4	-0.07269	-0.89329	-0.03393	-0.06562	+0.09501	+0.27901
0.5	-0.10597	-1.09762	-0.05053	-0.07474	+0.14221	+0.33025
0.6	-0.14008	-1.29192	-0.06862	-0.07977	+0.19440	+0.37112
0.7	-0.17209	-1.47644	-0.08717	-0.08059	+0.24900	+0.40126
0.8	-0.19935	-1.65227	-0.10516	-0.07732	+0.30354	+0.42100
0.9	-0.21966	-1.82119	-0.12167	-0.07035	+0.35580	+0.43129
1.0	-0.23152	-1.98552	-0.13596	-0.06028	+0.40397	+0.43352
	$Re P_B$	$Im P_B$	$Re Q_B$	$Im Q_B$	$Re R_B$	$Im R_B$
0	-0.00000	-0.00000	+0.00000	+0.00000	+0.00000	+0.00000
0.1	-0.01011	-0.22941	+0.00529	+0.03279	+0.01909	+0.15205
0.2	-0.03862	-0.44994	+0.02066	+0.06241	+0.07453	+0.29293
0.3	-0.08036	-0.65409	+0.04465	+0.08599	+0.16102	+0.41266
0.4	-0.12754	-0.83689	+0.07501	+0.10129	+0.27046	+0.50358
0.5	-0.17092	-0.99675	+0.10892	+0.10687	+0.39282	+0.56110
0.6	-0.20119	-1.13576	+0.14331	+0.10225	+0.51735	+0.58413
0.7	-0.21032	-1.25948	+0.17515	+0.08792	+0.63378	+0.57511
0.8	-0.19280	-1.37620	+0.20176	+0.06526	+0.73341	+0.53951
0.9	-0.14650	-1.49589	+0.22108	+0.03637	+0.81007	+0.48518
1.0	-0.07308	-1.62877	+0.23184	+0.00382	+0.86064	+0.42123
	$Re P_T$	$Im P_T$	$Re Q_T$	$Im Q_T$	$Re R_T$	$Im R_T$
0	-0.00000	-0.00000	-0.00000	-0.00000	+0.00000	+0.00000
0.1	-0.00382	-0.15355	-0.00191	-0.01524	+0.00511	+0.05734
0.2	-0.01489	-0.30470	-0.00753	-0.02952	+0.02011	+0.11233
0.3	-0.03210	-0.45129	-0.01647	-0.04198	+0.04408	+0.16280
0.4	-0.05376	-0.59159	-0.02815	-0.05187	+0.07558	+0.20692
0.5	-0.07770	-0.72453	-0.04182	-0.05862	+0.11277	+0.24335
0.6	-0.10156	-0.84972	-0.05662	-0.06193	+0.15355	+0.27128
0.7	-0.12299	-0.96752	-0.07165	-0.06169	+0.19576	+0.29052
0.8	-0.13990	-1.07900	-0.08604	-0.05805	+0.23733	+0.30144
0.9	-0.15602	-1.18576	-0.09902	-0.05138	+0.27645	+0.30494
1.0	-0.15408	-1.28984	-0.10997	-0.04222	+0.31170	+0.30229

TABLE 8.

 $M = + 2.50000.$ 

$k$	$Re F_B$	$Im F_B$	$Re G_B$	$Im G_B$	$Re H_B$	$Im H_B$
0	-0.00000	-0.00000	+ 0.00000	+ 0.00000	+ 0.00000	+ 0.00000
0.1	-0.00659	-0.34836	+ 0.00325	+ 0.02513	+ 0.01599	+ 0.17336
0.2	-0.02557	-0.69210	+ 0.01279	+ 0.04868	+ 0.06305	+ 0.33952
0.3	-0.05472	-1.02707	+ 0.02804	+ 0.06917	+ 0.13848	+ 0.49178
0.4	-0.09056	-1.35005	+ 0.04805	+ 0.08534	+ 0.23799	+ 0.62440
0.5	-0.12873	-1.65911	+ 0.07161	+ 0.09619	+ 0.35608	+ 0.73295
0.6	-0.16442	-1.95379	+ 0.09730	+ 0.10108	+ 0.48640	+ 0.81463
0.7	-0.19286	-2.23518	+ 0.12360	+ 0.09975	+ 0.62223	+ 0.86835
0.8	-0.20981	-2.50588	+ 0.14902	+ 0.09232	+ 0.75699	+ 0.89479
0.9	-0.21202	-2.76969	+ 0.17214	+ 0.07929	+ 0.88467	+ 0.89626
1.0	-0.19748	-3.03136	+ 0.19177	+ 0.06147	+ 1.00028	+ 0.87639
	$Re F_T$	$Im F_T$	$Re G_T$	$Im G_T$	$Re H_T$	$Im H_T$
0	-0.00000	-0.00000	-0.00000	-0.00000	+ 0.00000	+ 0.00000
0.1	-0.00220	-0.17438	-0.00149	-0.01445	+ 0.00401	+ 0.05795
0.2	-0.00866	-0.34759	-0.00589	-0.02829	+ 0.01587	+ 0.11445
0.3	-0.01892	-0.51855	-0.01302	-0.04094	+ 0.03513	+ 0.16813
0.4	-0.03225	-0.68632	-0.02256	-0.05190	+ 0.06106	+ 0.21775
0.5	-0.04773	-0.85022	-0.03408	-0.06073	+ 0.09271	+ 0.26227
0.6	-0.06427	-1.00979	-0.04711	-0.06710	+ 0.12892	+ 0.30089
0.7	-0.08072	-1.16489	-0.06110	-0.07079	+ 0.16846	+ 0.33309
0.8	-0.09594	-1.31569	-0.07547	-0.08638	+ 0.21001	+ 0.35862
0.9	-0.10886	-1.46263	-0.08967	-0.06992	+ 0.25229	+ 0.37754
1.0	-0.11759	-1.60642	-0.10317	-0.06555	+ 0.29409	+ 0.39014
	$Re P_B$	$Im P_B$	$Re Q_B$	$Im Q_B$	$Re R_B$	$Im R_B$
0	-0.00000	-0.00000	+ 0.00000	+ 0.00000	+ 0.00000	+ 0.00000
0.1	-0.00438	-0.17398	+ 0.00260	+ 0.01882	+ 0.01199	+ 0.11541
0.2	-0.01691	-0.34451	+ 0.01022	+ 0.03633	+ 0.04719	+ 0.22507
0.3	-0.03580	-0.50852	+ 0.02236	+ 0.05131	+ 0.10335	+ 0.32365
0.4	-0.05831	-0.66373	+ 0.03821	+ 0.06269	+ 0.17693	+ 0.40665
0.5	-0.08100	-0.80890	+ 0.05673	+ 0.06969	+ 0.26337	+ 0.47068
0.6	-0.10014	-0.94400	+ 0.07674	+ 0.07180	+ 0.35747	+ 0.51374
0.7	-0.11213	-1.07029	+ 0.09694	+ 0.06886	+ 0.45377	+ 0.53526
0.8	-0.11388	-1.19019	+ 0.11608	+ 0.05462	+ 0.54698	+ 0.53617
0.9	-0.10315	-1.30706	+ 0.13301	+ 0.04878	+ 0.63239	+ 0.51872
1.0	-0.07889	-1.42494	+ 0.14674	+ 0.03286	+ 0.70618	+ 0.48625
	$Re P_T$	$Im P_T$	$Re Q_T$	$Im Q_T$	$Re R_T$	$Im R_T$
0	-0.00000	-0.00000	-0.00000	-0.00000	+ 0.00000	+ 0.00000
0.1	-0.00165	-0.11623	-0.00124	-0.01155	+ 0.00320	+ 0.04344
0.2	-0.00648	-0.23152	-0.00491	-0.02258	+ 0.01268	+ 0.08568
0.3	-0.01410	-0.34502	-0.01083	-0.03260	+ 0.02804	+ 0.12557
0.4	-0.02392	-0.45599	-0.01874	-0.04117	+ 0.04867	+ 0.16209
0.5	-0.03518	-0.56391	-0.02827	-0.04792	+ 0.07374	+ 0.19439
0.6	-0.04697	-0.66845	-0.03899	-0.05258	+ 0.10228	+ 0.22183
0.7	-0.05836	-0.76956	-0.05043	-0.05498	+ 0.13323	+ 0.24401
0.8	-0.06694	-0.86743	-0.04268	-0.05505	+ 0.16550	+ 0.26077
0.9	-0.07634	-0.96249	-0.07353	-0.05285	+ 0.19801	+ 0.27220
1.0	-0.08141	-1.05538	-0.08425	-0.04851	+ 0.22977	+ 0.27861

TABLE 9.

 $M = + 3.00000.$ 

$k$	$Re F_B$	$Im F_B$	$Re G_B$	$Im G_B$	$Re H_B$	$Im H_B$
0	-0.00000	-0.00000	+ 0.00000	+ 0.00000	+ 0.00000	+ 0.00000
0.1	-0.00350	-0.28245	+ 0.00197	+ 0.01652	+ 0.01174	+ 0.14063
0.2	-0.01366	-0.56256	+ 0.00778	+ 0.03217	+ 0.04643	+ 0.27655
0.3	-0.02940	-0.83822	+ 0.01714	+ 0.04611	+ 0.10248	+ 0.40331
0.4	-0.04907	-1.10772	+ 0.02956	+ 0.05762	+ 0.17739	+ 0.51696
0.5	-0.07055	-1.36990	+ 0.04444	+ 0.06609	+ 0.26785	+ 0.61424
0.6	-0.09145	-1.62430	+ 0.06101	+ 0.07107	+ 0.36996	+ 0.69278
0.7	-0.10928	-1.87119	+ 0.07847	+ 0.07231	+ 0.47947	+ 0.75117
0.8	-0.12174	-2.11156	+ 0.09597	+ 0.06973	+ 0.59199	+ 0.78899
0.9	-0.12686	-2.34709	+ 0.11269	+ 0.06347	+ 0.70331	+ 0.80687
1.0	-0.12320	-2.57995	+ 0.12785	+ 0.05382	+ 0.80954	+ 0.80632
	$Re F_T$	$Im F_T$	$Re G_T$	$Im G_T$	$Re H_T$	$Im H_T$
0	-0.00000	-0.00000	-0.00000	-0.00000	+ 0.00000	+ 0.00000
0.1	-0.00117	-0.14132	-0.00112	-0.01172	+ 0.00294	+ 0.04698
0.2	-0.00462	-0.28206	-0.00443	-0.02302	+ 0.01167	+ 0.09302
0.3	-0.01012	-0.42165	-0.00980	-0.03351	+ 0.02592	+ 0.13720
0.4	-0.01734	-0.55962	-0.01706	-0.04283	+ 0.04526	+ 0.17869
0.5	-0.02582	-0.69559	-0.02593	-0.05066	+ 0.06914	+ 0.21676
0.6	-0.03504	-0.82928	-0.03610	-0.05674	+ 0.09685	+ 0.25080
0.7	-0.04443	-0.96058	-0.04723	-0.06088	+ 0.12762	+ 0.28036
0.8	-0.05338	-1.08949	-0.05891	-0.06296	+ 0.16063	+ 0.30514
0.9	-0.06133	-1.21617	-0.07077	-0.06296	+ 0.19502	+ 0.32502
1.0	-0.06778	-1.34092	-0.08243	-0.06091	+ 0.22997	+ 0.34003
	$Re P_B$	$Im P_B$	$Re Q_B$	$Im Q_B$	$Re R_B$	$Im R_B$
0	-0.00000	-0.00000	+ 0.00000	+ 0.00000	+ 0.00000	+ 0.00000
0.1	-0.00233	-0.14112	+ 0.00158	+ 0.01238	+ 0.00880	+ 0.09365
0.2	-0.00904	-0.28050	+ 0.00622	+ 0.02403	+ 0.03476	+ 0.18353
0.3	-0.01928	-0.41657	+ 0.01367	+ 0.03426	+ 0.07565	+ 0.26611
0.4	-0.03174	-0.54809	+ 0.02353	+ 0.04248	+ 0.13213	+ 0.33827
0.5	-0.04473	-0.67431	+ 0.03527	+ 0.04818	+ 0.19872	+ 0.39748
0.6	-0.05640	-0.79502	+ 0.04824	+ 0.05101	+ 0.27312	+ 0.44198
0.7	-0.06486	-0.91061	+ 0.06177	+ 0.05079	+ 0.35185	+ 0.47080
0.8	-0.06836	-1.02208	+ 0.07514	+ 0.04747	+ 0.43136	+ 0.48385
0.9	-0.06552	-1.13092	+ 0.08767	+ 0.04121	+ 0.50828	+ 0.48185
1.0	-0.05542	-1.23904	+ 0.09871	+ 0.03228	+ 0.57956	+ 0.46628
	$Re P_T$	$Im P_T$	$Re Q_T$	$Im Q_T$	$Re R_T$	$Im R_T$
0	-0.00000	-0.00000	-0.00000	-0.00000	+ 0.00000	+ 0.00000
0.1	-0.00088	-0.09420	-0.00093	-0.00937	+ 0.00235	+ 0.03522
0.2	-0.00345	-0.18793	-0.00369	-0.01838	+ 0.00933	+ 0.06966
0.3	-0.00755	-0.28076	-0.00816	-0.02670	+ 0.02070	+ 0.10255
0.4	-0.01288	-0.37229	-0.01418	-0.03402	+ 0.03611	+ 0.13321
0.5	-0.01907	-0.46224	-0.02152	-0.04006	+ 0.05506	+ 0.16103
0.6	-0.02569	-0.55041	-0.02992	-0.04462	+ 0.07697	+ 0.18553
0.7	-0.03227	-0.63673	-0.03905	-0.04754	+ 0.10118	+ 0.20634
0.8	-0.03832	-0.72123	-0.04859	-0.04871	+ 0.12700	+ 0.22324
0.9	-0.04340	-0.80408	-0.05821	-0.04813	+ 0.15370	+ 0.23615
1.0	-0.04710	-0.88554	-0.06757	-0.04584	+ 0.18060	+ 0.24515

TABLE 10.

 $M = + 3.50000.$ 

$k$	$Re F_B$	$Im F_B$	$Re G_B$	$Im G_B$	$Re H_B$	$Im H_B$
0	-0.00000	-0.00000	+0.00000	+0.00000	+0.00000	+0.00000
0.1	-0.00210	-0.23828	+0.00134	+0.01176	+0.00933	+0.11867
0.2	-0.00821	-0.47521	+0.00529	+0.02295	+0.03697	+0.23386
0.3	-0.01773	-0.70954	+0.01168	+0.03305	+0.67771	+0.34226
0.4	-0.02972	-0.94024	+0.02022	+0.04158	+0.08183	+0.44086
0.5	-0.04299	-1.16661	+0.03053	+0.04811	+0.14217	+0.52710
0.6	-0.05615	-1.38828	+0.04214	+0.05234	+0.21572	+0.59901
0.7	-0.06775	-1.60532	+0.05456	+0.05407	+0.29971	+0.65523
0.8	-0.07640	-1.81821	+0.06722	+0.05318	+0.31909	+0.69510
0.9	-0.08087	-2.02782	+0.07960	+0.04971	+0.48666	+0.71863
1.0	-0.08018	-2.23535	+0.09118	+0.04379	+0.58322	+0.72652
	$Re F_T$	$Im F_T$	$Re G_T$	$Im G_T$	$Re H_T$	$Im H_T$
0	-0.00000	-0.00000	-0.00000	-0.00000	+0.00000	+0.00000
0.1	-0.00070	-0.11920	-0.00090	-0.00988	+0.00234	+0.03964
0.2	-0.00277	-0.23806	-0.00357	-0.01946	+0.00928	+0.07857
0.3	-0.00609	-0.35625	-0.00791	-0.02841	+0.02066	+0.11614
0.4	-0.01046	-0.47350	-0.01380	-0.03646	+0.03617	+0.15170
0.5	-0.01563	-0.58956	-0.02105	-0.04337	+0.05543	+0.18469
0.6	-0.02130	-0.70427	-0.02942	-0.04891	+0.07794	+0.21464
0.7	-0.02713	-0.81754	-0.03866	-0.05293	+0.10317	+0.24116
0.8	-0.03279	-0.92936	-0.04847	-0.05532	+0.13052	+0.26397
0.9	-0.03792	-1.03979	-0.05857	-0.05602	+0.15937	+0.28291
1.0	-0.04223	-1.14898	-0.06866	-0.05503	+0.18909	+0.29792
	$Re P_B$	$Im P_B$	$Re Q_B$	$Im Q_B$	$Re R_B$	$Im R_B$
0	-0.00000	-0.00000	+0.00000	+0.00000	+0.00000	+0.00000
0.1	-0.00140	-0.11908	+0.00107	+0.00881	+0.00700	+0.07904
0.2	-0.00544	-0.23715	+0.00423	+0.01715	+0.02769	+0.15529
0.3	-0.01164	-0.35329	+0.00932	+0.02458	+0.06117	+0.22612
0.4	-0.01927	-0.46675	+0.01611	+0.03071	+0.10600	+0.28916
0.5	-0.02736	-0.57705	+0.02425	+0.03518	+0.16029	+0.34241
0.6	-0.03485	-0.68401	+0.03337	+0.03776	+0.22176	+0.38437
0.7	-0.04062	-0.78778	+0.04303	+0.03828	+0.28791	+0.41407
0.8	-0.04362	-0.88885	+0.05277	+0.03669	+0.35614	+0.43113
0.9	-0.04295	-0.98803	+0.06214	+0.03301	+0.42385	+0.43572
1.0	-0.03795	-1.08637	+0.07071	+0.02738	+0.48862	+0.42859
	$Re P_T$	$Im P_T$	$Re Q_T$	$Im Q_T$	$Re R_T$	$Im R_T$
0	-0.00000	-0.00000	-0.00000	-0.00000	+0.00000	+0.00000
0.1	-0.00053	-0.07946	-0.00075	-0.00791	+0.00187	+0.02972
0.2	-0.00207	-0.15864	-0.00297	-0.01554	+0.00742	+0.05885
0.3	-0.00454	-0.23730	-0.00659	-0.02265	+0.01650	+0.08684
0.4	-0.00777	-0.31520	-0.01148	-0.02898	+0.02887	+0.11317
0.5	-0.01155	-0.39217	-0.01748	-0.03434	+0.04417	+0.13737
0.6	-0.01564	-0.46808	-0.02439	-0.03854	+0.05200	+0.15905
0.7	-0.01975	-0.54287	-0.0319	-0.04144	+0.08190	+0.17790
0.8	-0.02362	-0.61654	-0.04003	-0.04297	+0.10337	+0.19372
0.9	-0.02696	-0.68918	-0.04825	-0.04306	+0.12587	+0.20637
1.0	-0.02953	-0.76092	-0.05639	-0.04175	+0.14889	+0.21584

TABLE 11.

 $M = + 4.00000.$ 

$k$	$Re F_B$	$Im F_B$	$Re G_B$	$Im G_B$	$Re H_B$	$Im H_B$
0	-0.00000	-0.00000	+0.00000	+0.00000	+0.00000	+0.00000
0.1	-0.00137	-0.20641	+0.00097	+0.00882	+0.00778	+0.10282
0.2	-0.00534	-0.41196	+0.00386	+0.01725	+0.03085	+0.20287
0.3	-0.01155	-0.61585	+0.00853	+0.02491	+0.06839	+0.29751
0.4	-0.01942	-0.81742	+0.01479	+0.03145	+0.11910	+0.38433
0.5	-0.02819	-1.01618	+0.02239	+0.03659	+0.18123	+0.46122
0.6	-0.03699	-1.21190	+0.03100	+0.04008	+0.25268	+0.52648
0.7	-0.04489	-1.40456	+0.04029	+0.04176	+0.33109	+0.57890
0.8	-0.05099	-1.59444	+0.04986	+0.04154	+0.41394	+0.61774
0.9	-0.05447	-1.78205	+0.05934	+0.03941	+0.49867	+0.64281
1.0	-0.05466	-1.96810	+0.06836	+0.03544	+0.58278	+0.65441
	$Re F_T$	$Im F_T$	$Re G_T$	$Im G_T$	$Re H_T$	$Im H_T$
0	-0.00000	-0.00000	-0.00000	-0.00000	+0.00000	+0.00000
0.1	-0.00046	-0.10324	-0.00076	-0.00857	+0.00195	+0.03433
0.2	-0.00180	-0.20627	-0.00300	-0.01688	+0.00774	+0.06811
0.3	-0.00396	-0.30887	-0.00666	-0.02468	+0.01725	+0.10080
0.4	-0.00682	-0.41087	-0.01164	-0.03176	+0.03025	+0.13189
0.5	-0.01021	-0.51210	-0.01778	-0.03789	+0.04644	+0.16093
0.6	-0.01394	-0.61247	-0.02492	-0.04291	+0.06546	+0.18751
0.7	-0.01782	-0.71190	-0.03282	-0.04668	+0.08688	+0.21132
0.8	-0.02160	-0.81038	-0.04128	-0.04908	+0.11025	+0.23209
0.9	-0.02509	-0.90793	-0.05006	-0.05007	+0.13508	+0.24967
1.0	-0.02807	-1.00466	-0.05891	-0.04962	+0.16087	+0.26396
	$Re P_B$	$Im P_B$	$Re Q_B$	$Im Q_B$	$Re R_B$	$Im R_B$
0	-0.00000	-0.00000	+0.00000	+0.00000	+0.00000	+0.00000
0.1	-0.00091	-0.10317	+0.00078	+0.00661	+0.00583	+0.06848
0.2	-0.00354	-0.20569	+0.00308	+0.01289	+0.02310	+0.13476
0.3	-0.00759	-0.30698	+0.00681	+0.01854	+0.05114	+0.19761
0.4	-0.01261	-0.40655	+0.01178	+0.02325	+0.08885	+0.25244
0.5	-0.01798	-0.50408	+0.01779	+0.02680	+0.13479	+0.30029
0.6	-0.02304	-0.59943	+0.02457	+0.02900	+0.18723	+0.33897
0.7	-0.02707	-0.69267	+0.03181	+0.02970	+0.24421	+0.36758
0.8	-0.02938	-0.78407	+0.03920	+0.02886	+0.30369	+0.38565
0.9	-0.02938	-0.87411	+0.04642	+0.02648	+0.36359	+0.39315
1.0	-0.02659	-0.96344	+0.05315	+0.02263	+0.42192	+0.39045
	$Re P_T$	$Im P_T$	$Re Q_T$	$Im Q_T$	$Re R_T$	$Im R_T$
0	-0.00000	-0.00000	-0.00000	-0.00000	+0.00000	+0.00000
0.1	-0.00034	-0.06882	-0.00062	-0.00685	+0.00156	+0.02574
0.2	-0.00135	-0.13747	-0.00250	-0.01348	+0.00619	+0.05102
0.3	-0.00296	-0.20579	-0.00555	-0.01968	+0.01378	+0.07540
0.4	-0.00507	-0.27362	-0.00968	-0.02526	+0.02414	+0.09844
0.5	-0.00755	-0.34085	-0.01477	-0.03003	+0.03702	+0.11978
0.6	-0.01025	-0.40739	-0.02067	-0.03385	+0.05210	+0.13909
0.7	-0.01299	-0.47321	-0.02718	-0.03660	+0.06902	+0.15611
0.8	-0.01559	-0.53830	-0.03412	-0.03820	+0.08740	+0.17063
0.9	-0.01788	-0.60269	-0.04127	-0.03861	+0.10682	+0.18254
1.0	-0.01970	-0.66648	-0.04844	-0.03781	+0.12686	+0.19178